The role of AHK5 in abiotic and biotic stress signalling

Jasmine Pham

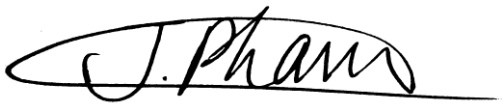
Imperial College London, Department of Life Sciences

Submitted for examination for the degree of PhD

Declaration of originality

I hereby declare the work within to be that of my own which was produced under the supervision of Dr Radhika Desikan and Professor John Mansfield in the Department of Life Sciences, Imperial College London.

This thesis is submitted for examination for the qualification of PhD and has not previously been submitted for examination. Any references to the work of others has been indicated and acknowledged as such.

Signed:  **Date:** 20/06/2011

The candidate: Jasmine Pham

Acknowledgements

Firstly, I would like to thank my supervisors, Dr Radhika Desikan and Professor John Mansfield, for their continued support and patience, with special thanks to Dr Radhika Desikan whose boundless enthusiasm for science and encyclopaedic knowledge has been a real inspiration. Thank you for working as hard as I have on this project. I couldn't have done it without you.

I would also like to thank my advisors, Dr Thorsten Hamann and Dr Colin Turnbull for ensuring that I was on track and for their invaluable advice. Thanks Thorsten for making sure I ate everyday during my PhD and watching me whilst I did. It really helped.

Apologies to my former supervisor Dr Ken Bruce who, after all these years, is finding that he is still advising and supporting me – sorry, but you can't get rid of me that easily.

My thanks to Mark Bennett for his help with LC-MS/MS and HPLC analysis and for acting as official cake taster. There is more cake on the way.

Very special thanks to my friend and colleague Natalia Dinischiotu (and Apostolos) for all the lunches, discussions and for teaching me a very valuable lesson: that you can be stylish and do science. Thanks also to my colleagues Maija Sierla and Timothy Simpson for their company on those many long nights in the lab. Maija, the taste of reindeer and salted liquorice will stay with me forever. Tim, your jokes are inappropriate but funny. You are my favourite Welshman.

Special thanks to my Sifu Jeffrey Guishard and my fellow Sung Chuanies for their encouragement, for making sure it wasn't just my brain getting a work out and for keeping me on my toes – literally.

To Christine, Kani and Karen – thank you for believing and supporting me and showing me that there was light at the end of the tunnel.

A special mention to Neghat, Malcolm, Scrumpy, Ksenia, Kabira, Khareen and Ian. There should be more people like you in the world. It would be mad, but in a good way.

Lastly but most importantly, I would like to thank my parents, my sisters Nina and Katty and my long suffering husband Dean for putting up with me for all these years. Your unwavering love and support has allowed me to come this far. This is all for you.

Abstract

In *Arabidopsis thaliana,* eight histidine kinases (HKs) have been identified which function in hormone signalling, stimuli perception, and plant development. To better elucidate HK roles in signalling, the function of the least characterised HK, AHK5, in stress tolerance was investigated using a T-DNA insertion knockout line (*ahk5-1*).

Reduced inhibition of seedling root growth was seen in *ahk5-1* in response to salinity when compared to wild-type Col-0 in tissue culture assays. In mature plants, *ahk5-1* showed greater fresh weight gain under either salinity or drought stress. Loss of AHK5 function did not alter cold stress tolerance, nor basal and acquired heat stress tolerance in terms of seedling root elongation.

Infection with the biotrophic pathogen *Pseudomonas syringae* pv. *tomato* DC3000 revealed *ahk5-1* is compromised in disease resistance, exhibiting increased chlorosis and *in planta* bacterial growth. Levels of the plant hormones salicylic acid, jasmonic acid, and abscisic acid, alongside the bacterial phytotoxin coronatine, were lower in pathogen challenged *ahk5-1* mutants compared to wild-type plants. The *ahk5-1* mutant was also more susceptible to the necrotrophic pathogen *Botrytis cinerea,* supporting more fungal growth and displaying accelerated symptom development. Hydrogen peroxide production has been linked with both resistance and susceptibility towards *B. cinerea*; in *ahk5-1*, 3,3-diaminobenzidene (DAB) staining suggested reduced hydrogen peroxide production in response to infection.

Complementation and expression of *AHK5* with either full-length genomic *AHK5* under the 35S CaMV promoter or full-length *AHK5* cDNA under the native promoter rescued the *ahk5-1* mutant stress response phenotypes.

In summary, AHK5 was found to negatively regulate abiotic stress tolerance whilst positively contributing towards resistance against pathogens employing different lifestyles. To begin to establish an AHK5 signalling network, tandem affinity purification coupled with LC-MS/MS was employed for identification of possible AHK5 interacting proteins. Suggestions for further optimisation of the purification method are presented. The role of AHK5 in regulation of plant stress responses through modulation of reactive oxygen species and hormone signalling and through protein-protein interactions are reviewed. Suggestions for further investigation are also discussed.

Table of contents

Abstract.....4

List of figures.....13

List of tables.....19

List of abbreviations.....21

Chapter 1:.....29

1 Introduction.....30

1.1 Perception of stress - how do plants perceive stimuli?.....32

1.2 Abiotic stress – drought and salinity stress.....32

1.2.1 Drought stress.....33

1.2.2 Salinity stress.....40

1.2.3 Overlaps in drought and salinity stress.....45

1.3 Biotic stress – the impact of bacterial and fungal disease of plants.....46

1.4 Lifestyle of a bacterial pathogen – *Pst*DC3000 as an example.....48

1.4.1 PAMP-triggered immunity.....50

1.4.2 Bacterial effector proteins – concepts in compatible, incompatible and non-host interactions.....53

1.4.3 The *P. syringae* phytotoxin coronatine.....58

1.5 Lifestyle of a fungal phytopathogen – *B. cinerea* as an example.....61

1.5.1 Fungal virulence factors.....63

1.5.2 Plant defences against necrotrophic fungi.....65

1.5.3 Hormone signalling in defence against biotrophic and necrotrophic pathogens.....68

1.6 Reactive oxygen species in stress signalling.....70

1.6.1 ROS as signalling molecules.....71

1.6.2 ROS detoxification.....73

1.7 ROS sensing.....74

1.8 Histidine kinases in perception of stimulus and signal transduction 77
1.8.2 Histidine kinases in *A. thaliana* 82
1.8.3 HPt domain proteins and response regulators in *A. thaliana* 88
1.9 AHK5: an integrator of abiotic and biotic stress signalling? 89
1.10 General aims and objectives 90

Chapter 2: 93
2 Methods 94
2.1 General methods for growth of plants 94
2.1.1 Plant lines and growth conditions 94
2.1.2 Generation and selection of complemented lines 95
2.1.3 Growth of *A. thaliana* in tissue culture 95
2.2 Molecular methods 96
2.2.1 DNA extraction 96
2.2.2 Genotyping of plants by PCR 96
2.2.3 Total RNA extraction and cDNA generation 98
2.2.4 Confirmation of complementation by RT-PCR 99
2.2.5 TAP purification 101
2.2.6 Analysis of proteins by SDS-PAGE 102
2.2.7 Western blotting 102
2.3 Abiotic stress treatments 103
2.3.1 Stress treatments in tissue culture 103
2.3.2 Analysis of seedling growth 104
2.3.3 Salinity stress in mature plants 104
2.3.4 Drought stress in mature plants 105
2.4 Biotic stress treatments 105
2.4.1 Bacterial strains and growth 105

2.4.2 Bacterial inoculation and symptom scoring 106
2.4.3 Estimation of chlorophyll content 107
2.4.4 Electrolyte leakage 107
2.4.5 Inoculation with *Botrytis cinerea* and assessment of disease progression 108
2.5 Histological observations 109
2.5.1 Trypan Blue staining for cell death 109
2.5.2 Trypan blue staining of leaves infected with *B. cinerea* 109
2.5.3 Detection of ROS via DAB staining 110
2.5.4 Aniline blue staining for callose deposition 110
2.5.5 Preparation and analysis of slides 110
2.6 Analytical methods 110
2.6.1 Amplex red 110
2.6.2 Determination of Na^+ and K^+ content 111
2.6.3 Induction of camalexin by silver nitrate and extraction for use as a standard 112
2.6.4 Extraction of camalexin in lesions induced by *Botrytis cinerea* 113
2.6.5 Measurement of camalexin by high-pressure liquid chromatography 113
2.6.6 Identification of proteins 114
2.6.7 Hormone extraction and analysis 115
2.7 Statistical analysis 117

Chapter 3: 119

3 Characterisation of lines used 120
3.1 *AHK5* gene expression pattern 120
3.2 AHK5 structure 124
3.3 Genotyping lines used 128
3.4 Isolation of complemented lines in the *ahk5-1* background 130
3.5 Morphological analysis of the *ahk5-1* mutant 131

3.6 Effect of ABA on root growth....133
3.7 Conclusions....133

Chapter 4:....136
4 The role of AHK5 in abiotic stress responses....137
4.1 Introduction....137
4.1.1 Temperature stress....137
4.1.2 Salinity and drought stress....138
4.1.3 Complexity of abiotic signalling....139
4.1.4 Histidine kinases as sensors for environmental stimuli....140
4.2 Aims....141
4.3 Results....142
4.3.1 Heat stress....142
4.3.2 Cold stress....145
4.3.3 Salinity stress....145
4.3.4 Osmotic stress and specificity of ion toxicity of NaCl....148
4.3.5 Measurement of ion uptake in response to salt stress by ion chromatography ...151
4.3.6 Quantification of ROS production in response to salt stress....154
4.3.7 Effect of salt stress on soil grown mature plants....155
4.3.8 Effect of drought stress on soil grown mature plants....158
4.4 Discussion....161
4.4.1 The *ahk5-1* mutant is not defective in response to low and elevated temperatures 161
4.4.2 AHK5 contributes to salt sensitivity....162
4.4.3 AHK5 contributes to drought stress sensitivity....166
4.5 Conclusions....168

Chapter 5: 170

5 The role of AHK5 in response to bacterial infection 171

5.1 Introduction 171

5.1.1 Different types of plant-bacteria interactions 171

5.1.2 The type-III secretion system and effector proteins 172

5.1.3 Plant hormones in immune signalling 172

5.2 Aims 180

5.3 Results 182

5.3.1 Compatible interaction – *Pst*DC3000 182

5.3.2 Incompatible interaction – *Pst*DC3000(*avrRpm1*) 194

5.3.3 Response to the non-pathogenic *Pst*DC3000(*hrpA*$^-$) mutant 197

5.3.4 Non-host interaction – the bean pathogen *Pph*1448A 200

5.4 Discussion 202

5.4.1 The *ahk5-1* mutant is more susceptible to *Pst*DC3000 after surface inoculation but not after syringe infiltration 202

5.4.2 The *ahk5-1* mutant is altered in hormone responses to *Pst*DC3000 203

5.4.3 A novel metabolite is present in *ahk5-1* leaves but not wild-type Col-0 leaves 205

5.4.4 The *ahk5-1* mutant is more resistant to infection with *Pst*DC3000(*avrRpm1*) but unaltered in response to the avirulent *hrpA*$^-$ mutant and the bean pathogen *Pph*1448A 207

5.5 Conclusions 208

Chapter 6: 211

6 AHK5 function in response to the necrotrophic pathogen *Botrytis cinerea* 212

6.1 Introduction 212

6.1.1 Infection by *B. cinerea* 212

6.1.2 The role of cell death and ROS 213

6.1.3 Camalexin in defence against *B. cinerea* 214

6.2 Aims 215

6.3 Results 216
6.3.1 The *ahk5-1* mutant is more susceptible to infection with *B. cinerea* 216
6.3.2 The *ahk5-1* mutant is not defective in camalexin production 220
6.3.3 The growth of *B. cinerea* on the *ahk5-1* mutant is accelerated 224
6.4 Discussion 227
6.4.1 The *ahk5-1* mutant is more susceptible to infection with *B. cinerea* which is not due to a defect in camalexin production 227
6.4.2 The growth of *B. cinerea* on the *ahk5-1* mutant is accelerated and ROS production in the *ahk5-1* mutant in response to infection is attenuated 229
6.4.3 A role for AHK5 in hormone signalling in response to *B. cinerea*? 232
6.5 Conclusions 233

Chapter 7: 236
7 Function of AHK5 through protein-protein interactions 237
7.1 Introduction 237
7.1.1 Prediction of AHK5 interacting proteins 237
7.1.2 Investigating protein-protein interactions experimentally 240
7.1.3 Tandem Affinity Purification 241
7.2 Aims 243
7.3 Results 245
7.3.1 TAP purification of the TAPa-AHK5 protein 245
7.4 Discussion 253
7.4.1 Proteins identified from TAP purification of P_{35S}-*AHK5/ahk5-3* seedling material 253
7.4.2 Improving recovery of AHK5 interactors 256
7.5 Conclusions 257

Chapter 8: 259

8 Final discussion 260

8.1 The histidine kinase AHK5 negatively regulates salt and drought resistance and contributes towards resistance against *Pst*DC3000 and *B. cinerea* 260

8.2 Does AHK5 modulate hormone responses to multiple stimuli? 260

8.2.1 Abiotic stress 260

8.2.2 Biotic stress 262

8.3 AHK5 as an integrator of multiple stimuli 263

8.4 ROS – the missing link? 266

8.5 AHK5 may participate in responses to multiple stimuli through interaction with different proteins 268

8.6 Conclusions and future work 270

Appendices 275

References 293

List of figures

Figure 1.1 Schematic model showing ABA-mediated stomatal closure.

Figure 1.2 Schematic showing the gene products produced in response to drought stress.

Figure 1.3 Schematic showing the biosynthetic pathway of ABA and the enzymes involved.

Figure 1.4 Schematic showing the SOS pathway activated upon salt stress to maintain cellular ion homeostasis.

Figure 1.5 Schematic showing the transcription factors which activate drought and salinity stress responses.

Figure 1.6 Infection of leaves by *Pst*DC3000.

Figure 1.7 Diagram depicting detection of bacterial flagellin leading to resistance through PTI.

Figure 1.8 Models proposed for the recognition of pathogen derived effector proteins by plant nucleotide leucine rich repeat (NB-LRR) type receptors.

Figure 1.9 Schematic summarising the defences which bacterial pathogens must overcome in order to establish disease.

Figure 1.10 Structure of the *P. syringae* phytotoxin coronatine.

Figure 1.11 Infection life-cycle of *B. cinerea.*

Figure 1.12 Biosynthesis of camalexin from tryptophan involving the action of CYP (cytochrome P450) enzymes.

Figure 1.13 Generation of different types of ROS through energy transfer or sequential addition of electrons.

Figure 1.14 Diagram depicting the different sources of cellular ROS.

Figure 1.15 The ascorbate-glutathione (A-G) cycle in which H_2O_2 is converted to H_2O.

Figure 1.16 Oxidation of cysteine thiol groups by H_2O_2 in proteins.

Figure 1.17 Redox control of Rap2.4a transcriptional activity.

Figure 1.18 Schematic depicting the histidine kinase and hybrid histidine kinase of the single- and multi-step two-component signalling systems (respectively).

Figure 1.19 The EnvZ/OmpR phosphotransfer system of *E. coli*.

Figure 1.20 The high-osmolarity glycerol response (HOG) pathway of yeast.

Figure 1.21 Structures of the eight histidine kinases and the three divergent histidine kinases identified in *A. thaliana*.

Figure 2.1 Gene structure of *AHK5* and the position of T-DNA insertion in the *ahk5-1* (Col-0 background) and *ahk5-3* (Ws-4 background) mutants.

Figure 2.2 Schematic depiction of the arrangement of seeds on square plates used to assess seedling responses to abiotic stress.

Figure 2.3 Watering regime used to treat mature plants with a solution of 250mM NaCl.

Figure 2.4 Photograph showing experimental setup for assessment of symptom development in detached leaves in response to inoculation with *B. cinerea*.

Figure 3.1 Output provided by the Development tool interface of the Genevestigator database.

Figure 3.2 Output provided by the Anatomy tool interface of the Genevestigator database.

Figure 3.3 Detailed view of *AHK5* expression pattern in root tissue shown within the boxes in Figure 3.2

Figure 3.4 SMART Genomes output of the predicted protein structure of AHK5 showing the domains identified.

Figure 3.5 Multiple alignment of *A. thaliana* histidine kinases within the region of the HK domain containing the conserved H, N, G1, F and G2 boxes.

Figure 3.6 Multiple alignment of *A. thaliana* histidine kinases within the region of the receiver domain containing the conserved aspartate residue.

Figure 3.7 Cladogram generated from multiple alignment of the protein sequences of the eight *A. thaliana* histidine kinase in ClustalW.

Figure 3.8 Gene structure of *AHK5* showing the site of T-DNA insertion within the HK domain of *AHK5* giving rise to the *ahk5-1* mutant.

Figure 3.9 Genotyping of Col-0, *ahk5-1* and the complemented P_{35S}*-AHK5/ahk5-1* lines for presence of T-DNA insertion and presence of wild-type *AHK5*.

Figure 3.10 Genotyping of plant lines.

Figure 3.11 Morphological analysis of five week old Col-0 and *ahk5-1* plants.

Figure 3.12 Profile view of soil grown mature wild-type Col-0 and *ahk5-1* mutant plants.

Figure 3.13 Inhibition of root length growth in response to ABA in wild-type and *ahk5-1* seedlings.

Figure 4.1 Seedling root growth in responses to different heat stress regimes

Figure 4.2 Seedling root length in response to cold stress of 10°C for 1, 2 and 3 days

Figure 4.3 Root growth response of wild-type Col-0 and *ahk5-1* seedlings to salt stress

Figure 4.4 Root growth of wild-type Col-0, *ahk5-1* mutant and seedlings of the complemented lines P_{AHK5}*-AHK5/ahk5-1-1* and P_{AHK5}*-AHK5/ahk5-1-4* under salt stress

Figure 4.5 Effect of osmotic stress on seedling root growth

Figure 4.6 Growth of seedlings germinated and grown for seven days on half-strength Murashige and Skoog medium supplemented with KCl

Figure 4.7 Measurement of Na^+ and K^+ content in seedling treated with 100mM NaCl by ion chromatography

Figure 4.8 Measurement of H_2O_2 extracted from seedlings treated with 100mM NaCl in liquid culture for various times using Amplex Red

Figure 4.9 The effect of salt treatment on shoot fresh weigh of mature soil grown plants watered for two weeks with salt solution

Figure 4.10 Shoot fresh weight of mature soil grown plants watered with 250mM NaCl for two weeks

Figure 4.11 Appearance of soil grown plants after 10 days of withholding water to simulate drought stress

Figure 4.12 Effect of drought stress on (a) fresh shoot weight and (b) water content of shoots

Figure 5.1 Figure showing activation of SA signalling triggered by recognition of pathogen effector proteins by the CC-NB-LRR and TIR-NB-LRR classes of R proteins

Figure 5.2 Schematic depicting the role of NPR1 in activation of SA-responsive genes

Figure 5.3 *In planta* bacterial populations in wild-type Col-0 leaves after syringe infiltration with *Pst*DC3000 at various densities

Figure 5.4 Photographs depicting disease symptoms caused by syringe infiltration of Col-0 leaves infiltrated with *Pst*DC3000

Figure 5.5 Response of plants to syringe infiltration with 5×10^5 cfu ml^{-1} of *Pst*DC3000

Figure 5.5 Response of plants to syringe infiltration with 5×10^5 cfu ml^{-1} of *Pst*DC3000

Figure 5.6 Response of wild-type and *ahk5-1* mutant plants to surface inoculation with 4×10^8 cfu ml^{-1} *Pst*DC3000

Figure 5.7 Total chlorophyll extracted from leaves of wild-type, *ahk5-1* mutant and P_{AHK5}*-AHK5/ahk5-1-1*surface inoculated with 4×10^8 cfu ml^{-1} *Pst*DC3000

Figure 5.8. Measurement of *in planta* levels of plant hormones and bacterial phytotoxin in response to surface inoculation of leaves with $4x10^8$ cfu ml^{-1} *Pst*DC3000

Figure 5.9 Pattern of accumulation of unknown compound with a parent ion of 160Da and a daughter ion of 132Da in *ahk5-1* leaf tissue in response surface inoculation

Figure 5.10 Analysis of parent ions of 160Da with a main daughter ion of 132Da (160/132Da) from LC-MS/MS of wild-type and *ahk5-1* mutant leaves surface inoculated with 4 x 10^8 cfu ml^{-1} *Pst*DC3000 at 6dpi

Figure 5.11 Response of wild-type Col-0 and the *ahk5-1* mutant to syringe infiltration with 1 x 10^6 cfu ml^{-1} *Pst*DC3000(*avrRpm1*)

Figure 5.12 ROS production in leaves infiltrated with 5 x 10^6 cfu ml^{-1} *Pst*DC3000 (*avrRpm1*)

Figure 5.13 Response of wild-type and *ahk5-1* mutant plants to infiltration with the non-pathogenic *Pst*DC3000(*hrpA*$^-$) mutant

Figure 5.14 Response of wild-type and *ahk5-1* mutant plants to infiltration with the bean pathogen *Pph*1448A

Figure 6.1 Scoring system used to determine disease progression in leaves inoculated with *B. cinerea*

Figure 6.2 Lesion scores observed in wild-type and *ahk5-1* mutant leaves infected with 2 x 10^5 spores ml^{-1} of *B. cinerea*

Figure 6.3 The appearance and proportion of different lesion types in leaves of wild-type, *ahk5-1*mutant and the complemented P_{35S}*-AHK5/ahk5-1* line inoculated with 2 x 10^5 spores ml^{-1} of *B. cinerea*

Figure 6.4 Average lesion size in wild-type and *ahk5-1* mutant leaves caused by inoculation with 2 x 10^5 spores ml^{-1} of *B. cinerea* at 3dpi

Figure 6.5 Optimisation of camalxin extraction

Figure 6.6. Camalexin production of leaves of wild-type and *ahk5-1* mutant plants in response to (a) inoculation with 2 x 10^5 spore ml^{-1} of *B. cinerea* infection up to 4dpi and (b) spraying with 10mM silver nitrate at 3dpi

Figure 6.7 Wounding before inoculation with *B. cinerea* prevents symptom development

Figure 6.8 ROS production in wild-type and *ahk5-1* mutant leaves associated with the area of inoculation with 2 x 10^5 spore ml^{-1} of *B. cinerea* visualised by DAB staining

Figure 6.9. The increased ROS staining seen in the *ahk5-1* mutant is associated with fungal hyphae

Figure 6.9 ROS associated with fungal hyphae of *B. cinerea* growing on wild-type and *ahk5-1* mutant leaves at 12hpi

Figure 6.10 Growth of *B. cinerea* on wild-type and *ahk5-1* mutant leaves at 8hpi

Figure 6.11 ROS production in wild-type and *ahk5-1*mutant leaves in response to inoculation with 2 x 10^5 spores ml^{-1} of *B. cinerea* 24hpi

Figure 7.1 Predicted interactors of AHK5 (referred to in the diagram as CKI2) generated by the Predicted Arabidopsis Interactome Resource (PAIR) database

Figure 7.2 Structure of the C-terminal TAPa tag used in this study

Figure 7.3 Schematic summarising the TAPa purification protocol as described in the text

Figure 7.4 Proteins obtained from TAP purification

Figure 7.5 Western blot of proteins extracted from 18 day old P_{35S}*-AHK5/ahk5-3* seedlings separated into soluble and insoluble fractions

Figure 7.6 SDS-PAGE of proteins obtained from TAP purification of total protein extracts from 15g of 18 day old P_{35S}*-AHK5/ahk5-3* seedling material with modifications

Figure 8.1 Schematic showing the hypothesised opposing functions of AHK5 in tolerance to abiotic stress and resistance towards pathogen infection

List of tables

Table 1.1 Summary of transcription factors which act in drought stress and the consensus sequences of the *cis*-elements recognised by these transcription factors.

Table 1.2 Summary of the functions and targets of a selection of *Pst*DC3000 effector proteins.

Table 1.3 Interaction matrix summarising known interactions between HKs and AHPs of *A. thaliana.*

Table 2.1 Strains of *Pseudomonas* used in this study and antibiotic concentrations used to culture these strains.

Table 2.2 Conditions under which plant hormones and coronatine were measured by LC-MS/MS.

Table 3.1 Summary of *cis*-acting elements identified by the PLACE database upstream of *AHK5.*

Table 3.2 Expected product size from different primer pairs used to genotype plant lines used in this study.

Table 4.1 Germination of wild-type Col-0 and *ahk5-1* seeds on various concentrations of NaCl

Table 4.2 Germination of wild-type Col-0 and *ahk5-1* seeds in the presence of sorbitol

Table 4.3 Germination of wild-type and *ahk5-1* seeds in the presence of KCl

Table 4.4 Mean water content of shoots of wild-type and *ahk5-1* mutant plants watered with 250mM NaCl for two weeks

Table 7.1 Identification of proteins obtained from TAP purification of proteins extracted from 18 day old P_{35S}*-AHK5/ahk5-3* seedlings analyses by LC-MS/MS and matched using the MASCOT algorithm

Table 7.2 Identification of proteins obtained from TAP purification of proteins extracted from 18 day old *P_{35S}-AHK5/ahk5-3* seedlings analysed by LC-MS/MS and matched using the MASCOT algorithm

List of abbreviations

$^1O_2$	Singlet oxygen
2CPA	2-Cys peroxiredoxin
AAO	Abscisic acid oxidase
ABA	Abscisic acid
ABC	ATP-binding cassette
ABI1	ABA insensitive 1
ABI2	ABA insensitive 2
ABRE	ABA-responsive *cis*-acting element
ACC	Aminocyclopropyl
acd	*accelerated cell death*
A-G cycle	Ascorbate-glutathione cycle
AHP	*Arabidopsis* histidine-containing phosphotransfer protein
Ala	Alanine
APX	Ascorbate peroxidase
AR	Amplex red
ARR	Arabidopsis response regulator
as-1	Activating sequence 1
ASC	Ascorbate
BAK1	BRI-associated receptor kinase 1
BOS1	*Botrytis* susceptible 1
bre1	*botrytis resistant 1*
BRI1	Brassinosteroid insensitive 1
bZIP	Basic leucine zipper
Ca^{2+}	Calcium

CAT	Catalase
CBF	CRT-binding factor
CC-NB-LRR	Coiled-coil nucleotide-binding leucine rich repeat
CFA	Coronafacic acid
CKI1	Cytokinin independent 1
CMA	Coronamic acid
CO_2	Carbon dioxide
COI1	Coronatine insensitive 1
COR	Coronatine
COR6.6/KIN2	Cold regulated 6.6/inducible 2
CPR1	Constitutive expressor of PR gene 1
CRT	C-repeat *cis*-acting element
CYP	Cytochrome P450
Cys	Cysteine
DAB	3, 3'-diaminobenzidine
DAMP	Damage associated molecular pattern
DHA	Dehydroascorbate
DHAR	Dehydroascorbate reductase
DNA	Deoxyribonucleic acid
dnd1	*defence, no death 1*
DPI	Diphenyleneiodonium
dpi	Days post inoculation
dpt	Days post treeatment
DRE	Dehydration responsive *cis*-acting element
DREB	DRE-binding

EDS1	Enhanced disease susceptibility 1
EFR	EF-Tu receptor
EF-Tu	Elongation factor Tu
Elf26	EF-Tu peptide 26
EPI	Enhanced product ion
ETI	Effector triggered immunity
ETR1	Ethylene response 1
FLS2	Flagellin sensing 2
GA	Gibberellin
GPI	Glycosylphosphatidyl-inositol
GPX	Glutathione peroxidase
GR	Glutathione reductase
GSH	Glutathione (reduced)
GSSH	Glutathione (oxidised)
H_2O	Water
H_2O_2	Hydrogen peroxide
HAB1	Hypersensitive to ABA 1
His	Histidine
HK	Histidine kinase
HOG	High-osmolarity glycerol response
HPLC	High-pressure/performance liquid chromatogrphy
HPt	Histidine-containing phosphotransfer domain
hpt	Hours post treatment
HR	Hypersensitive response
HSP	Heat shock protein

IAOx	Indole-3-acetaldoxime
IgG-BD	Protein A IgG binding domain
INA	2, 6-dichloroisonicotinic acid
JA	Jasmonic acid
JAZ	Jasmonate ZIM domain
K^+	Potassium
lacs2	*long-chain acyl-CoA synthetase 2*
LC/MS-MS	Liquid chromatography tandem mass spectrometry
LEA	Late embryogenesis abundant
LRR-RLK	Leucine-rich repeat receptor-like kinase
lsd1	*lesion stimulating disease 1*
LsyM	Lysin motif
MAMP	Microbe associated molecular pattern (sometimes used interchangeably with PAMP)
MAPK	Mitogen-activated protein kinase
MeJA	Methyl jasmonate
$MgCl_2$	Magnesium chloride
MoCo	Molybdenum cofactor
MPK6	Mitogen activated kinase 6
MRM	Multiple reaction monitoring
MS	Murashige and Skoog medium
Na^+	Sodium
NaCl	Sodium chloride
NB-LRR	Nucleotide-binding leucine rich repeat
NCED	9-*cis*-epoxycarotenoid dioxygenase

NDPK2	Nucleoside diphosphate kinase 2
NDR1	Non race-specific disease resistance 1
NO	Nitric oxide
NOS	Nitric oxide synthase
NSCC	Non-selective cation channels
O_2	Oxygen
$O_2^{\cdot -}$	Superoxide
OG	Oligogalacturonide
$OH^{\cdot}$	Hydroxyl radical
OST1	Open stomata 1
P5CS	Δ^1-pyrroline-5-carboxylate synthase
PA	Phosphatidic acid
PAD3	Phytoalecin deficient 3/CYP71B15
PAD4	Phytoalexin deficient 4
PAIR	Predicted Arabidopsis Interactome Resource
PAMP	Pathogen associated molecular pattern (sometimes used interchangeably with MAMP)
PDB	Potato dextrose broth
PG	Endopolygalacturonase
PLD	Phospholipase D
PP2C	Protein phosphatase 2C
PR	Pathogenesis-related
***Pst*DC3000**	*Pseudomonas syringae* pv. *tomato* DC3000
PTI	PAMP triggered immunity

PYL	Pyrabactin resistance 1-like
PYR	Pyrabactin resistance
RBOH	Respiratory burst homolog
RCAR	Regulator component of ABA receptor
RCD	Runaway cell death
RCD1	Radical-induced cell death 1
***R*-gene**	*Resistance* gene
RIN4	RPM1-interacting protein 4
RNS	Reactive nitrogen species
ROS	Reactive oxygen species
R-protein	Resistance protein
RR	Response regulator
SA	Salicylic acid
SAG101	Senescence associated gene 101
SAMT	*S*-adenosyl-L-Met: salicylic acid carboxyl methyl transferase
SBFI	Sodium-binding bezofuran isophthalate
SCF^{COI1}	Skp/Cullin/F-box-COI1 complex
SDW	Sterile distilled water
SID2	SA induction-deficient 2
SOD	Superoxide dismutase
SOS	Salt overly sensitive
STZ	Salt tolerance zinc finger
TAP	Tandem affinity purification
TAPa-tag	Alternative tandem affinity purification tag
TCS	Two-component system

TIR-NB-LRR	Toll interleukin nucleotide-binding leucine rich repeat
TRX	Thioredoxins
TTSS	Type-three secretion system
Tyr	Tyrosine
Val	Valine
VIGs	Virus-induced gene silencing
XIC	Extracted ion current
XOD	Xanthine oxidase
ZEP	Zeathantin oxidase
ψ_w	Water potential

Chapter 1:

Introduction

1 Introduction

On a daily basis, plants face changes in environmental conditions, such as alterations in humidity, light intensity and temperature (abiotic factors), and are also challenged by many different organisms, such as insects, herbivores and bacterial and fungal pathogens (biotic factors). The ability of plants to recognise external stimuli and stresses and to adapt accordingly is paramount to plant survival. Since plants are not able to avoid unfavourable conditions due to their sessile nature, they have developed numerous sensing and signalling pathways to coordinate the physiological adaptation of the plant to environmental stimuli and stresses.

Stimuli can be defined as any factor which the plant can detect and which induces a response. Thus, the term stimulus also encompasses stress, but what is the definition of stress? In simple terms, stress can be described as the result of unfavourable conditions which adversely affect plant productivity and/or which causes physiological changes which result in injury (Hopkins, 1999; Nilsen and Orcutt, 2000). However, the concept of stress in plants is not completely clear cut as the definition depends on the context in which it is being considered. In the short term, a particular 'stress' may induce physiological changes which lead to a reduction in productivity but these changes may, in the long term, be of benefit to the plant.

For example, the leaf surface contains pores called stomata which allow gaseous exchange between the leaf interior and exterior required for uptake of carbon dioxide (CO_2), which is reduced to plant sugars using water and energy derived from sunlight by the process of photosynthesis (Hopkins, 1999). Opening and closing of stomata are controlled through changes in turgidity of the two guard cells surrounding the pore (Schroeder et al., 2001). Stomata also provide a route through which water is lost from the plant through transpiration. Under drought stress, stomata close to prevent water loss, which ultimately leads to decreased productivity due to inhibition of photosynthesis (Chaves et al., 2009). However, in the long term, these changes may be of benefit to the plant as it prevents complete desiccation, which reduces the amount of permanent tissue damage, thus increasing the survival rate of the plant on return to more favourable conditions (Nilsen and Orcutt, 2000).

When referring to environmental factors as stressors, it is also difficult to determine the point at which these factors become stressors as these factors are continuous, rather than discrete, variables. The difficulty in defining this point can be illustrated with light intensity. Although

light is required for photosynthesis, high light intensity has detrimental effects on the plant and actually inhibits photosynthesis (Long and Humphries, 1994) – at what point does light go from being 'favourable' to 'unfavourable'? This is difficult to determine given that many fluctuations in environmental conditions, such as temperature and light intensity, occur on a daily basis without detrimental effect to the plant. Thus 'favourable' conditions can become 'unfavourable' depending on the duration for which the plant is exposed. Perhaps a more useful definition is the capability of certain conditions to cause injury or disease to the plant as different plants have different tolerance levels (Gaspar et al., 2002).

Even when considering infection of plants by pathogens where disease is obviously detrimental to the plant, there are examples where there is a benefit, such as the systemic acquired resistance (SAR) triggered by incompatible pathogens resulting in systemic resistance to subsequent infection with other pathogens (Sticher et al., 1997; Durrant and Dong, 2004).

Although the goal of this study is not to define precisely what constitutes 'stress' and 'unfavourable' conditions, it is worth noting that a universal definition accepted by all is still lacking. This aside, we can use a working definition of stress whereby plant productivity/ growth is negatively impacted on for the duration of the stress and shortly after when compared to plants grown under 'ideal' conditions, which is more easily assessed under controlled laboratory conditions as used in this study.

There are three strategies which plants utilise to deal with stress:

1. Stress avoidance: avoiding exposure to stressful conditions
2. Stress tolerance: being able to tolerate stressful conditions
3. Acclimation: adaptation of physiology to stressful conditions

Avoidance of stress can be seen as the first line of defence against exposure to unfavourable conditions, examples of which are the closure of stomata in response to drought stress to prevent water loss (dehydration stress) as mentioned earlier and shade avoidance (Taiz and Zeiger, 1998). However in some cases, avoidance is not possible or is only a temporary measure and the plant therefore has to tolerate or acclimatise to such conditions. This may be the case where unfavourable conditions persist for long durations of time. In the case of tolerance, the plant is able to function under suboptimal conditions, 'tolerating' the effects of stress. An example can again be provided by the example of drought stress. Where water is

limiting for long periods, stomatal closure cannot compensate for the deficit in water and the plant, as a tolerance mechanism, may produce (for example) compatible solutes to adjust the osmotic status of the cell to prevent water loss (Verslues et al., 2006). In the case of acclimation, the plant is able to adjust its metabolism and physiology to withstand stress where the stressor is introduced gradually. A well known example it that seen in the phenomenon of acquired heat stress in which plants pre-exposed to a mild heat stress are resistant to subsequent higher temperatures which, in the absence of pre-treatment with the milder heat stress, would cause tissue damage and death (Larkindale et al., 2005). It is apparent that key to stress response is the ability to perceive stress.

1.1 Perception of stress - how do plants perceive stimuli?

In order to respond to a stimulus, the plant must first be able to detect/sense the stimulus and to differentiate between different stimuli in order to respond accordingly. It is clear from the numerous studies thus far that plants are able to recognise and differentiate between different stresses and stimuli and to react in terms of gene expression and physiological adaptation that is specific to the situation. In many cases however, what the plant perceives and how this perception is mediated is not clearly understood. In some cases, the plant may sense stimuli through changes in cellular physiology caused as a result of the stimuli rather than the stimuli itself, such as increased and decreased membrane fluidity caused by elevated and depressed temperatures, respectively (Sangwan et al., 2002). In other cases, the plant may detect the source of the stimuli, such as the perception of constituents of bacterial and fungal cells mediated through plant cell receptors (Jones and Dangl, 2006; Miya et al., 2007).

In the following sections, the physiological basis of abiotic and biotic stresses, how they are perceived by plants and the signalling pathways activated on perception will be introduced. The role of reactive oxygen species (ROS) as signalling molecules and the function of plant histidine kinases in response to endogenous and exogenous stimuli will be discussed. To conclude this chapter, the aims of this study will be presented.

1.2 Abiotic stress – drought and salinity stress

In nature, plants are exposed to a number of environmental factors that influence and impact on plant growth and development. Environmental stresses in various parts of the world have resulted in loss of crops, therefore impacting on food security and economic output of arable

land. In addition, climate change is predicted to have negative effects on future productivity, creating new challenges (Huang et al., 2002; Mittler, 2006; Lobell et al., 2008).

In addition to climate change, intensive agricultural practices have also had negative impacts on world crop production; for example, irrigation of land has led to increased soil salinity caused by raising water tables and continuous growth of single plant species (known as 'monocropping') resulting in depletion of soil nutrients and encouragement of the proliferation of plant pests (Huang et al., 2002).

A common response to abiotic stress is the retardation of plant growth and diversion of plant resources towards plant survival, leading to decreased crop productivity and increasing the time between planting to harvest (Munns, 2002; Skirycz and Inzé, 2010). A better understanding of the mechanisms that control plant responses to environmental stress will aid in the development of crops which are able to survive under normally sub-optimal conditions. Here, the discussion will focus on the effects of drought and salinity stress.

1.2.1 *Drought stress*

Drought stress occurs when there is low water availability and reduction in water uptake also limits nutrient acquisition, photosynthesis and plant growth (Taiz and Zeiger, 1998; Chaves et al., 2009; Skirycz and Inzé, 2010). Water loss from the plant surface is prevented to a certain extent through leaf hairs/trichomes which act to maintain humidity close to the leaf surface and a waxy cuticle which prevents evaporation of water through the leaf surface (Taiz and Zeiger, 1998). However, the majority of water loss from the plant is through the stomata and as such, stomatal closure is triggered in the event of drought stress (Schroeder et al., 2001; Yang et al., 2010). This stomatal closure is mediated by the plant hormone abscisic acid (ABA) and has been well studied (Blatt, 2000; Schroeder et al., 2001).

Stomatal closure is regulated by the turgidity of the guard cells surrounding the stomatal pore, with loss of guard cell turgor resulting in stomatal closure. Upon perception of ABA, calcium ions (Ca^{2+}) are released from intracellular stores resulting in increased cytosolic calcium concentration ($[Ca^{2+}]_{cyt}$), triggering the efflux of anions from the guard cells through slow-activating sustained (S-type) and rapid transient (R-type) anion channels. Efflux of anions results in membrane depolarisation, which inhibits potassium ion (K^+) uptake through inward rectifying channels (K^+_{in}) whilst promoting efflux of K^+ through outward rectifying K^+ channels (K^+_{out}). An increase in cytosolic pH also enhances K^+_{out} activity. The efflux of

both anions and K^+ also leads to the efflux of water from the guard cells and loss of turgor resulting in stomatal closure (Figure 1.1) (Schroeder et al., 2001; Kwak et al., 2008).

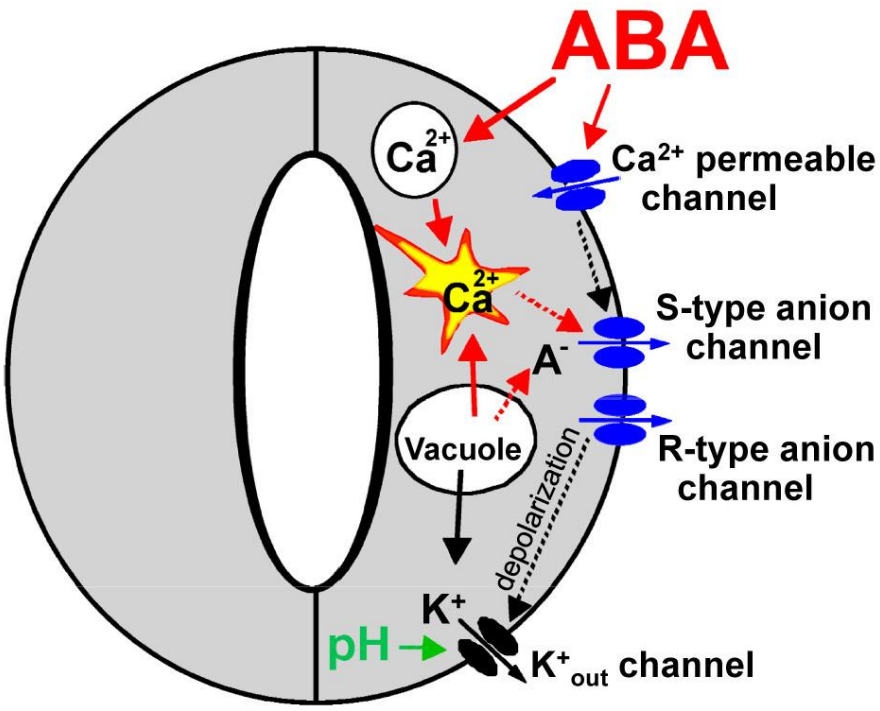


Figure 1.1 Schematic model showing ABA-mediated stomatal closure. See text for details. Figure taken from Kwak et al. (2008).

In addition to stomatal closure, other cellular changes also occur in response to drought stress. Proteins which are involved in drought stress responses can be divided into two classes of proteins: those that function in protection against drought stress (functional proteins) and those which regulate drought stress responses (regulatory proteins) (Shinozaki and Yamaguchi-Shinozaki, 2007) (Figure 1.2).

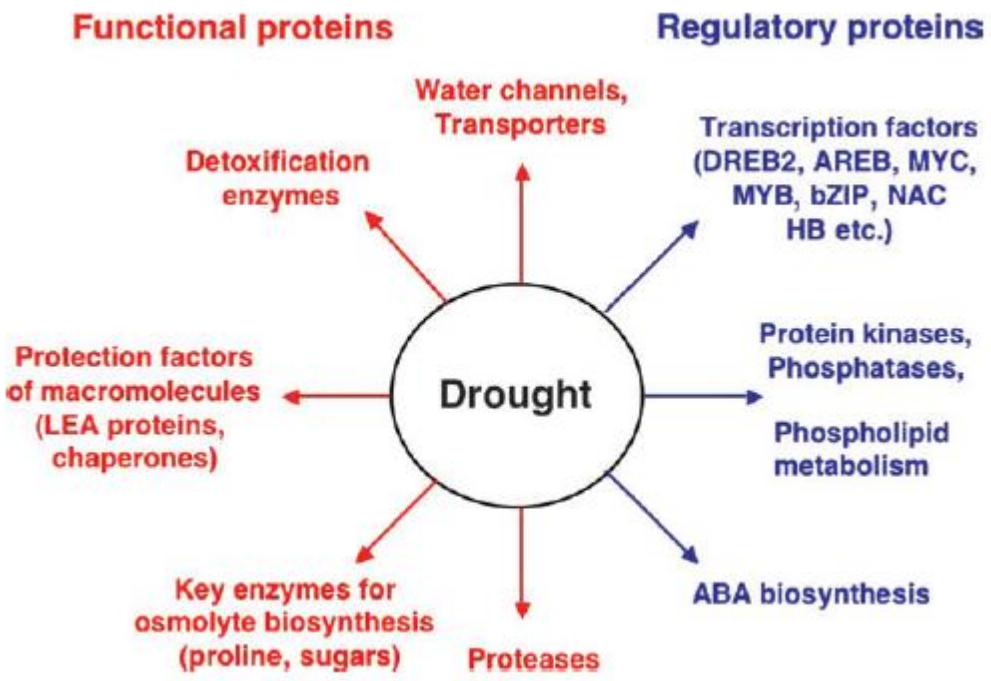


Figure 1.2 Schematic showing the gene products produced in response to drought stress. These can be divided into two classes of proteins: functional proteins and regulatory proteins. Figure taken from Shinozaki and Yamaguchi-Shinozaki (2007).

The functions of some of the proteins shown in Figure 1.2 in drought tolerance are discussed in the following sections.

1.2.1.1 Functional proteins in drought stress

To counteract the effects of drought stress, plant cells synthesise a number of proteins which function to restore cellular homeostasis and to minimise cellular damage and can be classed as functional proteins.

The primary stress caused by drought is osmotic stress due to the lack of water available (Verslues et al., 2006). One mechanism by which plants can avoid water stress at the cellular level is to increase the synthesis of compatible solutes/osmolytes, such as the amino acid proline, which acts to raise the osmotic potential and thus water content of the cell (Verslues et al., 2006). Biosynthesis of proline has been shown to occur in response to drought stress; in *A. thaliana*, the enzyme Δ^1-pyrroline-5-carboxylate synthase (AtP5CS) is a key enzyme in the biosynthesis of proline, expression of which is known to increase in response to ABA and drought stress and precedes increases in proline levels (Yoshiba et al., 1995). As transcript levels of *AtP5CS* decreases on rehydration of drought stress plants, followed by a decrease in

proline levels *in planta*, this suggests that AtPCS5 functions in response to water deficit (Yoshiba et al., 1995). Given the link between drought stress and ABA, *AtPCS5* may be up-regulated by an ABA-dependent pathway (Yoshiba et al., 1995). Petunia plants over-expressing *PCS5* from rice (*OsP5CS*) or *A. thalinana AtPCS5* showed constitutively higher levels of proline and increased survival under drought stress, indicating proline positively contributes to drought resistance (Yamada et al., 2005). In transgenic tobacco plants constitutively expressing the *PCS5* gene of *Vigna aconitifolia*, proline production was over 10-fold that in wild-type plants and correlated with a delay in wilting and smaller decreases in the water potential (ψ_w) of leaves under drought stress compared to wild-type plants (Kishor et al., 1995). Thus proline acts to protect against drought stress by increasing the ψ_w within leaves to prevent cellular dehydration. Other osmolytes produced in response to drought stress include mannitol, trehalose, raffinose, galactionol and fructan (Valliyodan and Nguyen, 2006).

Also noted to increase on drought stress are the late embroyogenesis abundant (LEA) proteins which may act as chaperones to stabilise membranes and protein structure (Wang et al., 2003). Evidence for the role of LEAs in membrane protection under dessication was obtained by Tolleter et al. (2007) in a study investigating the function of the mitochondrial pea (*Pisum sativun*) LEA protein, LEAM which is expressed in the seed during dessication. Using a liposome drying assay in which liposomes were used to mimic the mitochondrial membrane, Tolletter et al. (2007) found that addition of LEAM before dessication prevented fusions of the liposomes (indicative of membrane rearrangements) on rehydration; whereas dessication and rehydration of liposomes in the absence of LEAM shifted average liposome diameter size to greater than 8000nm from an original average diameter of 150nm, addition of LEAM before dessication resulted in retention of a large proportion of liposome of the original size on rehydration. This result suggests that LEAM may interact with the mitochondrial membrane to prevent membrane damage during seed dessication (Tolleter et al., 2007). Although LEAs are known to accumulate in many plants in response to drought stress, direct evidence for their function in drought stress tolerance is scarce. In a recent report by Olvera-Carrillo et al. (2010) however, evidence suggesting the group 4 LEA proteins positively contribute to drought stress tolerance in *Arabidopsis* was presented. It was shown that whereas over-expression of *AtLEA4-5* resulted in higher relative water content and dry weight and increased survival and bud formation after recovery from drought stress, loss of function of AtLEA4-5 or AtLEA4-1 and AtLEA4-2 had the opposite effect.

In addition to cellular dehydration, drought stress also causes oxidative stress through the production of reactive oxygen species (ROS) which accumulate due to perturbation of normal metabolic processes, leading to oxidative damage (Apel and Hirt, 2004; Halliwell, 2006). Accumulation of ROS to toxic levels results in damage to cellular membranes through lipid peroxidation, irreversible oxidation of proteins leading to denaturation and loss of function and oxidation of other biomolecules such as DNA (Moller et al., 2007). In order to limit oxidative damage to cells, plants up-regulate components of the antioxidant system in order to remove excess ROS (Wang et al., 2003). These include enzymes involved catalysing the removal of ROS, such as superoxide dismutase (SOD), ascorbate peroxidase (APX) and glutathione reductase (GR), and also molecules which act as ROS scavengers, such as ascorbate (ASC) and glutathione (GSH) (Apel and Hirt, 2004). The chemistry of ROS, their roles in cellular signalling and ROS detoxification are discussed in more detail in Section 1.6.

1.2.1.2 Regulatory proteins in drought stress

Upstream of the functional proteins are those which regulate their production, such as transcription factors which up-regulate the expression of genes encoding for drought functional proteins and proteins involved in stress signalling.

As discussed earlier, ABA plays an important role in drought stress tolerance by initiating stomatal closure to prevent water loss through transpiration. Drought stress is known to up-regulate the ABA biosynthetic genes zeaxanthin epoxidase (*ZEP/ABA1*), 9-*cis*-epoxycarotenoid dioxygenase (*NCED*), abscisic acid oxidase 3 (*AAO3*) and *LOS5/ABA3* (Zhu, 2002; Tuteja, 2007; Nambara et al., 2010). Conversion of zeaxanthin to violaxanthin is catalysed by zeathanthin epoxdase (ZEP/ABA1) which, with neoxanthin, is then cleaved by the action of NCED into xanthoxin (Duckham et al., 1991; Nambara and Marion-Poll, 2005). Conversion of xanthoxin to ABA is then catalysed in two sequential steps by the short chain alcohol dehydrogenase ABA2 and by abscisic acid oxidase (AAO) (Schwartz et al., 1997; Nambara and Marion-Poll, 2005). The action of AAO requires a molybdenum cofactor (MoCo) which is produced by the molybdenum cofactor sulfurylase LOS5/ABA3 (Schwartz et al., 1997; Zhu, 2002). The ABA biosynthetic pathway and the stage at which each of the ABA biosynthetic enzymes act is shown Figure 1.3.

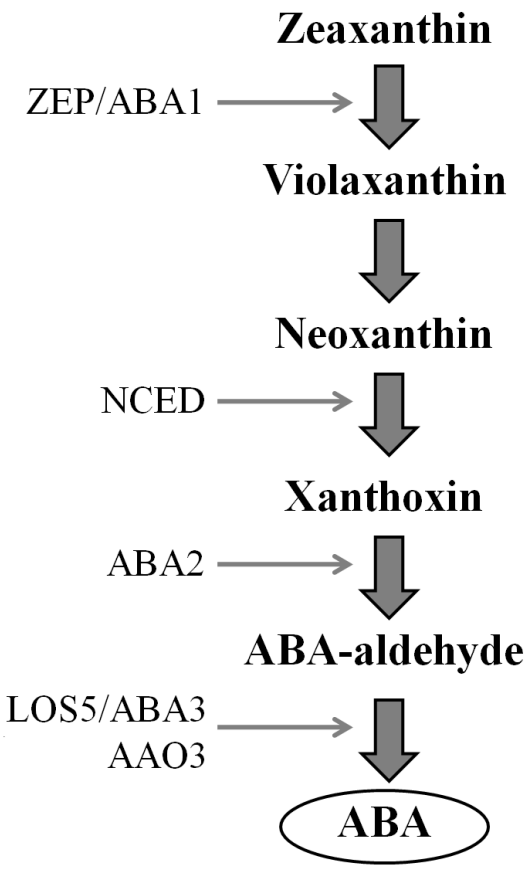


Figure 1.3 Schematic showing the biosynthetic pathway of ABA and the enzymes involved. ZEP/ABA1 = zeaxanthin epoxidse, NCED = 9-*cis*-epoxycarotenoid dioxygenase, AAO3 = abscisic acid oxidase 3. See text for details. Figure modified from Zhu et al. (2002) and Nambara et al. (2005).

The importance of ABA in drought stress tolerance is evident from the increased sensitivity and 'wilty' phenotypes of ABA-biosynthetic mutants. For example, the *aba1, aba2, aba3* and *aao3* mutants show reduced levels of ABA and increased water loss through transpiration (Leon-Kloosterziel et al., 1996; Seo et al., 2000). The ABA-signalling pathway leading to stomatal closure is regulated by the SnRK2 protein kinase OST1 (open stomata 1)/SnRK2.6 (Mustilli et al., 2002). Under conditions in which water is not a limiting factor, the ABA-signalling pathway is negatively regulated by the protein phosphatase 2C (PP2C) proteins HAB1 (hypersensitive to ABA 1), ABI1 (ABA insensitive 1) and ABI2 (ABA insensitive 2) which dephosphorylates and deactivate OST1, resulting in open stomata; under drought stress which triggers increased ABA biosynthesis, deactivation of OST1 is prevented, leading to closure of stomata (Vlad et al., 2009). Evidence suggests that the inhibition of PP2C phosphatase activity under drought stress is mediated by interaction of the ABA sensors PYR (pyrabactin resistance)/PYL (pyrabactin resistance 1-like)/RCAR (regulator component of

ABA receptor) family proteins with the PPC2 phosphatases (Cutler et al., 2010). Phosphorylated OST1 is then able to interact with, modify and stabilise, through its kinase activity, downstream transcription factors of the bZIP family which control expression of ABA-responsive genes (Sirichandra et al., 2009; Cutler et al., 2010).

The majority of genes encoding for drought functional proteins that are under the control of ABA contain ABA-responsive *cis*-acting elements (ABRE) in the promoter region (Mundy et al., 1990; Zhu, 2002; Wang et al., 2003). Genes containing ABREs are regulated by transcription factors of the basic leucine zipper (bZIP) family and transcription factors belonging to the MYB/MYC family (Urao et al., 1996; Abe et al., 1997; Zhu, 2002; Wang et al., 2003).

Other than ABREs, some drought responsive genes contain dehydration-responsive (DRE) or C-repeat (CRT) *cis*-acting elements which are recognised by dehydration responsive (DREB) and C-repeat binding factors (CBF) and these genes can also be up-regulated in an ABA-dependent manner (Yamaguchi-Shinozaki and Shinozaki, 1994; Wang et al., 2003).

In addition to the ABA-dependent pathway, ABA-independent pathways leading to regulation of drought responsive genes also exists and are regulated by the NAC and ZF-HDR transcription factors, although some regulation by the ABA pathway may occur (Tran et al., 2004; Tran et al., 2006). One member of the DREB class of transcription factors, DREB2A, appears to be induced by drought stress independent of ABA (Liu et al., 1998) and thus forms part of the ABA-independent pathway.

A summary of the transcription factors which act in response to ABA and drought stress and the corresponding *cis*-elements which they recognise are shown in Table 1.1.

Table 1.1 Summary of transcription factors which act in drought stress. Consensus sequences of the *cis*-elements recognised by these transcription factors are also shown. Py = pyrimidine, N = A/T/C/G.

Transcription factor class	*cis*-element	Consensus sequence	Reference
DREB/CBF	DRE/CRT	A/GCCGAC	(Yamaguchi-Shinozaki and Shinozaki, 1994)
AREB	ABRE	PyACGTGGC	(Mundy et al., 1990)
MYC	MYCRS	CANNTG	(Abe et al., 1997)
MYB	MYBRS	C/TAACNA/G	(Urao et al., 1996)
NAC	NACRS	CACGCATGT	(Tran et al., 2004)
ZFHD	ZFHDR	CACTAAATTCTCAC	(Tran et al., 2006)

In summary, stomatal closure in response to drought stress is mediated by ABA and the importance of this response is seen in the ABA biosynthetic mutants which are hypersensitive to drought stress and low humidity (Leon-Kloosterziel et al., 1996; Seo et al., 2000; Xiong et al., 2001). In addition to stomatal closure, proteins which function in protection against water stress, such as osmolytes and LEAs, are produced on the cellular level (Zhu, 2002; Wang et al., 2003). Regulation of genes encoding for drought functional and regulatory proteins are under the control of transcription factors which recognise conserved *cis*-elements in the promoter regions of stress responsive genes (Zhu, 2002; Wang et al., 2003).

1.2.2 *Salinity stress*

In the environment, high soil salinity is common in dry areas where the low water content of the soil in effect acts to concentrate the salts present (Navarro-Pedreño et al., 2007). Salinisation of land is also caused by agricultural practices such as irrigation leading to rising water tables bringing salts from ground water to the upper layers of the soil where they accumulate due to improper drainage/leaching or through evaporation of water from the soil (Qadir et al., 2000; Lynch and St.Clair, 2004). High soil salinity essentially reduces the water available to the plant, resulting in osmotic stress (Munns, 2002; Munns and Tester, 2008).

However, in addition to osmotic stress, salt also caused ion toxicity and it is this latter component that causes the most damage to plants in the long term (Munns, 2002; Munns and Tester, 2008). Excessive uptake of sodium ions (Na^+) which interferes with nutrient uptake, is toxic to cellular enzymes and causes further cellular dehydration if deposited in the plant cell wall (Munns, 2002; Zhu, 2003). Salinity stress results in loss of photosynthetic capacity through premature senescence of older leaves and reduction in plant growth (Munns, 2002; Munns and Tester, 2008).

1.2.2.1 Regulation of Na^+ in plants

Na^+ can enter into the cell by the Na^+ transporter HKT1 and through non-selective cation channels (NSCC) and under conditions of high salinity results in the excess entry of Na^+ into the cell (Kronzucker and Britto, 2011). In response this, the Salt Overly Sensitive (SOS) signalling pathway is activated in order to control Na^+ uptake and extrusion and mutants of this pathway show increased uptake of Na^+ coupled with reduced absorption of K^+ (Wu et al., 1996; Shi et al., 2000; Zhu et al., 2007).

In the SOS pathway, salt tolerance is mediated by the plasma membrane Na^+/H^+ antiporter SOS1 which mediates extrusion of Na^+ from plant cells (Shi et al., 2000). Expression and activation of SOS1 through phosphorylation is mediated by the myristolated calcium sensor SOS3 and the serine/threonine protein kinase SOS2 (Ishitani et al., 2000; Liu et al., 2000; Zhu et al., 2007). Increased [Ca^{2+}_{cyt}] as a result of increased intracellular Na^+ levels is detected by SOS3 through binding of Ca^{2+} with the EF-hand motifs of SOS3 which then interacts with and activates the kinase activity of SOS2 (Ishitani et al., 2000) (Figure 1.4). In addition to the SOS pathway, Na^+ can also be sequestered in the vacuole by the action of the Na^+/H^+ antiporter NHX to remove Na^+ from the cytosol (Shi and Zhu, 2002; Yokoi et al., 2002).

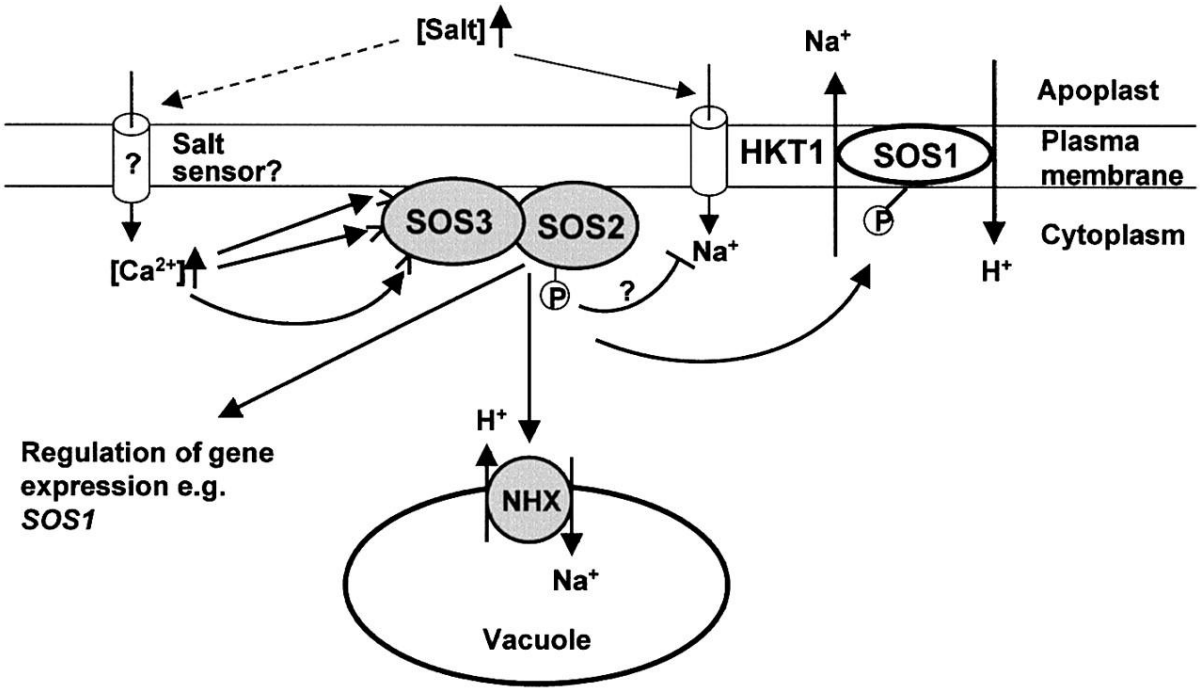


Figure 1.4 Schematic showing the SOS pathway activated upon salt stress to maintain cellular ion homeostasis. Under high salt stress, excessive Na^+ enters the cell through the plasma membrane-located Na^+ transporter HKT1 and non-selective cation channels (NSCCs) (not shown). Sensing of elevated Na^+ levels results in increased $[(Ca^{2+})_{cyt}]$ which is detected through binding of Ca^{2+} to SOS3. On binding of Ca^{2+} with SOS3, SOS3 interacts with and activates the serine/threonine protein kinase SOS2 which in turn activates *SOS1* expression and function. In addition to SOS1, the vacuolar H^+/Na^+ antiporter is also activated and acts to compartmentalise Na^+ in the vacuole. Figure taken from Chinnusamy et al. (2004).

Salinity stress also results in oxidative stress in plants and links between the SOS pathway and ROS signalling have been found. SOS1 was found to interact with the oxidative stress regulator RCD1 (radical-induced cell death 1) and SOS2 with the catalases CAT2 and CAT3, and with NDPK2 (nucleoside diphosphate kinase 2) which acts in ROS signalling (Katiyar-Agarwal et al., 2006; Verslues et al., 2007). In addition, the *SOS1* transcript is stabilised in response to both salt stress and the ROS hydrogen peroxide (H_2O_2); since salt stress is known to cause oxidative stress, ROS may act as an indirect indicator of high salinity to enhance SOS1 activity through stabilisation of its transcript (Shi et al., 2003; Chung et al., 2008).

In addition to ROS signalling, the SOS pathway is also linked to the mitogen-activated protein kinase MPK6 which was found to phosphorylate SOS1 under conditions of high salinity and required the presence of phosphatidic acid (PA) produced through the action of phospholipase Dα (PLDα) (Yu et al., 2010). Furthermore, interaction of SOS2 with the

negative regulator of ABA signalling ABI2 has also been reported (Ohta et al., 2003). These observations suggest complex regulation of the SOS pathways mediating tolerance to salinity.

In a screen for SOS regulated genes, Gong et al. (2001) found that SOS3 is involved in the negative regulation of known salt-responsive genes, namely *SAMT* (*S*-adenosyl-L-Met: salicylic acid carboxyl methyltransferase), *COR6.6/KIN2* (cold regulated 6.6/inducible 2) and *STZ* (salt tolerance zinc finger). Although *COR6.6/KIN2* and *SAMT* expression are known to be induced on salt stress, their primary functions are not in salt tolerance and as such, Gong et al. (2001) suggests that the SOS pathway may act to suppress expression of genes not specifically related to salt tolerance.

The importance of the SOS pathway in mediating salt tolerance is evident in the increased sensitivity to high salinity of plants mutated in components of this pathway. This increased sensitivity to salinity manifests phenotypically as reduction in root growth, shoot fresh weight, survival rate and germination rate (Wu et al., 1996; Shi et al., 2000; Katiyar-Agarwal et al., 2006; Batelli et al., 2007; Verslues et al., 2007; Zhu et al., 2007). On the cellular level, loss of SOS1 function results in greater increase in Na^+ accumulation at the root tip, disruption of cellular pH homeostasis and deformation of the vacuole on salt stress (Oh et al., 2010). Analysis of four *A. thaliana* ecotypes (Col-0, Ler, Ws and C24) which naturally vary in their tolerances towards salinity stress revealed a negative correlation between *SOS1* expression and total Na^+ tissue content (Jha et al., 2010). Conversely, over-expression of either *SOS1* or *SOS3* resulted in increased survival and root growth together with decreased chlorophyll loss and Na^+ uptake (Shi et al., 2003; Yang et al., 2009).

The NHX Na^+/H^+ antiporter which acts to remove Na^+ from the cytoplasm and sequester this ion within the vacuole also contributes to salt tolerance. In *A. thaliana*, expression levels of *AtNHX1* correlated with salt resistance (Jha et al., 2010) and loss of AtNHX1 function reduced establishment of seedlings under saline conditions (Aspe et al., 2003). Over-expression of *NHX* has also been shown to increase salt tolerance in a number of species, suggesting an important role of NHX in salt tolerance (Kronzucker and Britto, 2011). In addition to its role as an Na^+/H^+ antiporter, AtNHX1 may also act to store K^+ ions in the vacuole and to play a general role in ion homeostasis in addition to a protective role under salt stress (Aspe et al., 2003; Jiang et al., 2010).

1.2.2.2 Disruption of K^+ transport under salt stress

In addition to the cytoxicity of Na^+ to the cell at high concentrations, the indirect effect of increased Na^+ uptake on reducing K^+ uptake is also a factor contributing to the stress caused by high salinity. K^+ is an essential plant nutrient which is required, for example, as a co-factor for cellular enzymes, membrane transport processes, osmotic adjustment of the cell and plant growth and development (Szczerba et al., 2009). That plants actively transport K^+ from the soil is reflected in the high cellular concentrations of K^+ (approximately 100mM) compared to the K^+ content of the soil which, under ideal conditions which supports healthy plant growth, ranges from 10µM to 100mM (Alemán et al., 2009).

In plants, the uptake of K^+ ions is mediated mostly by transporters belonging to the KUP/HAK/KT and AKT families which act as high and low affinity transporters of K^+, respectively (Very and Sentenac, 2003; Szczerba et al., 2009; Kronzucker and Britto, 2011). Differential regulation of expression of the KUP/HAK/KT K^+ transporter HAK5 has been linked to the differences in salt sensitivities of the halophyte (salt tolerant) *Thellungiella halophila* and the glycophyte (salt sensitive) *A. thaliana* (Alemán et al., 2009). Under conditions of restricted K^+ availability, the expression of *HAK5* was induced in both *T. halophila* and *A. thaliana* but whereas salt stress in addition to low K^+ availability completely suppressed *HAK5* expression in *A. thaliana, HAK5* was still detectable in *T. halophila* (Alemán et al., 2009). The inhibition of *HAK5* expression in *A. thalina* was linked to a marked decrease in K^+ uptake compared to *T. halophila* under the same conditions, suggesting the ability to maintain K^+ absorption is also an important component of salt tolerance (Alemán et al., 2009) .

An indirect role for SOS1 in maintenance of K^+ uptake by the low affinity K^+ transporter AKT1 under salinity stress was also found. The observation that ammonium (NH_4^+) can selectively inhibit the activities of the KUP/HAK/KT family of K^+ transporters without affecting AKT function has been used to investigate the role of AKT1 function in K^+ transport in plants (Very and Sentenac, 2003; Szczerba et al., 2009). Under conditions in which only K^+ was limiting, K^+ dependent growth of the *sos1* mutant was found to be similar to that of wild-type whereas the *akt1* mutant showed less enhancement of growth in response to increasing external K^+ concentrations, suggesting K^+ transport by AKT1 contributes to plant growth and was not defective in the *sos1* mutant (Qi and Spalding, 2004). However, in the presence of mild salinity, the permeability of the cell membrane to K^+ was reduced in the

sos1 mutant but unaffected in wild-type plants, suggesting that in addition to Na^+ homeostasis, SOS1 also regulates AKT1 activity and thus K^+ homeostasis under conditions of salt stress (Qi and Spalding, 2004).

Thus salt stress inhibits plant growth, prevents uptake of K^+ and is toxic to plant cells and in order to prevent build up of Na^+, Na^+ can either be extruded from the cell or compartmentalised in the cell vacuole.

1.2.3 *Overlaps in drought and salinity stress*

Some aspects of drought and salinity stress are common and as such are reflected in the overlap in signalling pathways utilised by the plant in response to theses stresses. In effect, both stresses result in water/osmotic stress as the water available to the plant is restricted either through lack of water in the growth medium, such as is the case with drought stress, or through unfavourable cellular ψ_w caused by excessive presence of salt in the growth medium. Thus the early events occurring in response to salinity and drought stress are similar (Munns, 2002). In addition, both salt and drought stress induces the production of the compatible solutes such as proline to retain osmotic homeostasis, as well as up-regulation of antioxidants to prevent oxidative stress (Zhu, 2002; Wang et al., 2003; Verslues et al., 2006). ABA signalling is also involved in both drought and salt and is reflected in some of the overlaps in the genes up-regulated by these two stresses. In rice, analysis of 1,700 independent cDNAs to identify genes commonly regulated by ABA, drought and salt stress by cDNA microarray and RNA gel-blot analysis included those encoding for components of the antioxidant system (catalase, thioredoxin), an LEA protein and a protein phosphatase 2C (Rabbani et al., 2003). In *A. thaliana,* cDNA microarray analysis of 7000 genes identified 277 and 194 genes were regulated by drought and salt stress, respectively, with 141 of these genes commonly regulated by both stresses (Seki et al., 2002). Genes up-regulated in response to both drought and salt stress included those encoding for the proline biosynthetic enzyme PCS5, a number of genes encoding for LEAs, ROS detoxifying enzymes and the ABA biosynthetic enzymes NCED3 and ZEP/ABA1 (Seki et al., 2002). A summary of the regulation of genes in response to drought and salinity stress is shown in Figure 1.5.

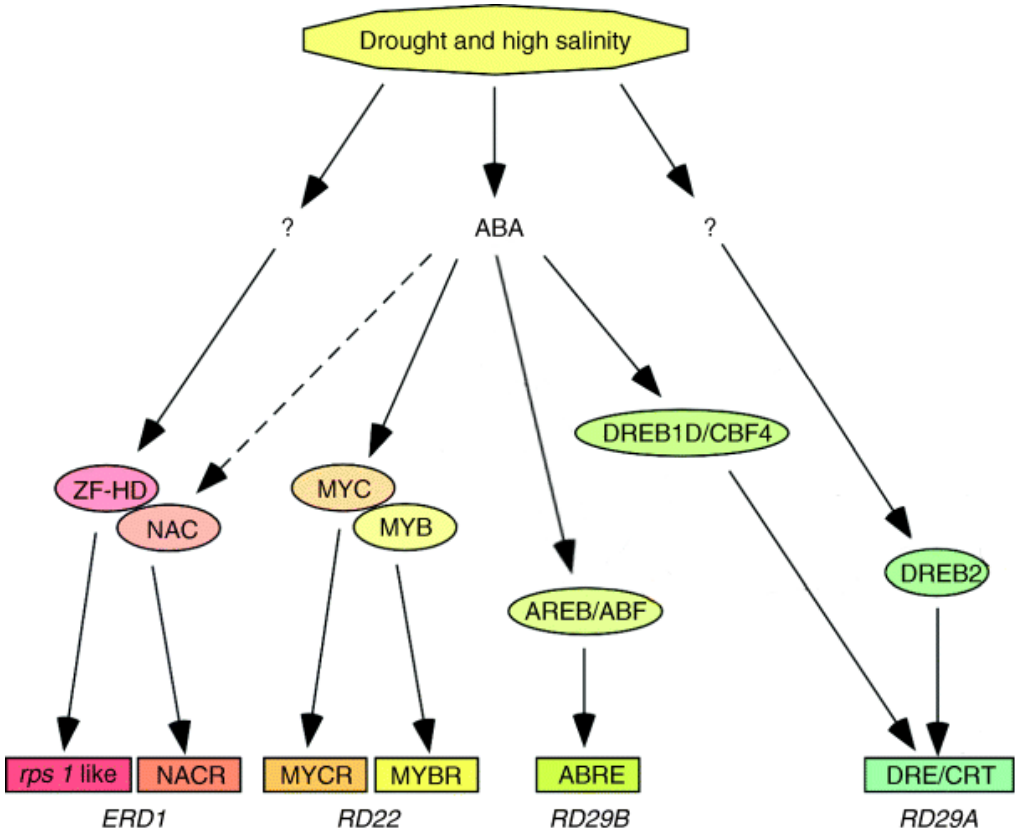


Figure 1.5 Schematic showing the transcription factors which activate drought and salinity stress responses. The *cis*-elements within the promoter regions of the genes recognised by the transcription factors are also shown. Transcription factors are shown as ovals and *cis*-elements as rectangles. Examples of genes containing these *cis*-elements are shown underneath. Figure modified from Nakashima et al. (2006).

It is apparent that plant stress signalling is complex and overlaps in the mechanisms employed by plants in response to diverse stimuli add to this complexity. A picture of plant stress responses is emerging in which plant responses to multiple stresses is not necessarily the sum of the responses to the individual stresses (Mittler, 2006). This begs the question of how plants are able to coordinate responses tailored to specific stresses. It is clear that a better understanding of how plants perceive stress and identification of key integrators of multiple stress responses is required if progress is to be made in the field in terms of generating more stress resistant crops to meet the world's growing demand for food and fuel.

1.3 Biotic stress – the impact of bacterial and fungal disease of plants

In addition to abiotic stresses, the infection of plants with pathogens is a growing problem in agriculture, with the over-use of chemicals and monocropping exacerbating the situation by providing breeding grounds for more robust and resistant pathogens (Huang et al., 2002).

With respect to disease caused by microbes, the use of antibiotics such as streptomycin to control bacterial disease in the field has been hampered by the development of antibiotic resistant strains and possible implications in human health (McManus et al., 2002), with a similar situation arising for fungicides (Waard et al., 1993). In light of these problems and public perceptions on the impact of chemical control of plant disease on human health and the environment, alternative approaches to agriculture and disease management, such as organic farming and the use of biocontrols, have been utilised, although these approaches are not without problems (Trewavas, 2001; Schneeberger et al., 2002; Brimner and Boland, 2003; Johansson et al., 2004; Trewavas, 2004). Although the source of biotic stress to plants is not limited to microbial pathogens and includes, for example, insect pests, the focus of discussion here will be on bacterial and fungal pathogens of plants.

The plant surface is an environment rich in micro-organisms such as yeast, fungi and bacteria, with up to 10^7 bacterial cells estimated to reside on each cm^2 of leaf surface at any one time (Lindow and Leveau, 2002). As such, plants have developed physical barriers to prevent microbial ingress, such as the waxy leaf cuticle which prevents direct access to plant epidermal cells and is also hydrophobic and repels moisture, the build up of which can encourage fungal infection (Freeman and Beattie, 2008). In addition to structural barriers, plants also possess the ability to perceive the presence of potential pathogens and mount an immune response. In response, pathogens have developed mechanisms to evade detection through the production and actions of effector proteins (discussed in Section 1.4.2) and in turn, plants have developed means of recognising these proteins, resulting in what has been described as an evolutionary ‘arms race’ between plant and pathogen (Boller and He, 2009). It is clear that a better understanding of the virulence mechanisms of plant pathogens and the immune responses of plants is required for robust and integrated approaches to crop protection.

To better understand the mechanisms of disease and disease resistance, model organisms have been employed to dissect the molecular components and signalling pathways involved. Two pathogens commonly used to study bacterial and fungal infection of plants are the bacterium *Pseudomonas syringae* pv. *tomato* DC3000 (*Pst*DC3000), which causes bacterial speck disease in *A. thaliana* and tomato (Preston, 2000; Katagiri et al., 2002), and the fungus *Botrytis cinerea,* which causes soft-rot in over 200 plant species (Williamson et al., 2007). Similarly, *Arabidopsis thaliana* is also used as a model plant to study plant physiology, signalling and development (Arabidopsis Genome Initiative, 2000; Nishimura and Dangl,

2010). As such, much of the discussion here will focus on these two phytopathogens and their interaction with *A. thaliana*.

1.4 Lifestyle of a bacterial pathogen – *Pst*DC3000 as an example

Plant pathogenic bacteria can exist within the plants, as parasites, as epiphytes on the leaf surface or as saprophytes in the soil, with each environment providing a possible source of bacterial pathogens (Agrios, 2005). Disease symptoms caused by *Pst*DC3000 is characterised by circular, necrotic water-soaked lesions (in *Arabidopsis*) or dark spots/specks (in tomato) surrounded by a yellow/chlorotic halo with infection favoured by cool, damp conditions (Preston, 2000; Agrios, 2005).

*Pst*DC3000 is considered a hemi-biotrophic pathogen as the initial stages of infection requires living host tissue with cell death occurring later on in infection (Glazebrook, 2005). As bacteria do not possess mechanisms to penetrate plant tissue, the bacterium enters through wounds in the plant surface or natural openings such as stomata, broken trichomes, hydathodes, lenticels and nectaries (Bashan et al., 1981; Melotto et al., 2008a). Stomata form numerous openings in the leaf surface and are utilised by *Pst*DC3000 as a point of entry (Melotto et al., 2008a). Once in the intercellular spaces of the leaf, the bacteria multiply within the apoplast, assimilating nutrients from within the apoplastic fluid (Rico and Preston, 2008) (Figure 1.6).

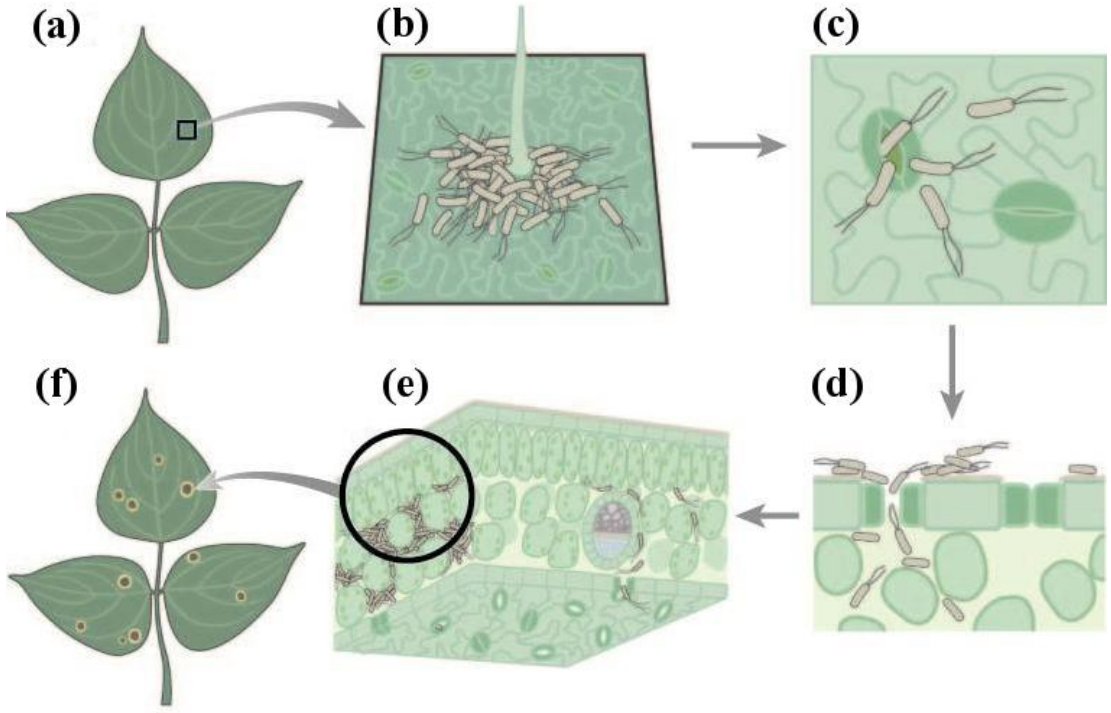


Figure 1.6 Infection of leaves by *Pst*DC3000. (a) Healthy leaf showing no symptoms may harbour bacteria on the leaf surface. (b) Bacteria can form aggregates around leaf structures such as trichomes. (c) Bacteria can enter the leaf through open stomata to (d) gain access to the leaf apoplastic space. (e) Bacteria are able to utilise nutrients in the apoplastic fluid and multiply rapidly. (f) Death of leaf tissue at the later stages of infection results in the formation of macroscopic lesions. Figure taken from Melotto et al. (2008a).

To aid infection, *Pst*DC3000 secretes toxins such as coronatine and effector proteins which act as pathogenicity and virulence factors. Clear distinctions between the terms 'pathogenicity' and 'virulence' and precise definitions which are universally accepted are lacking, as the considerations used to define these terms depends on the nature of the pathogen, the host and their interaction (Schneider and Collmer, 2010). As such, these terms are sometimes used interchangeably. However, a loose description of pathogenicity can be stated as the 'potential ability' of the pathogen to cause disease, whereas virulence can be described as the 'severity of disease' caused by the pathogen, whereby virulence can be viewed as a measurement of pathogenicity (Agrios, 2005; Shapiro-Ilan et al., 2005).

Although pathogens have evolved mechanism and factors to gain entry into the plant interior and to cause disease, plants are by no means defenceless and are able to detect the presence of pathogens and trigger responses which prevent establishment of disease. Where a potential pathogen is unable to overcome the structural barriers and pathogen-associated molecular pattern triggered immunity (PTI, discussed in Section 1.4.1) of the plant, the plant is said to

show non-host resistance (Thordal-Christensen, 2003). In cases where the pathogen can overcome pre-formed and induced resistance, a compatible interaction is formed.

1.4.1 *PAMP-triggered immunity*

In order to detect the presence of potential pathogens, plants have taken advantage of physiological differences between plants and microbes by targeting structural components inherent to the pathogen (termed pathogen-associated molecular patterns (PAMPs)) for detection. Since structural components can also be found in non-pathogenic microbes, this broad recognition also extends to microbes which are not plant pathogens, and therefore PAMPs are also known more accurately as MAMPs (microbe-associated molecular patterns). However, since this study is mainly concerned with the interaction between plants and pathogenic microbes, the term PAMP will be used here.

PAMPs make good targets for immune surveillance as they:

- are essential to the physiology of the pathogen and are therefore conserved and show little variation between species
- are found in different pathogens
- are not normally present in the plant and therefore can be recognised as 'non-self'

Recognition of PAMPs is mediated by pattern recognition receptors (PRRs) at the plant cell membrane which physically interacts with the PAMP. This broad recognition of pathogens triggers what is known as basal immunity/PAMP-triggered immunity (PTI) (Jones and Dangl, 2006).

Although the importance of PAMP-perception is indicated in the hundreds of potential PRRs encoded for by the *Arabidopsis* genome (Zipfel, 2008; Gimenez-Ibanez and Rathjen, 2010), examples of PRRs demonstrated to be required for PTI and to directly interact with bacterial PAMPs is scarce. Many putative receptors have been shown to mediate detection of bacterial PAMPs, but the mechanisms by which they do so is unknown for the majority. In *Arabidopsis,* the flagellin receptor FLS2 and the receptor for bacterial elongation factor Tu (EF-Tu) EFR are two PRRs for which both physical interaction with and requirement of detection of bacterial PAMP has been demonstrated. Both FLS2 (Flagellin Sensing2) and EFR (EF-Tu Receptor) are transmembrane leucine-rich repeat receptor-like kinases (LRR-RLKs).

PTI that is triggered by the bacterial flagellin and mediated by FLS2 is the most well studied example. Bacteria such as *Pst*DC3000 have flagella made up of flagellin subunits which the bacterium uses for motility (Naito et al., 2008). The conserved sequence of 22 amino acids at the N-terminus of flagellin (flg22) is recognised in *A. thaliana* by FLS2 (Zipfel et al., 2004). Chinchilla et al. (2006) demonstrated through immunopreciptation and chemical cross-linking that flg22 binds to the leucine-rich transmembrane receptor-like protein kinase (LRR-RLK) FLS2 in *Arabidopsis* extracts. The *fls2-17*-insensitive line containing a point mutation in the kinase domain of FLS2 showed increased susceptibility to surface-inoculated bacteria (Zipfel et al., 2004), demonstrating that plants are able to perceive the presence of bacteria through recognition of components of the bacterial cell.

Interaction of a PAMP to the extracellular LRR domain of the PRR leads to activation of the cytoplasmic serine/threonine protein kinase domain of the receptor which in turn activates downstream signalling components to initiate an immune response (Nürnberger and Kemmerling, 2006). In the case of FLS2, interaction of FLS2 with flg22 stimulates binding of the FLS2 with BAK1 (BRI1-associated receptor kinase 1), another LRR-RLK, which activates the kinase activity of FLS2 (Chinchilla et al., 2006; Chinchilla et al., 2007). BAK1 was initially identified as an interactor of the LRR-RLK BRI1 (Brassinosteroid Insensitive1) involved in brassinosteroid signalling (Li et al., 2002), suggesting a general role of BAK1 interaction with LRR-RLKs, like PRRs, to form signalling complexes. Loss of BAK1 function leads to insensitivity to both flg22 and elf18, a peptide of EF-Tu recognised by EFR, suggesting that BAK1 may mediate PTI (Chinchilla et al., 2007). Activation of the kinase activity of FLS2 by BAK1 through change in conformation and auto-phosphorylation of the FLS2 kinase domain leads to activation of a downstream mitogen-activated protein kinase (MAPK) cascade through a relay of phosphorylation events which results in the up-regulation and expression of defence related genes, including the PRRs themselves (Zipfel et al., 2006) (Figure 1.7).

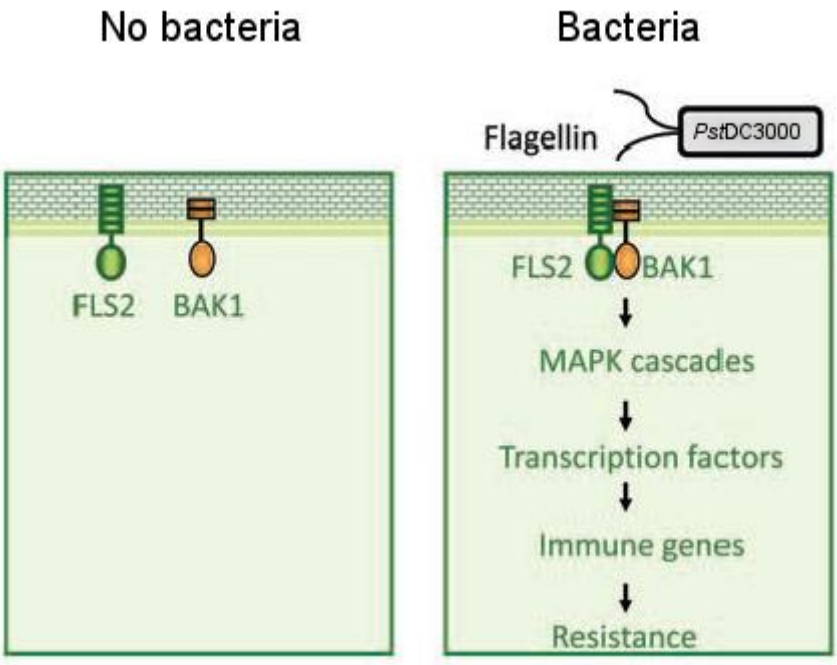


Figure 1.7 Diagram depicting detection of bacterial flagellin leading to resistance through PTI. In the absence of flagellin, there is no interaction between FLS2 and BAK1; immune responses are not activated. On interaction of FLS2 with bacterial flagellin, FLS2 is activated by autophosphorylation and interacts with BAK1 to form an immune signalling complex that activates a MAPK signalling cascade leading to transcription of immune genes and activation of resistance. Figure modified from Lu et al. (2010).

Some of the responses activated by PRRs do not seem to be PAMP-specific, suggesting that there is a generic response triggered by PAMPs (Nürnberger and Kemmerling, 2006; Zipfel et al., 2006). Common defence mechanisms activated by PTI include:

- formation of callose deposits which act as reinforcements of the cell wall,
- the generation of reactive oxygen species, also known as the 'oxidative burst' and
- production of various pathogenesis-related (PR) proteins with anti-microbial functions (Hopkins, 1999; Gómez-Gómez and Boller, 2000; Agrios, 2005).

More recently, it has emerged that stomatal guard cells at the leaf surface are able to detect and respond to the presence of bacteria in an FLS2-dependent manner (Melotto et al., 2006; Underwood et al., 2007; Zeng et al., 2010). Although bacteria utilise stomata as entry points into the leaf, the presence of *Pst*DC3000 or the flg22 peptide was found to cause active closure of stomata (Melotto et al., 2006; Zeng and He, 2010). This stomatal response requires functional FLS2 as *fls2* mutants mutated in the kinase domain were insensitive to both *Pst*DC3000 and the flg22 peptide and more susceptible to bacterial infection (Zipfel et al.,

2004; Melotto et al., 2006; Zeng and He, 2010). These findings provide an example of how detection of a pathogen can lead to a physiological response in plants which prevent infection.

1.4.2 *Bacterial effector proteins – concepts in compatible, incompatible and non-host interactions*

Bacteria have evolved numerous effector proteins to overcome PTI, with over 30 effector proteins secreted by *Pst*DC3000 (Schechter et al., 2006; Zipfel and Rathjen, 2008; Hann et al., 2010). These effector proteins act to suppress and subvert PTI through targeting host proteins such as immune receptors and components of the plant immune signalling pathways to 'mask' the presence of PAMPs (Grant et al., 2006). The effector proteins are delivered to the host cell through the bacterial Type-III secretion system (TTSS) and the importance of these proteins are reflected in the non-pathogenic nature of mutants with defects in the TTSS and which are therefore unable to secrete effector proteins (Yuan and He, 1996; Taira et al., 1999; Wei et al., 1999). Thus effector proteins can be defined as proteins which are delivered to the host cell through the TTSS and which act to modify the host cell structure and function, modification which either aid infection or elicit an immune response (Hogenhout et al., 2009).

Where the bacterium is successful in evasion/suppression of PTI through the action of effector proteins, the pathogen is able to establish disease in what is known as a 'compatible interaction' with the host. Prediction of effector protein function through bioinformatics is difficult as the sequence and structure of bacterial effector proteins are diverse and as such, the mechanisms by which many of these effector proteins act are unknown (Abramovitch et al., 2006; Zipfel and Rathjen, 2008). In total, 62 effector proteins have been found in *P. syringae*, with each strain expressing a subset of 20-30 of these effector proteins (Hann et al., 2010). For those in which function has been determined (some of which are summarised in Table 1.2), it is clear that the actions of these effectors are diverse.

Table 1.2 Summary of the functions and targets of a selection of *Pst*DC3000 effector proteins. Reproduced from Hann and Rathjen (2010) with modifications.

Effector	Function	Action	Host target	Function of host target	Reference
AvrPto	Unknown	Prevents initiation of PAMP/MAMP signalling	FLS2, EFR, other PRRs(?)	PAMP/MAMP perception and signalling	Shan et al. (2008) Xiang et al. (2008) Xiang et al. (2011)
AvrPtoB	E3 ubiquitin protein ligase	Prevents initiation of PAMP/MAMP signalling	BAK1, FLS2, EFR, other PRRs(?)	PAMP/MAMP perception and signalling	Shan et al. (2008) Göhre et al. (2008) Gimenez-Ibanez et al. (2009b)
HopAI1	Phosphothreonine lyase	Suppression of MAPK signalling	MAPKs	Kinase activity/ PAMP/MAMP signalling	Zhang et al. (2007)
HopM1	Unknown - initiates target degradation	Prevents callose deposition	AtMIN7 and others	ARF-GEF involved in exocytosis	Nomura et al. (2006)
HopU1	ADP-ribosyl transferase (ADP-RT)	Suppresses flagellin-induced callose and cell death	GRP7	RNA binding protein	Fu et al. (2007)
HopAA1-1	Potential GTPase-activating protein (GAP) domain	Contributes to lesion formation	Unknown	Unknown	Munkvold et al. (2009)
HopI1	Putative J domain	Thylakoid remodelling and suppression of SA	Unknown	Unknown	Jelenska et al. (2007)
HopAM1	Unknown	Increases sensitivity to ABA; contributes to virulence in water-stressed plants	Unknown	Unknown	Goel et al. (2008)

A well studied example of an effector protein for which a mode of action has been demonstrated is AvrPto of *Pst*DC3000. AvrPto was found to physically interact with FLS2 and EFR in *Arabidopsis* both *in vivo* and *in vitro,* inhibiting activation of these receptors and downstream signalling components (Xiang et al., 2008). Another example is AvrPtoB, which is known to suppress basal defences, such as callose deposition in response to flagellin (Abramovitch et al., 2006; de Torres et al., 2006; Shan et al., 2008). AvrPtoB was found to target BAK1, thereby disrupting formation of FLS2-BAK1 signalling complexes (Shan et al., 2008). As BAK1 may interact with other PRRs, such as EFR, by targeting BAK1 it is possible that recognition of multiple PAMPs and the signalling pathways activated by their corresponding PRRs can be disrupted though the action of the effector protein (Chinchilla et al., 2006; Shan et al., 2008; Lu et al., 2010).

To counteract suppression of PTI by bacterial effector proteins, plants have evolved resistance genes (*R*-genes) encoding for proteins which detect the presence of pathogen effector proteins (Dangl and Jones, 2001). Although the presence of specific *R*-genes can be attributed to resistance against pathogens carrying certain effector proteins, evidence of direct interaction between effector and R protein is lacking for many, leading to the 'guard hypothesis' first proposed by Van Der Biezen and Jones (1998). In this scenario, the R protein 'guards' a cellular target of the effector protein and recognises modification of this target host protein by the effector, thus indirectly detecting the presence of the effector protein to trigger immunity. Modifications of this model, such as the 'decoy' model and the 'bait and switch' model have also been proposed and are depicted in Figure 1.8 (Dodds and Rathjen, 2010).

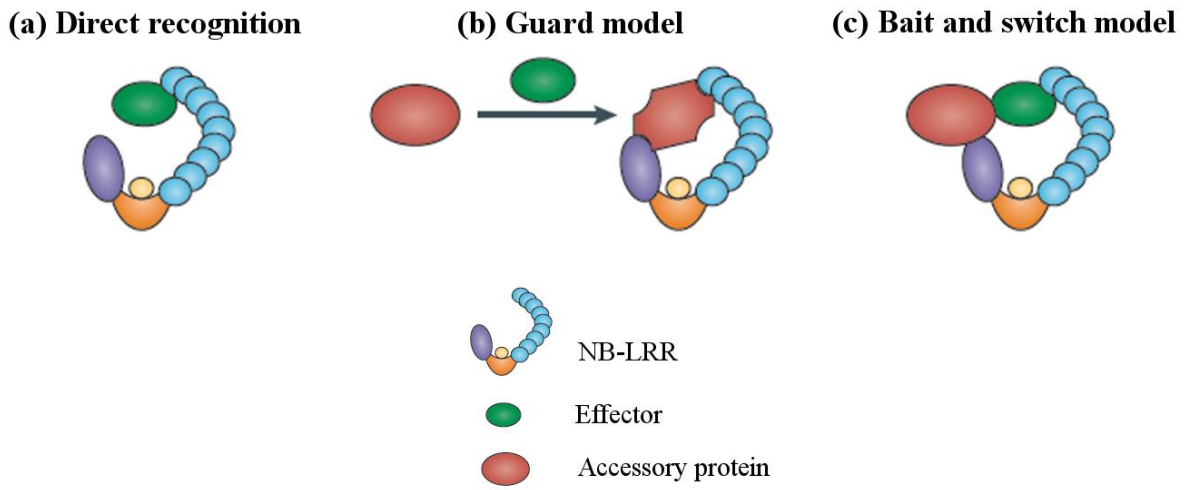


Figure 1.8 Models proposed for the recognition of pathogen derived effector proteins by plant nucleotide leucine rich repeat (NB-LRR) type receptors. (a) Effector proteins can be recognised through direct interaction with an NB-LRR type receptor. (b) In the guard model, the receptor recognises modifications of accessory proteins as a result of effector protein activity. The accessory protein is either a virulence target of the effector protein or is a decoy of the real target, facilitating indirect detection of the effector protein. (c) In the bait and switch model, the accessory protein ('bait') is associated with the receptor. On binding of the effector protein to the 'bait', the receptor is then able to interact with the effector to initiate immune signalling. Figure modified from Dodds and Rathjen (2010).

There are five classes of R-proteins in plants, the largest of which are the nucleotide-binding leucine rich repeat (NB-LRR) type receptors (Dangl and Jones, 2001). The recognition of effectors mediated by R-proteins triggers what is known as effector-triggered immunity (ETI), resulting in an 'incompatible interaction' as establishment of infection is prevented. Since the effector protein is negatively impacting on the pathogen's ability to cause infection in this context, the effector protein is referred to as an avirulence (avr) protein (Dangl and Jones, 2001). Historically, effector proteins were discovered as causing avirulence of the pathogen on resistant host plants and thus were initially named avirulence proteins as their true functions were not known (Schneider and Collmer, 2010). Since the primary function of these proteins is to positively contribute to virulence in the context of a compatible interaction, whether an effector acts as an avirulence or a virulence factor depends on the context of the interaction (i.e., whether it is an incompatible or compatible interaction, respectively).

In cases where the plant only recognises a single effector protein, immunity is not robust as the pathogen may evolve different forms of the effector protein or produce others which mask the recognition of the single effector protein (Jones and Dangl, 2006). In situations where

multiple effector proteins are recognised by the plant, immunity is more robust and can lead to non-host resistance (Thordal-Christensen, 2003).

Cellular responses most commonly associated with *R*-gene mediated resistance are:

- a biphasic oxidative burst characterised by an initial short burst followed by a more prolonged period of production three to six hours after inoculation with avirulent pathogen (Levine et al., 1994; Lamb and Dixon, 1997)
- increase in cytosolic Ca^{2+} and production of nitric oxide (NO) (Ma et al., 2009)
- the hypersensitive response (HR), a type of defence response which involves cell death triggered on recognition of pathogen effector proteins to prevent further pathogen spread (Yu et al., 1998)

Thus plant immunity towards bacterial pathogens can be viewed as layers of responses, summarised in Figure 1.9 below.

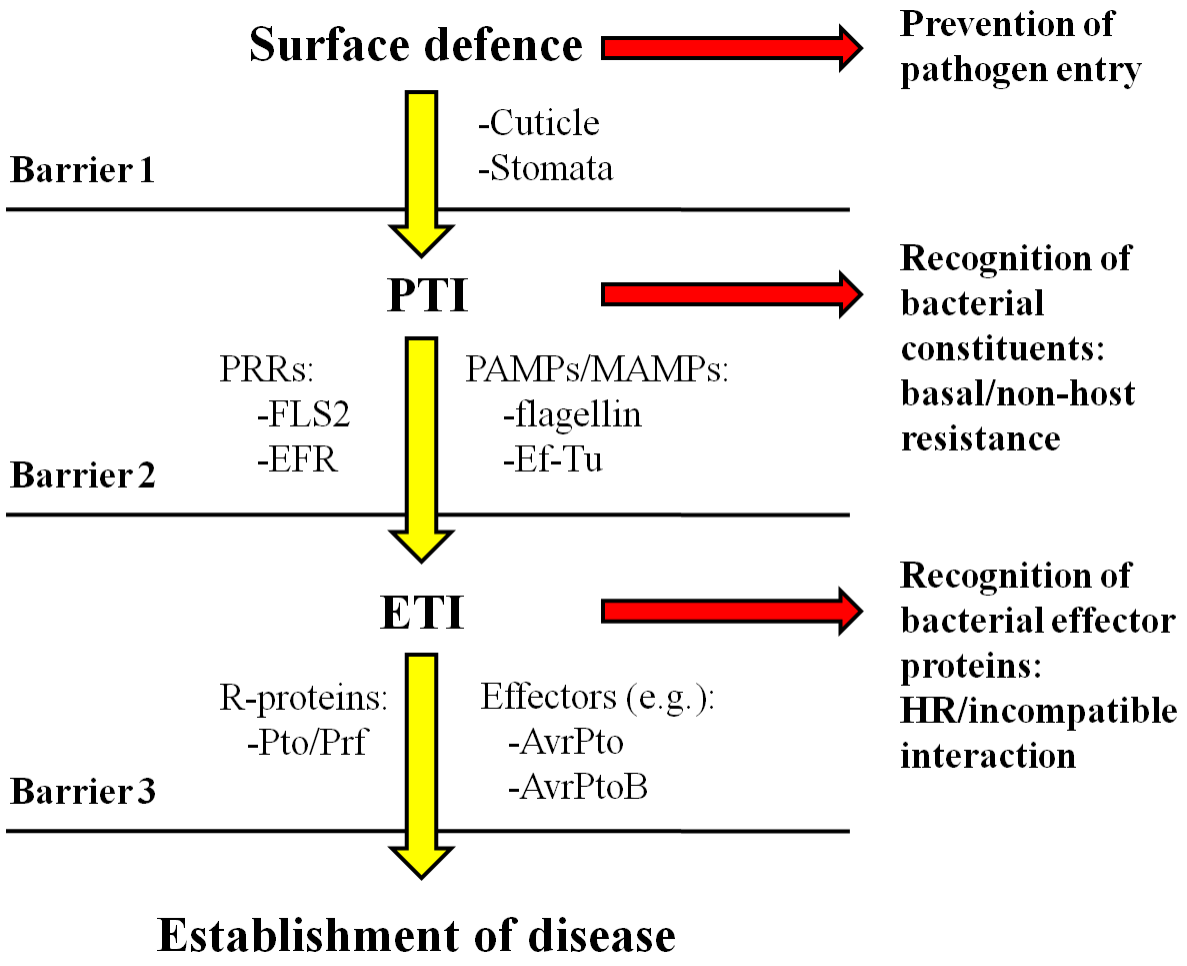


Figure 1.9 Schematic summarising the defences which bacterial pathogens must overcome in order to establish disease. Yellow arrows represent barriers overcome by the bacterial pathogen with examples of PRRs, PAMPs/MAMPs, R-proteins and effector proteins. Red arrows represent immune response associated with an inability to overcome each barrier.

1.4.3 *The* P. syringae *phytotoxin coronatine*

In addition to effector proteins, *Pst*DC3000 also secretes the phytotoxin coronatine. Coronatine is a secondary metabolite that is non-host specific and produced by pathovars of *P. syringae* (Bender et al., 1998). Coronatine is required for full virulence of *Pst*DC3000 and symptom development as mutants in coronatine biosysnthesis show reduced growth *in planta* and chlorosis (Ma et al., 1991; Mittal and Davis, 1995; Brooks et al., 2004). Application of purified coronatine to tomato plants or inoculation with TTSS mutants which are unable to secrete virulence factors but are still able to produce coronatine resulted in chlorosis of tissue (Penaloza-Vazquez et al., 2000; Uppalapati et al., 2008; Ishiga et al. 2010).

Coronatine was found to down-regulate expression of photosynthetic genes, cause shrinkage of and increased oxidative stress in chloroplasts and up-regulate expression of *ATHCOR1* encoding for a chlorophyll degrading enzyme ,resulting in loss of chlorophyll content (Benedetti et al., 1998; Benedetti and Arruda, 2002; Uppalapati et al., 2005; Uppalapati et al., 2008; Ishiga et al., 2009a). This evidence suggests that disruption of the photosynthetic machinery by coronatine is the cause of the chlorotic symptoms seen. The accumulation of ROS and down regulation of thylakoid Cu/Zn SOD in a light-dependent manner was shown to occur on treatment of tomato seedlings with purified coronatine or infection with wild-type *Pst*DC3000 but not with a coronatine deficient mutant, indicating manipulation of redox balance is an important virulence mechanism (Ishiga et al., 2009a; Ishiga et al., 2009b). Furthermore, in support of the role of ROS manipulation in disease development, inhibition of ROS production by pre-treatment of tomato seedlings with the NADPH oxidase inhibitor diphenyleneiodonium (DPI) resulted in a reduction in necrotic symptoms on infection with *Pst*DC3000 (Ishiga et al., 2009a).

Tn5 insertion mutants defective in coronatine production showed reduced growth *in planta* (100-1000 fold less growth compared to wild-type *Pst*DC3000) and caused very little or no disease symptoms on surface inoculation, suggesting that coronatine is required for full pathogenicity and virulence of the pathogen (Mittal and Davis, 1995; Brooks et al., 2004). More recently, coronatine was found to be required for the ability of bacteria to overcome stomatal defences (Melotto et al., 2006). Mutants in coronatine production could not reopen stomata and were therefore unable to utilise these natural openings as a route to the leaf interior (Melotto et al., 2006; Zeng and He, 2010). This finding correlates with previous observations showing that growth defects of coronatine biosynthetic mutants *in planta* were less pronounced on infiltration of the bacteria directly into the leaf apoplast, a method which by-passes surface defences (Mittal and Davis, 1995; Brooks et al., 2004). However, since coronatine deficient mutants did not grow to wild-type levels even when directly infiltrated into the leaf apoplast, coronatine may also contribute to persistence or growth of the bacteria *in planta* in addition to its role at the plant surface (Brooks et al., 2005; Zeng and He, 2010).

The biosynthetic pathway of coronatine involves the production of two moieties, coronafacic acid (CFA) and coronamic acid (CMA) which are chemically linked together to form coronatine (Brooks et al., 2004) (Figure 1.10).

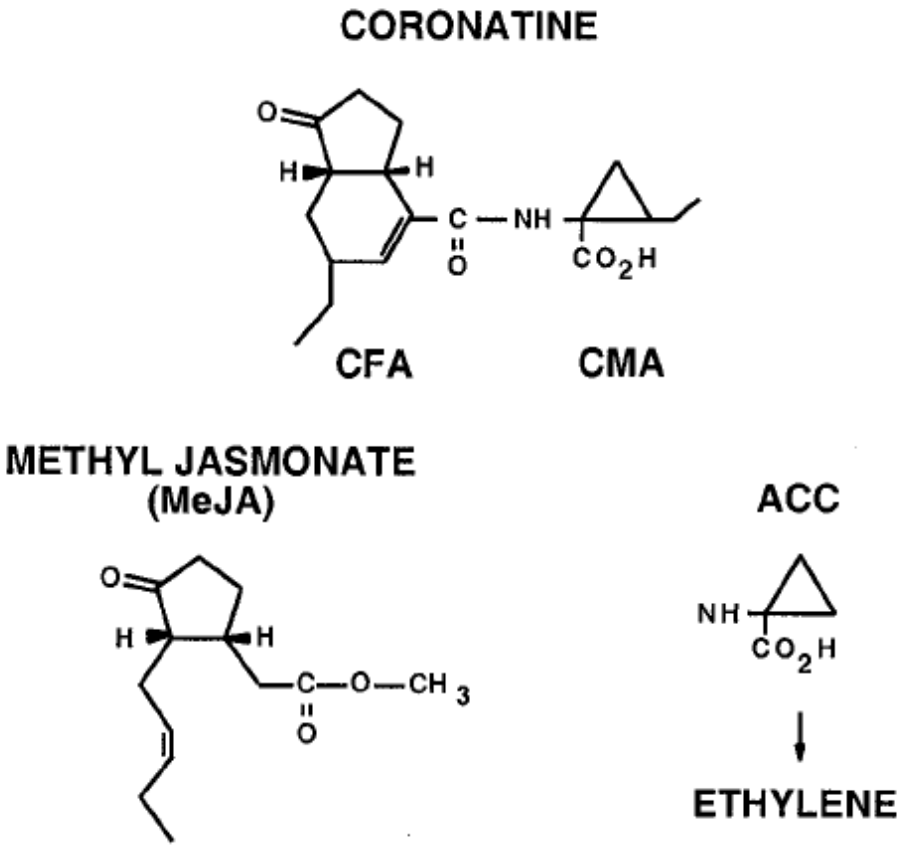


Figure 1.10 Structure of the *P. syringae* phytotoxin coronatine. Coronatine consists of the moieties coronafacic acid (CFA), a polyketide, and coronamic acid (CMA), a cyclised isoleucine derivative, which are chemically linked by an amide bond. Also shown are the chemical structures of the plant hormone methyl jasmonate (MeJA) and aminocyclopropyl carboxylic acid (ACC), the precursor of ethylene in plants. CFA and CMA show structural similarity to MeJA and ACC, respectively. Figure taken from Brooks et al. (2004).

Coronatine has been shown to stimulate the jasmonic acid (JA) signalling pathway of plants by targeting the F-box protein coronatine insensitive 1 (COI1); in the presence of JA, COI1 activates JA signalling (Katsir et al., 2008). JA signalling is suppressed by jasmonate ZIM domain (JAZ) proteins which, in the presence of JA, are targeted for ubiquitin-dependent degradation upon binding with COI1 (Katsir et al., 2008). Mutation of the *COI1* gene confers both resistance to *Pst*DC3000 infection and insensitivity to coronatine and methyl jasmonate (MeJA). Coupled with data showing that coronatine up-regulates expression of JA biosynthetic genes and JA accumulation in plants, *Pst*DC3000 targets JA signalling as a virulence strategy through the action of coronatine (Uppalapati et al., 2005; Uppalapati et al., 2007; Ishiga et al., 2010).

Given the structural similarities between CFA and CMA with the plant hormone MeJA and the ethylene precursor aminocyclopropyl carboxylic acid (ACC), respectively, it had been suggested that coronatine may exert its actions on plants by acting as molecular mimics of plant hormones. Although CMA does not seem to mimic ACC function *in planta*, evidence suggests that CFA may mimic the function of MeJA, although the complete coronatine molecule has a larger impact on JA signalling in plants (Brooks et al., 2005; Uppalapati et al., 2007; Ishiga et al., 2010).

Thus coronatine has multiple functions in bacterial virulence, mediating chlorosis and necrosis, overcoming stomatal defences and manipulation of ROS and hormone signalling.

It is clear that effector proteins and the phytotoxin coronatine have important roles in bacterial pathogenicity and virulence. Although the mechanisms by which effector proteins and coronatine exert their effects vary, the main functions of these factors are to suppress and manipulate plant responses and to induce conditions favourable to establishment of infection. As *Pst*DC3000 is a (hemi)biotroph, this pathogen relies on a living host from which to derive its nutrients from, a situation in contrast to necrotrophic pathogens, such as *Botrytis cinerea*, the difference in which is reflected in the virulence mechanisms utilised.

1.5 Lifestyle of a fungal phytopathogen – *B. cinerea* as an example

The fungal necrotroph *Botrytis cinerea* causes soft-rot disease in over 200 plant species and as a necrotrophic pathogen, relies on the release of nutrients from dead/dying cells (Glazebrook, 2005). Characteristic of *B. cinerea* infection is the production of a grey mould on the surface of infected tissue which is favoured by cool temperatures and high humidity (Agrios, 2005). Infection is mediated by fungal spores/conidia which on contact with the leaf surface germinate to produce a germ tube/ hyphae. The hyphae invades tissues through wounds, upon which the fungus releases digestive enzymes and phytotoxins which promote breakdown and death of plant tissue resulting in the soft rot associated with *B. cinerea* infection (van Kan, 2006). At the later stages of infection, the fungus produces conidiophores bearing conidia, which is the characteristic grey mould caused by this fungus, which can then go on to infect another part of the plant/other plants, completing the lifecycle (Agrios, 2005) (Figure 1.11). In addition to infection through wounds, *B. cinerea* is also able to directly penetrate the host surface using a specialised infection structure which differentiates at the tip of the fungal hyphae called an appressorium (van Kan, 2006). To breach the plant cuticle, the

appressorium forms a penetration peg which penetrates into the host tissue where it is then able to grow and degrade plant tissue to release nutrients (Akutsu et al., 1981; Agrios, 2005; van Kan, 2006).

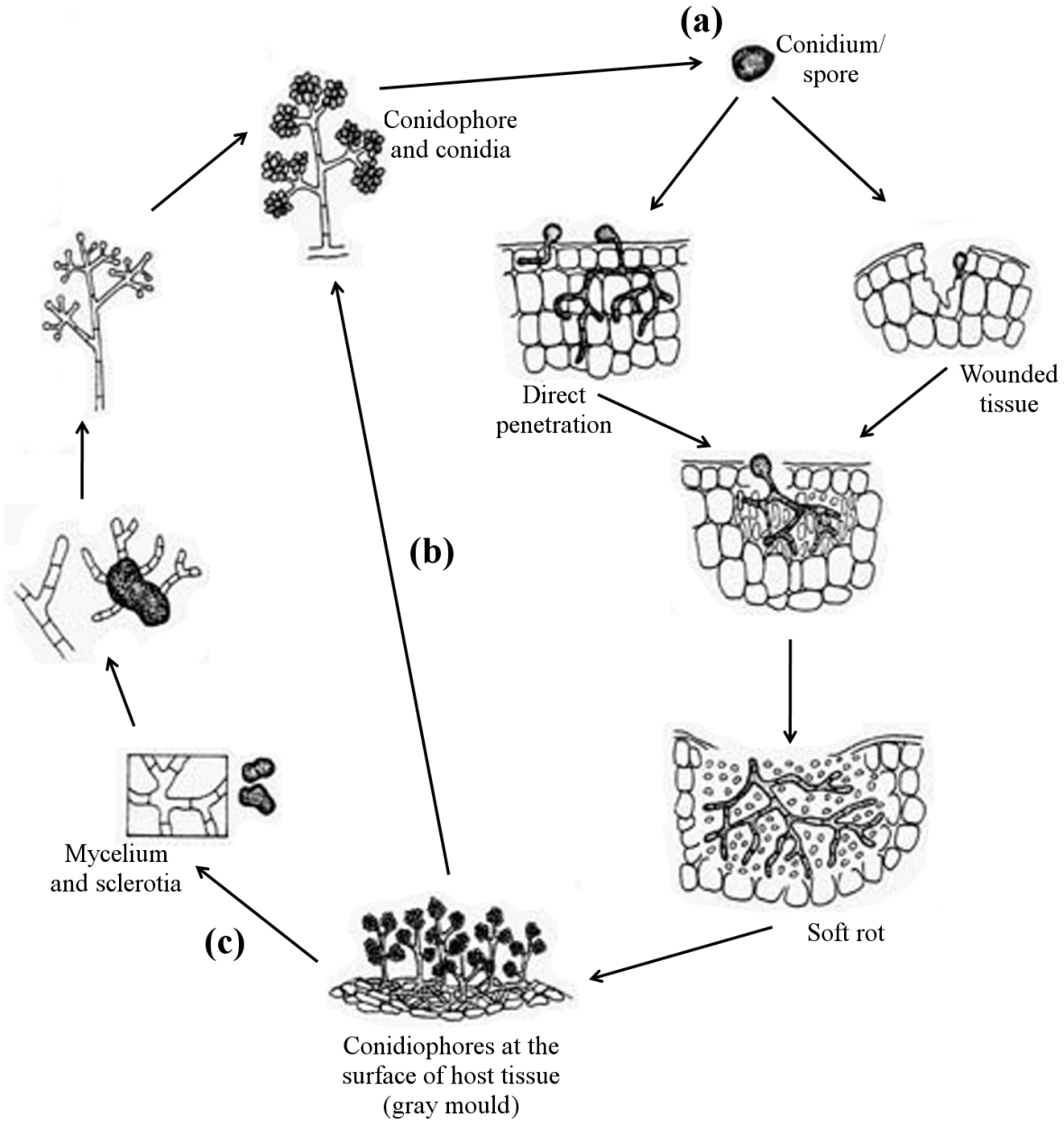


Figure 1.11 Infection life-cycle of *B. cinerea*. (a) A conidium/spore on contact with the host germinates and can either penetrate directly into host tissue through the formation of an infection structure called the appressorium, or can gain entry through wounds. Once inside the host, fungal hyphae grow into host tissue and secrete cell wall degrading enzymes to release nutrients from the plant cells, leading to collapse of tissue (soft rot). The fungus then produces conidiophores at the surface of the host tissue which can be seen as the characteristic grey mould caused by *B. cinerea.* The conidiophores can then (b) shed conidia to repeat the infection cycle or (c) survive in the soil as fungal mycelia or sclerotia. On return to favourable conditions, sclerotia can produce mycelia which then go on to produce conidiophores carrying conidia to restart the infection cycle. Figure modified from Agrios (2005).

1.5.1 *Fungal virulence factors*

1.5.1.1 Factors triggering host cell death

As mentioned earlier, *B. cinerea* is a necrotrophic pathogen and characteristic of infection with this fungus is host cell death. The importance of host cell death in infection by this necrotroph is demonstrated in the *A. thaliana dnd1* (defence, no death) mutant which is defective in the HR, as *B. cinerea* was unable to cause lesions on this mutant (Yu et al., 1998; Govrin and Levine, 2000). Additionally, *B. cinerea* growth and lesion formation was greater on leaves which had been infiltrated with HR-inducing bacteria beforehand (Govrin and Levine, 2000). Induction of cell death in leaves treated with the intercellular fluid extracted from *B. cinerea* infected leaves and the observation that collapse of host tissue occurs before invasion of fungal hyphae suggests that the fungus triggers host cell death through the secretion of virulence factors (Govrin et al., 2006).

To enable *B. cinerea* to have a wide host range, the fungus secretes many non-host specific phytotoxic metabolites, two of which are botrydial, a sequiterpene, and botcinic acid, a polyketide. These phytotoxins have been shown to act redundantly in virulence of the fungus through mutation of botrydial and botcinic acid biosynthesis genes (Siewers et al., 2005; Pinedo et al., 2009; Dalmais et al., 2011). Botrydial is the most phytotoxic compound secreted by *B. cinerea* and application of purified botrydial to host *Phaseolus vulgaris* leaves resulted in chlorosis and cell collapse (Colmenares et al., 2002). Pre-treatment of leaves with this phytotoxin prior to inoculation with *B. cinerea* led to accelerated infection, suggesting that botrydial promotes virulence by triggering cell death (Colmenares et al., 2002). Oxalic acid secreted by *Botrytis* has also been shown to trigger host cell death and mutants in oxalic acid production in the related necrotrophic pathogen *Sclerotinia sclerotiorum* results in avirulence (van Kan, 2006).

As well as phytotoxic metabolites, *B. cinerea* also produces phytotoxic proteins, such as the effectors BcNEP1 and BcNEP2, which were shown to induce necrosis/cell death in a range of plants including *Arabidopsis, Vicia faba, Nicotiana benthamiana, Glycine max* and *Phaseolus vulgaris* (Schouten et al., 2008). Microscopic examination revealed that BcNEP1 and BcNEP2 associated with the plasma and nuclear membranes and with the nucleolus in dying leaf protoplasts, the chloroplasts of which showed H_2O_2 production (Schouten et al., 2008). However, mutants in either BcNEP1 or BcNEP2 did not have any effect on the

virulence of the fungus, suggesting redundancy in function between the numerous *B. cinerea* virulence factors (Arenas et al., 2010).

The requirement of host derived ROS in virulence of *B. cinerea,* which accumulates at the site of lesion formation, is implicated by the restriction of symptom development in plants pre-treated with the NADPH oxidase inhibitor DPI (Govrin and Levine, 2000). Furthermore, infiltration of leaves with xanthine oxidase plus xanthine which produces superoxide ($O_2^{\cdot-}$) or with glucose plus glucose oxidase to produce H_2O_2 increases infection with *B. cinerea* (Govrin and Levine, 2000).

Genes associated with ROS production have also been identified in *B. cinerea.* The *B. cinerea* genome encodes for a Cu-Zn-superoxide dismutase (BCSOD1) with mutants of this gene showing decreased virulence, suggesting generation of toxic levels of H_2O_2 through dismutation of $O_2^{\cdot-}$ may be required to trigger host cell death (Rolke et al., 2004). Two NADPH oxidases (which catalyse the production of $O_2^{\cdot-}$ from O_2) BCNOXA and BCNOXB were subsequently identified in *B. cinerea* and shown to contribute to host colonisation and penetration of host tissue, respectively (Segmuller et al., 2008). It was therefore suggested that these NADPH oxidases may provide a source of $O_2^{\cdot-}$ for dismutation to H_2O_2 by BCSOD1. However, addition of the NADPH oxidase inhibitor DPI did not affect H_2O_2 or $O_2^{\cdot-}$ production nor virulence of the fungus when added to the inoculation media (Govrin and Levine, 2000; Segmuller et al., 2008). Additionally, mutants of these NADPH oxidases were not compromised in ROS production, suggesting alternative sources of ROS exist in *B. cinerea* (Segmuller et al., 2008). How BCNOXA and BCNOXB contribute to virulence is therefore unclear. However, in contradiction with NADPH oxidase function in generation of ROS, BCNOXA and BCNOXB were implicated in resistance to oxidative stress (Segmuller et al., 2008). Although the importance of fungal ROS in virulence and development of *B. cinerea* is implicated in the presence of genes encoding for ROS generating enzymes and the negative impact of which mutation of these genes has on fungal virulence, the precise roles of these enzymes remain to be determined.

1.5.1.2 Digestive enzymes

A recent study by Espino et al. (2010) investigating proteins secreted by *B. cinerea* 16 hours after induction with plant extracts (from tomato and kiwi fruit) found the fungus secreted a range of proteins including proteases, lipases and proteins involved in pectin, hemicellulose

and cellulose degradation. Therefore *Botrytis* appears to secrete a large range of virulence factors aimed at degradation of the plant cell wall in order to release nutrients (Choquer et al., 2007). Pectin is a major component of the plant cell wall and mutants in the pectin methyl-esterase BCPME1 and the endopolygalacturonases (PGs) BCPG1 and BCPG2 show reduced virulence and ability to colonise host tissue, highlighting cell wall degradation as a virulence strategy (Valette-Collet et al., 2003; Kars et al., 2005).

Clearly, *Botrytis* is armed with a large number virulence factors which contributes to its success as a pathogen. Given the wide host range of this fungus, there is no doubt that more effectors and mechanism of virulence will be identified in the coming years. Whether plant defences will overcome *Botrytis* virulence to enable durable resistance remains to be seen. However, plants are by no mean defenceless against necrotrophic fungi and the defence mechanisms utilised by plants is the topic of discussion in the following section.

1.5.2 *Plant defences against necrotrophic fungi*

1.5.2.1 Recognition of PAMPs and DAMPs

Similar to bacteria, fungi also possess structural components which are utilised by plants to trigger PTI. Chitin is a common component of the fungal cell wall and consists of unbranched β-1-4-linked *N*-acetyl glucosamine (GlcNAc) (Bulawa, 1993). Recognition of chitin in plants is mediated by the receptor-like kinase CERK1 which contains three extracellular Lysin motifs (LysM) that recognise the *N*-acetyl glucosamine moiety and is typically found in glycan binding proteins (Buist et al., 2008). The importance of CERK1 in PTI by chitin was demonstrated in *cerk1* mutants containing either a Ds transposon insertion or a T-DNA insertion in the intracellular serine/threonine kinase domain of CERK1 (Miya et al., 2007; Wan et al., 2008). These mutants did not exhibit responses typically triggered by chitin in wild-type plants, such as production of ROS, up-regulation of chitin-responsive genes and activation of the downstream MAPKs MPK3 and MPK6 involved in defence signalling (Miya et al., 2007; Wan et al., 2008). Mutation of CERK1 also leads to increased susceptibility to the biotrophic fungal pathogen *Eryisiphe cichoracearum* and enhanced symptom development in response to *Alternaria brassicicola*, a necrotrophic fungal pathogen (Miya et al., 2007; Wan et al., 2008). Direct binding of CERK1 to chitin was shown *in vitro* with yeast- and *Nicotiana benthamiana*-expressed CERK1 which required the three LysM motifs in the extracellular domain of CERK1 (Iizasa et al., 2010; Petutschnig et al. 2010). In

rice, the chitin elicitor binding protein CEBiP and the receptor kinase OsCERK1 which both contribute to recognition of chitin also contain LysM motifs (Shimizu et al., 2010). Interestingly, CERK1 has also been implicated in PTI against bacterial infection, although the identity of the bacterial PAMP recognised by this PRR remains unknown (Gimenez-Ibanez et al., 2009a).

In addition to indirect recognition of effector proteins, the products of pathogen activity such as the breakdown products of plant tissue can also elicit an immune response. Break down of pectin in the plant cell wall by fungal PGs releases oligogalacturonides (OGs) which are detected by the plants immune system (Ferrari et al., 2007; Galletti et al., 2009) and pre-treatment of plants with OGs 24h before inoculation with *B. cinerea* restricted lesion spread (Ferrari et al., 2003; Ferrari et al., 2007). These elicitors, derived from the host and released through the action of the pathogen are termed damage associated molecular patterns (DAMPs).

Thus, in addition to recognition of structural components specific to the fungus, plants have also adapted to perceive damage caused as a result of the necrotrophic lifestyle of *B. cinerea.*

1.5.2.2 Secondary metabolites

Due to the differences in the lifestyles of biotrophic and necrotrophic pathogen, aspects of the defences employed by plants against *B. cinerea* differ in some aspects for a pathogen such as *Pst*DC3000 discussed previously. For example, where as recognition of PAMPs/MAMPs holds true for defence against both *B. cinerea* and *Pst*DC3000, *R*-gene mediated resistance does not seem to play a role in defence against necrotrophs (Denby et al., 2004). Most noticeable in plant defence against *B.cinerea* are secondary metabolites, such as the phytoalexin camalexin.

Camalexin is an indolic compound synthesised from tryptophan and is a major secondary metabolite produced by *Arabidopsis* with demonstrated antifungal activity (Glawischnig, 2006, 2007) (Figure 1.12). The final step of camalexin biosynthesis is catalysed by CYP71B15/PAD3 (Phytoalexin Deficient3) which is up-regulated in response to the DAMP OG and on infection with *B. cinerea,* with a mutation in this enzyme resulting in deficiency in camalexin production and susceptibility to infection (Ferrari et al., 2003; Denby et al., 2004; Schuhegger et al., 2006; Ferrari et al., 2007; van Baarlen et al., 2007).

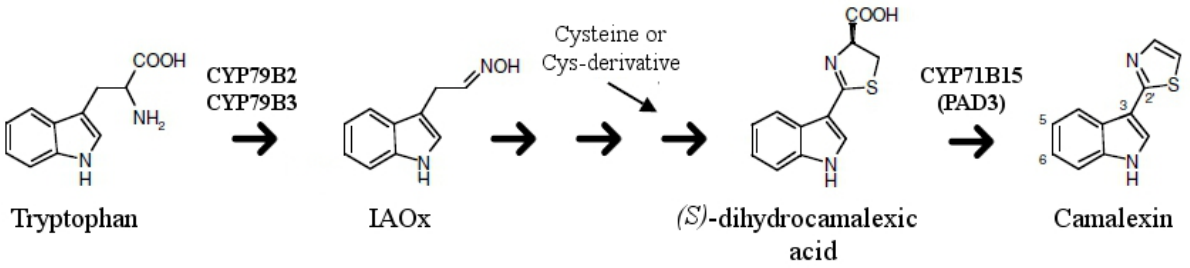


Figure 1.12 Biosynthesis of camalexin from tryptophan involving the action of CYP (cytochrome P450) enzymes. Tryptophan is converted to indole-3-acetaldoxime (IAOx) by CYP79B2 and CYP79B3. A thiozole ring derived from cysteine is incorporated to form *(S)*-dihydrocamalexic acid, which is decarboxylated by CYP71B15 (PAD3) in the last step of the pathway to form camalexin. Modified from Glawischnig (2007).

In vivo, camalexin inhibits growth of *B. cinerea* in a dose-dependent manner and increased accumulation in infected leaf tissue correlates with restriction of lesion spread (Ferrari et al., 2003; Denby et al., 2004). However, it was found that *B. cinerea* isolated from different host plants differed in their sensitivity to camalexin, suggesting that some isolates are able to detoxify camalexin (Ferrari et al., 2003; Denby et al., 2004; van Baarlen et al., 2007). Accordingly, an ATP-binding cassette (ABC) transporter BcatrB was identified in *B. cinerea* which was up-regulated in the presence of camalexin (Stefanato et al., 2009). Mutants of the *BcatrB* gene were more sensitive to camalexin *in vivo* and *in planta* but virulent on the *pad3* mutant, suggesting BcatrB is required for detoxification of camalexin in the fungus (Stefanato et al., 2009). BcatrB also prevented accumulation of the fungicides fludioxonil and fenpiclonil and the secondary metabolite eugenol produced by basil, suggesting a general role in the detoxification of toxic compounds (Vermeulen et al., 2001; Schoonbeek et al., 2003). Evidence of detoxification of camalexin by conversion to less growth inhibitory compounds by *B. cinerea* has also been found (Pedras et al., 2011).

In addition to phytoalexins, plants produce a range of secondary metabolites such as phenylpropanoids (e.g., sinapates and flavonols), glucosinolates (e.g., tryptophan and phenylalanine) and terpenoids (Kliebenstein, 2004). To determine whether other secondary metabolites play a role in resistance to *B. cinerea* in *Arabidopsis,* Kliebenstein et al. (2005) investigated the spatial distribution of glucosinolates, flavonols and sinapate in addition to camalexin in leaves in relation to the inoculation site. It was found that whereas camalexin accumulation was highest in tissue surrounding the lesion, glucosinolates, sinapoyl malate and flavanoid concentrations increased further away from the lesion. Considering that accumulation of camalexin is triggered by stimuli which induce ROS production, such as UV

light, silver nitrate and ROS generating compounds (such as paraquat and acifluorfen), this accumulation at the site of infection may be in response to plant ROS production triggered by the fungus (Tierens et al., 2002; Glawischnig, 2007; Stefanato et al., 2009).

Interestingly, the extent to which these metabolites accumulated was dependent on the fungal strain used, with camalexin and flavonoids induced to a lower and higher extent, respectively, in response to a more virulent, camalexin insensitive strain (Kliebenstein et al., 2005). Kliebenstein et al. (2005) suggested that reduced camalexin in response to the more virulent strain was due to either degradation of the phytoalexin, insufficient accumulation due to the rapid growth of the fungus or lack of induction. The exact roles of the other metabolites were difficult to determine, as mutants blocked in biosynthesis of these secondary metabolites had plieotrophic effects. However, the *cyp79B2/B3* mutant which is defective in both camalexin and glucosinolate production was more susceptible to infection than the *pad3* mutant, suggesting glucosinolates may also play a defensive role (Kliebenstein et al., 2005).

Downstream of the recognition of pathogens are the signalling networks which activate immune response, of which plant hormones play an important role.

1.5.3 *Hormone signalling in defence against biotrophic and necrotrophic pathogens*

To potentiate immune responses, plant hormones such as salicylic acid (SA), JA and ethylene are utilised by the plant. In the case of biotrophic pathogens, SA has been shown to be most important, whereas JA and ethylene are associated with resistance against necrotrophic pathogens (Thomma et al., 1998; Glazebrook, 2005; Chague et al., 2006; Kliebenstein and Rowe, 2008). This division of labour is a result of the different lifestyles employed by biotrophic and necrotrophic pathogens and is reflected in the antagonism between SA and JA/ethylene responses. For example, inoculation of *A. thaliana* leaves prior to infection with SA-inducing *Pst*DC3000 prior to infection with the JA/ethylene-inducing necrotroph *Alternaria brassicicola* resulted in an increased susceptibility towards this fungi, which was not seen in the SA-biosynthetic *sid2* mutant (Spoel et al., 2007). Application of SA to wild-type plants which are normally resistant also increased susceptibility towards *A. brassicicola* and suppressed expression of the JA/ethylene-dependent *PDF1.2* marker gene, indicating antagonism of responses towards biotrophic and necrotrophic defences mediated by SA (Spoel et al., 2007). Additionally, mutants of JA and ethylene signalling *coi1-1* and *etr1-1*, respectively, were more susceptible to infection with *B. cinerea* and treatment of plants with

methyl jasmonate (MeJA) increased resistance to a number of necrotrophic pathogens (Thomma et al., 2000; Zimmerli et al., 2001). As discussed previously, biotrophic pathogens require a living host on which to survive, whereas necrotrophs elicit host cell death as a virulence mechanism. Therefore whereas cell death, such as the HR elicited by avirulent bacteria prevents the spread and establishment of infection by a biotroph, with respect to necrotrophic pathogens, cell death facilitates rather than hinders infection (Govrin and Levine, 2000).

SA signalling is important in activation of defences associated with biotrophic pathogens such as the HR triggered by ETI, callose deposition and expression of pathogenesis-related (PR) proteins (SA signalling is discussed in more detail in Section 5.1.3.1). In the case of necrotrophs, JA/ethylene responses include expression of anti-microbial proteins, such as the plant defensin PDF1.2, PR-3 chitinase and production of camalexin which is partially dependent on a functional JA signalling pathway (Glazebrook, 2005; Rowe et al., 2010).

Although there is division of defences against pathogens with different lifestyles, this separation is not absolute and overlaps in the signalling pathways do exist. In both tomato and *A. thaliana*, transgenic lines expressing the SA-degrading enzyme salicylate hydroxylase encoded by the *nahG* gene displayed a greater number of spreading lesions on infection with *B.cinerea,* suggesting a role for SA in resistance towards this pathogen (Zimmerli et al., 2001; Audenaert et al., 2002; Govrin and Levine, 2002; Achou et al., 2004). Synergy between SA and JA has also been shown to occur at low levels of JA in relation to SA, suggesting the outcome of interaction between hormones may also be concentration dependent (Mur et al., 2006).

More recently, ABA which has well known roles in abiotic stress signalling is emerging as an important hormone in biotic stress signalling, contributing to plant interactions with both biotrophic and necrotrophic pathogens. In *A. thaliana*, ABA mediates both resistance and susceptibility towards *Pst*DC3000. Whereas ABA is required for stomatal defences against bacteria at the early stages of infection, ABA contributes to susceptibility to *Pst*DC3000 at later stages and is linked to suppression of basal (including SA) defences (Mohr and Cahill, 2003; Melotto et al., 2006; de Torres Zabala et al., 2007; Mohr and Cahill, 2007; de Torres Zabala et al., 2009). The role of ABA in stomatal closure is well studied and is triggered in response to low water availability/drought stress to prevent water loss through transpiration as discussed previously in Section 1.2.1. Although stomatal closure mediated by ABA

prevents access to the leaf interior, once inside the plant, manipulation of ABA responses may benefit the bacterium through protection against water stress. Restriction of water availability to bacteria within the leaf has been linked to the HR and found to occur during incompatible interactions, whereas compatible interaction with *Pst*DC3000 did not reduce water availability to levels inhibitory to the bacterium (Wright and Beattie, 2004; Freeman and Beattie, 2009). This suggests that plants may subject bacteria to osmotic stress as a mechanism to prevent bacterial multiplication. Additionally, increasing ABA levels in plants through exposure to drought stress also increased susceptibility towards *Pst*DC3000, with expression of the *Pst*DC3000 effector protein HopAM1 in the weakly pathogenic *P. syringae* pv. *maculicola (Pma)* resulting in increased bacterial growth in water-stressed plants (Goel et al., 2008; Fan et al., 2009). Thus *Pst*DC3000 may manipulate ABA levels in order to suppress basal defences and to increase water availability within the plant.

Whereas ABA has been shown to contribute to *Pst*DC3000 infection post-invasion, the ABA deficient tomato *sitiens* mutant was found to be more resistant to infection with *B. cinerea* (Asselbergh et al., 2007; Curvers et al., 2010). Similarly, the ABA biosynthetic mutants *aba2-12* and *aao3-2* of *A. thaliana* were also more resistant to *B. cinerea* (Adie et al., 2007). However, ABA was also shown to contribute to callose formation in response to *B. cinerea,* suggesting complex hormonal regulation of resistance responses (Asselbergh and Hofte, 2007).

It is clear that hormone signalling in plants is complex with overlap in pathways serving to 'fine-tune' responses. Whereas division of immune responses is seen according to the lifestyle of the pathogen, these divisions are not absolute. Indeed, overlaps in signalling pathways also extends to abiotic and biotic stresses, an example of which is seen in the case of ROS utilised for signalling purposes.

1.6 Reactive oxygen species in stress signalling

Reactive oxygen species (ROS), of which hydrogen peroxide (H_2O_2) is the most well studied, are produced as normal by-product of cellular processes in plants such as respiration and photosynthesis and are produced from the incomplete reduction of molecular oxygen (Desikan et al., 2005a). Different forms of ROS occur as a result of energy transfer to oxygen or from sequential addition of electrons (Apel and Hirt, 2004) (Figure 1.13).

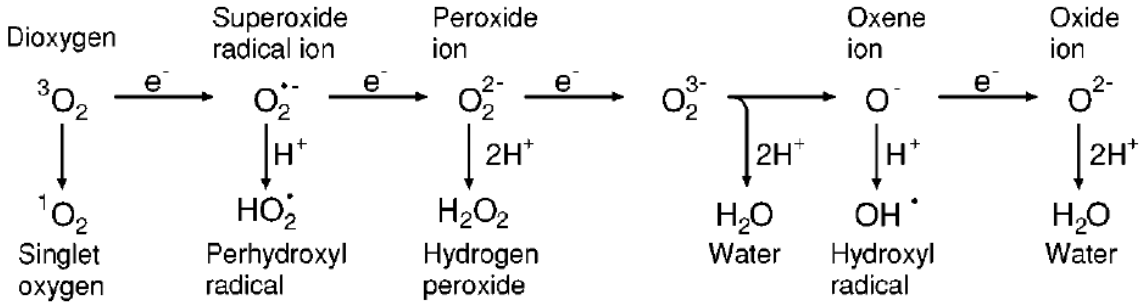


Figure 1.13 Generation of different types of ROS through energy transfer or sequential addition of electrons. Taken from Apel and Hirt (2004).

Under conditions of stress, disruption of cellular homeostasis can lead to the build up of ROS which can cause oxidative damage due to their reactive nature (Halliwell, 2006). For example, ROS can lead to damage of cellular membranes by reacting with lipids in the membranes to cause lipid peroxidation (Moller et al., 2007). Thus ROS have traditionally been linked with cellular damage and the complex mechanism evolved by plants in order to detoxify ROS produced by metabolism and stress reinforce the notion of ROS as sources of cellular stress (Apel and Hirt, 2004).

1.6.1 *ROS as signalling molecules*

However, it is becoming clear that ROS are not just toxic, unwanted by-products of metabolism and stress, but are actively produced by the plant as important signalling molecules which are required for normal developmental processes and cellular signalling in addition to acting in stress responses (Bailey-Serres and Mittler, 2006). ROS as signalling molecules are produced in response to a number of different stresses and stimuli such as hormones (Kwak et al. 2003), high light (Mullineaux et al., 2006), UV irradiation (Jansen and van den Noort, 2000), cold, drought, salt (Xiong et al., 2002) and fungal (Allan and Fluhr, 1997) and bacterial elicitors (Desikan et al., 2008).

Since ROS are produced in response to such a wide range of stresses and stimuli, it is perhaps not surprising to find that ROS act as ‘cellular indicator of stress’ and therefore utilised for signalling purposes (Mittler, 2002). However, there are key differences in the ROS produced as signalling molecules by the plant as opposed to ROS produced as a result of perturbation of cellular homeostasis, one of which is the source of the ROS.

Enzymes dedicated to ROS production for the purpose of signalling have been identified, the most well studied being NADPH oxidase, called RBOH (respiratory burst oxidase homolog) in *Arabidopsis*. In *Arabidopsis*, 10 *RBOH* genes (*Atrboh A-J)* have been identified (Torres et al., 1998), of which *AtrbohD* and *F* encode for NADPH oxidase subunits involved in responses to pathogen attack and hormone-triggered stomatal closure (Torres et al., 2002; Kwak et al., 2003; Torres et al., 2005). In addition to NADPH oxidases, cell wall-bound peroxidases, xanthine oxidase (XOD) and amine oxidase also act as enzymatic sources of ROS in plants (del Rio et al., 2002; Mittler, 2002; Mahalingam and Fedoroff, 2003; Desikan et al., 2005a).

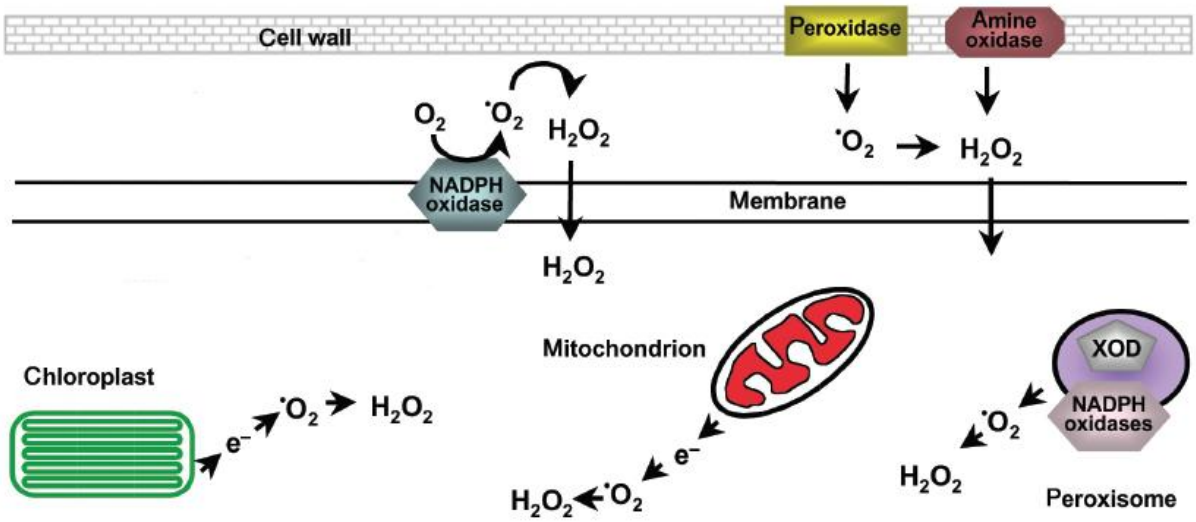


Figure 1.14 Diagram depicting the different sources of cellular ROS. ROS are produced as by-products of normal cellular respiration in the mitochondrion and during photosynthesis in the chloroplast. Additionally, ROS are produced as signalling molecules by membrane bound NADPH oxidases, by xanthine oxidase (XOD) in peroxisomes and also by cell wall bound peroxidases and amine oxidases. Figure taken from Mahalingam and Federoff (2003).

Although ROS include other molecules in addition to H_2O_2, such as superoxide ($O_2^{\cdot-}$), singlet oxygen ($^1O_2$) and the hydroxyl radical ($OH^{\cdot}$) (Desikan et al., 2005a), H_2O_2 is the most well studied as it has the characteristics needed to act as a signalling molecule: it is relatively stable, can cross biological membranes to move some distance from its source of production and plants possess the mechanisms needed to detoxify this molecule (Foyer and Noctor, 2005).

In addition to ROS, reactive nitrogen species (RNS) are also emerging as important signalling molecules, although the discussion here will focus on ROS.

1.6.2 *ROS detoxification*

As ROS are essentially cytotoxic, mechanisms for detoxification are in place to remove ROS and thus detoxification also play a role in signalling in plants. Cellular detoxification of ROS includes both enzymatic and non-enzymatic mechanisms. Enzymes which contribute to removal of ROS include superoxide dismutase (SOD) which converts $O_2^{\cdot-}$ to the less reactive H_2O_2 and catalase (CAT) which can convert H_2O_2 to H_2O and O_2 (Apel and Hirt, 2004). The enzymes ascorbate peroxidase (APX), dehydroascorbate peroxidase (DHAR) and glutathione reductase (GR) form part of the ascorbate-glutathione (A-G) cycle which catalyses the reduction of H_2O_2 using the antioxidants ascorbate (ASC) and glutathione (GSH) (Apel and Hirt, 2004) (Figure 1.15). In addition to contributing to the A-G cycle, GSH can also directly act as a reductant for H_2O_2 catalysed by glutathione peroxidase (GPX) (Apel and Hirt, 2004). As the ratio of reduced and oxidised forms of the antioxidants is dependent on the amount of ROS present, the cycling of antioxidants between reduced and oxidised states can provide information regarding the cellular redox status of the cell (Foyer and Noctor, 2005).



Figure 1.15 The ascorbate-glutathione (A-G) cycle in which H_2O_2 is converted to H_2O. This reaction is catalysed by ascorbate peroxidase (APX) using ascorbate (ASC) as the reducing agent which is oxidised to dehydroascorbate (DHA). Regeneration of ASC is mediated by dehydroascorbate reductase (DHAR) using reduced glutathione (GSH) which is in turn oxidised (GSSH). At the end of the cycle, GSH is regenerated by the action of glutathione reductase (GR) with NAPDH acting as the reducing agent. Figure modified from Neill et al. (2002)

In summary, ROS play a dual role in stress responses acting as both cellular stressors and important signalling molecules. The role of ROS as signalling molecules can be separated from its potential to cause cellular stress through controlled, enzymatic production and detoxification of ROS, control of the spatial distribution and timing of production. In order to act as a signal, mechanisms to sense ROS need to be in place in order to initiate downstream responses, such as changes in target protein activity or activation of target gene transcription. How exactly ROS are sensed and the mechanisms by which this is transduced into

physiological responses in plants is still not entirely clear, although modification of protein structure appear to be an important mode by which ROS signalling exerts its cellular effects.

1.7 ROS sensing

Modification of protein structure by ROS is an important mechanism for perception of ROS and modification of protein activity. In this way, the activity/function of proteins can be 'switched' on or off depending on the oxidative state of the cell (Paget and Buttner, 2003). One mechanism by which ROS can modify the activity of target proteins is through the oxidation of amino acid thiol groups, such as those of cysteine and methionine residues, where modification possibly leads to changes in protein conformation and therefore protein activity (Desikan et al., 2005a; Hancock et al., 2006; Moller et al., 2007) (Figure 1.16). Reversal of these modifications is also possible through reduction of the oxidised thiol groups by the action of thioredoxins and glutaredoxins, allowing redox-sensitive proteins to adjust activity according to cellular redox status (Paget and Buttner, 2003; Hancock et al., 2006).

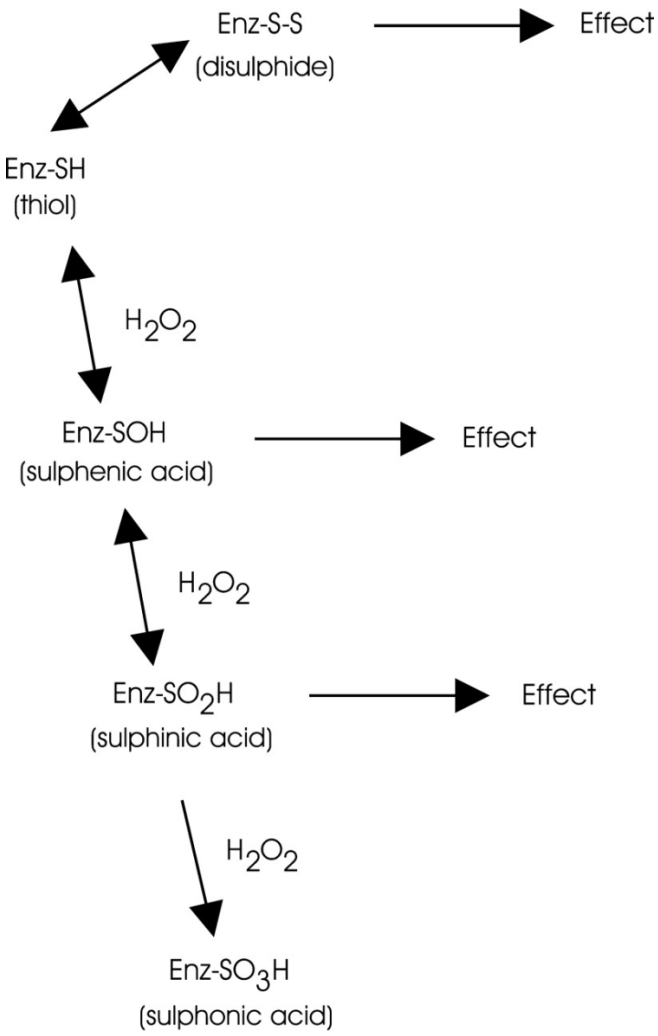


Figure 1.16 Oxidation of cysteine thiol groups by H_2O_2 in proteins. Disulphide bonds can form in the presence of two thiol groups. The product of single oxidation gives rise to unstable sulphenic acid, with further successive oxidations possible resulting in more stable products which may result in irreversible changes to protein structure. Modification of protein structure through oxidation may also affect protein activity. Taken from Hancock et al. (2006).

An example of a redox sensitive protein is the transcription factor Rap2.a which regulates expression of 2-Cys Peroxiredoxin-A (2CPA), a chloroplastic antioxidant enzyme which prevents oxidative damage of chloroplastic proteins, in a redox-dependent manner (Konig et al., 2002). Shaikhali et al. (2008) showed that under mild oxidising conditions, Rap2.4a formed dimers, the formation of which correlated with increased Rap2.4a activity and transcription of the *2CPA* gene. Under reducing conditions, Rap2.4a was present as inactive monomers. By altering the activity of Rap2.4a according to redox status, expression of the 2CPA antioxidant occurs only when needed (i.e., under oxidative stress) (Figure 1.17). Under high oxidative stress, Rap2.4a formed oligomers, which were inactive and unable to bind DNA. Rap2.4a was found to have three cysteine residues outside of the DNA-binding motif

which were proposed to mediate disulphide bond formation in the dimers and oligomers under oxidising conditions, although this was not shown conclusively (Shaikhali et al., 2008).

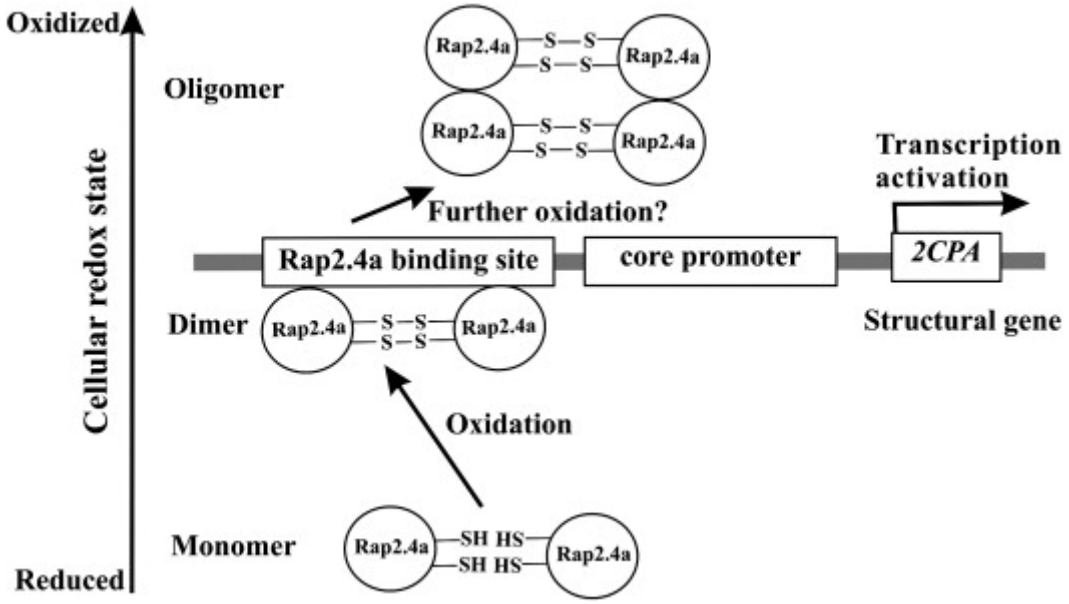


Figure 1.17 Redox control of Rap2.4a transcriptional activity. Under reducing conditions, Rap2.4a exists mainly as monomers, which are inactive. Under mildly oxidising conditions, Rap2.4a forms dimers through disulphide bonds between cysteine residues in Rap2.4a, which then binds to a Rap2.4a binding site (CE3-like element) to activate transcription of the *2CPA* gene. Under highly oxidising conditions, Rap2.4a form inactive oligomers. Taken from Lushchak (2011).

In addition to transcription factors, redox control of proteins involved in signalling is also possible. An example is NPR1 (non-expressor of *PR* genes 1) which controls the transcription of SA-responsive genes and is discussed in Section 5.1.3.5. Another example is the ethylene receptor ETR1 which mediates H_2O_2-induced stomatal closure. This activity requires the presence of the Cys-65 residue as the *etr1-1* mutant (which carries a Cys-65Tyr mutation) but not the *etr1-3* mutant (which carries an Ala-31Val mutation) was defective in H_2O_2-induced stomatal closure (Desikan et al., 2005b). It is possible that H_2O_2 modifies ETR1 activity through oxidation of the Cys-65 residue, although this has not yet been demonstrated. ETR1 belongs to the plant histidine kinases of the two-component system, which mediate responses to stimuli by activating downstream proteins though a series of phosphorylation events (Hwang et al., 2002; Desikan et al., 2005a). Histidine kinases involved in ROS sensing have also been identified in yeast and cyanobacteria (Singh, 2000; Kanesaki et al. 2007), suggesting this group of kinases may have key roles in ROS perception and signalling although how exactly ROS is perceived by the histidine kinases is not known.

1.8 Histidine kinases in perception of stimulus and signal transduction

An important mechanism used for intracellular signalling is the phosphorylation of proteins mediated by protein kinases which transfer the phosphoryl group from ATP to a histidine, serine, threonine or tyrosine residue within the target protein (Grefen and Harter, 2004). One class of proteins which function in this way are the histidine kinases.

Histidine kinases (HKs) of the two-component systems (TCS) were originally identified in prokaryotes, but in addition to bacteria are now known to function in yeast, amoeba and, more recently, in plants where they act as sensors of environmental and endogenous signals and in stress and developmental signalling (West and Stock, 2001; Schaller et al., 2008).

Upon detection of stimuli, HKs autophophorylate on a histidine residue, triggering a relay of phosphotransfer events resulting in the phosphorylation of a response regulator (RR), the activity of which is modified to effect cellular changes in response to the stimuli (Grefen and Harter, 2004; Schaller et al., 2008). HKs have a modular structure, each domain of which shows conservation of structure and function and are key to the phosphorelay events (Stock et al., 2000). These key HK modules are:

- the input/sensor domain that detects stimuli
- the transmitter/HK domain, containing a conserved histidine residue that gets autophosphorylated and
- the receiver domain, containing a conserved aspartic acid residue which gets phosphorylated

There are two types of HKs:

- the orthodox/prototypical HKs consisting of an input domain and a transmitter/HK domain, found mostly in prokaryotes
- the hybrid HKs consisting of an input domain, a transmitter/HK domain and a receiver domain, found mostly in eukaryotes

The RR which is the final recipient of the phosphoryl group consists of a receiver domain and an output domain. The response regulator is responsible for mediating cellular responses to stimuli and can act as transcription factors or act to modify the function of downstream proteins (Stock et al., 2000; Grefen and Harter, 2004; Romir et al. 2009).

The general structures of the two types of HKs are shown in Figure 1.18. In the prototypical TCS, detection of a stimulus by the input domain of the HK leads to autophosphorylation of the conserved histidine residue within the transmitter/HK domain (Grefen and Harter, 2004). This phosphoryl group is then transferred to the conserved aspartic acid residue of the receiver domain of the RR, leading to a conformational change in the output domain of the protein (Lohrmann and Harter, 2002). This conformational change leads to activation (or inactivation) of RR activity (Lohrmann and Harter, 2002) (Figure 1.18a). As phosphotransfer occurs between two components (the HK and the RR), this system was named the two-component system. However in the case of hybrid HKs, a multistep phosphorelay mechanism is used and involves an intermediary histidine-containing phosphotransfer domain (HPt) protein. After autophosphorylation of the transmitter/HK domain, the phosphoryl group is first transferred to the conserved aspartic acid residue of the receiver domain of the HK before being transferred to the conserved histidine residue of the HPt protein and finally to the RR (Grefen and Harter, 2004) (Figure 1.18b).

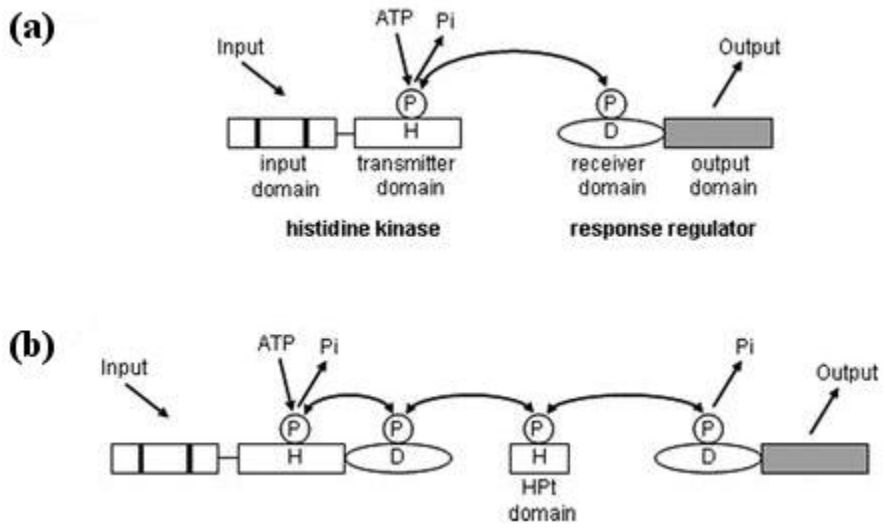


Figure 1.18 Schematic depicting the histidine kinase and hybrid histidine kinase of the single- and multi-step two-component signalling systems (respectively). Stimulus ('input') is perceived by the input domain, causing autophosphorylation on a conserved histidine (H) residue within the transmitter domain of the histidine kinase. (a) In the single-step two-component signalling pathway, the phosphoryl group is transmitted directly to the conserved aspartic acid (D) residue within the receiver domain of the response regulator. (b) In the multi-step two-component signalling pathway, a relay of phosphotransfer events occur, where the phosphoryl group is transferred first to the receiver domain of the histidine kinase, subsequently to an intermediate histidine-containing phosphotransfer (HPt) domain protein and finally to the receiver domain of the response regulator. Phosphorylation of the response regulator causes a conformational change in the output domain, resulting in a response ('output') mediated by the altered activity of the response regulator. Figure modified from Grefen and Harter (2004).

The following two subsections will describe two examples in which a prototypical HK and a hybrid HK have been studied in detail and shown to have important roles in sensing and reacting to external stimuli.

1.8.1.1 The Escherichia coli EnvZ/OmpR phosphotransfer system

Initially identified in bacteria, the prototypical HK is more prevalent in bacteria such as *E. coli* in which 23 orthodox HKs have been identified along with five hybrid HKs (Mizuno, 1997). The *E. coli* HK EnvZ which is involved in bacterial response to osmotic stress is an example of a prototypical HK. On detection of osmotic stress, EnvZ autophosporylates on the conserved histidine residue and the phosphoryl group is transferred in a single step to the RR OmpR (Forst and Roberts, 1994). OmpR acts as a transcription factor to differentially regulate the expression of OmpF and OmpC, proteins which form pores in the outer membrane of gram-negative bacteria and allow the diffusion of hydrophilic molecules across the membrane (Benz, 1988; Lan and Igo, 1998) (Figure 1.19). Under low osmotic stress, OmpF is expressed at low levels, the expression of which is increased under mild osmotic stress in addition to activation of expression of OmpC (Forst and Roberts, 1994; Lan and Igo, 1998). On high osmotic stress however, the expression of OmpF is repressed and expression of OmpC increases (Forst and Roberts, 1994; Lan and Igo, 1998). Although loss of OmpF and OmpC function result in sensitivity to osmotic stress, how exactly these proteins mediate tolerance to hyperosmolarity is not clear (Kaeriyama et al., 2006; Wang et al., 2007).

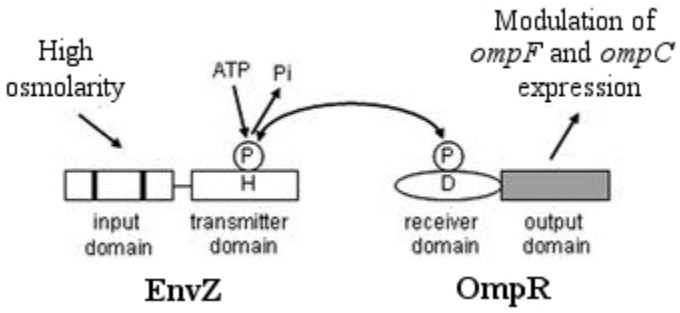


Figure 1.19 The EnvZ/OmpR phosphotransfer system of *E. coli.* This system modulates the expression of the bacterial outer membrane porins OmpF and OmpC in response to high osmolarity. High osmolarity is sensed by the input domain of the HK EnvZ, causing autophosphorylation on the conserved histidine (H) residue within the transmitter/HK domain. The phosphoryl group is transferred to a conserved aspartic acid (D) residue within the receiver domain of the RR OmpR, activating OmpR the activity of which modulate expression of the *ompF* and *ompC* porin genes. Figure modified from Grefen and Harter (2004)

1.8.1.2 The high-osmolarity glycerol (HOG) pathway of yeast

More prevalent in the eukaryotes are the hybrid HKs which use a multistep phosphorelay mechanism involving intermediary phosphotransfer proteins. The function of hybrid HKs in sensing/response mechanisms can be illustrated by the well studied high-osmolarity glycerol response (HOG) pathway in yeast (*Saccharomyces cerevisae*) which is activated by and required for tolerance to hyperosmotic conditions.

The HOG pathway can be activated by two branches, one of which involves the hybrid HK SLN1 which possesses an extracellular sensory domain and cytoplasmic HK and receiver domains (Posas et al., 1996). In this example SLN1 activity inhibits, rather than activates, signalling. Under normal conditions, the hybrid HK SLN1 autophosphorylates, triggering phosphorylation of the response regulator SSK1 via the intermediary HPt protein YPD1 (Hayashi and Maeda, 2006). SSK1 is responsible for activation of the downstream MAPK cascade in response to osmotic stress and in its phosphorylated form, SSK1 is inactive and unable to do so, resulting in suppression of osmotic responses (Hayashi and Maeda, 2006). Under high osmolarity, SLN1 is not phosphorylated preventing downstream phosphorelay events, leaving SSK1 unphosphorylated and active; active SSK1 is then able to activate the downstream MAPK cascade through sequential phosphorylation of the MAPK kinase kinase (MAPKKK) SSK2/SSK22, the MAPK kinase (MAPKK) PBS2 and finally the MAPK HOG1 which then activates responses to osmotic stress (Posas et al., 1996; Saito and Tatebayashi, 2004) (Figure 1.20). An alternative branch of the HOG pathway is the SHO1 branch which converges with the SLN1 branch at PBS2 (Saito and Tatebayashi, 2004) (Figure 1.20). Activation of the HOG pathway leads to protective responses such as increase in intracellular glycerol content to raise the water potential of the cell in to reduce water loss (Albertyn et al., 1994).

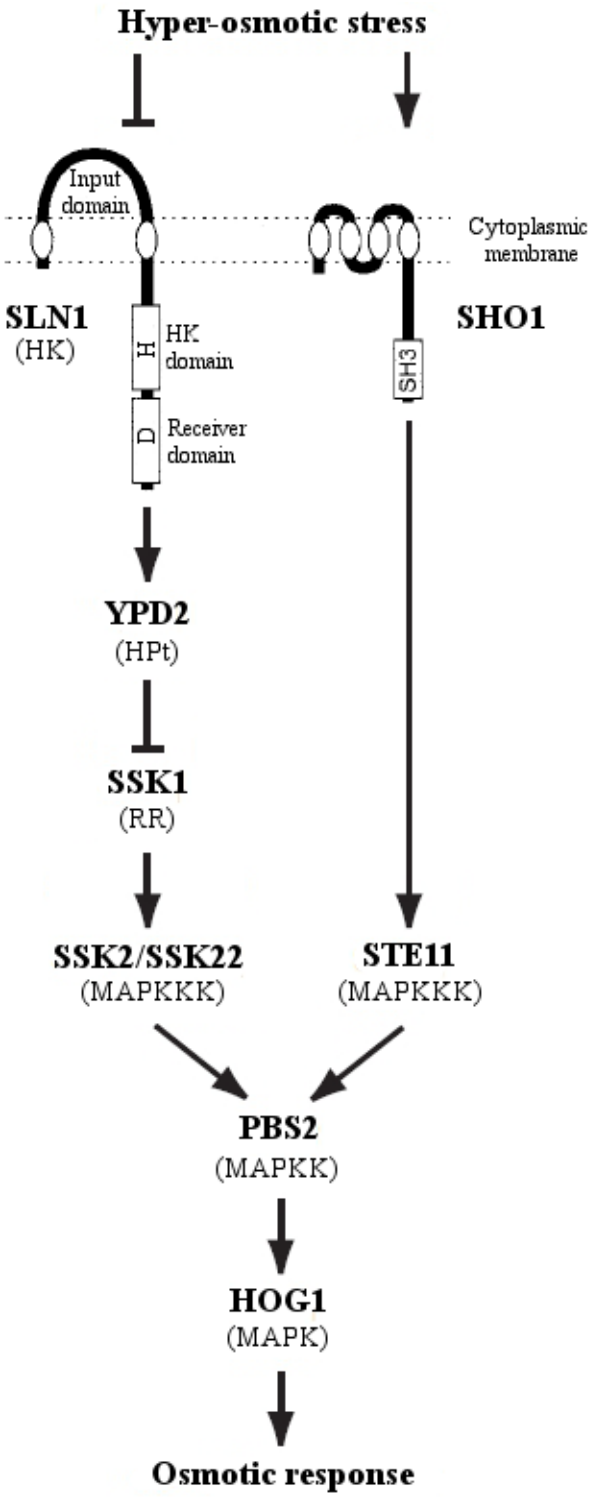


Figure 1.20 The high-osmolarity glycerol response (HOG) pathway of yeast. Under high osmolarity, inhibition of the autophosporylative activity of SLN1 leads to inhibition of the phophorelay from SLN1 to the HPt containing protein YPD1 and subsequently to the response regulator (RR) SSK1. In its unphosphorylated form, SSK1 is active and able to trigger the downstream MAPK signal signalling pathway involving SSK2/SSK22 (MAPKKKs), PBS2 (MAPKK) and HOG1 (MAPK) which leads to activation of osmotic stress responses. In addition to the SLN1 branch of the HOG pathway, the SHO1 branch is also activated in response to hyper-osmotic stress which converges with the SLN1 branch at PBS2 which is activated by the MAPKKK STE1 (Saito and Tatebayashi, 2004). Figure modified from Hayashi and Maeda (2006) and Reiser et al. (2003).

Although the SLN1 signalling cascade has been extensively studied and well understood, how SLN1 detects osmotic stress is still not clear, but possibly does so through detection of changes in turgor pressure. In a study by Reiser et al. (2003), mimicking loss of turgor caused by osmotic stress through permeabilisation of the yeast membrane with the antifungal agent nystasin led to activation of the HOG pathway. The HOG pathway was activated in wild-type and the *ste11* mutant but not in either the *ssk2* or the *ssk2 ssk22* double mutant, suggesting the SLN1 branch of the HOG pathway was specifically activated (Reiser et al., 2003). Additionally, removal of the cell wall to mimic the loss of contact of the cytoplasm with the plasma membrane that occurs under osmotic stress also resulted in phosphorylation of HOG1 and required functional SSK2/SSK22 (Reiser et al., 2003).

Interestingly, a number of hybrid HKs from *A. thaliana* are able to complement loss of SLN1 function in yeast (Tran et al., 2007; Tran et al., 2010), suggesting conservation of function of HKs across different species.

1.8.2 *Histidine kinases in* A. thaliana

In plants, the histidine kinases of the two-component system are emerging as important sensors of environmental and endogenous stimuli and mediators of cellular signalling (Urao et al., 2000a; Hwang et al., 2002; Grefen and Harter, 2004).

To date, eight HKs have been identified in *Arabidopsis* that are known to function in ethylene signalling (ETR1 and ERS1, which are class I ethylene receptors (Gamble et al., 2002)), as an osmosensor (AHK1/AtHK1) (Urao et al., 1999), as cytokinin receptors (AHK2, AHK3 and AHK4/CRE1/WOL) (Kakimoto, 1996, 2003), in megagametophyte development (CKI1) (Pischke et al., 2002) and more recently as an integrator of environmental and endogenous signals (AHK5/CKI2) (Desikan et al., 2008). In addition, roles of HKs as important mediators in stress signalling in plants is emerging with links to responses to temperature (Jeon et al., 2010), salt, osmotic and drought stress (Zhao and Schaller, 2004; Tran et al., 2007; Wang et al., 2008a; Wohlbach et al., 2008; Tran et al., 2010).

Of these eight HKs, all bar one (ERS1) are of the hybrid type, and in addition to these eight HKs, three divergent HKs have also been identified, all of which are ethylene receptors (Urao et al., 2001; Hwang et al., 2002; Grefen and Harter, 2004; Schaller et al., 2008) (Figure 1.21). These divergent HKs, ETR2, EIN4 and ERS2 which are classed as class II ethylene receptors

based on sequence homology, seem to lack conserved residues which are required for HK activity (Urao et al., 2001; Moussatche and Klee, 2004; Mizuno, 2005).

There are five motifs which are conserved and characteristic of the HK domain: the H box which contains the conserved histidine residue that is autophosphorylated on activation of the HK, and the N, G1, G2 and F box motifs which form a nucleotide binding cleft to which ATP, the source of the phosphoryl group, binds to and is hydrolysed by the ATPase activity of the HK (Stock et al., 2000; Hwang et al., 2002). Although both ETR2 and ERS2 have C-terminal receiver domains typical of the hybrid HKs, ETR2 lacks four of the conserved HK motifs (the H, N, G1 and F box) and ERS2 lacks all five and both also have the conserved histidine residue substituted with glutamate and aspartate residues, respectively (Hwang et al., 2002; Moussatche and Klee, 2004). Whereas EIN4 possesses the conserved histidine residue found in the H box, it lacks the other four motifs (Hwang et al., 2002; Moussatche and Klee, 2004). Evidence suggests that ETR2, ERS2 and EIN4 may not act as HKs, but as serine/threonine kinases as they have been shown to autophosphorylate on serine residues *in vitro* (Moussatche and Klee, 2004).

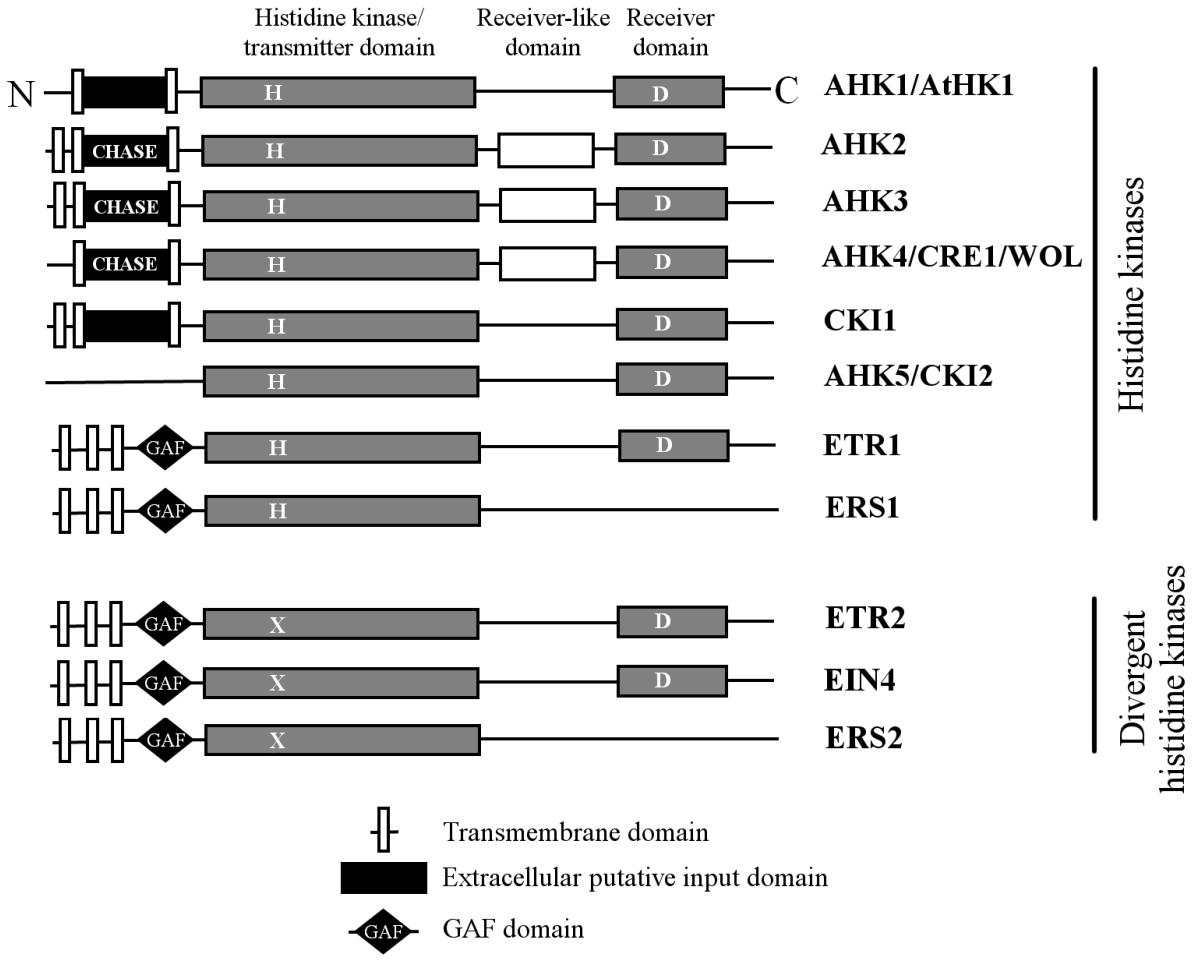


Figure 1.21 Structures of the eight histidine kinases and the three divergent histidine kinases identified in *A. thaliana*. An 'X' denotes the absence of conserved HK motifs. The CHASE domain binds cytokinin; the function of the GAF domain is unknown. (Figure adapted from Hwang et al. (2002) and Schaller et al. (2008)).

The functions of each of the eight HKs of *A. thaliana* are described in the following sections.

1.8.2.1 ETR1 (Ethylene Response 1)

ETR1 was the first of the *A. thaliana* HKs to be identified as having homology to HKs of the TCS and shows partial functional redundancy with the other ethylene receptors ERS1, ERS2, ETR2 and EIN4 (Chang et al., 1993; Taiz and Zeiger, 1998). Although the high homology between ETR1 with HKs and the ability of ETR1 to autophosphorylate on the conserved histidine residue at position 353 would suggest that HK activity is involved in ETR1 function, abolition of HK activity, mutation of the G2 box or truncation of the ethylene receptor did not seem to affect ethylene signalling through ETR1 (Gamble et al., 2002; Moussatche and Klee, 2004). In addition, H_2O_2-induced stomatal closure mediated by ETR1

did not require HK activity since the truncated version of ETR1consisting of the first 349 N-terminal amino acids (and therefore lacking the HK domain) and the G2 box mutant were still able to trigger stomatal closure in response to H_2O_2 (Desikan et al., 2005b).

Evidence has emerged implicating the HK activity of ETR1 in promotion of plant growth independent of ethylene, which may explain why its HK activity seems to be dispensable for ethylene signalling (Gamble et al., 2002; Cho and Yoo, 2007). A common assay to test for ethylene sensitivity is by the 'triple response' of seedlings in response to growth under darkness; ethylene production induced under darkness inhibits hypocotyl and root elongation, exaggerates apical hook formation and causes thickening of the hypocotyl of seedlings (Taiz and Zeiger, 1998). By transforming a HK-inactive form of *ETR1* cDNA in which the conserved histidine residue was replaced with a glutamine residue (*cETR1*^{H353Q}) into the *etr1-7* loss of function background, Cho and Yoo (2007) found that hypocotyl growth of these transgenic seedlings were much slower than that of the *etr1-7* mutant or wild-type plants, suggesting ETR1 HK activity contributes to growth. Furthermore, the presence of silver (a competitive inhibitor of ethylene signalling) resulted in increased hypocotyl elongation in the *etr1-7* mutant (through inhibition of the other four ethylene receptors which act redundantly to ETR1) to the same extent seen in wild-type plants; inhibition of ethylene signalling by silver did not enhance elongation in *cETR1*^{H353Q} seedlings (Cho and Yoo, 2007). It was therefore suggested that the defect in growth of the *cETR1*^{H353Q} line was not due to modulation in ethylene production or sensitivity, but to the loss of the HK activity of ETR1, suggesting the function of ETR1 as an ethylene receptor can be separated from its function as a HK (Cho and Yoo, 2007). In further support of this, Cho et al. (2007) found that whereas growth of *etr1-7* mutant plants under light was indistinguishable from wild-type plants, *cETR1*^{H353Q} transgenic plants were much smaller.

Interestingly, transfection of *etr1-7* protoplast with a luciferase reporter gene construct under the control of the Type-B *Arabidopsis* response regulator (ARR) ARR6 promoter resulted in increased reporter gene activity when cotransfected with wild-type *ETR1*or a constitutively active form of *ETR1,* but not when transfected with a HK-inactive versions of *ETR1* (Cho and Yoo, 2007). This suggests that ETR1 acts as a HK as part of the TCS.

However, Voet-van-Vormzeele and Groth (2008) found that full-length ETR1 and a truncated version missing the transmembrane domains ($ETR1_{165\text{-}738}$) autophosphorylated *in vitro* and whereas this autophosphorylation of full-length ETR1 was inhibited in the presence of

ethylene or the ethylene agonist cyanide, autophosphorylation of $ETR1_{165-738}$ was not inhibited by these compounds, suggesting a link between the function of ETR1 as an ethylene receptor and as a HK (i.e., HK activity of ETR1 is modulated by ethylene). More recently, Bisson and Groth (2010) found evidence to suggest modulation of ETR1 phosphorylation by ethylene influences its interaction with EIN2, an integral membrane protein required for ethylene signalling (Taiz and Zeiger, 1998). It was shown that the unphosphorylated form of ETR1, which occurs in the presence of ethylene, promotes interaction of ETR1 with EIN2 and absence of ethylene which results in autophosphorylation of ETR1 decreased the affinity of ETR1 for EIN2. Whether this interaction is required for ethylene signalling was not shown and together with studies indicating ETR1 HK activity is not required for ethylene signalling leaves the question as to whether the TCS is involved in modulating ethylene signalling unanswered.

1.8.2.2 AHK2, AHK3, AHK4/CRE1/WOL

The cytokinin receptors AHK2, AHK3 and AHK4/CRE1/WOL have very similar structures and loss of function of these HKs leads to insensitivity to cytokinin, as measured by typical cytokinin responses such as inhibition of root growth and formation, cell proliferation and greening of calli (Higuchi et al., 2004). AHK3 and AHK4/CRE1/WOL were shown to bind cytokinin in a heterologous system (*E. coli*) using a *lacZ* reporter gene driven by an *E. coli* promoter regulated by the RcsB bacterial RR; in this system, reporter gene activity was shown to increase in the presence of AHK3 or AHK4/CRE1/WOL in a cytokinin-dependent manner (Yamada et al., 2001). Additionally, direct binding of cytokinin to these receptors observed *in vitro* suggest direct activation of signalling through the TCS by binding of cytokinin to AHK3 and AHK4/CRE1/WOL (Yamada et al., 2001).

The cytokinin receptors are also involved in tolerance to salt and drought stress and AHK2, AHK3 and AHK4/CRE1/WOL were able to complement loss of function of SLN1 in the yeast *sln1/sho1* double mutant when grown on media containing 0.3M NaCl, conditions under which the mutant could not survive (Tran et al., 2007; Tran et al., 2010). That AHK2, AHK3 and AHK4/CRE1/WOL can interact with HPts to activate a response regulator in a heterologous system suggests conserved function of HKs in different organisms. Interestingly, AHK4/CRE1/WOL was only able to complement the *sln1/sho1* mutant in the presence of cytokinin (Tran et al., 2007; Tran et al., 2010). This finding reflects the function of AHK4/CRE1/WOL as both a kinase and a phosphatase, the activity of which is modulated

by cytokinin; in the presence of cytokinin, the phosphatase activity of AHK4/CRE1/WOL is inhibited and kinase activity activated, with the opposite seen in the absence of cytokinin (Mähönen et al., 2006a). Presence of cytokinin also enhanced salt and drought tolerance conferred to the *sln1/sho1* mutant by AHK2 and AHK3, albeit to a lesser extent (Tran et al., 2007; Tran et al., 2010). In plants, AHK2 and AHK3 seem to act as negative regulators of salt and drought tolerance, as *ahk2* and *ahk3* knockout mutants were more tolerant to both salt and drought stress (Tran et al., 2007). AHK4/CRE1/WOL was also found to negatively regulate salt tolerance as the *ahk4* mutant was also more resistant to high salinity (Tran et al., 2007). In addition to functions in salt and drought stress tolerance, AHK2 and AHK3 are also required for normal development of vascular tissue (Hejatko et al., 2008). Thus the cytokinin receptors function in both developmental processes and in stress responses.

1.8.2.3 CKI1 (Cytokinin Independent 1)

CKI1 was first identified in a T-DNA activation tagging screen for genes involved in cytokinin signalling (Kakimoto, 1996, 1998). However, CKI1 does not contain the extracellular CHASE domain involved in cytokinin binding (Heyl et al., 2007) and phylogenetic analysis suggests CKI1 is not closely related to the cytokinin receptors AHK2, AHK3 and AHK4/CRE1/WOL (Urao et al., 2001; Hwang et al., 2002; Schaller et al., 2008). Additionally, cytokinin binding activity of CKI1 could not be shown and it was therefore suggested that CKI1 does not act as a cytokinin receptor (Yamada et al., 2001). CKI1 plays a role in plant development and has been shown to be required for the process of megagametogenesis (Pischke et al., 2002; Hejátko et al., 2003). However, overlap between CKI1 and AHK2/AHK3 signalling has been demonstrated. Hetjatko et al. (2008) found that loss of function mutants *ahk2* and *ahk3* which are defective in cytokinin regulated vascular tissue development could be partially rescued by over-expression of CKI1 in a cytokinin-independent manner. In addition, active CKI1 could phosphorylate the Type-B ARR2, which is also activated in a cytokinin-dependent manner by AHK2 and AHK3, with inactive CKI1 inhibiting ARR2 activation by AHK2, AHK3 and AHK4/CRE1/WOL (Hejatko et al., 2008). This overlap in CKI1 and AHK2, AHK3 and AHK4/CRE1/WOL activity on downstream components of the TCS would explain how CKI1 may be linked to cytokinin signalling without acting as a cytokinin receptor.

1.8.2.4 AHK1/AtHK1

AHK1/AtHK1 was first identified as acting as an osmosensor and similar to AHK2 and AHK3, AHK1/AtHK1 was also shown to have a function in salt and drought tolerance, but as a positive regulator of tolerance to these stresses (Tran et al., 2007). *ahk1* knockout mutants were less tolerant to salt and drought stress, whereas *AHK1/AtHK1* over-expression lead to increased tolerance (Urao et al., 1999; Tran et al., 2007; Wohlbach et al., 2008).

1.8.3 *HPt domain proteins and response regulators in* A. thaliana

Downstream of the HKs are the histidine-containing phosphotransfer domain (HPt) proteins which act to transfer the phosphate group from the HK receiver domain to an *Arabidopsis* response regulator (ARR) (Figure 1.18b). The *Arabidopsis* genome encodes five *Arabidopsis* HPt proteins (AHPs), AHP1, AHP2, AHP3, AHP4 and AHP5, and a pseudo-AHP APHP1/AHP6 (Schaller et al., 2008). Table 1.3 summarises interactions known to occur between *A. thaliana* HKs and AHPs.

Table 1.3 Interaction matrix summarising known interactions between HKs and AHPs of *A. thaliana.* Letters denote method used to study interaction: Y = yeast two-hybrid, PD = pull down, F = fluorescence spectroscopy, B = bimolecular fluorescence complementation. [1] Urao et al. (2000b), [2] Dortay et al. (2006), [3] Scharein et al. (2008), [4] R. Desikan, personal communication.

	AHP1	**AHP2**	**AHP3**	**AHP4**	**AHP5**
AHK1/AtHK1		Y[1]			
AHK2	Y[2], PD[2]	Y[2], PD[2]	Y[2], PD[2]		Y[2], PD[2]
AHK3	Y[2], PD[2]	Y[2], PD[2]	Y[2], PD[2]		Y[2], PD[2]
AHK4/CRE1/WOL	Y[2], PD[2]	Y[2], PD[2]	Y[2], PD[2]		Y[2], PD[2]
CKI1		Y[1]	Y[1]		
AHK5	B[4]	B[4]			B[4]
ETR1	Y[1], F[3]	Y[1]	Y[1]		
ERS1					

The *Arabidopsis* genome also encodes for 23 ARRs and nine pseudo-responses regulators (Schaller et al., 2008). Active, phosphorylated ARRs mediate the activity of downstream proteins (Type-A ARRs) or acts as transcription factors to modify gene expression (Type-B ARRs) (Sakai et al., 2000; Schaller et al., 2008).

To date, the role of ARRs and HPt proteins in signal transduction has been most well studied in cytokinin responses. Type-A ARRs act as negative regulators of cytokinin responses (To et al., 2004), whereas Type-B ARRs act as positive regulators in addition to activating transcription of some Type-A ARR genes in a cytokinin-dependent manner (Mason et al., 2005; Argyros et al., 2008; Ishida et al., 2008). Additionally, all five HPt proteins function in cytokinin signalling, with AHP1, AHP2, AHP3 and AHP5 mediating positive responses to cytokinin and AHP4 and the pseudo-HPt protein AHP6 acting in a negative capacity (Hutchison et al., 2006; Mähönen et al., 2006b). The Type-A ARR2 has also been linked to ethylene signalling downstream of ETR1 (Hass et al., 2004).

It can be envisaged that signalling through the HKs in plants is controlled by the cellular location of the different HKs, AHPs and ARRs and the outcomes of signalling dependent on the combinations of AHPs and ARRs utilised by each HK (Urao et al., 2000b; Schaller et al., 2008). A yeast two-hybrid screen carried out by Dortay et al. (2008) to identify potential interactors of the three HK cytokinin receptors of *Arabidopsis*, AHP5 and 13 ARRs known to be involved in cytokinin signalling identified 160 interactions, indicating the complexity of HK signalling networks. Downstream interactors identified included those involved in signal transduction, protein metabolism, and metabolic and cellular processes. In addition, Dortay et al. (2008) found all three HKs interacted with non-TCS proteins, implicating interactions with signalling pathways outside of the TCS. It is apparent that there is still much to be learnt about TCS signalling in plants.

1.9 AHK5: an integrator of abiotic and biotic stress signalling?

AHK5/CKI2 is the most poorly characterised member and the only predicted cytosolic hybrid histidine kinase in *A. thaliana*, but has been shown to localise to both the cytosol and the plasma membrane (Hwang et al., 2002; Grefen and Harter 2004; Desikan et al. 2008). Recently, evidence has emerged placing AHK5 as a central mediator of abiotic and biotic stress signalling in *Arabidopsis* (Desikan et al. 2008).

AHK5 was initially identified with CKI1 in a T-DNA activation tagging screen for mutants altered in cytokinin responses, although the HK activity of AHK5 was found to be independent of cytokinin (Kakimoto, 1996, 1998; Iwama et al., 2007). The first report to investigate the function of AHK5 found that it was most highly expressed in the roots where it acts as a negative regulator of ETR1 dependent ABA/ethylene-induced inhibition of root elongation (Iwama et al. 2007). A more recent study by Desikan et al. (2008) suggests the action of AHK5 is not restricted to the roots and may act to integrate exogenous and endogenous stimuli in stomatal guard cells through regulation of H_2O_2 homeostasis.

Since guard cells are responsive to a number of stimuli due to their role in controlling gaseous exchange and in limiting water loss through transpiration, guard cells form attractive models for studying plant cell signalling (Blatt, 2000; Schroeder et al., 2001). Mutants of AHK5 were found to be defective in stomatal responses to H_2O_2, ethylene, darkness, presence of bacteria and to the bacterial flagellin peptide flg22 (Desikan et al., 2008). Although *AHK5* expression was found to be low in guard cells, application of exogenous H_2O_2 resulted in up-regulation of the *AHK5* transcript and AHK5 was also found to be redox-regulated (Desikan et al. 2008). Taken together, the evidence suggests that AHK5 acts as a central mediator of abiotic and biotic stress signalling triggered by H_2O_2 and the aim of this study was to investigate further the role of AHK5 in abiotic and biotic stress signalling.

1.10 General aims and objectives

Given the importance of AHK5 in stomatal responses to both abiotic and biotic stimuli, it was hypothesised that the role of AHK5 in stress signalling extends beyond that demonstrated in stomatal guard cells. To test this hypothesis, the requirement of AHK5 in response to various abiotic and biotic stresses was investigated and assessed phenotypically by comparison of wild-type *A. thaliana* Col-0 responses to the *ahk5-1* mutant carrying a T-DNA insertion in the receiver domain of the HK. This mutant was previously characterised by Iwama et al. (2007) and Desikan et al. (2008).

To extend on the study carried out by Iwama et al. (2007), the role of AHK5 in root growth response to heat, cold, salinity and osmotic stress was investigated. Root growth assays are commonly used to investigate plant responses to abiotic stress and have successfully been used to identify genes required for resistance to such stresses (Davletova et al., 2005; Verslues et al., 2006; Lee and Zhu, 2009). Where AHK5 was implicated in mediating

response to stress in seedling assays, validation of the findings was confirmed through studies in vegetative tissue.

Recent studies suggest that stomata actively prevent bacterial invasion of the leaf apoplast by detecting and closing in response to the presence of bacteria at the leaf surface (Melotto et al., 2006; Underwood et al., 2007; Zeng and He, 2010; Zeng et al., 2010). As AHK5 was implicated in stomatal defences against bacteria (Desikan et al., 2008), the role of AHK5 in mediating immune responses against the hemi-biotrophic pathogen *Pseudomonas syringae* pv. *tomato* DC3000 (*Pst*DC3000) beyond the initial infection stage was monitored by symptom development and *in planta* bacterial population growth. Since hormone signalling is known to play an important role in defence against bacterial pathogens, changes in the plant hormones salicylic acid (SA), abscisic acid (ABA) and jasmonic acid (JA) were monitored during the course of infection using LC-MS/MS.

In addition to *Pst*DC3000, infection with the necrotrophic fungal pathogen *Botrytis cinerea* was also investigated to determine whether the function of AHK5 extends across signalling pathways/responses activated by pathogens with different lifestyles.

Finally, in order to elucidate how AHK5 functions in signal transduction, identification of AHK5 interacting proteins through a tandem affinity purification (TAP) approach coupled with LC-MS/MS was attempted.

Chapter 2:

Methods

2 Methods

2.1 General methods for growth of plants

2.1.1 *Plant lines and growth conditions*

The wild-type and the *ahk5* mutant lines used in this study were of the Col-0 and Ws-4 background. The *ahk5-1* mutant line (SAIL_50_H11) in the Col-0 background was originally obtained from Syngenta and contains a T-DNA insertion in the receiver domain of *AHK5*. A complemented line (P_{35}-*AHK5/ahk5-1*) containing a construct for the expression of a GFP-fusion protein under the control of a 35S promoter was also used and generated as previously described by Desikan et al. (2008). In addition, plants containing a T-DNA insertion in the histidine kinase domain of *AHK5* in the Ws-4 background complemented with a TAPa tag fused to the C-terminal (C-TAPa tag; Rubio et al. (2005)) (referred to as P_{35S}-*AHK5/ahk5-3*) was used for the TAP purification procedure described in Section 2.2.5. All plant lines used here were previously characterised by Desikan et al. (2008) and genotyped by PCR. Figure 2.1 shows the position of T-DNA insertions in the *ahk5-1* and *ahk5-3* mutant lines.

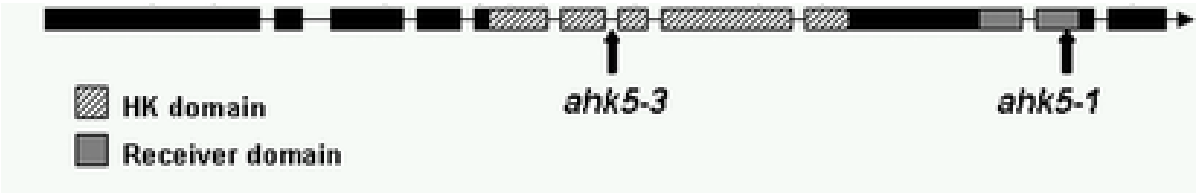


Figure 2.1 Gene structure of *AHK5* and the position of T-DNA insertion in the *ahk5-1* (Col-0 background) and *ahk5-3* (Ws-4 background) mutants. In the *ahk5-1* mutant, the T-DNA is positioned within an exon encoding part of the receiver domain whereas the *ahk5-3* mutant contains a T-DNA insertion within an intron of the predicted histidine kinase (HK) domain.

Plants were grown under short day conditions of 10 hours light/14 hours dark cycles with a light intensity of 120-150 µE m^{-2} s^{-1} at 23˚C and 55-65% relative humidity in seed and modular compost plus sand (Levington's F2+sand) (Scotts, UK) and were used when approximately 5-6 weeks old, unless otherwise stated.

2.1.2 *Generation and selection of complemented lines*

ahk5-1 was also complemented with full-length *AHK5* under the control of its endogenous promoter (3205 bases upstream of the ATG start codon). The construct was previously generated and inserted into the pENTRD/TOPO entry vector (Invitrogen, UK) and cloned by the LR reaction into the Gateway destination vector pMDC99 to generate vector pMKC111 as described by Desikan et al. (2008). pMKC111 was transformed into *Agrobacterium tumefaciens* strain GV101 and transformed into *ahk5-1* plants by vacuum transformation. Transformants were selected by resistance to Hygromycin B conferred by the presence of a Hygromycin-resistance maker gene carried on pMKC111. To select for complementation, seeds were surface sterilised by soaking in 100% ethanol for five minutes, followed by 10% bleach, 0.1% SDS for five minutes and subsequent rinsing in SDW six times. Sterilised seeds were suspended in 0.4% agarose and plated onto full-strength Murashige and Skoog (MS) medium (including vitamins) (pH 5.7) (Duchefa, The Netherlands) containing 1.5% agar and supplemented with 1% sucrose and 50µg ml^{-1} Hygromycin B (Duchefa, The Netherlands). Transformants were subjected to three rounds of selection to obtain homozygotes.

2.1.3 *Growth of* A. thaliana *in tissue culture*

Seeds were surface sterilised as described in Section 2.1.2. Surface-sterilised seeds of each line tested were sown onto the same 120mm square plate containing 50ml of half-strength Murashige and Skoog (MS) medium (Duchefa, UK) media in the same row to minimise variation caused by positional and plate to plate variation; each plate was divided vertically into sections for each line being tested so that seeds from each line were placed side by side as described by Davletova et al. (2005) and schematically shown in Figure 2.2. Plated seeds were incubated at 4°C in a cold room for 2 days before transfer to a growth chamber and maintained vertically under a 16 hours light/8 hours dark cycle with a light intensity of 120-150 µE m^{-2} s^{-1} at 23˚C and 55-65% relative humidity. The start of the seedling assays (day 0) was the day on which plates were transferred from the cold room to the growth facilities.

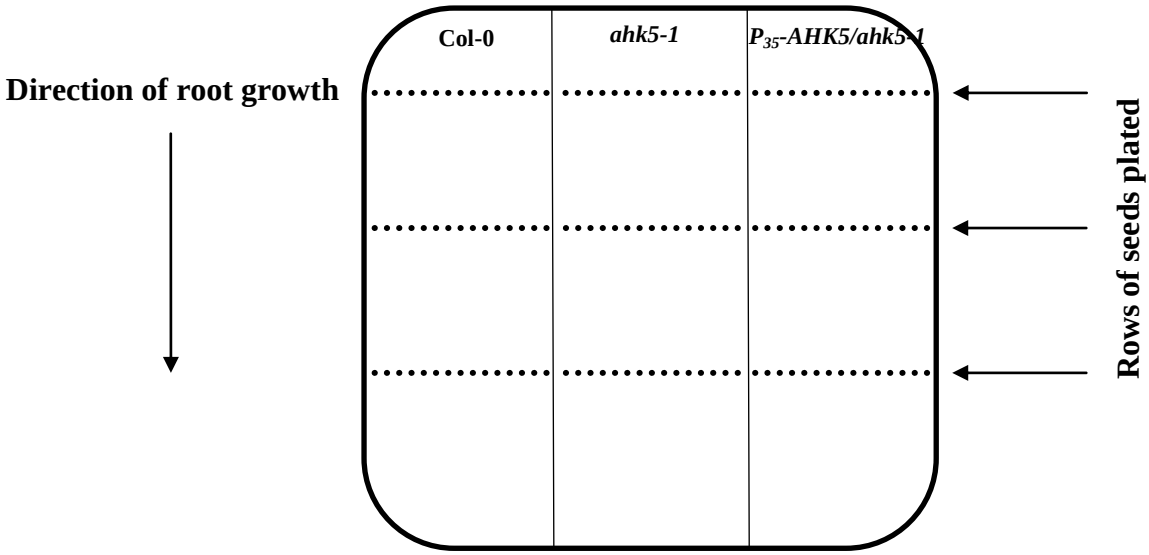


Figure 2.2 Schematic depiction of the arrangement of seeds on square plates used to assess seedling responses to abiotic stress. Plates were divided into columns for each line being tested and seeds for each line plated side by side so that seeds from each line were on the same plate and the same row. This example shows how three different lines (Col-0, *ahk5-1* and *P_{35}-AHK5/ahk5-1*) were arranged.

2.2 Molecular methods

2.2.1 *DNA extraction*

For genotyping of plants by PCR, crude DNA extracts were obtained by grinding leaf or seedling material in an eppendorf for 15-30 seconds before addition of 400µl DNA Extraction Buffer (200mM Tris-HCl (pH 7.5), 200mM NaCl, 25mM EDTA, 0.5% SDS). Samples were briefly mixed by vortexing and centrifuged at 14,000 x g for 1 minute to remove cellular debris. Three hundred microlitres of the supernatant was then mixed with an equal volume of isopropanol and centrifuged at 14,000 x g for 5 minutes. The DNA pellet was washed with 70% ethanol, air-dried and re-suspended in 100µl SDW.

2.2.2 *Genotyping of plants by PCR*

DNA extracted from plant tissue as described above was used to genotype plants. For genotyping of plants in the Col-0 and *ahk5-1* backgrounds, two primer pairs were used. Forward primer 5'-GCTGTGACGTATGGGACACTGG-3' (primer 1) and reverse primer 5'-CTCAGTGCAAATACTGTTGC-3' (primer 2) were used to detect the presence of wild-type *AHK5* in wild-type Col-0 and complemented lines. To test for the presence of T-DNA

insertion in the receiver domain of AHK5 in the *ahk5-1* background, forward primer 1 was used with reverse primer 5'- GCTTCCTATTATATCTTCCCAAATTACCAATACA-3' (primer 3) which binds within the T-DNA sequence.

For genotyping plants in the Ws-4 and *ahk5-3* background, two primer pairs were used which differed from those used for the Col-0 and *ahk5-1* background as the T-DNA insertion causing the *ahk5-3* mutation is located in the HK domain of AHK5. Forward primer 5'-TGTTTACAACAAAGCTCGCG-3' (primer 4) and reverse primer 5'-CAAATTGGTGAGGATCTGCC-3' (primer 5) were used to detect the presence of wild-type *AHK5* in wild-type Ws-4 and the P_{35S}-*AHK5/ahk5-3* complemented line. To test for the presence of T-DNA insertion, forward primer 4 and reverse primer 5'-CTACAAATTGCCTTTTCTTATCGAC-3' (primer 6) which binds within the T-DNA sequence were used.

PCR was performed using KAPA Taq DNA Polymerase (GRI, UK) in the following reaction mix:

10 x KAPA Taq Buffer B	2.5µl
25mM $MgCl_2$	2.3µl
10mM dNTPs	1µl
Forward primer (10µM)	1µl
Reverse primer (10µM)	1µl
Taq (1U μl^{-1})	1µl
DNA	2.5µl
SDW	13.7µl
Total reaction volume	25µl

General PCR conditions were as follows: initial denaturation at 95°C for five minutes followed by 35 cycles of denaturation at 95°C for 30 seconds, annealing for one minute at a

temperature dependent on the primer pair used and extension at 72°C for one minute. At the end of the 35 cycles, a final extension step at 72°C for 10 minutes was performed. Annealing temperature used for each primer pair were as follows:

- Primers 1 and 2: 55°C
- Primers 1 and 3: 55°C
- Primers 4 and 5: 50°C
- Primers 4 and 6: 48°C

PCR reactions were mixed with Orange G loading dye (30% glycerol, 0.2% (w/v) Orange G (Sigma)) and electrophoresed on a 1% agarose gel made up with 1xTAE (Tris-acetate-EDTA) buffer containing SYBR Safe DNA gel stain (Invitrogen, UK) at a concentration of 1 in 50,000. DNA was visualised on a Safe Imager blue-light transilluminator (Invitrogen, UK) and the image captured using the Gel Doc EQ scanner function of the Quantity One Image analysis software, version 4.5.2 (Biorad).

2.2.3 *Total RNA extraction and cDNA generation*

Total RNA was obtained from approximately 100mg of leaf tissue or seedling material by grinding the tissue in liquid nitrogen with a pestle and mortar and extracting total RNA with TRIZol Reagent (Invitrogen) according to manufacturer's instructions. RNA pellets obtained from the extraction were re-suspended in 20-50µl SDW (depending on the size of the pellet) and quantified using a Nano Drop Spectrophotometer ND-1000 (Labtech International, UK). Purity of the RNAs were determined by the ratio of absorbance at 260 and 280nm (A_{260}:A_{280}).

Total RNA used for cDNA generation was first treated with DNAse to remove contaminating DNA. Ten micrograms of total RNA was treated with two units of RQ1 RNase-Free DNase (Promega, UK) at 37°C for an hour and the reaction terminated at 65°C for 10 minutes. RNA was subsequently precipitated by sodium acetate/ethanol precipitation as described in Section 2.2.1 and resuspended in water to obtain the original volume of RNA used. The DNase treated RNA was used as template for cDNA generation using M-MLV Reverse Transcriptase (Promega) with Oligo(dT)$_{15}$ primer (Promega) in the following reaction mix:

Oligo(dT)$_{15}$ primer, 50ng µl^{-1} stock	1µl
5 x M-MLV RT buffer	8µl
dNTPs, 10mM stock	3.2µl
Template RNA	5µg
SDW	to 38µl
Total volume	38µl

The reaction mixture was incubated at 94°C for 5 minutes, then at 4°C for 5 minutes after which 1µl of M-MLV Reverse Transcriptase (200U µl^{-1}) (Promega) and 1µl of RNasin Ribonuclease Inhibitor (20-40U µl^{-1}) (Promega) was added to the mix and the reaction left to proceed at 42°C for 40 minutes. The reaction was terminated at 94°C for 5 minutes and subsequently used for RT-PCR or stored at -20°C.

2.2.4 *Confirmation of complementation by RT-PCR*

To determine whether the complemented *P$_{AHK5}$-AHK5/ahk5-1* lines described in Section 2.1.2 expressed the complementing *AHK5* gene, cDNA generated as described in Section 2.2.3 was used to test for the presence of the *AHK5* transcript. For this purpose, primers targeted to the end of *AHK5* after the site of T-DNA insertion were used. Forward primer 5'-CAAACCGGCTGCCTATAATC-3' (AHK5-F) and reverse primer 5'-TTGCAACGTTACAGGTTTCG-3' (AHK5-R) were used for RT-PCR. For normalisation of RT-PCR, forward primer 5'-GTGCCAATCTACGAGGGGTA-3' (ACT7-F) and reverse primer 5'-TTCTGCGGTAGTGGTGAACA-3' (ACT7-R) targeted to the Actin-7 gene were used.

The following reaction mixtures were used for each primer pair:

Sybr Green PCR Master Mix (Invitrogen)	5µl
AHK5-F, 2µM stock	1µl
AHK5-R, 2µM stock	1µl
cDNA	up to 3µl
Water	to 10µl
	10µl

Sybr Green PCR Master Mix (Invitrogen)	5µl
ACT7-F, 10µM stock	1µl
ACT7-R, 10µM stock	1µl
cDNA	up to 3µl
Water	to 10µl
	10µl

Amplification was carried out using the conditions as follows: initial denaturation at 95°C for 15 minutes followed by 40 cycles of denaturation at 94°C for 15 seconds, annealing for 30 seconds at 60°C (AHK5-F/AHK5-R) or 50°C (ACT7-F/ACT7-R) and extension at 72°C for 30 seconds. On completion of the 40 cycles, a final extension step at 72°C for 3 minutes was performed. PCR products were assessed by gel electrophoresis as described in Section 2.2.2.

2.2.5 *TAP purification*

The *P_{35S}-AHK5/ahk5-3* line containing a C-terminal TAPa tag was used for purification of AHK5 and interacting proteins. This line was previously generated and genotyped by Desikan et al. (2008). Seeds of this line were sown on 1% agar, 1xMS (pH 5.7) supplemented with 1% sucrose and grown under the conditions described in Section 2.1.3. Approximately 15g of 18 day old seedling material was collected and snap-frozen in liquid nitrogen for extraction of proteins for TAP purification.

Seedling material was ground to a fine powder using a pestle and mortar, thawed in 2x volume of Extraction Buffer (Appendix I) and centrifuged at 1,000 x g, 4°C for 10 minutes to pellet homogenised leaf tissue. The supernatant was collected and filtered through a layer of Miracloth to remove remaining debris. The protein extract was then either separated into cytosolic/soluble and microsomal membrane/insoluble proteins before concentration by acetone precipitation or concentrated by ultrafiltration using Amicon Ultra-15 Centrifugal Filter Units (Millipore, UK) with a molecular cut-off weight of 10KDa following manufacturers' instructions. Cytosolic and microsomal membrane proteins were extracted from the seedling material as described by Rivas et al. (2002) by ultracentrifugation of whole seedling extract in a Beckman Coulter Optima L-100 XP Ultracentrifuge at 100,000 x g, 4°C for 1 hour. The supernatant containing cytosolic proteins was collected and the remaining microsomal pellet re-suspended in Solubilisation Buffer (Appendix I) and ultracentrifuged at 100,000 x g, 4°C for 1 hour. Supernatant containing microsomal membrane proteins were then collected.

Concentration of cytosolic and microsomal proteins prior to TAP purification by acetone precipitation was as follows: four volumes of ice-cold acetone was added to the sample, vortexed and incubated at -20°C for one hour. Samples were then centrifuged for 10 minutes at 15,000 x g to pellet precipitated proteins. The supernatant was decanted and the pellet left to air dry for approximately 30 minutes before re-suspension in Extraction buffer (for cytosolic proteins) or Solubilisation buffer (for microsomal proteins) before commencement of the purification procedure. Cytosolic proteins were re-suspended in 12ml of buffer and microsomal proteins in 2ml of buffer.

Concentrated protein samples were subjected to TAP purification as described by Rubio et al. (2005) with some modifications. For the first purification step, IgG Sepharose^{TM} Fast-Flow beads (Amersham Biosciences, Sweden) were washed in 5x volume of Tris-Saline Tween

Buffer (Appendix I) and equilibrated with 3x volume of Wash Buffer (Appendix I) three times before incubation of beads with protein sample at 4°C for 2 hours with rotation. Five hundred microlitres of IgG beads was used for the cytotolic fraction and 200µl was used for the microsomal fraction. IgG beads were then washed three times in 10ml Wash Buffer and once with 10 ml Cleavage Buffer (Appendix I) before incubation of the beads for 1 hour at 4°C with rotation in 5 ml Cleavage Buffer containing 10 units of 3C protease (Prescision protease, Amersham Biosciences) to release IgG-bead bound proteins.

For the second step of purification, the resulting supernatant was incubated with 1ml of Ni-NTA His-Bind beads® Resin (Qiagen) at 4°C for 60 minutes. Prior to this, the Ni-NTA beads were equilibrated with 4ml of 1 x Ni-NTA Bind Buffer (Appendix I) in 15ml Falcon tubes. The beads were allowed to settle before the Ni-NTA Bind Buffer was pipetted off and sample added. The sample/bead mixture was then loaded onto polyprep chromatography columns (Novagen, UK). The flow-through was allowed to drip through the column by gravity, collected and re-loaded onto the column. The Ni-NTA beads were then washed three times with 10ml Wash Buffer and bead-bound proteins were eluted through the column with 5ml Elution Buffer (Appendix I) to obtain the final 'TAP' fraction containing the purified proteins. Fractions from each step of the purification process were collected and concentrated by acetone precipitation as described above in preparation for SDS-PAGE.

2.2.6 *Analysis of proteins by SDS-PAGE*

Protein samples were heated at 95°C for five minutes with 3x Laemmli SDS Sample Buffer (0.1875M Tris-HCl pH 6.8, 6% SDS, 0.3M DTT, 30% (v/v) glycerol, 0.03% (w/v) Bromophenol Blue) for analysis by SDS-PAGE on a 12.5% SDS gel. Pre-stained Broad Range SDS-PAGE Standards (Bio-Rad, UK) were run with the samples for estimation of protein size. SDS-PAGE gels were fixed for one hour in 7% acetic acid, 40% methanol, stained overnight with Brilliant Blue G (Sigma-Aldrige, UK) and then de-stained with 10% acetic acid, 25% methanol. Before Western Blotting, an image of the SDS-PAGE gel was captured using a Canon Scanner.

2.2.7 *Western blotting*

Western blotting was performed by sandwiching the SDS-PAGE gel with Hybond-P PVDF membrane (GE Healthcare, UK) between three pieces of Chromatography Paper (Whatman,

UK) and a Scotch Brite pad on either side as described by Sambrook and Russell (2006). The 'sandwich' was clamped together between two solid supports and the cassette placed in a blotting tank containing Transfer Buffer (Appendix II). Proteins were transferred overnight at 25mA at 4°C. Following transfer, the cassette was disassembled and the membrane blocked with Blocking Buffer (Appendix II) for one hour.

The blot was probed with a primary antibody raised in mouse against the 9xmyc epitope of the TAPa tag at a dilution of 1:1,000 in Blocking Buffer for one hour and then probed with secondary antibody (peroxidase conjugated anti-mouse IgG (Sigma-Aldrich, Germany)) at a dilution of 1:5,000 and the signal developed using Amersham ECL^{TM} Western Blotting Analysis System (GE Healthcare, UK) according to manufacturer's instructions. Membranes were developed using chemiluminescence and autoradiography.

2.3 Abiotic stress treatments

2.3.1 *Stress treatments in tissue culture*

Salinity, osmotic, heat stress and cold stress treatments were performed on seedlings grown in tissue culture as described in Section 2.1.3.

For salt and osmotic stress, the media on which seeds were sown were supplemented with the appropriate stressor. Salinity stress was achieved by the addition of sodium chloride (NaCl) to the medium to concentrations of 25, 50, 100 and 150mM and osmotic stress by addition of sorbitol to concentrations of 50, 100, 200 and 300mM. The osmolarity of these concentrations of NaCl and sorbitol were measured using an Osmometer (Camlab Roebling, UK). The ionic effect of NaCl was compared to KCl by growth of seedling on plates supplemented with 50 and 100mM KCl.

For heat stress, seedlings were tested for both basal and acquired heat tolerance. To test basal heat tolerance, 7 day old seedlings in light were stressed by incubation at 38°C for 8 hours or 42°C for 1, 1.5 or 2 hours and root length measured after an additional 2 days in a growth chamber at 23°C. For acquired heat tolerance, 7 day old seedlings were subjected to the following stress regime as described by Larkindale et al. (2005): 38°C for 90 minutes, followed by recovery for 120 minutes at 22°C, heat stress at 45°C for 120 minutes and recovery for 3 days in a growth chamber at 23°C before measurement of root length.

In addition to heat stress, plants were also subjected to cold stress of 10°C for 24, 48 and 72 hours and root length measured after 3 days recovery in a growth chamber at 23°C. Controls for heat and cold stress remained in a growth chamber for the duration of the experiments and measured at the same time point as stressed seedlings.

2.3.2 *Analysis of seedling growth*

At the appropriate time point, seedlings were removed from the plates and root length measured with a ruler to an accuracy of +/- 0.5mm. For salinity and osmotic stress, root length was measured after 7 days growth. Root length of heat and cold stressed plants were measured after three days recovery in growth conditions described in Section 2.1.3.

2.3.3 *Salinity stress in mature plants*

For salinity stress in mature plants, 3 week old plants were watered with 250mM NaCl five times during a two week period and control plants treated with water. On Day 0, plants were given the first dose of saline solution by watering with 30ml of salt solution directly into each pot. Plants were watered in the same fashion three times a week for two weeks, resulting in a total of six watering events. The aerial portion of the plant was then harvested on the third day after the last watering dose for determination of fresh shoot weight. Figure 2.3 depicts the treatment regime used.

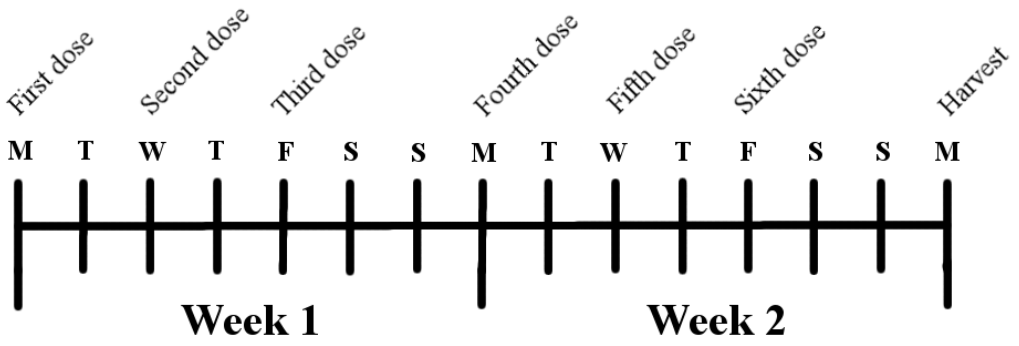


Figure 2.3 Watering regime used to treat mature plants with a solution of 250mM NaCl. Each dose consisted of 30ml of 250mM NaCl. Controls were treated with the same volume of water.

After determination of fresh weight, each shoot was individually wrapped in foil, dried at 120°C in an oven for at least 24h and re-weighed for determination of water content as a proportion of dry weight (FW-DW/DW).

2.3.4 *Drought stress in mature plants*

Drought stress was performed by withholding water for 10 days, after which shoots were harvested for determination of fresh weight and water content as described above in Section 2.3.3. Wild-type and *ahk5-1* mutant plants were placed on the same tray and the tray rotated on a daily basis to prevent positional effects on drying during the experiment.

2.4 Biotic stress treatments

2.4.1 *Bacterial strains and growth*

Strains of *Pseudomonas syringae* pv. *tomato* DC3000 (*Pst*DC3000) and *Pseudomonas syringae* pv. *phaseolicola* 1448A (*Pph*1448A) used in this study were provided by J. Mansfield (Imperial College London) and are listed in the Table 2.1 below. Bacteria were grown on solid Pseudomonas Agar F Base medium (Merck, Germany) at 25°C for two days for maintenance of bacterial strains and enumeration of bacterial populations or in liquid Luria Bertani (LB) broth with the appropriate antibiotics (see Table 2.1) overnight at 25°C with shaking for inoculation of plants.

Table 2.1 Strains of *Pseudomonas* used in this study and antibiotic concentrations used to culture these strains.

Strain	Antibiotics
*Pst*DC3000	Rifampicin 50µg ml^{-1}
*Pst*DC3000(*hrpA*-)	Rifampicin 50µg ml^{-1}, Kanamycin 20µg ml^{-1}
*Pst*DC3000(*avrRpm1*)	Rifampicin 50µg ml^{-1}, Kanamycin 20µg ml^{-1}
*Pph*1448A	Rifampicin 50µg ml^{-1}

2.4.2 *Bacterial inoculation and symptom scoring*

Bacterial cells grown overnight in liquid culture were pelleted by centrifugation at 4,000 x g for 10 minutes, re-suspended in 10mM $MgCl_2$ and diluted to the appropriate bacterial density by estimation from the optical density reading at 600nm (OD_{600}) using a spectrophotometer.

For correlation of OD_{600} to number of colony forming units per ml (cfu ml^{-1}) of bacterial suspension, serial dilutions of the bacterial suspension in Ringer's solution (Merck, Germany) were plated onto solid media and the resulting number of colonies formed used to correlate OD_{600} readings with cfu ml^{-1} (Appendix III).

For syringe infiltration of bacteria, bacterial cultures were processed and adjusted to the appropriate OD_{600} as described above. Bacterial suspension was infiltrated into the leaf by lightly nicking the abaxial leaf surface with a razor blade and then infiltrating with a needleless syringe. Plants were maintained in a growth chamber for the duration of the experiments. Leaf discs were removed either side of the site of infiltration at the appropriate time points using a 0.5cm diameter cork borer and both leaf discs placed in a 1.5ml eppendorf containing 500µl Ringer's Solution. Leaf discs were homogenised using plastic grinders and serial dilutions plated onto solid media described above. After two days growth, colonies were counted and the number of colonies per cm^2 of leaf area calculated. Visual development of symptoms of infiltrated leaves were monitored over days and severity scored on a scale of 0 (no symptoms) to 7 (complete collapse and dried) as devised by J. Mansfield.

For surface inoculation of bacteria, 0.04% Silwet L-77 (Lehle Seeds, USA) (v/v) was added to the bacterial suspension as a wetting agent and gently coated onto both the adaxial and abaxial sides of the leaf. Plants were maintained in a growth chamber for the duration of the experiment and covered with a lid to increase humidity. To determine *in planta* population counts of bacteria after surface inoculation, leaves were weighed before surface sterilisation with 70% ethanol for one minute. The leaves were then blotted with tissue, rinsed for one minute in SDW to remove residual ethanol and blotted again before grinding in 500µl of Ringer's solution. Serial dilutions were then plated onto solid media as described above for enumeration of bacterial populations.

2.4.3 *Estimation of chlorophyll content*

To quantify the severity of symptoms as a result of surface inoculation of *Pst*DC3000 onto leaves of wild-type and mutant plants, the chlorophyll content of inoculated leaves were measured. Leaves were removed at different time points post-inoculation, weighed, snap-frozen in liquid nitrogen and stored at -80°C until use. Chlorophyll was extracted from whole leaves in 10ml of 100% methanol at 50°C for 1 hour in a waterbath and absorbance of the methanolic extracts were measured at wavelengths of 665 and 652nm in a spectrophotometer. Chlorophylls a and b (nmol ml^{-1}) content was calculated using Equation 2.1 and Equation 2.2 below, respectively, as described by Porra et al. (1989). Total chlorophyll content was expressed as the sum of chlorophylls a and b.

Equation 2.1: **Chl a =** $(16.29 \times A_{665}) - (8.54 \times A_{652})$

Equation 2.2: **Chl b =** $(30.66 \times A_{652}) - (13.58 \times A_{665})$

2.4.4 *Electrolyte leakage*

Electrolyte leakage as a measure of cell death was performed as described by Mackey et al. (2003) with modifications. Ten leaf discs of 1cm diameter from five leaves were immediately removed after syringe infiltration with *Pst*DC3000(*avrRpm1*) and floated on 10ml SDW for 30 minutes with gentle shaking to wash the leaf discs. The wash water was then replaced with 10ml fresh SDW (this point was considered as the starting point of the experiment (t=0)) and the leaf discs were placed under conditions used for plant growth (see Section 2.1.1) and electrolyte leakage measured at different time points using an inoLab TetraCon 325 conductivity meter (WTW GmbH & co. KG, Germany). At the end of the experiment, the leaf discs were boiled in the water in which they were floated for 20 minutes and once cooled, the amount of electrolytes released was measured as above. This measurement was considered as total amount of releasable electrolytes and electrolyte leakage at the time points measured was expressed as a percentage of this as shown in Equation 2.3 below.

Equation 2.3:

$$\textbf{Electrolyte leakage (\%)} = \frac{\text{Electrolyte leakage at given time point}}{\text{Total amount of releasable electrolytes}} \times 100$$

2.4.5 *Inoculation with* Botrytis cinerea *and assessment of disease progression*

Botrytis cinerea isolated from strawberry (provided by JW Mansfield) was cultured on potato glucose agar (Fluka Sigma-Aldrich) supplemented with 500µg ml^{-1} spectinomycin and incubated at 18-20°C under Mini Black Light Blue fluorescent lamps emitting long-wave UV lighting (Phillips) for seven days. Spores were harvested by flooding the plate with SDW and fungal hyphae removed by passing the suspension through a layer of Miracloth (Calbiochem Merck) without centrifugation. Spore concentration was determined using a haemocytometer and adjusted to a concentration of $4x10^5$ spores ml^{-1} and then mixed with an equal volume of quarter-strength Potato Dextrose Broth (PDB) (Fluka Sigma-Aldrich) to give a final spore suspension of $2x10^5$ spores ml^{-1} in 1/8th strength PDB.

Symptom development was assessed on detached leaves. Leaves were cut at the base of the plant so that the petiole remained attached to the leaf. The petiole was wrapped in tissue to act as a wick for water uptake to prevent wilting during the course of the experiments. The leaves were placed in transparent boxes onto strips of plastic mesh placed on top of moist tissue lining the boxes with their abaxial surface facing upwards and their tissue-wrapped petioles in contact with the moist tissue. The moist tissue was used to maintain humidity and the plastic mesh was used to prevent the leaf blade from touching the tissue lining the box, as this encouraged rotting of the leaves. The leaves were then inoculated with 10µl droplets of spore suspension on the abaxial side either side of the midrib of the leaf. The photo in Figure 2.4 shows how the leaves were arranged for the experiment. Symptom development/ lesion spread was assessed by visual inspection using a numerical scoring system with a minimum score of 0 representing no symptoms and a maximum score of 4 denoting collapse of the leaf and sporulation of the fungus.



Figure 2.4 Photograph showing experimental setup for assessment of symptom development in detached leaves in response to inoculation with *B. cinerea*.

To assess the effect of wounding prior to infection with *B. cinerea* as previously described by Chassot et al. (2008b), the abaxial side of the excised leaf was scraped with a razor blade and *B. cinerea* inoculated as described above at the site of wounding.

2.5 Histological observations

2.5.1 *Trypan Blue staining for cell death*

To visualise cell death *in planta* in response to infiltration with *Pst*DC3000(*avRpm1*), leaves were stained by boiling for two minutes in 0.025% (w/v) Trypan Blue (Sigma-Aldrich, UK) in a mixture of glycerol, lactic acid, phenol and water in a 1:1:1:1 ratio. The leaves were left to cool in the staining solution for 2-3hours before de-staining in saturated chloral hydrate (5g of chloral hydrate to every 1ml of water).

2.5.2 *Trypan blue staining of leaves infected with B. cinerea*

Fungal hyphae on leaves were visualised by Trypan Blue staining as described by Xiao et al. (2003). Leaves were decolourised in an 8:1:1:1 mixture of ethanol:phenol:lactic acid: glycerol for 24 hours, during which the solution was changed twice. Leaves were then soaked for 30 minutes in 0.025% (w/v) Trypan Blue in a 1:1:1 mixture of lactic acid:glycerol:water, cleared in saturated chloral hydrate as described above.

2.5.3 *Detection of ROS via DAB staining*

Presence of reactive oxygen species in leaves was detected by staining with DAB (3,3-diaminobenzidine) (Sigma-Aldrich, UK) at a concentration of 1mg ml^{-1} water (pH 3.8). Excised leaves were floated on DAB solution with the abaxial side of the leaf in contact with the stain and vacuum infiltrated for 5 minutes. The leaves were then incubated at room temperature in the dark for four hours, after which leaves were de-stained in 100% ethanol.

2.5.4 *Aniline blue staining for callose deposition*

To visualise callose deposits in response to fungal infection, leaves were de-stained in 100% ethanol and stained in 0.05% (w/v) Aniline Blue (Sigma-Aldridge) in 150mM K_2HPO_4 buffer (adjusted to pH 8 with KOH) overnight.

2.5.5 *Preparation and analysis of slides*

Stained leaves were washed in 10% glycerol and mounted in 60% glycerol on glass slides in preparation for observation under a stereo and/or light microscope.

Leaves and fungal hyphae prepared for microscopic examinations were examined with either a stereomicroscope (Leica MZ16F, UK) and images captured by an attached Leica DFC300FX camera or with a Zeiss AxioSkop2 Plus Microscope and Images captured by an attached Zeiss AxioCam and analysed with the AxioVision 3.1 software (Zeiss).

Measurement of fungal hyphae was performed using a Leica compact microscope and analysed with Leica QWin Software. Analysis and quantification of staining was performed using the ImageJ software (Abramoff, 2004).

2.6 Analytical methods

2.6.1 *Amplex red*

Seedlings were plated and grown for five days on half-strength Murashige and Skoog medium as described in Section 2.1.3. Seedlings were then transferred to half-strength liquid Murashige and Skoog in 24 well plates. Each well contained 1ml of media and four seedlings per well, with a total of 48 seedlings used per time point per treatment per line. After a further three days of growth under conditions described in Section 2.1.3, the media was replaced

with fresh medium supplemented with 100mM NaCl. The time at which the media was replaced was considered as time t=0. At the appropriate time point, seedlings were removed from the wells, briefly blotted dry and ground in liquid nitrogen. Ground tissue was weighed and H_2O_2 extracted from samples in potassium phosphate buffer, pH 6.5 using 200µl buffer per 30mg of tissue. Samples were spun at maximum speed on a bench top centrifuge for two minutes to remove cellular debris. The supernatant was then diluted 1 in 2 in potassium phosphate buffer and 50µl of this dilution was added to a 950µl Amplex Red (Invitrogen) reaction mixture. The complete reaction mixture contained:

Amplex Red (Invitrogen)	5µl
Horseradish peroxidise	4µl
Potassium phosphate buffer, pH 6.5	941µl
1 in 2 dilution of sample supernatant	50µl
	1000µl

The reaction mixture was incubated at room temperature for 30 minutes in the dark and fluorescence measured using a Luminescence Spectrophotometer (Perkin Elmer Instruments, USA) with excitation set at 530±12.5nm and emission at 580±25nm.

Known amounts of H_2O_2 (Sigma-Aldrich) were added to Amplex Red reaction mixtures to construct a calibration curve to relate fluorescence of samples to H_2O_2 concentration in the sample (Appendix IV).

2.6.2 *Determination of Na^+ and K^+ content*

Seedlings grown on 100mM NaCl for analysis of salt stress in tissue culture as described in Section 2.3.1 were harvested after seven days growth for determination of Na^+ and K^+ content. Seedlings were rinsed four times in SDW, blotted on filter paper (Whatman International Ltd, UK), wrapped in foil and dried in an oven at 80°C for 24 hours. The dried tissue was milled with a steel ball using a Tissue Lyser (Retsch for Qiagen) at 20Hz for two minutes. Ions were extracted from 5mg of milled tissue by boiling in 2ml of Ion

Chromatography grade water (Fluka Analytical Sigma-Aldrich) for 30 minutes. Samples were spun at 14,000 x g for 20 minutes and the supernatants filtered through Amincon Ultracel Ultra Centrifugal Filters with a molecular cut off weight of 10,000 (Millipore, Ireland) to remove debris. 1ml of sample was injected into an 861 Advanced Compact Ion Chromatography machine (Metrohm, Switzerland) and eluted through a 200µl loop with Cation Eluent (1.7mM Nitric acid (Fluka Analytical, UK), 0.7mM 2-6-pyridine carboxylic acid (Fluka Analytical, UK) in water purified with a Milli-Q Plus 185 purifier (Millipore)) and ions detected by conductivity. Identification and concentration of Na^+ and K^+ in samples were based on the known retention times of these ions and by comparison of the conductivity measurement of the samples to those of a calibration curve constructed from a dilution series of a Multication Standard solution containing 10.0mg kg^{-1} ± 0.2% of each of the cations of Li^+, Na^+, K^+, Mg^{2+}, Ca^{2+} (Fluka Analytical Sigma-Aldrich) (Appendix V).

2.6.3 *Induction of camalexin by silver nitrate and extraction for use as a standard*

Six five week old plants were sprayed with a 10mM solution of silver nitrate ($AgNO_3$) (VWR, UK) with 0.002% Silwet L-77. Treated plants were kept under a plastic cover and leaves collected three days after treatment when discrete lesions were apparent.

Camalexin was extracted from approximately 5g of treated leaf tissue in 50ml 60% methanol overnight. The methanolic extract was heated in a water bath at 37°C and solvent evaporated off under vacuum using a rotary evaporator. The extract was re-suspended in 2ml ethanol and solvent evaporated off under vacuum to remove residual water. The extract was then re-suspended in 2ml ethanol and applied to 2cm origins over two thin-layer chromatography (TLC) polyamide 11 F_{254} plates (Merck). The plates were developed in chloroform: methanol (20:1). Plates were examined under UV light at a wavelength of 375nm using a Universal UV Unit (model number 51438) (Gelman Instrument Company) under which camalexin can be seen as a fluorescent band. The fluorescing band of camalexin was marked using a pencil and the silica gel containing the camalexin scraped from the plate using a razor blade. Camalexin was extracted from the silica gel by soaking in 5ml methanol. The extracts were spun at 4,000 x g prior to analysis to remove the silica gel and stored at -80°C until use.

To measure the amount of camalexin obtained, a scan of the absorption spectrum of the methanolic extract at wavelengths in the range of 240-400nm was performed using a spectrophotometer. Camalexin has a distinct an extinction coefficient of 14,800M^{-1} cm^{-1} at

318nm in methanol (Soylu, 1998) and absorption at this wavelength was used to calculate camalexin concentration using the Beer-Lambert equation $A=\xi CL$, where A=absorption, ξ=extinction coefficient, C=concentration and L=length of light path (cm).

2.6.4 *Extraction of camalexin in lesions induced by* **Botrytis cinerea**

Leaves were inoculated with *B. cinerea* spores suspended in $1/8^{th}$ strength PDB as described in Section 2.4.5 above. Ten lesions from five leaves were collected by carefully cutting around the lesion perimeter with a razor blade and weighed for separate extractions of camalexin from each individual lesion.

The lesions were freeze-dried and camalexin extracted in 200µl of 30% methanol with a tungsten bead using a Tissue Lyser at 30Hz for 1 minute and left to soak for 15 minutes. Samples were then centrifuged at 13,200rpm for 15 minutes and the supernatant collected. The remaining pellet was re-extraction as above a further two times. The supernatants from the successive extractions were collected and pooled for analysis by high-pressure liquid chromatography.

2.6.5 *Measurement of camalexin by high-pressure liquid chromatography*

For measurement of extracted camalexin, samples were subjected to high-pressure liquid chromatography (HPLC) using an Agilent 1200 HPLC system with a Phenomenex C-18 column (100x2mm dimension, 3µm particle size). Sample injections of 20µl were used and solvent consisting of H_2O:CH_3CN (7:3) pumped isocratically at a temperature of 35^oC and a flow rate of 0.25ml min^{-1}. Detection and identification of camalexin was based on a retention time of 13.5 min and detection of camalexins characteristic fluorescent spectra (excitation = 318nm, emission = 385nm) using a Shimadzu RF535 fluorescence detector. An authenticated standard provided by B. H. Halkier, University of Copenhagen, was used as a reference. Quantification of camalexin in samples was calculated in reference to a calibration curve obtained by running known amounts of camalexin standard to produce a calibration curve (Appendix VI). Acquisition and integration of data was performed using Agilent Chemstation software.

2.6.6 *Identification of proteins*

For LC-MS/MS analysis of proteins obtained from the TAP purification, proteins in the fractions from each step of the purification were separated by SDS-PAGE on a 12% SDS gel and bands of interest were excised and subjected to in-gel tryptic digest. Gel bands were destained twice for 25 minutes at 37°C in 200mM ammonium bicarbonate in 50% acetonitrile and then dehydrated by Speed Vac. The gel bands were then rehydrated with 20µl of 10mM DTT in 100mM ammonium bicarbonate at 57°C for one hour. This solution was then replaced with 20µl of 55mM iodoacetamide in 100mM ammonium bicarbonate, incubated in the dark for 45 minutes and then dehydrated with acetonitrile and washed with 100mM ammonium bicarbonate twice. The gel slice was then dehydrated by Speed Vac and subsequently rehydrated in 20µl of Working Trypsin (Appendix VII) Solution containing Promega Sequencing Grade Trypsin for 20 minutes at room temperature, after which 50µl of Trypsin Digestion Buffer (Appendix VII) was added and in-gel trypsin digestion performed by incubation at 37°C overnight. After digestion, the supernatant containing peptides was removed to a clean silated tube. The remaining gel slice was washed with enough volume of 50% acetonitrile to cover the gel slice and the wash added to the supernatant. The volume of the peptide sample was reduced to 2µl and the volume made up to 15µl with 1% acetonitrile acidified with 0.1% formic acid.

Proteins obtained from the tryptic digest were analysed by LC-MS/MS on an Agilent 1100 G1376A system nanoflow LC. Eight microlitres of sample was injected onto a C18 nanoflow trap column and washed isocratically with 2.5% acetonitrile and 0.1% formic acid. A 59 minute gradient at a flow rate of 0.3µl min^{-1} was applied to elute the sample onto a separation column (25µm fused silica capillary). Buffer A consisted of 94.9% water, 5% acetonitrile and 0.1% formic acid and buffer B contained 4.9% water, 95% acetonitrile and 0.1% formic acid. The column oven was heated to and maintained at 40°C for the analysis using a Linear Ion Trap Quadrupole LC-MS/MS Mass Spectrometer (QTrap, AB Sciex Instruments). The acquisition program was set to select for the four most intense peaks with *m/z* ratios between 400 and 1500 and charge states of +2 and +3 (first MS step) for further analysis by collision-induced dissociation with the application of rolling collision energy (second MS step). LC-MS/MS outputs were acquired using the Analyst 1.4.2 software and processed using the MASCOT algorithm (Hirosawa et al., 1993).

Reliable identification of proteins by MASCOT were based on:

1. the significance of the score given to the match by MASCOT
2. matching one or more peptides to the same protein
3. the origin of the protein (i.e., whether or not they are identified as *Arabidopsis* proteins)
4. the correlation of the molecular weight of the matched protein to the size at which the protein band migrated on SDS-PAGE gel.

Further information based on BLASTP analysis of each protein identified was obtained using The Arabidopsis Information Resource (TAIR) website (www.arabidopsis.org) (Swarbreck et al., 2008).

2.6.7 *Hormone extraction and analysis*

Leaves for hormone extraction were inoculated by syringe infiltration as described previously (Section 2.4.2) and harvested at the appropriate time points. For each biological sample, three leaves from three plants were pooled. For each plant line, treatment (i.e., inoculated with bacterial suspension or 10mM magnesium chloride) and time point used, three biological replicates were analysed. Harvested leaves were wrapped in foil, frozen in liquid nitrogen and stored at -80°C until freeze-drying prior to extraction.

Hormones were extracted as described by Forcat el al. (2008). Freeze-dried leaf tissue was milled with a steel ball in 2ml eppendorfs and 396µl of extraction solution was added to each sample. The extraction solution consisted of 25% methanol and 1% acetic acid in water with the following internal standards: 2µl of jasmonic acid ($^{13}C_2$-JA) (5µg ml^{-1}), 1µl salicylic acid ($^{2}H_4$-SA) (100µM) and 2µl of abscisic acid ($^{2}H_6$-ABA) (0.5µg ml^{-1}). Hormones were extracted by beating samples in a bead beater for two minutes at 30Hz with a 3mm tungsten ball. Samples were then placed on ice for 30 minutes, centrifuged at maximum speed in a table top centrifuge for 10 minutes, the supernatant removed and a second extraction performed with 400µl extraction solution without internal standards. Supernatants from the two extractions were pooled and transferred to glass vials for LC-MS/MS analysis.

Samples were analysed by LC-MS/MS using an Agilent 1100 LC coupled to an Applied Biosystems Q-TRAP LC/MS/MS system fitted with a Turbo Ion Spray source operating in negative mode. Chromatographic separation of molecules based on hydrophobicity was carried out using a Phenomenex Luna 3µm C18(2) 100mm x 2.0mm column maintained at 35°C and an acetonitrile gradient (5% acetonitrile to 94.9% acetonitrile) containing 0.1% formic acid as shown in Table 2.2.

Table 2.2 Conditions under which plant hormones and coronatine were measured by LC-MS/MS.

Step	**Total time** (min)	**Flow rate** (µl/min)	**Solution A (%)** (5% acetonitrile, 0.1% formic acid, 94.9% water)	**Solution B (%)** (94.9% acetonitrile, 0.1% formic acid, 5% water)
0	10	200	100	0
1	0	200	100	0
2	20	200	0	100
3	25	200	0	100
4	27	200	100	0
5	29	200	100	0

An injection volume of 50µl for each sample was used for analysis and measurement of plant hormones and coronatine performed simultaneously.

Labelled and endogenous JA, SA and ABA ion pairs of the following mass transitions were monitored: JA 209.2>59, $^{13}C_2$-JA 211.2>61, SA 137.1>93, $^{2}H_4$-SA 141.1>97, ABA 263.2>153 and $^{2}H_6$-ABA 269.2>159. For coronatine, a calibration curve was constructed from data obtained by injection of known quantities of coronatine and the amount detected by monitoring the coronatine mass transition pairs 318>163 in samples.

2.7 Statistical analysis

Statistical significance of data was determined using the Student's t-test, One-way ANOVA with Tukey's post hoc test or Kruskal-Wallis One-way ANOVA with Dunn's multiple comparison test. The Student's t-test was used to compare wild-type and mutant responses to biotic and abiotic stresses at a given time-point. The Student's t-test was performed with Microsoft Excel inbuilt statistical function. One-way ANOVA was used to analyse data where more than two plant lines were being compared to determine whether there were statistically significant differences between groups. Tukey's post hoc test was used to determine between which groups the difference was significant. In the case of non-parametric data (in this case, symptom scores) where more than two plant lines were compared, Kruskal-Wallis One-way ANOVA was used to determine whether there were statistically significant differences between the groups analysed. Dunn's multiple comparison test was used to determine between which groups the difference was significant. One-way ANOVA with Tukey's post hoc test and Kruskal-Wallis One-way ANOVA with Dunn's multiple comparison test were carried out using GraphPad Prism version 5 for Windows (GraphPad Software, San Diego, California USA, www.graphpad.com).

For data presented as percentages, the percentages were arcsine transformed prior to statistical analyses by the Student's t-test. For the arcsine transformation of data, the square root of the percentages as a proportion were taken and the arcsine of the resulting values used for statistical analysis.

Chapter 3:

Characterisation of lines used

3 Characterisation of lines used

3.1 *AHK5* gene expression pattern

Analysis of the expression pattern of *AHK5* during the life cycle of *A. thaliana* using the Genevestigator Development tool (https://www.genevestigator.com/gv/) (Hruz et al., 2008) revealed overall *AHK5* expression to be low at all developmental stages. The highest levels of *AHK5* expression occurred during the germination, seedling and young rosette stages (Figure 3.1).

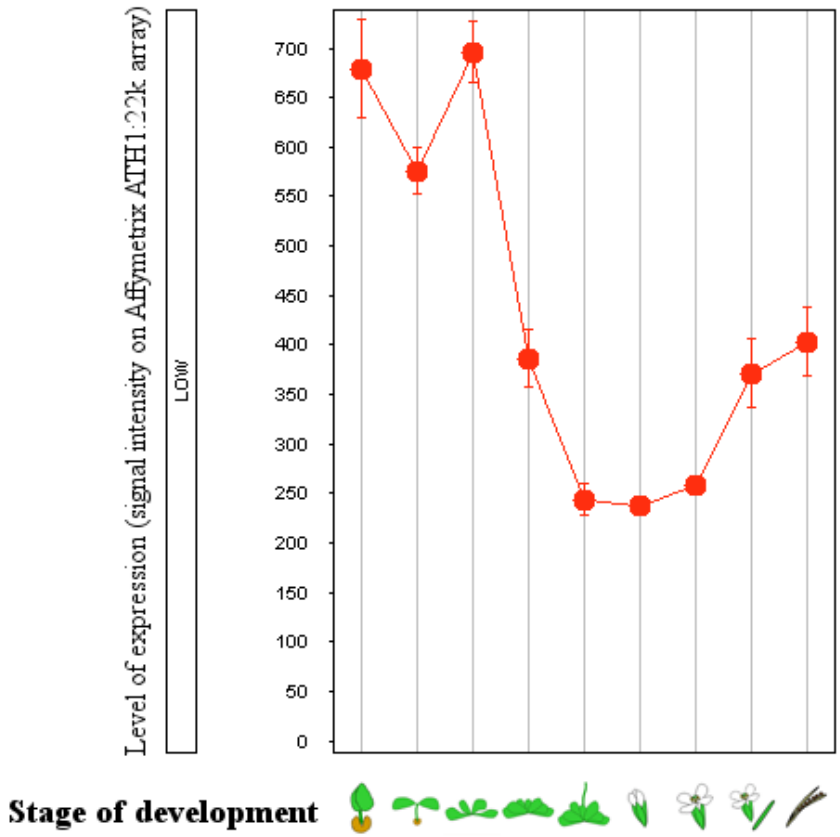


Figure 3.1 Output provided by the Development tool interface of the Genevestigator database. The output shows expression levels of *AHK5* at different developmental stages from Affymetrix experimental data stored in the Genevestigator database

Previous analysis of *AHK5* expression in different plant tissue types revealed *AHK5* to be most highly expressed in the roots (Iwama et al., 2007; Desikan et al., 2008). A search for *AHK5* expression levels across different tissues in the Genevestigator database using the Anatomy tool corroborated these previous findings (Hruz et al., 2008) (Figure 3.2 and Figure 3.3).

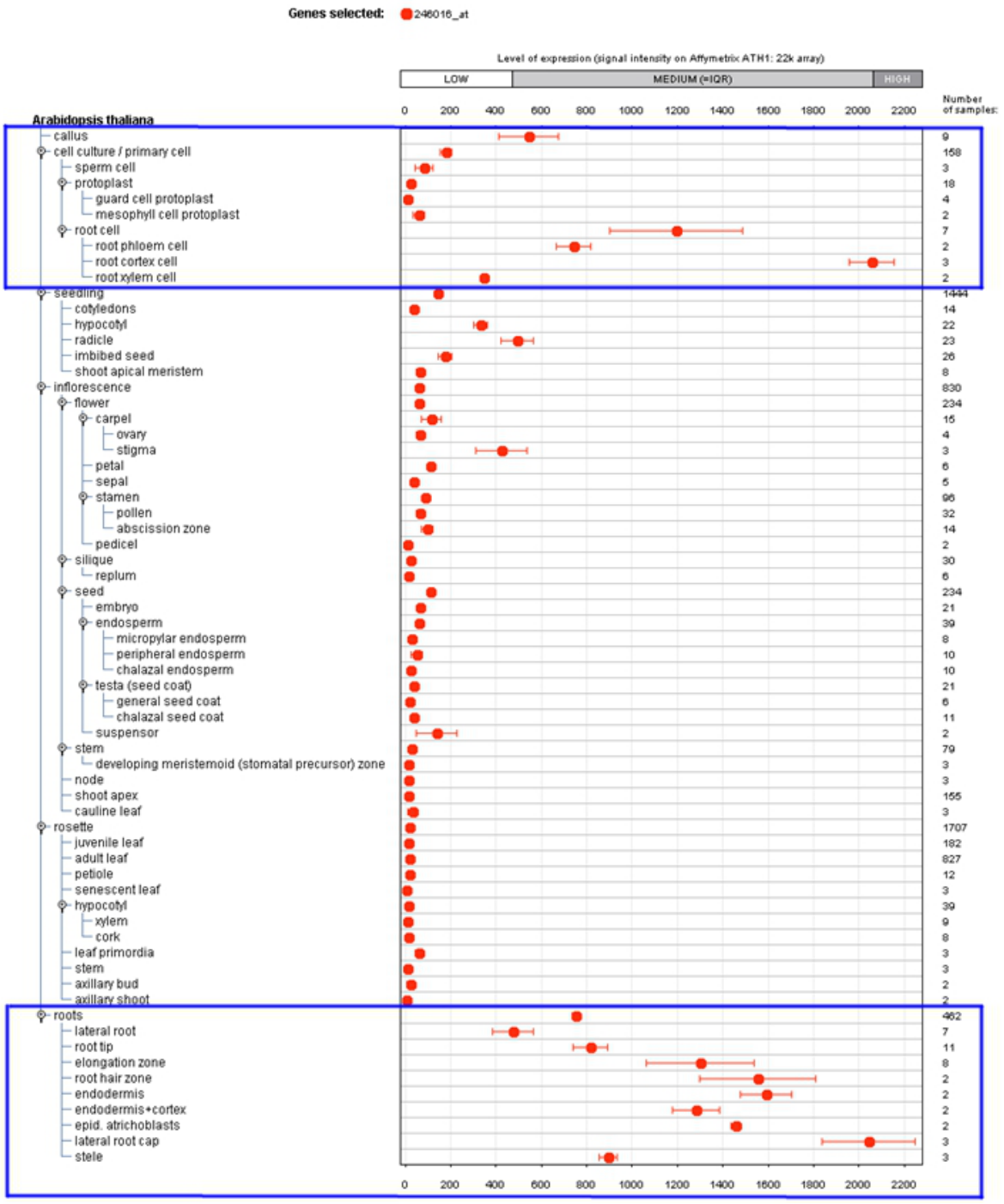


Figure 3.2 Output provided by the Anatomy tool interface of the Genevestigator database. The output shows expression pattern of *AHK5* in different tissue types from Affymetrix experimental data stored in the Genevestigator database. Areas within the two boxes are shown in detail in Figure 3.3.

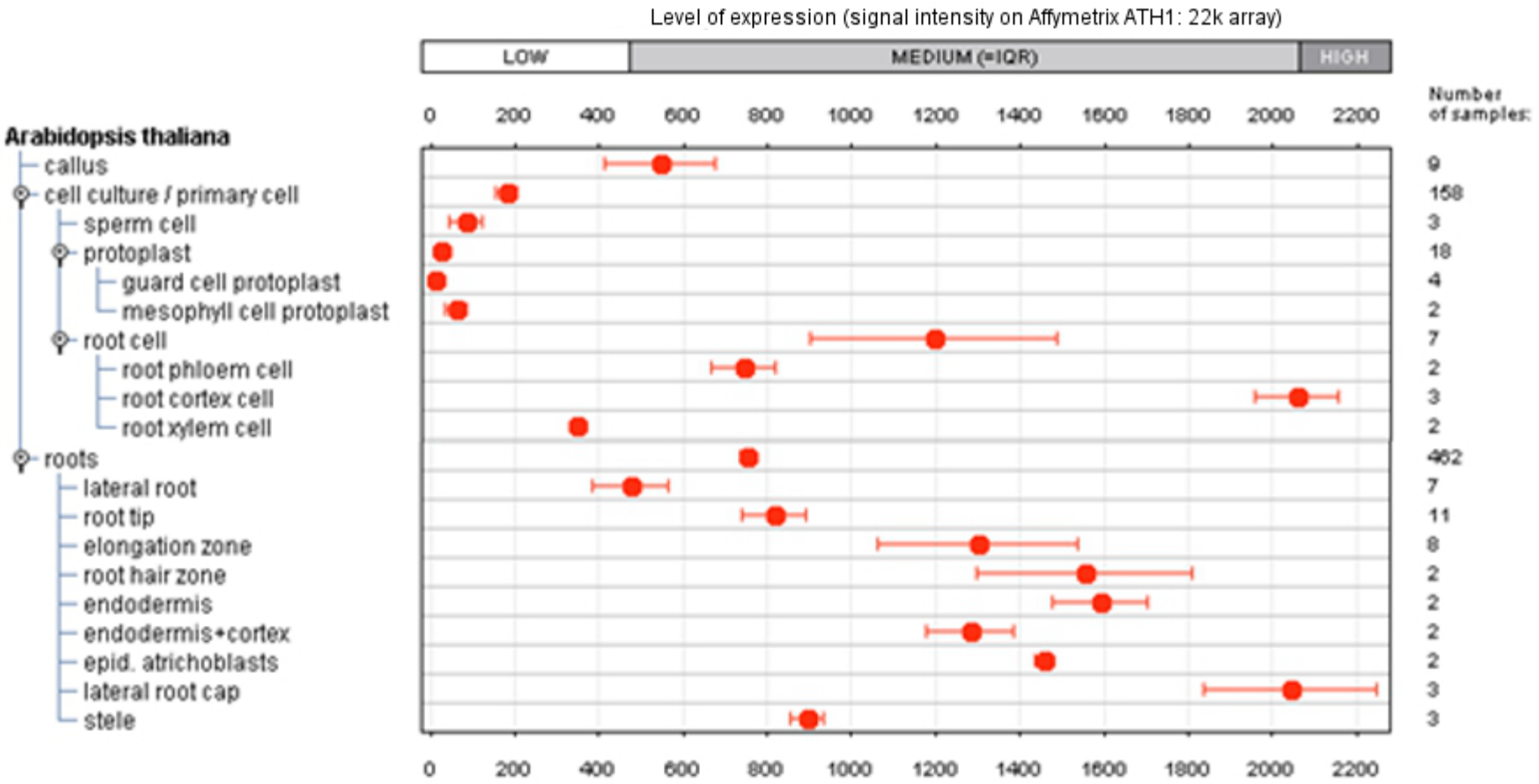


Figure 3.3 Detailed view of *AHK5* expression pattern in root tissue shown within the boxes in Figure 3.2.

To investigate the presence of possible *cis*-elements in the 5' UTR of *AHK5* which may regulate *AHK5* transcription and therefore function, 3205bp of genomic sequence upstream of the *AHK5* start codon was queried against the PLACE database of plant *cis*-acting regulatory DNA elements (http://www.dna.affrc.go.jp/PLACE/) (Higo et al., 1999). Interestingly, *cis*-elements found upstream of ABA and drought/dehydration responsive genes were identified upstream of *AHK5.* Also found upstream of *AHK5* was a *cis*-element which acts as a binding site for the *Arabidopsis* response regulator ARR1. These findings suggest that *AHK5* may be regulated by stress and other members of the TCS. The *cis*-elements identified upstream of *AHK5* are summarised in Table 3.1.

Table 3.1 Summary of *cis*-acting elements identified by the PLACE database upstream of *AHK5.* Functions of *cis*-elements are as assigned by annotation in the PLACE database.

***Cis*-element**	**Consensus sequence**	**Function**
ABRELATERD1	ACGTG	Dehydration
ARR1AT	NGATT	ARR1 binding element
ACGTATERD1	ACGT	Dehydration
LTRECOREATCOR15	CCGAC	Cold, drought, ABA
MYB1AT	WAACCA	Dehydration
MYB2CONSENSUSAT	YAACKG	Dehydration, ABA
MYBATRD22	CTAACCA	Dehydration, ABA, water stress
MYBCORE	CNGTTR	Dehydration, water stress
MYCATRD22	CACATG	Dehydration, ABA, water stress
MYCCONSENSUSAT	CANNTG	Dehydration, cold, ABA
Nucleotide key:	N=G/C/A/T	K=G/T
	W=A/T	R=A/G
	Y=C/T	

To determine under which conditions and to what extent *AHK5* transcript levels are up- or down-regulated, the Genevestigator Conditions tool (https://www.genevestigator.com/gv/) (Hruz et al., 2008) was used to analyse *AHK5* expression levels in response to stimuli. In response to exogenously applied ABA, over two-fold and just under two-fold induction of the *AHK5* transcript was seen in germinating seedlings and stomatal guard cells, respectively. The up-regulation of the *AHK5* transcript in response to ABA is in agreement with the presence of *cis*-elements in the 5'UTR of *AHK5* which are associated with ABA-responsive genes (Table 3.1). In seedling roots, *AHK5* transcript level was down-regulated almost two-fold in response to cold stress (4°C) and increased approximately 1.5-fold on treatment with 150mM NaCl. No large increase or decrease (i.e., less than 1.5-fold up-or down-regulation, respectively) in *AHK5* transcript levels was seen in response to drought, heat, osmotic stress or infection with *Pst*DC3000 or *B. cinerea.*

3.2 AHK5 structure

AHK5 has previously been shown to have histidine kinase activity (Iwama et al., 2007). To confirm that AHK5 has the features of a histidine kinase, the amino acid sequence of AHK5, which is a total of 922aa in length, was analysed by the SMART Genomes interface (http://smart.embl-heidelberg.de/) (Schultz et al., 2000) and the Scan Prosite tool (http://expasy.org/tools/scanprosite/) (de Castro et al., 2006) to identify conserved protein domains. From this analysis, a histidine kinase domain (position 373-614) and a C-terminal receiver domain (position 778-917), both characteristic of HKs, was identified in AHK5 by the ScanProsite tool. Within the HK domain, a HK phosphoacceptor region containing the conserved histidine residue was predicted to reside at position 366-431, upstream of an ATPase domain (position 477-431) by SMART Genomes. The SMART Genomes output also identified two coiled coil domains (positions 86-121 and 169-204) and three segments of low complexity in AHK5. A summary of the predicted protein structure of AHK5 is shown in Figure 3.4.

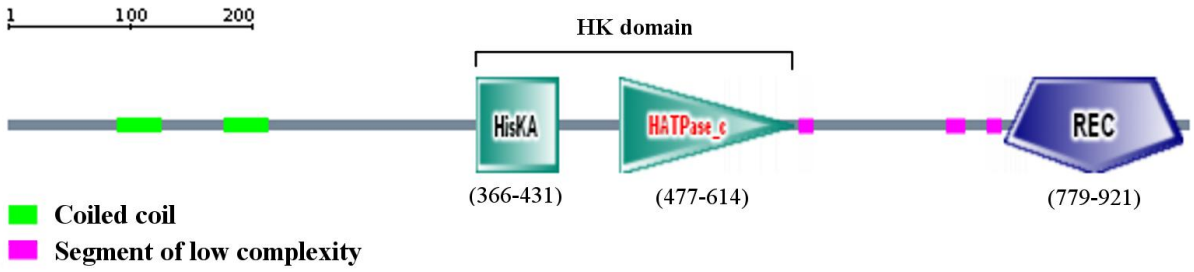


Figure 3.4 SMART Genomes output of the predicted protein structure of AHK5 showing the domains identified. Numbers within parentheses indicate amino acid positions of the domains. HisKA = HK phosphoacceptor region, HATPase_c = ATPase, REC = receiver domain. Scale shown refers to sequence length in amino acids.

Within the HK domain, the conserved histidine residue was predicted at position 376 in addition to a conserved aspartate residue within the receiver domain at position 828. Visualisation of a multiple alignment of AHK5 with the other seven *A. thaliana* HKs using ClustalW (http://www.ebi.ac.uk/Tools/msa/clustalw2/) (Chenna et al., 2003) and the Box Shade program (http://www.ch.embnet.org/software/BOX_form.html) showed the predicted conserved histidine and aspartate residues aligned with those of the other *A. thaliana* HKs (Figure 3.5, Figure 3.6 and Appendix VIII). In addition the conserved histidine residue of the H box, the N, G1, F and G2 boxes which form part of the ATP binding site in HKs were also found within the HK domain predicted to have ATPase activity (Figure 3.5).

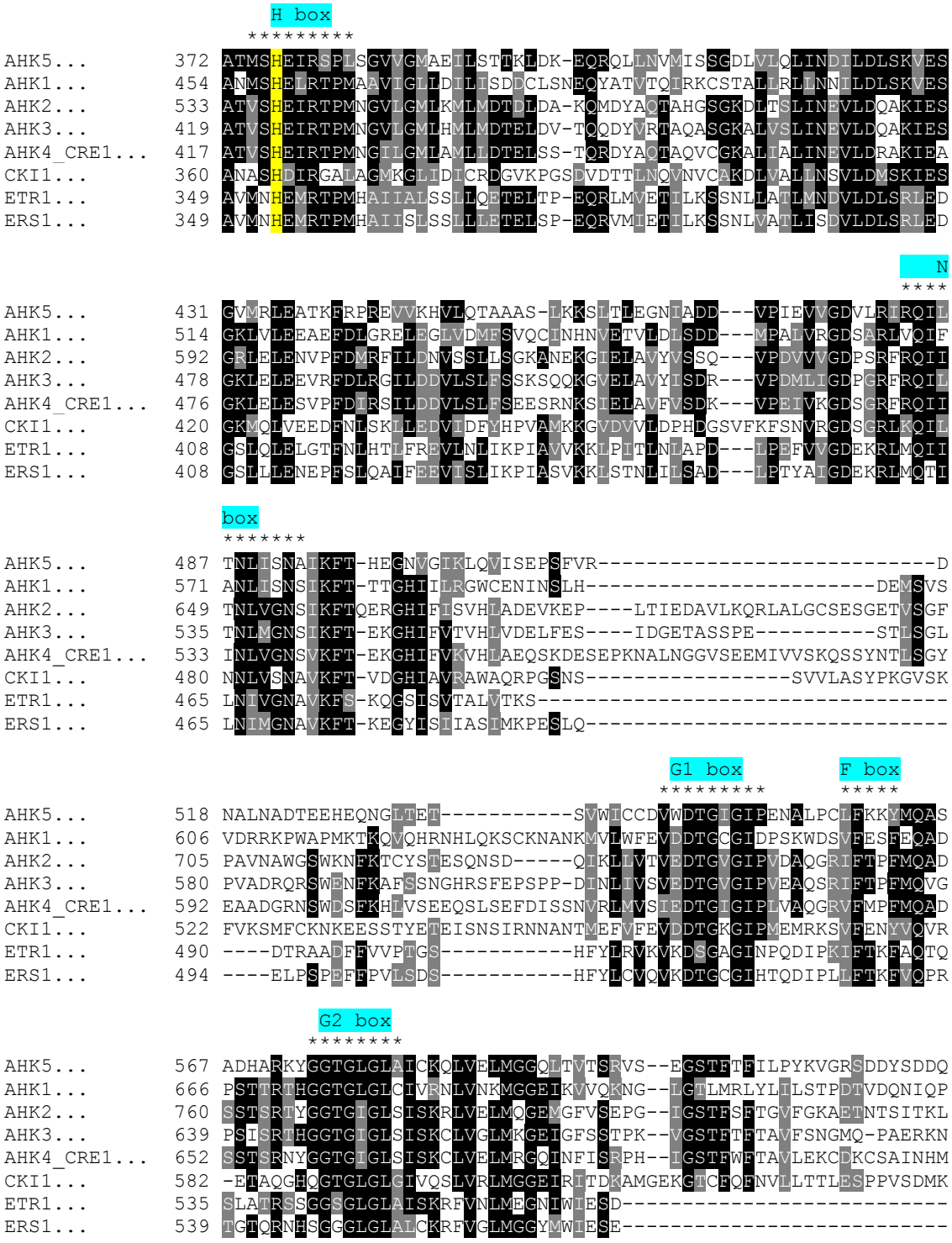


Figure 3.5 Multiple alignment of *A. thaliana* histidine kinases within the region of the HK domain containing the conserved H, N, G1, F and G2 boxes. Positions of the conserved boxes are as described in Ueguchi et al. (2001). The conserved histidine residue within the H box of each histidine kinase is highlighted in yellow.

```
AHK1...      1049 SFEEETANKVTTRETSLRNSSPYDLILMDCQMPKMDGYEATKAIRRAEIGT---------
AHK2...      1018 ----------------------HNFDACFMDLQMPEMDGFEATRRVRELEREINKKIASGE-
AHK3...       896 ----------------------HEFDACFMDIQMPEMDGFEATRRIRDMEEEMNKRIKNGE-
AHK4_CRE1...  927 ----------------------HTFDACFMDIQMPQMDGFEATRQIRMMEKETKEKTN----
CKI1...       989 --------LTQREEQGSVDKLPFDYIFMDCQMPEMDGYEATREIRKVEKSYG---------
AHK5...       821 ----------------------SYDLVLMDVCMPVLDGLKATRLIRSYEETGNWNAAIEAG
ETR1...       651 ----------------------HEHKVVFMDVCMPGVENYQIALRIHEKFTKQRHQRP----
ERS1...           ------------------------------------------------------------
```

Figure 3.6 Multiple alignment of *A. thaliana* histidine kinases within the region of the receiver domain containing the conserved aspartate residue. ERS1 lacks the receiver domain and therefore does not contain the conserved aspartate residue. The conserved aspartate residue is highlighted in green

A cladogram generated by ClustalW (http://www.ebi.ac.uk/Tools/msa/clustalw2/) (Chenna et al., 2003) multiple alighment of the amino acid sequences of the *A. thaliana* HKs shows that the HKs cluster into groups, with the cytokinin receptors (AHK2, AHK3 and AHK4) clustering together, the ethylene receptors (ETR1 and ERS1) forming a group and AHK1 and CKI1 forming another group (Figure 3.7). AHK5 showed most sequence similarity with AHK4 in the pairwise analysis with ClustalW.

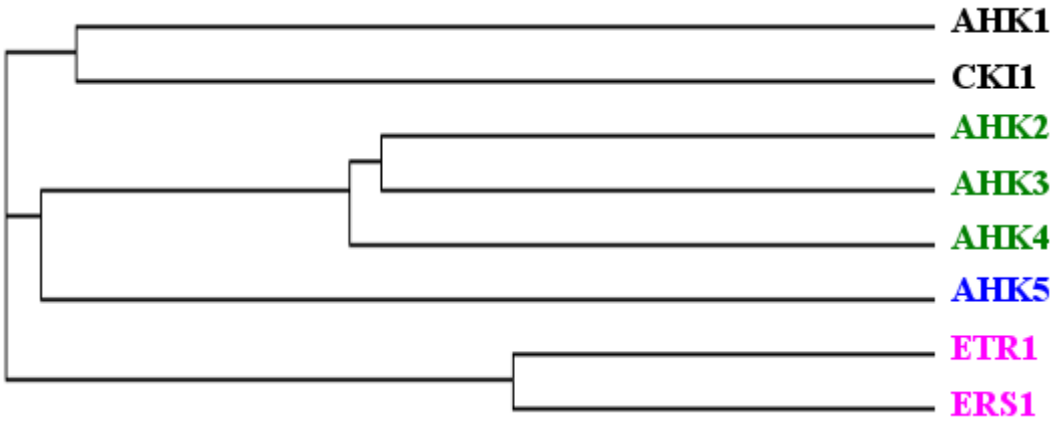


Figure 3.7 Cladogram generated from multiple alignment of the protein sequences of the eight *A. thaliana* histidine kinase in ClustalW.

In summary, AHK5 has the hallmarks of a histidine kinase and contains both a HK domain with the conserved histidine residue and a receiver domain with the conserved aspartate residue. In addition, the AHK5 protein is also predicted to possess two coiled-coil domains at the N-terminus, which are not found in the other *A. thaliana* HKs (Hwang et al., 2002).

3.3 Genotyping lines used

Throughout the study, the comparison of wild-type Col-0 and the T-DNA insertion mutant *ahk5-1* was used to investigate the role of AHK5 in response to various abiotic and biotic stresses. These lines were previously characterised by Iwama et al. (2007) and Desikan et al. (2008). In addition to these lines, the *P_{35S}-AHK5/ahk5-1* line containing a *GFP-AHK5* cDNA fusion construct (previously characterised by Desikan et al. (2008)) was also used.

To confirm the identity of these plants, these lines were genotyped by PCR. The *ahk5-1* mutant contains a T-DNA insertion which lies within an exon encoding for the AHK5 receiver domain (Figure 3.8). For genotyping of the lines used, two primer pairs were utilised - one pair which amplifies across the site of T-DNA insertion for detection of wild-type *AHK5* (primers 1 (5'-GCTGTGACGTATGGGACACTGG-3) and primer 2 (5'-CTCAGTGCAAATACTGTTGC-3')) (Figure 3.8) and a primer pair in which the reverse primer binds within the T-DNA sequence to test for presence of T-DNA insertion within the *AHK5* gene (primer 1 and primer 3 (5'-GCTTCCTATTATATCTTCCCAAATTACCAATACA-3')) (Figure 3.8).

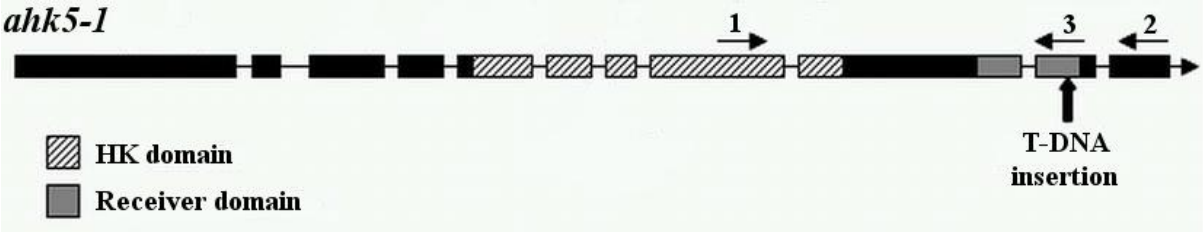


Figure 3.8 Gene structure of *AHK5* showing the site of T-DNA insertion within the HK domain of *AHK5* giving rise to the *ahk5-1* mutant. The positions of the primers used to genotype the lines in this study are also shown. Arrows denote binding position and orientation of each primer denoted by numbers; primer 1 = 5'-GCTGTGACGTATGGGACACTGG-3', primer 2 = 5'-CTCAGTGCAAATACTGTTGC-3', primer 3 = 5'-GCTTCCTATTATATCTTCCCAAATTACCAATACA-3'. Primers 1 and 2 were used to test for presence of wild-type *AHK5* and primers 1 and 3 were used to test for presence of T-DNA insertion in the *ahk5-1* background. Figure modified from Desikan et al. (2008).

In the case of detection of wild-type *AHK5*, the large T-DNA insertion leads to no PCR product being produced as the product is too large to be amplified under the conditions used (see Section 2.2.2 for details). In the case of detection of T-DNA insertion, a product is only produced in the *ahk5-1* mutant background as the reverse primer binds within the T-DNA

sequence and not within the *AHK5* sequence. Predicted PCR product sizes from the primers used for genotyping are summarised in Table 3.2.

Table 3.2 Expected product size from different primer pairs used to genotype plant lines used in this study. Primers 1 and 2 were used to detect wild-type *AHK5* and primers 1 and 3 were used to detect the presence of T-DNA insertion in the *ahk5-1* background. Primer 1 = 5'-GCTGTGACGTATGGGACACTGG-3', primer 2 = 5'-CTCAGTGCAAATACTGTTGC-3', primer 3 = 5'-GCTTCCTATTATATCTTCCCAAATTACCAATACA-3'. See text for binding positions of primers within the *AHK5* gene.

	Product size with primer pairs:	
Genotype	**Primers 1 and 2**	**Primers 1 and 3**
Col-0	1.5kb	-
ahk5-1	-	1.5kb
P_{35S}-AHK5/ahk5-1	1.5Kb	1.1Kb

In wild-type plants as expected, using primers 1 and 2 resulted in a product of approximately 1.5Kb, whereas primers 1 and 3 did not give any product (Figure 3.9). The opposite was seen in the *ahk5-1* mutant line, with primers 1 and 2 giving no PCR product due to the presence of the T-DNA and primers 1 and 3 giving a product of approximately 1.5Kb confirming the presence of the T-DNA (Figure 3.9). Since the complemented line *P_{35S}-AHK5/ahk5-1* is in the *ahk5-1* background and is complemented with a construct containing a cDNA copy of the wild-type *AHK5* gene, a product was expected and seen for both primer pairs (Figure 3.9). The PCR product obtained with primers 1 and 2 from the *P_{35}-AHK5/ahk5-1* line was smaller at approximately 1.1Kb compared to the product of 1.5Kb seen for genomic *AHK5* due to the exclusion of introns in the cDNA sequence.

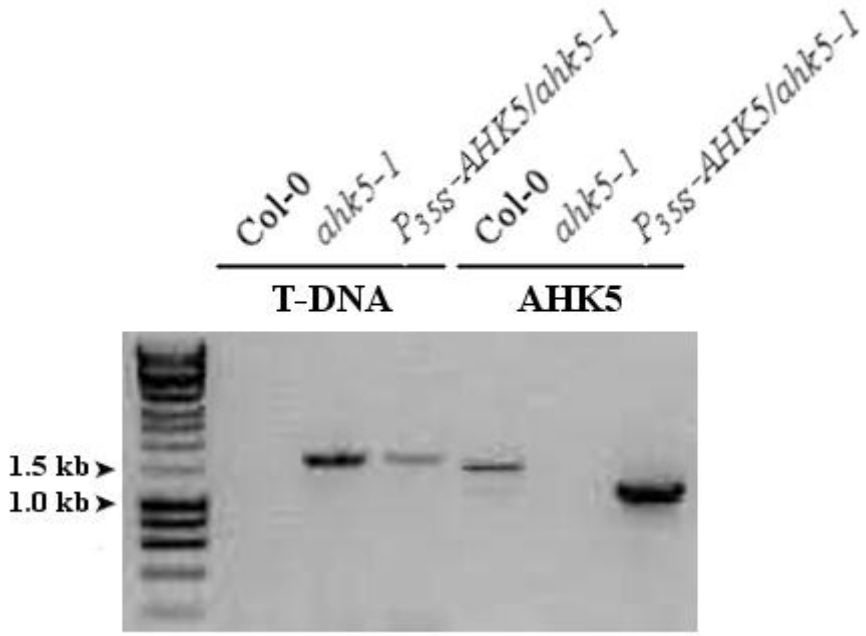


Figure 3.9 Genotyping of Col-0, *ahk5-1* and the complemented P_{35S}*-AHK5/ahk5-1* lines for presence of T-DNA insertion and presence of wild-type *AHK5*. Primers used are described in Figure 3.8 and Table 3.2. The product size for *AHK5* in line P_{35S}*-AHK5/ahk5-1* is smaller than that of Col-0 as this line was complemented with the cDNA of *AHK5*.

3.4 Isolation of complemented lines in the *ahk5-1* background

To obtain complemented lines in which *AHK5* expression was under the control of the endogenous promoter, *ahk5-1* plants previously transformed by *Agrobacterium*-mediated transformation with vector pMKC111were subjected to selection on hygromycin B (Desikan et al., 2008). Vector pMKC111 carries a full-length genomic *AHK5* construct which includes 3205 bases of sequence upstream of the *AHK5*ATG start codon and also carries the HygB resistance gene. Three rounds of selection were performed and 12 independent lines were chosen for genotyping by PCR using the primers described above (Figure 3.8 and Table 3.2) for presence of *AHK5* and T-DNA insertion. All 12 lines genotyped were positive for both wild-type *AHK5* and T-DNA insertion, suggesting all lines were true transformants (Figure 3.10a). To determine whether complementation led to expression of *AHK5,* four of the 12 lines genotyped (labelled 1-4 in Figure 3.10a) were selected for RT-PCR to test for expression of the complementing gene (Figure 3.10b). All four lines tested showed expression of *AHK5* and were subsequently named P_{AHK5}*-AHK5/ahk5-1-1,* P_{AHK5}*-AHK5/ahk5-1-2,* P_{AHK5}*-AHK5/ahk5-1-3* and P_{AHK5}*-AHK5/ahk5-1-4.*

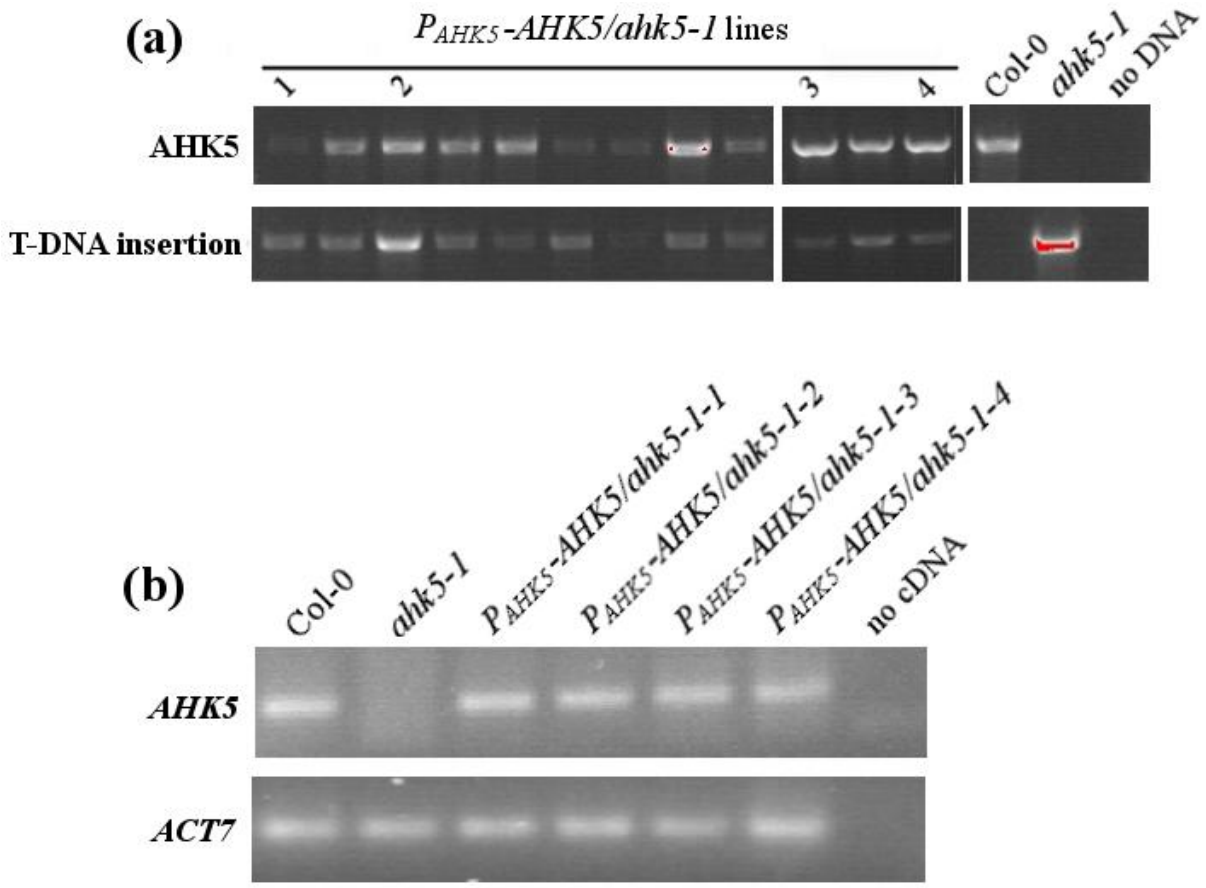


Figure 3.10 Genotyping of plant lines. (a) Genotyping of *ahk5-1* plants transformed with full-length genomic *AHK5* under the control of the endogenous promoter. A selection of hygromycin B resistant transformants were genotyped for complementation (presence of *AHK5*) and for the *ahk5-1* mutant background (presence of T-DNA insertion). Primers used and expected products sizes are as summarised in Table 3.2. (b) Testing for expression of *AHK5* in complemented lines. Four lines complemented with an *AHK5* construct under the control of the endogenous promoter (numbered 1 to 4 in (a)) were chosen for further testing by RT-PCR to test for expression of the *AHK5* transgene. RNA was extracted from 15 day old seedlings. The lines tested were named P_{AHK5}-*AHK5/ahk5-1-1*, P_{AHK5}-*AHK5/ahk5-1-2*, P_{AHK5}-*AHK5/ahk5-1-3* and P_{AHK5}-*AHK5/ahk5-1-4*. The *ACT7* gene was used as a control for normalisation (see Section 2.2.4 for primers and conditions used for RT-PCR).

3.5 Morphological analysis of the *ahk5-1* mutant

It was noted that mature soil grown plants of wild-type Col-0 and *ahk5-1* mutant plants differed in size, with rosettes of mutant plants appearing to be smaller than wild-type plants, which was reflected in a significant difference in the fresh weight of *ahk5-1* shoots compared to wild-type shoots grown under normal growth conditions (Figure 3.11). It was also noted that the leaves of the mutant tended to lie more flat on top of the surface of the soil, whereas wild-type leaves tended to grow away from the surface of the compost (Figure 3.12)

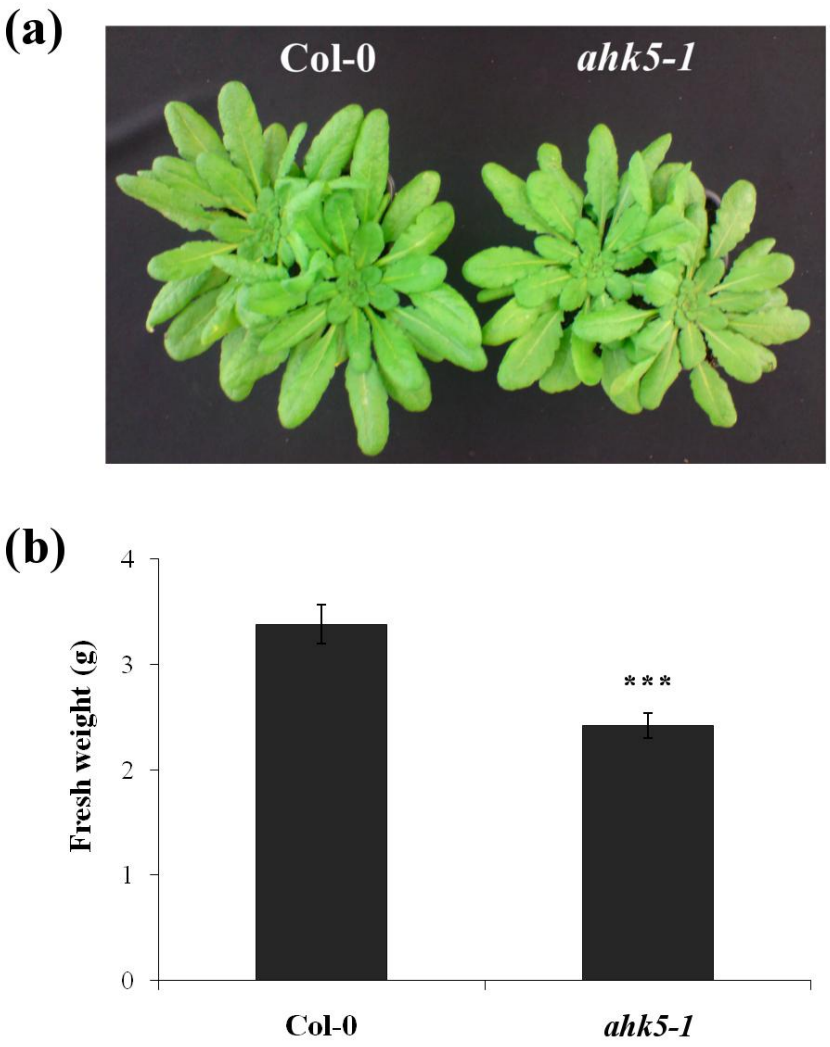


Figure 3.11 Morphological analysis of five week old Col-0 and *ahk5-1* plants. (a) appearance of wild-type Col-0 and *ahk5-1* mutant rosettes and (b) shoot fresh weights (data presented are mean ± SE of 26 plants). Asterisks denote a statistically significant difference as determined by the Student's t-test (*** = $p < 0.0005$).

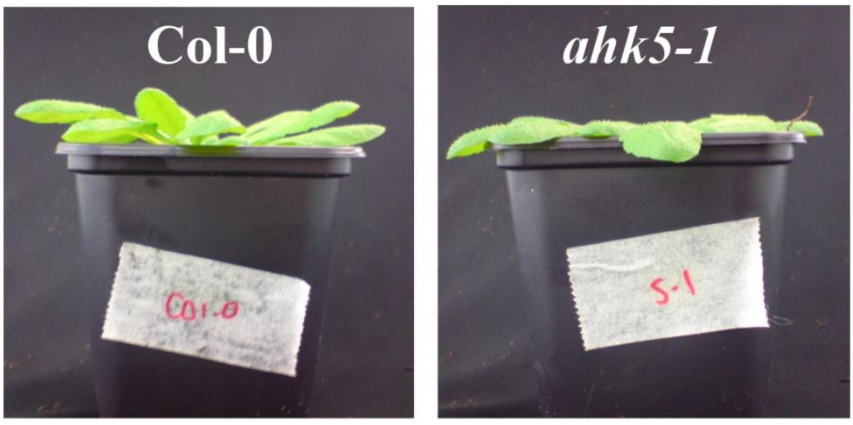


Figure 3.12 Profile view of soil grown mature wild-type Col-0 and *ahk5-1* mutant plants.

3.6 Effect of ABA on root growth

AHK5 was previously found to act as a negative regulator of the ABA/ethylene signalling pathway inhibiting root elongation, with *ahk5-1* seedlings more sensitive to inhibition of root growth by ABA (Iwama et al., 2007). To confirm this phenotype, wild-type and *ahk5-1* seeds were germinated and grown on half-strength Murashige and Skoog medium for four days, after which they were transferred to media containing various concentrations of ABA and root length measured after a further four days growth (Figure 3.13). At the lowest concentration of ABA used (0.1µM), a slight increase in root elongation was seen. At a concentration of 1µM ABA and above, inhibition of root growth was seen in both wild-type and *ahk5-1* mutant seedlings, with a greater inhibition in *ahk5-1* seedlings. This suggests that loss of AHK5 acts to negatively regulate ABA inhibition of root elongation, confirming the previous findings of Iwama et al. (2007).

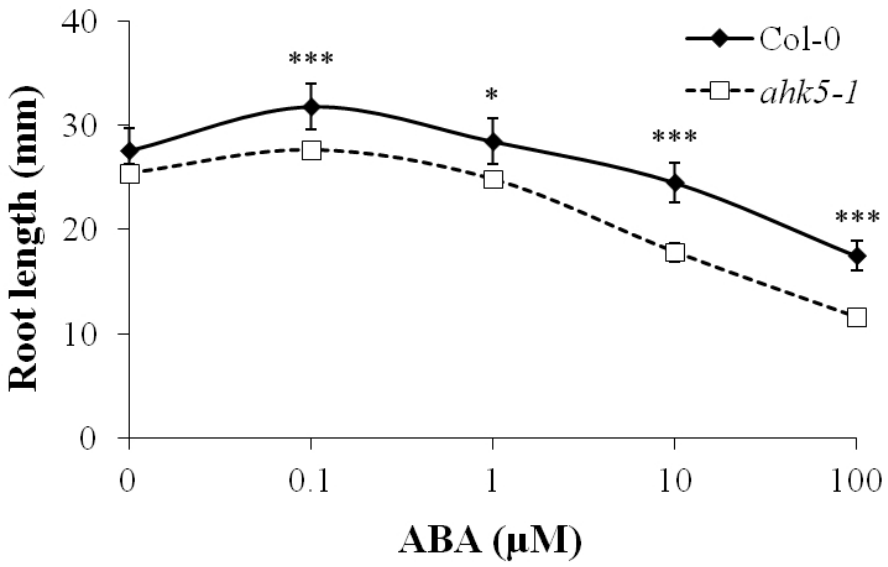


Figure 3.13 Inhibition of root length growth in response to ABA in wild-type and *ahk5-1* seedlings. Seedlings were grown on half strength Murashige and Skoog medium for four days, after which seedlings were transferred to plates containing various doses of ABA and root length measured after a further four days growth (mean ± SE, n = 33 seedlings). Asterisks denote a significant difference between treated and control seedlings as determined by the Student's t-test (** = $p<0.005$).

3.7 Conclusions

AHK5 is most highly expressed at earlier stages of development and in the roots and analysis of the 5'UTR of *AHK5* identified *cis*-elements associated with ABA-, drought- and water stress-responsive genes in addition to an ARR1 binding element. Analysis of expression data

using Genevestigator suggests expression of *AHK5* is up-regulated by ABA and salt and down-regulated by cold treatment.

Analysis of AHK5 protein sequence reveals that AHK5 possesses the HK and receiver domains conserved amongst the HKs and additionally possesses two coiled coil domains at the N-terminus of the protein. Coiled coil domains are not found in other *Arabidopsis* HKs and it has been suggested that these domains may mediate interaction of AHK5 with other proteins (Hwang et al., 2002).

The genotypes of the *ahk5-1* mutant described by Desikan et al. (2008) and the complemented line P_{35S}*-AHK5/ahk5* previously generated were confirmed here. In addition, *ahk5-1* lines complemented with genomic *AHK5* under the control of the endogenous promoter were confirmed and shown to express *AHK5*. Loss of function of AHK5 was shown to decrease the size of *ahk5-1* mutant rosettes, which was reflected in shoot fresh weight.

Chapter 4:

The role of AHK5 in abiotic stress responses

4 The role of AHK5 in abiotic stress responses

4.1 Introduction

In nature, plants are exposed to a number of environmental factors that influence and impact on plant growth and development. Environmental stresses in various parts of the world have already resulted in loss of crops, therefore impacting on food security and economic output of arable land. In addition, climate change is predicted to have negative effects on future productivity, creating new challenges (Huang et al., 2002; Mittler, 2006; Lobell et al., 2008). In addition to climate change, intensive agricultural practices have also negatively impacted on world crop production; for example, irrigation of land has led to increased soil salinity caused by rising water tables; continuous growth of single plant species (known as 'monocropping') results in depletion of soil nutrients and encourages proliferation of pests (Huang et al., 2002). A better understanding of the mechanisms that control plant responses to environmental stress will aid in the development of crops which are able to survive under sub-optimal conditions.

Variability in temperature, soil salinity and limitation of water availability/drought stress are conditions commonly encountered by plants in the environment and as such have received much attention. Of interest is how plants perceive these environmental stresses, the signalling cascades activated and cellular responses leading to tolerance.

4.1.1 *Temperature stress*

Fluctuations in temperature occur on a daily basis, and as such plants need to adapt to such changes rapidly as both extremes of temperature (i.e., temperatures below and above that optimal for growth) can be experienced in a short space of time.

Elevated temperature negatively impacts on plant growth through denaturation of proteins, alteration of membrane fluidity and permeability, oxidative stress and disturbance of cellular homeostasis (Wahid et al., 2007). Phenotypically, heat stress results in reduction in growth rate, scorching of leaves and stems and bleaching of photosynthetic tissue (Wahid et al., 2007). In response to heat stress, the accumulation of heat shock proteins (HSPs) is well documented and these proteins are thought to act as molecular chaperones to prevent protein denaturation and to facilitate re-folding of proteins under heat stress (Kotak et al., 2007). It is

apparent that factors other than HSPs influence heat tolerance. Studies indicate that abscisic acid (ABA), salicylic acid (SA), ethylene and ROS signalling positively contribute to heat tolerance in *Arabidopsis* (Larkindale and Knight, 2002; Larkindale et al., 2005).

Plants exhibit two types of tolerance to heat stress: basal heat tolerance and acquired heat tolerance. Basal heat tolerance refers to the ability of the plant to resist a sudden increase in temperature. Acquired heat tolerance is the capability of the plant to withstand normally lethal heat stress subsequent to exposure to mild (non-lethal) heat stress separated by a short recovery period (Larkindale et al., 2005). These two types of heat tolerance are activated by both overlapping and distinct pathways; for example, SA and ROS signalling play a role in both types of heat tolerance, ABA signalling contributes mainly to acquired heat tolerance and ethylene signalling and antioxidant activity are more important for basal thermotolerance (Larkindale et al., 2005).

On the other end of the spectrum, cold stress disrupts metabolic reactions, reduces water availability, causes oxidative stress and reduces membrane fluidity (Chinnusamy et al., 2007). Similar to drought and salt stress, cold stress can also lead to water deficit by preventing uptake of water (Chinnusamy et al., 2007). As such, ABA signalling is also involved in cold-stress responses and genes up-regulated in response to cold also show overlaps with those induced by salt and drought stress (Seki et al., 2001; Xiong et al., 2001; Seki et al., 2002).

4.1.2 *Salinity and drought stress*

Soil salinity is an important factor restricting the use of land for agriculture as high salinity reduces both water and nutrient uptake, affecting crop growth and yield, with loss of more than 50% of the worlds arable land predicted to be lost to salinisation by 2050 (Munns, 2002; Wang et al., 2003; Flowers, 2004). Reduction in availability of water through drought stress can also have the secondary effect of increasing salinisation of soil (Wang et al., 2003). Understanding the molecular mechanisms underlying salt and drought stress is therefore important for improving salt tolerance in plants.

Both salt and drought stress cause hyperosmotic stress and imbalance in ion homeostasis and as such overlaps in the response of plants to these two stresses are seen (Xiong et al., 2002; Mahajan and Tuteja, 2005). In response to drought and salt stress, up-regulation of ABA biosynthetic genes and production of late embryogenesis abundant (LEA) type proteins,

compatible solutes/osmolytes and antioxidants/ROS scavengers are seen (Xiong et al., 2002; Wang et al., 2003).

The large overlap in the genes induced by drought and salt stress with those induced by the plant hormone abscisic acid (ABA) suggests that ABA plays a role in both drought and salt stress signalling (Zhang et al., 2006). The role of ABA in mediating stomatal closure in response to drought stress is well documented. Under salt stress, increases in ABA levels are also associated with decreased stomatal conductance which may protect against salt stress through reduction of Na^+ uptake from the soil in the transpiration stream (Jakab et al., 2005; Maggio et al., 2007). In addition to the ABA-dependent pathway, ABA-independent pathways also act to mediate salt and drought tolerance; ABA-responsive genes typically contain *cis*-acting ABA responsive elements (ABRE) in the promoter region, whereas those genes which are part of the ABA-independent pathway may contain dehydration responsive elements (DRE) (Yamaguchi-Shinozaki and Shinozaki, 2005).

In addition to the osmotic stress that increased salinity imposes on plants, specific to salt stress is the ion toxicity caused by excessive uptake of Na^+ which inhibits cellular processes such as enzyme activities and disruption of K^+ uptake in the plant (Munns, 2002; Zhu, 2002). It is the ionic component of salt stress which causes the most cellular damage to plants (Munns, 2002). Build up of Na^+ within plant tissue leads to the death of older leaves and reduction in the photosynthetic capacity of the plant which negatively impacts on plant growth (Munns, 2002; Munns and Tester, 2008).

To deal with the ionic component of salt stress, the SOS (Salt Overly Sensitive) pathway, which mediates extrusion of Na^+ from the cell, is activated in addition to vacuolar Na^+/H^+ exchangers which act to sequester Na^+ in the vacuole (Shi and Zhu, 2002; Chinnusamy et al., 2005; Yang et al., 2009).

4.1.3 *Complexity of abiotic signalling*

Overlaps in the effects on plant physiology and metabolism and the types of cellular damage caused by different abiotic stresses exist and as such, overlapping cellular responses and signalling pathways are activated which are not necessarily specific to any one stress. For example, oxidative stress is a common outcome of various stresses such as extremes of temperatures, salinity and drought stress and as a result the production of antioxidants and ROS scavengers is a common response to these stresses (Xiong et al., 2002; Wang et al.,

2003; Suzuki and Mittler, 2006; Smith et al., 2009; Miller et al., 2010). Another example is the expression of LEA proteins in response to different stresses which may be due to their proposed general role in cellular protection (Battaglia et al., 2008). HSPs are also expressed in response to the stresses discussed here, hypothesised to be due to their general roles as molecular chaperones (Wang et al., 2004). It is therefore likely that sensors of environmental stress respond to specific aspects/outcome of the stress (e.g., increased ROS production, membrane fluidity) rather than to specifically detecting the stress itself (e.g., increased temperature).

Common to abiotic stresses is the negative impact on plant growth and survival. The natural variation in the ability of plants to survive under different conditions in nature is most clearly evident in the geographical restriction of plants to areas with certain climates and soil types in the absence of physical barriers (Mott, 2010). Physiologically, the impact of abiotic stress on plants can be measured in terms of impact on growth, where the degree and/or duration of the stress is not lethal and therefore reflects the plant's ability to avoid stress (Verslues et al., 2006). Methods of assessing the effect of abiotic stress on plant growth include measurement of root elongation in seedlings and plant biomass (Davletova et al., 2005; Verslues et al., 2006). The ability of plants to tolerate more extreme stress and/or longer durations of stress can be measured in terms of plant survival (Verslues et al., 2006). For the purpose of this study, the term 'stress tolerance' is used broadly to describe both ability to grow or survive under stress.

4.1.4 *Histidine kinases as sensors for environmental stimuli*

The histidine kinases of the two component system have been shown to act as important sensors of environmental stimuli, discussed in detail in Section 1.8.2. In response to osmolarity, the yeast histidine kinase SLN1 acts as an osmosensor together with the membrane protein SHO1 to activate the HOG pathway under hyperosmotic conditions (Saito and Tatebayashi, 2004). Loss of function of SLN1 can be complemented with the *Arabidopsis* histidine kinase AHK1/AtHK1, AHK2 or AHK3, demonstrating the importance of HKs in environmental sensing in different organisms (Tran et al., 2007; Wohlbach et al., 2008; Tran et al., 2010). In addition to its role as an osmosensor in *Arabidopsis,* AHK1/AtHK1 was also found to positively regulate drought tolerance in plants, whereas AHK2 and AHK3 act as negative regulators salt and drought stress (Tran et al., 2007; Tran et al., 2010). AHK2 and AHK3 have also been shown to play partially redundant roles in the

negative regulation of cold stress responses through regulation of Type-A ARR expression (Jeon et al., 2010). Expression of the ethylene receptor ETR1 was also shown to be regulated by abiotic stress, the expression of which is repressed under salt/osmotic stress (Zhao and Schaller, 2004). Whereas the loss of function mutant *etr1-7* was found to be more tolerant to salt or osmotic stress, the opposite was seen for the dominant negative *etr1-1* mutant which is ethylene insensitive, linking ETR1 to the salt stress signalling pathway (Wang et al., 2008a).

It is therefore clear that *Arabidopsis* HKs can function in abiotic stress signalling. The possible role of AHK5 in abiotic stress responses was therefore investigated in this study.

4.2 Aims

To date, AHK5 has been shown to integrate environmental and endogenous signals at the stomatal level (Desikan et al., 2008) and in root response to exogenous ABA (Iwama et al., 2007). To determine whether AHK5 functions in growth responses affected by abiotic stress in plants, the role of AHK5 in response to temperature stress (both cold and heat stress), salinity and osmotic stress in seedling root growth assays were investigated. This assay was chosen as it is commonly used to screen for alterations in plant tolerance towards abiotic stress (Davletova et al., 2005; Verslues et al., 2006). In addition to these seedling assays, the response of vegetative tissue to salt and drought stress was also tested to investigate AHK5 function at different growth stages.

4.3 Results

To test the involvement of AHK5 in response to abioic stresses, seedling root growth assays were also used to compare root growth of wild-type and *ahk5-1* seedlings to heat, cold, salinity and osmotic stress.

4.3.1 *Heat stress*

Plants display two types of heat tolerance: basal heat tolerance and acquired heat tolerance (Larkindale et al., 2005). The mechanisms involved in these two types of heat resistance are distinct and therefore, three aspects of heat tolerance were tested here to investigate the role of AHK5 in heat-induced root growth in *Arabidopsis*:

1. Tolerance to prolonged exposure to a mild heat stress of 38°C
2. Tolerance to short term exposure to a severe heat stress of 42°C
3. Ability to acquire tolerance to a severe heat stress of 45°C after conditioning by exposure to a mild heat stress of 38°C with a short recovery period at 22°C.

A mild stress of 38°C is non-lethal and seedling root growth was measured after exposure to 4, 6 and 8 hours heat stress and measured after three days recovery. At this temperature, a noticeable effect on seedling root length was seen in seedlings exposed to 8 hours heat stress, with similar decreases in root growth seen in both wild-type and mutant seedlings (Figure 4.1a). The average decrease in seedling root length at this exposure time compared to controls was 33% and 40% in wild-type and *ahk5-1* seedlings, respectively, with no significant difference between the two lines.

In contrast to mild heat stress, a more severe heat stress of 42°C was employed for the shorter durations of 1, 1.5 and 2 hours. Increasing the duration of heat stress resulted in greater inhibition of root length elongation, with a decrease in root length of 25.5% and 17.3% compared to controls seen in wild-type and *ahk5-1* seedlings after 2 hours at 42°C, respectively (Figure 4.1b). No significant difference in the growth of wild-type and mutant seedlings was seen, indicating AHK5 is not required for resistance to severe heat stress.

Distinct from basal heat tolerance of plants, the ability of seedlings to acquire heat tolerance was tested. In this assay, seedlings were exposed to a mild heat stress of 38°C for a period of 90 minutes, followed by a recovery period at 22°C for 120 minutes after which seedlings were exposed to a heat stress of 45°C for 120 minutes. Following this treatment regime to test

for acquired heat tolerance, seedlings survived the normally lethal treatment at 45°C with inhibition of root elongation similar in both Col-0 and *ahk5-1* seedlings; root growth was 88.3% and 92.7% of that of control seedlings in wild-type and *ahk5-1* mutant seedlings, respectively (Figure 4.1c). Treatment of seedlings at 45°C for 120 minutes alone without pre-treatment at 38°C resulted in bleaching and death of all seedlings, confirming previous studies showing that exposure to mild heat stress protects against subsequent heat stress (Larkindale and Knight, 2002). Since responses were similar in both wild-type and mutant seedlings, this indicates that acquired heat tolerance is not affected in the *ahk5-1* mutant.

Together, the above experiments show that AHK5 does not function in heat stress tolerance in *Arabidopsis.*

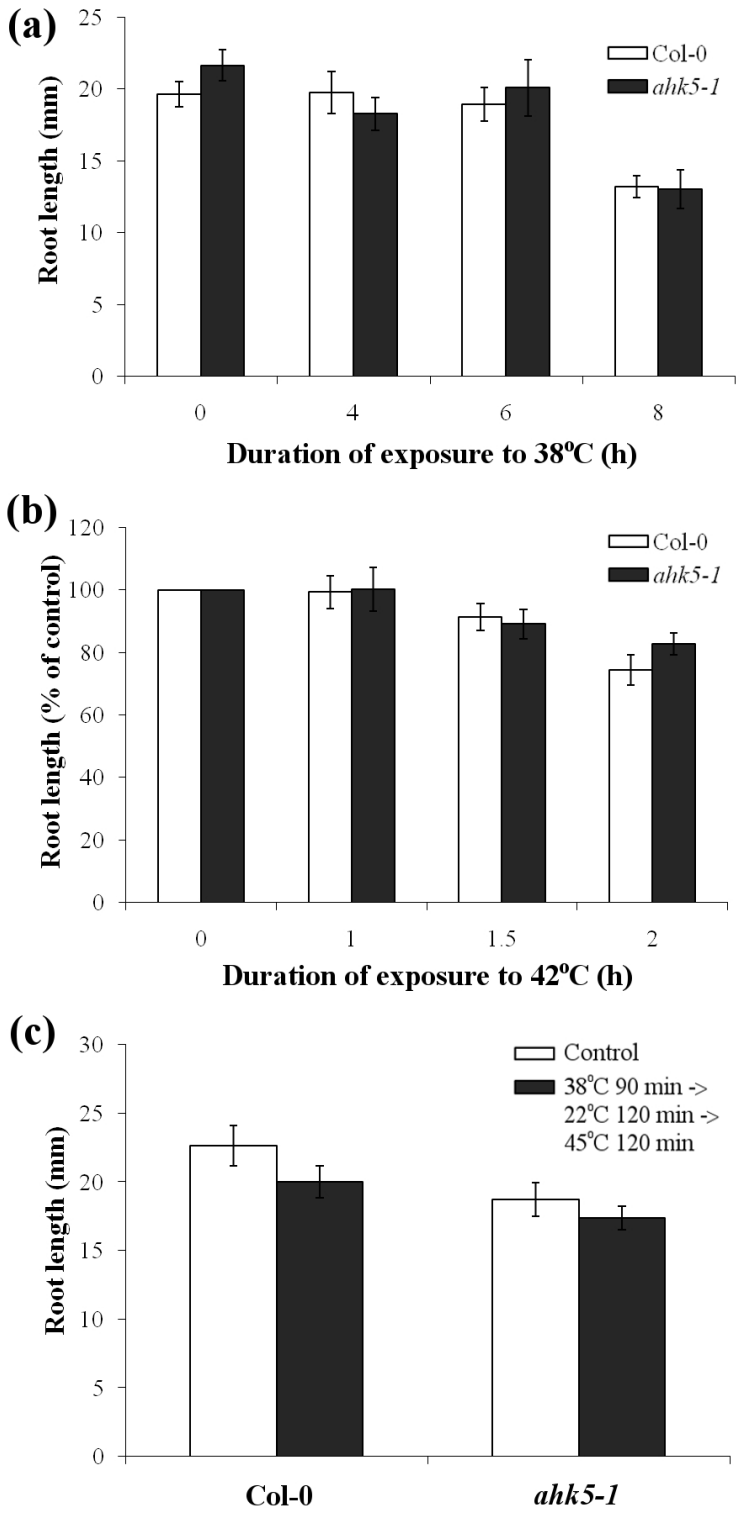


Figure 4.1 Seedling root growth in responses to different heat stress regimes. Seven-day old seedlings were subjected to heat stress and seedling root length measured after three days recovery. Graphs show root responses to (a) a mild heat stress of 38°C (n=96-144 seedlings, three independent experiments), (b) a severe heat stress of 42°C (n=120 seedlings, three independent experiments) and (c) a mild heat stress of 38°C for 90 minutes followed by a recovery period of 120 minutes at 22°C prior to heat stress at 45°C for 120 minutes (n=130 seedlings, three independent experiments). Data presented are mean ± SE.

4.3.2 *Cold stress*

Cold stress can be divided into two types: chilling stress which occurs at temperatures below 20°C or freezing stress which is caused by temperatures below 0°C (Chinnusamy et al., 2007). In this study, the cold stress applied falls within the range of chilling stress, which is inhibitory to plant growth. To test cold stress tolerance, five day old seedlings were treated to a cold stress of 10°C for up to three days (as used by Davletova (2005)) and seedling root length measured after three days recovery.

Seedlings treated at 10°C for 1, 2 and 3 days showed a reduction in root length of 18-28% compared to controls which were not subjected to cold stress, with similar reductions in root length between wild-type and *ahk5-1* seedlings at each duration of cold stress tested (Figure 4.2). This suggests that the loss of AHK5 function does not affect responses to cold stress under the conditions used here.

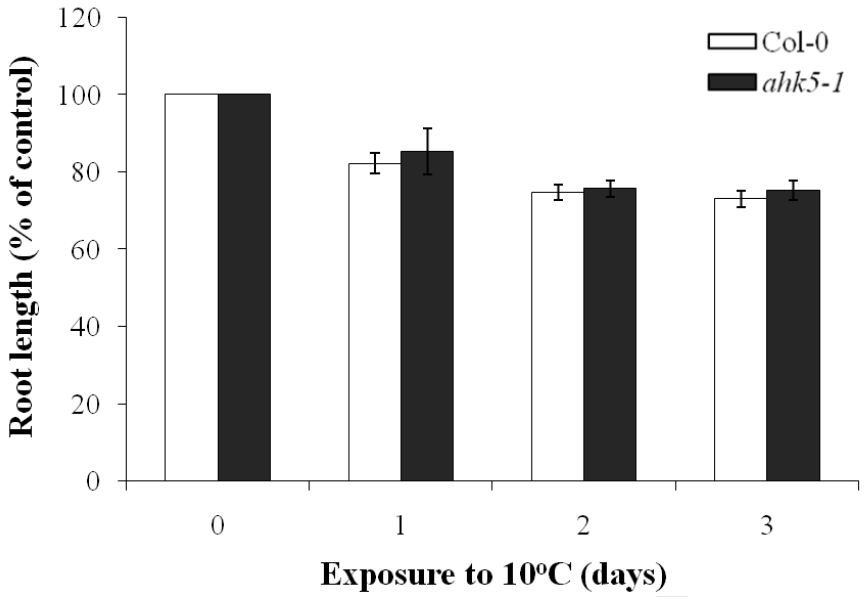


Figure 4.2 Seedling root length in response to cold stress of 10°C for 1, 2 and 3 days. Data are expressed as mean ± SE (n = 140-160 seedlings from four independent experiments).

4.3.3 *Salinity stress*

In soils of high salinity, the increased uptake of sodium ions negatively impacts on the growth of the plant and on the cellular level, build up of Na^+ in the cytoplasm inhibits enzymatic activity resulting in ion toxicity (Munns, 2002; Munns and Tester, 2008). Previously, Wu et al. (1996) isolated the salt sensitive *sos1* mutant using a seedling growth

assay and sensitivity of mutants in other components of the SOS pathway have also been shown to be hypersensitive to salinity in seedling root growth assays (Ishitani et al., 2000; Zhu et al., 2007). Therefore, to determine whether *ahk5-1* mutant seedlings were affected in root elongation in response to salt stress compared to wild-type plants, seedlings were grown on medium supplemented with different concentrations of NaCl within the range of 0 to 150mM and measured after seven days growth. In addition to root growth, germination of seeds was also monitored. In this assay, both seedling root length (Figure 4.3) and germination rate (Table 4.1) were greater in the *ahk5-1* mutant than wild-type in response to higher salt concentration, demonstrating that a knockout mutation of the *AHK5* gene results in decreased sensitivity to salt stress.

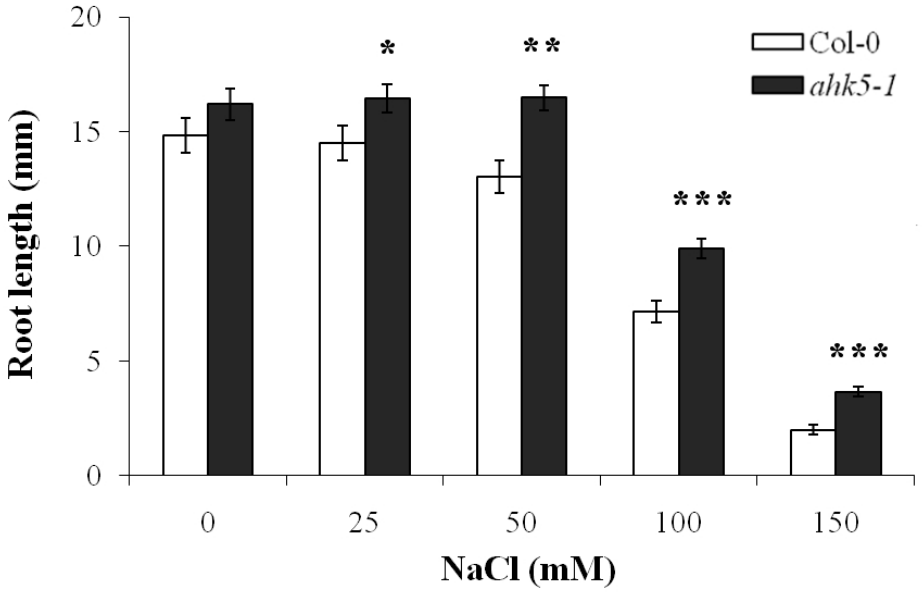


Figure 4.3 Root growth response of wild-type Col-0 and *ahk5-1* seedlings to salt stress. Seedlings were germinated and grown for seven days on half-strength Murashige and Skoog medium supplemented with NaCl. Data presented are mean ± SE (n = 90 seedlings for each dose from three independent experiments). Asterisks denote a significant difference as determined by the Student's t-test (* = $p<0.05$, ** = $p<0.005$, *** = $p<0.0001$).

Table 4.1 Germination of wild-type Col-0 and *ahk5-1* seeds on various concentrations of NaCl. Values are mean percentage germination rate of Col-0 and *ahk5-1* seeds on half-strength Murashige and Skoog medium supplemented with NaCl at the indicated doses. Germination was scored seven days after sowing of seeds (n = 90 seeds for each dose from three independent experiments). The asterisk denotes a significant difference as determined by the Student's t-test (* = $p<0.05$).

	NaCl (mM)				
	0	**25**	**50**	**100**	**150**
Col-0	100	100	95	91	72
ahk5-1	100	100	99	94	90*

To test the requirement of AHK5 function to increase sensitivity to salinity in seedlings, two independent complemented lines containing the *AHK5* gene under the control of the native promoter, lines P_{AHK5}*-AHK5/ahk5-1-1* and P_{AHK5}*-AHK5/ahk5-1-4*, were also analysed by the root growth assay in the presence of 100mM NaCl. Under these conditions, root length of the two complemented lines was as that seen in wild-type Col-0 seedlings, with root growth of the *ahk5-1* mutant line greater than that of wild-type or the complemented lines (Figure 4.4). This difference in the root growth of the *ahk5-1* mutant compared to wild-type and complemented lines were found to be significantly different by One-way ANOVA with Tukey's post hoc test. This result suggests that loss of AHK5 function is responsible for the salt insensitive phenotype of the *ahk5-1* seedlings.

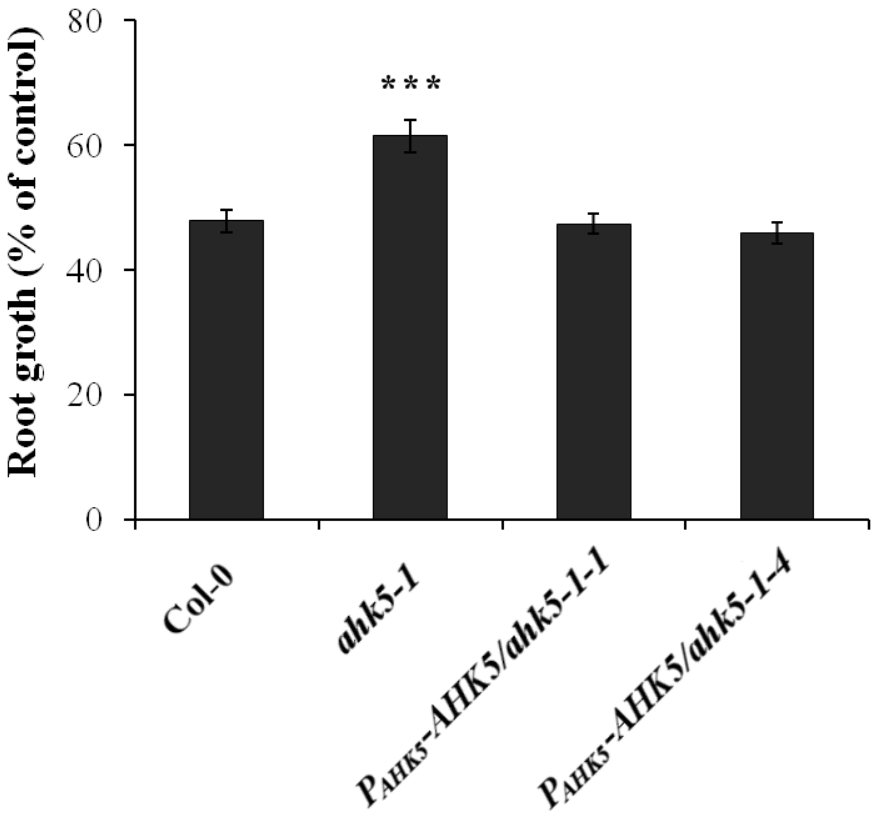


Figure 4.4 Root growth of wild-type Col-0, *ahk5-1* mutant and seedlings of the complemented lines P_{AHK5}*-AHK5/ahk5-1-1* and P_{AHK5}*-AHK5/ahk5-1-4* under salt stress. Seedlings were germinated and grown for seven days on half-strength Murashige and Skoog medium supplemented with 100mM NaCl. Data presented are mean ± SE from three independent experiments. *** = ANOVA analysis with Tukey's post hoc test to compare root growth of each line in a pairwise manner showed *ahk5-1* to be significantly different from all other lines tested ($p<0.0001$).

4.3.4 *Osmotic stress and specificity of ion toxicity of NaCl*

In addition to the ionic toxicity caused by salt stress, salinity also causes osmotic stress; build up of ions in the cell wall causes the cell to dehydrate resulting in osmotic stress (Munns, 2002; Munns and Tester, 2008). To determine whether germination and root length were affected by osmotic stress in the absence of the ionic component of salt stress, seedlings were sown on media containing sorbitol as the osmoticum (as used by Davletova et al. (2005)). To ensure the concentrations of sorbitol used would cause an equivalent osmotic stress to NaCl, the concentrations of sorbitol used were adjusted to match the osmolarities of the concentrations of NaCl used in the seedling assay (Figure 4.5a). Root growth of wild-type and *ahk5-1* mutant seedlings on these concentrations of sorbitol showed no difference (Figure 4.5b). In addition, germination rate of seeds in response to sorbitol was similar between wild-

type and mutant seeds (Table 4.2), suggesting that the differential growth of wild-type and *ahk5-1* seedlings on NaCl may be associated with the ionic component of salt stress.

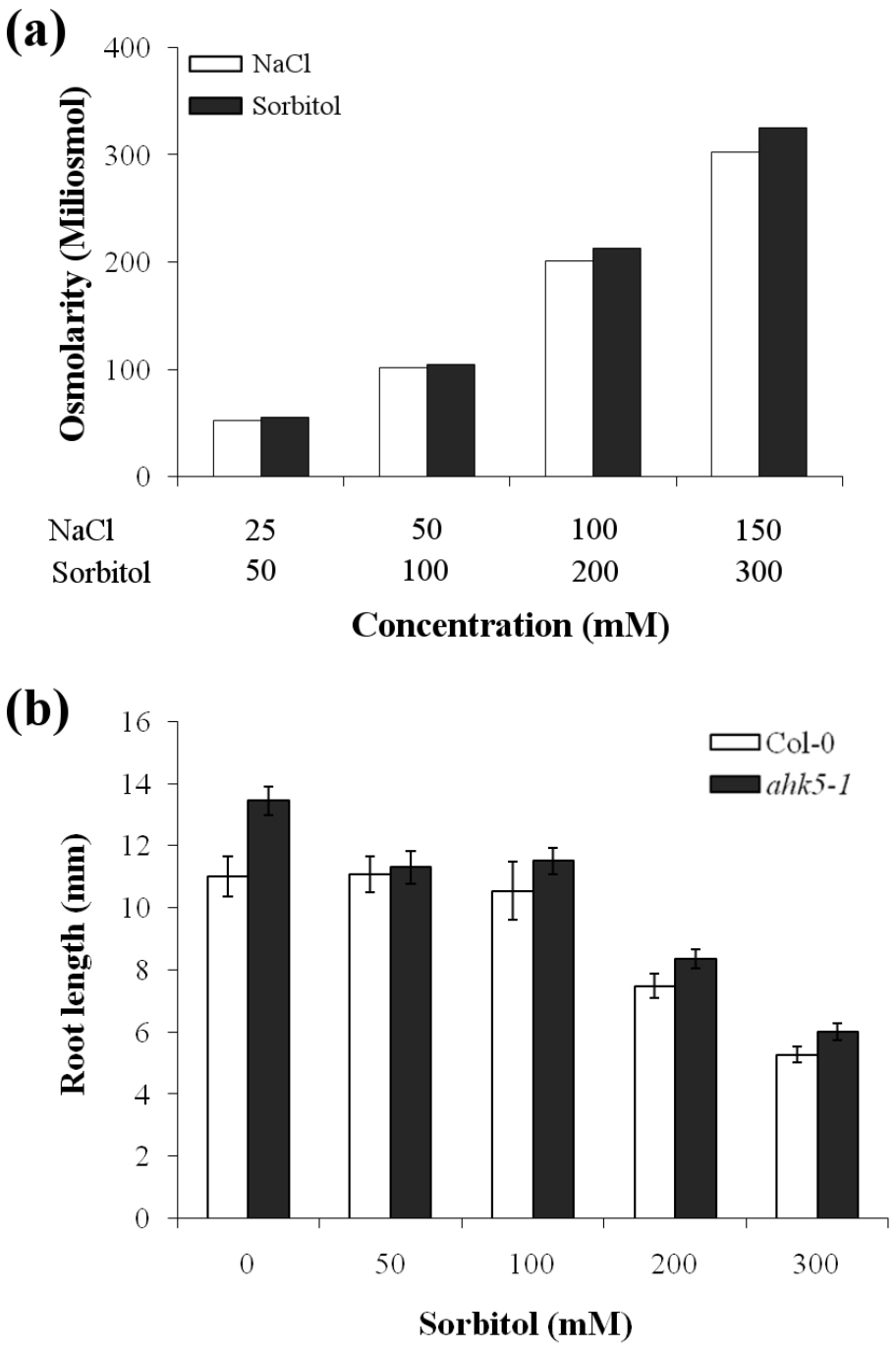


Figure 4.5 Effect of osmotic stress on seedling root growth. (a) Measurement of osmolarity of various concentrations of NaCl and sorbitol and (b) root growth of seedlings germinated and grown for seven days on half-strength Murashige and Skoog medium supplemented with sorbitol (mean ± SE, n = 144 seedlings for each dose from three independent experiments).

Table 4.2 Germination of wild-type Col-0 and *ahk5-1* seeds in the presence of sorbitol. Values are mean percentage germination rate of Col-0 and *ahk5-1* seeds on half-strength Murashige and Skoog medium supplemented with sorbitol at the indicated doses. Germination was scored seven days after sowing of seeds (n = 144 seeds for each dose from three independent experiments).

	Sorbitol (mM)				
	0	**25**	**50**	**100**	**150**
Col-0	95	99	97	94	93
ahk5-1	98	99	100	99	93

To determine whether the effect of NaCl on seedling growth was specific to Na^+, seedlings were also grown on KCl to eliminate the possibility of non-specific ion toxicity. No difference was seen between wild-type and mutant in root length (Figure 4.6) or germination of seeds (Table 4.3) in response to KCl.

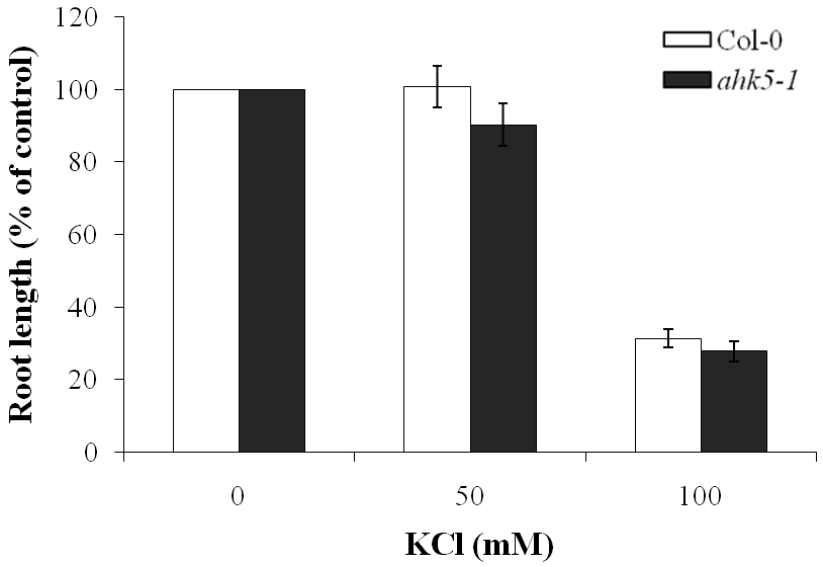


Figure 4.6 Growth of seedlings germinated and grown for seven days on half-strength Murashige and Skoog medium supplemented with KCl. Data presented are mean ± SE (n = 240 seedlings for each dose from four independent experiments).

Table 4.3 Germination of wild-type and *ahk5-1* seeds in the presence of KCl. Values are mean percentage germination rate of Col-0 and *ahk5-1* seeds on half-strength Murashige and Skoog medium supplemented with KCl at the indicated doses. Germination was scored seven days after sowing of seeds (n = 240 seeds for each dose from four independent experiments).

	KCl (mM)		
	0	**50**	**100**
Col-0	96	95	92
ahk5-1	96	95	91

In conclusion, these results suggest that *AHK5* contributes to salt sensitivity in *Arabidopsis* and this effect may be due to the ionic (Na^+) component of salt stress.

4.3.5 *Measurement of ion uptake in response to salt stress by ion chromatography*

Under salinity stress, Na^+ can build up in the cell leading to cellular toxicity and dehydration (Munns, 2002; Munns and Tester, 2008). In addition, uptake of K^+ by plants is inhibited as Na^+ competes with K^+ for uptake through non-selective cation channels, which has a negative impact on the plant as potassium is important for normal growth and development (Schroeder et al., 1994; Pardo and Quintero, 2002). In salt sensitive plants, poor performance under salinity stress has been linked to increased and decreased Na^+ and K^+ uptake, respectively, resulting in a low K^+ to Na^+ ratio in plant tissue (Zhu et al., 2007; Yang et al., 2009; Ellouzi et al., 2011).

To determine whether uptake of these ions was modified in the *ahk5-1* mutant, Na^+ and K^+ ions in seven day old seedlings grown on 100mM NaCl were measured by ion chromatography. A multi-ion standard containing known amounts of Na^+ and K^+ was also analysed in order to construct a calibration curve relating peak area measurements given by ion chromatography to ion content of the sample. This was used to calculate the concentrations of Na^+ and K^+ in samples (Appendix V). Na^+ and K^+ elute at approximately nine and 13 minutes, respectively.

As expected in control seedlings, Na^+ content was low whereas K^+ content was high in both wild-type and *ahk5-1* mutant seedlings with no significant difference in the levels of either

ion between these two lines (Figure 4.7a). Na^+ tissue content measured in control seedlings were 4.03mg gDW^{-1} for wild-type and 4.86mg gDW^{-1} in the *ahk5-1* mutant, whereas K^+ tissue content was 45.45mg gDW^{-1} and 47.26mg gDW^{-1} in wild-type and *ahk5-1*mutant, respectively.

In seedlings grown for seven days on 100mM NaCl, salt stress resulted in a greater than 10-fold increase in Na^+ content in both wild-type and *ahk5-1* mutant seedlings whereas K^+ content dropped to similar levels in both lines (38% and 37% of that measured in control seedlings for wild-type and *ahk5-1* mutant seedlings, respectively) (Figure 4.7a).

As mentioned previously, a low K^+ to Na^+ ratio in plants under salt stress is linked to sensitivity to salinity. Expressing K^+ and Na^+ content as a ratio, it can be seen that salt stress alters the balance of K^+ and Na^+ acquisition towards Na^+ uptake at the expense of K^+ in both wild-type and mutant seedlings (Figure 4.7b). Although a slightly lower K^+/Na^+ ratio was found in the *ahk5-1* mutant under control conditions, this was not statistically significant and no significant difference between the K^+/Na^+ ratio of *ahk5-1* mutant seedlings under salt stress compared to wild-type seedlings was seen.

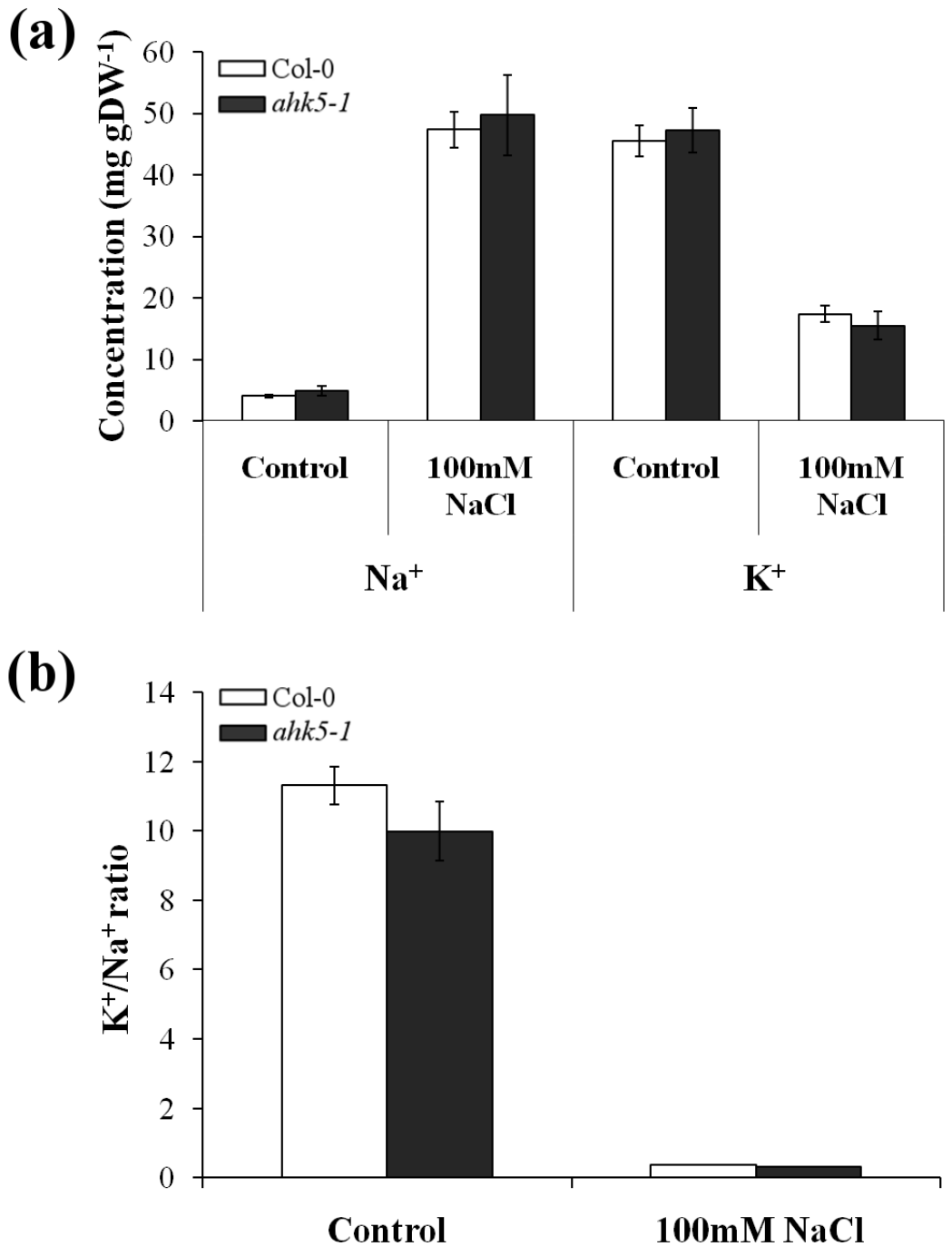


Figure 4.7 Measurement of Na^+ and K^+ content in seedling treated with 100mM NaCl by ion chromatography. (a) Na^+ and K^+ content in wild-type Col-0 and *ahk5-1* seedling grown on half-strength Murashige and Skoog medium with or without 100mM NaCl for seven days. (b) K^+ and Na^+ content of seedlings as a ratio. Ions were extracted from 5mg of seedling material. Data presented are mean ± SE of three independent extractions and two technical repeats for each extraction.

In conclusion, no significant difference in Na^+ or K^+ uptake in response to salt stress was seen between wild-type and the *ahk5-1* mutant suggesting loss of AHK5 function does not affect the concentrations of these ions within the plant.

4.3.6 *Quantification of ROS production in response to salt stress*

The production of ROS is known to be linked to salt stress and in salt-sensitive mutants such as the *sos2-1* mutant of the SOS pathway, increased accumulation of ROS is linked to salt sensitivity (Zhu et al., 2007; Ellouzi et al., 2011).

To further investigate the difference in wild-type and *ahk5-1* responses to salt stress, production of H_2O_2 was measured in response to treatment of seedlings with 100mM NaCl in liquid culture using the Invitrogen Amplex Red (AR) reagent. AR reacts with H_2O_2 to produce the highly fluorescent product resorufin which can be measured using a fluorimeter for calculation of H_2O_2 concentration in the sample (Towne et al., 2004). To correlate fluorescence with concentration of H_2O_2, a calibration curve was constructed using samples containing known concentrations of H_2O_2 which was used to calculate the amount of H_2O_2 extracted from seedling material (Appendix IV).

In a study by Zhu et al. (2007), increased ROS production in roots of salt sensitive *sos2-1* and *enh1-1* mutants over that seen in wild-type seedlings in response to 100mM NaCl was measurable using Amplex Red at 12 hours post treatment (hpt). Here, H_2O_2 mesurments in seedlings treated with 100mM NaCl was measured at 4, 8 and 14hpt. H_2O_2 levels were found to be induced by NaCl treatment at all time points in both wild-type and *ahk5-1* mutant seedlings over that of untreated seedlings (Figure 4.8). The increase in H_2O_2 levels in salt-treated *ahk5-1* seedlings was greater than that seen in Col-0 seedlings at 4, 6 and 8hpt, with levels of H_2O_2 1.2-fold higher at 4hpt and 1.6-fold higher at 6 and 8hpt (Figure 4.8).

Although there was high variability in values obtained between individual experiments and therefore no statistically significant differences were found between wild-type and *ahk5-1* responses, a consistent trend between experiments of higher H_2O_2 production in response to salt stress was seen in the *ahk5-1* mutant at the first three time points. At 14hpt however, the amount of H_2O_2 measured in the *ahk5-1* mutant was lower than that measured in wild-type. Additionally, whereas the levels of H_2O_2 at 14hpt in the *ahk5-1* mutant was reduced compared to earlier time points, H_2O_2 levels in the wild-type had risen compared to levels measured at earlier time points (Figure 4.8). Overall, H_2O_2 levels were initially greater in *ahk5-1* mutant seedlings than wild-type seedlings in response to 100mM NaCl, which decreased at the end point of the experiment, whereas H_2O_2 in wild-type tissue at 14hpt increased over that of earlier time points.

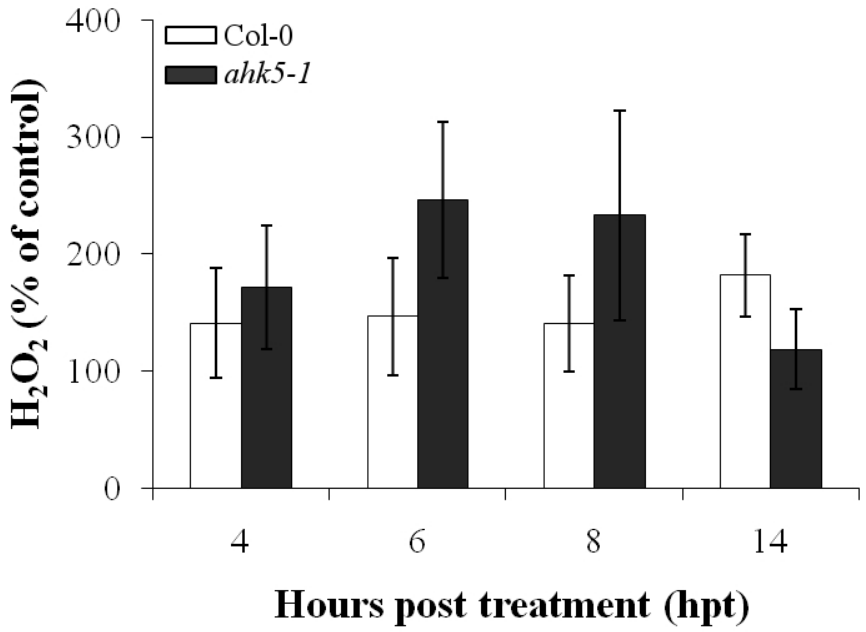


Figure 4.8 Measurement of H_2O_2 extracted from seedlings treated with 100mM NaCl in liquid culture for various times using Amplex Red. Data presented are mean ± SE from four independent experiments. Each sample consisted of H_2O_2 extracted from the tissue of approximately 100 seedlings.

4.3.7 *Effect of salt stress on soil grown mature plants*

The effect of salt treatment in vegetative tissues was also tested and measured in terms of shoot fresh weight. To determine the concentration of salt solution to treat plants with, a trial experiment in which mature soil grown wild-type plants were watered with solutions ranging in concentration from 0 to 500mM NaCl three times a week for two weeks. After this treatment regime, shoot fresh weight was measured (Figure 4.9a). From this trial, a difference in shoot fresh weight was seen at the lowest concentration used (100mM NaCl) compared to control plants treated with water only, with a similar impact on shoot fresh weight seen with 150 and 200mM NaCl. At 250 and 500mM NaCl, the impact on shoot fresh weight was greater. However, at 500mM NaCl, death of some of the plants was seen, and for this reason, a concentration of 250mM NaCl was chosen for the treatments as this concentration had the greatest impact on shoot fresh weight without causing death during the time frame of the experiment.

To investigate AHK5 function in salt tolerance in vegetative tissue, wild-type and *ahk5-1* mutant plants were watered with 250mM NaCl six times over the course of two weeks, after which a significant difference in shoot fresh weight was found, with shoots of *ahk5-1* plants

showing less of a decrease in fresh weight than salt-treated Col-0 plants when compared to the corresponding mock-treated plants (Figure 4.9b). However, this difference in fresh shoot weight was not reflected in the water content of the tissue (expressed as a proportion of shoot dry weight), which was similar between wild-type and *ahk5-1* plants treated with 250mM NaCl (Table 4.4). This suggests that the greater increase in shoot fresh weight in the *ahk5-1* mutant under salt stress is due to a proportional increase in both water and biomass production of the shoots.

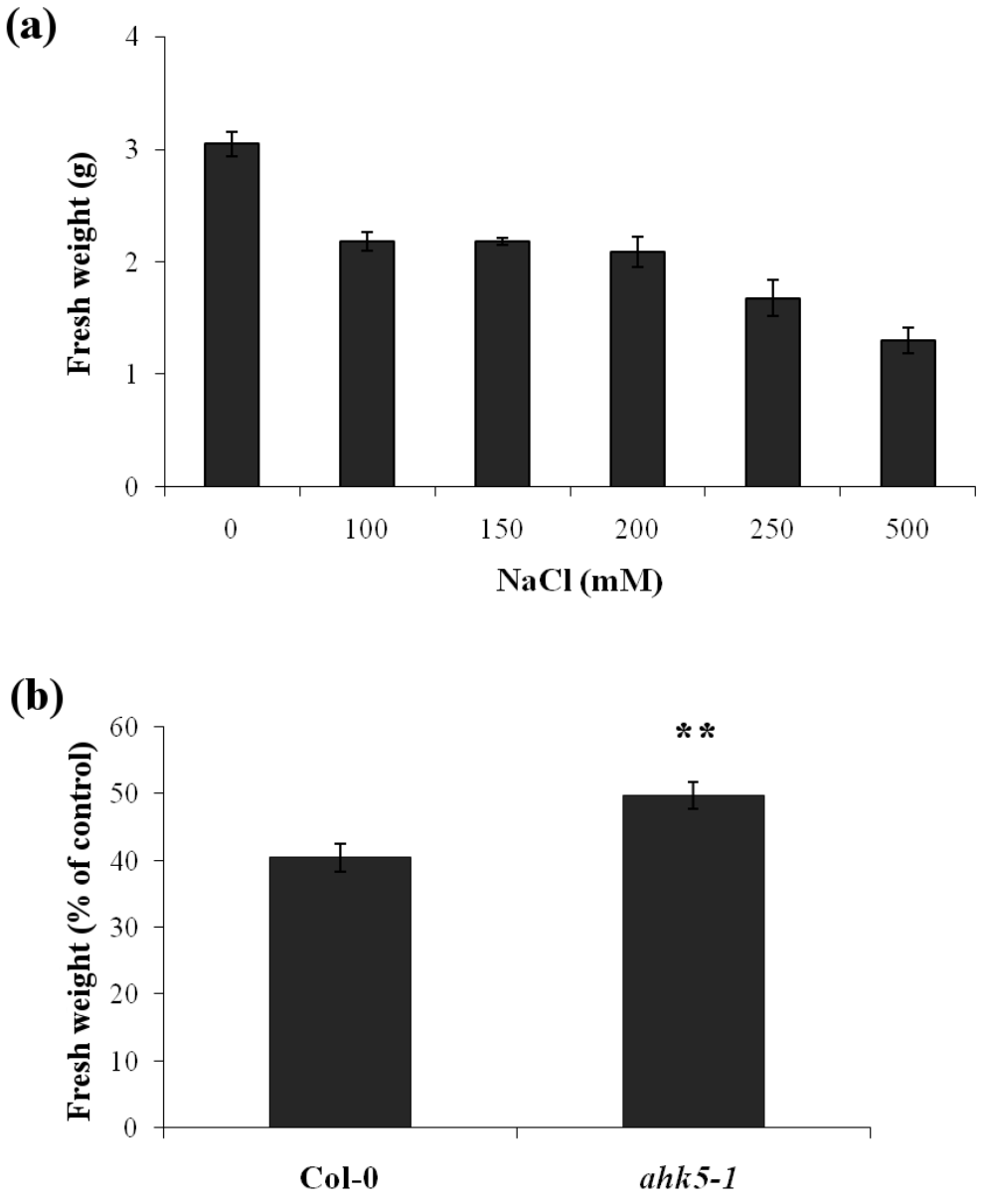


Figure 4.9 The effect of salt treatment on shoot fresh weigh of mature soil grown plants watered for two weeks with salt solution. (a) Trial experiment to test the effect of watering plants with various concentrations of salt solutions (n = three plants). (b) Shoot fresh weight of plants watered with 250mM NaCl (n = 27 plants). Data presented are mean ± SE. Asterisks denote a significant difference as determined by the Student's t-test (** = $p<0.005$).

Table 4.4 Mean water content of shoots of wild-type and *ahk5-1* mutant plants watered with 250mM NaCl for two weeks. Mean water content is expressed as a proportion of shoot dry weight ((FW-DW)/DW) (n = 13 plants from three independent experiments).

	Control	**250mM NaCl**
Col-0	11.69 ± 1.21 SEM	6.17 ± 0.53 SEM
ahk5-1	10.44 ± 0.26 SEM	6.58 ± 0.53 SEM

To test whether the greater gain in fresh weight of vegetative tissue in the *ahk5-1* mutant under salt stress was due to loss of AHK5 function, three complemented lines were also tested: P_{35S}-*AHK5/ahk5-1* containing a construct for the expression of GFP-AHK5 under the constitutive CaMV 35S promoter and lines P_{AHK5}-*AHK5/ahk5-1-1* and P_{AHK5}-*AHK5/ahk5-1-4*. This preliminary experiment showed that whereas the fresh weights of salt treated Col-0 and plants of the three complemented lines ranged from 39% to 47% of that of their corresponding control plants, fresh weight of the *ahk5-1* mutant under salt stress was 65% of that found for mock treated *ahk5-1* plants (Figure 4.10). As the impact of salt stress on shoot fresh weight was similar between wild-type plants and the three complemented lines, this suggests the phenotype seen in the *ahk5-1* mutant of greater fresh weight gain under salinity stress may be attributed to the loss of AHK5 function in this mutant.

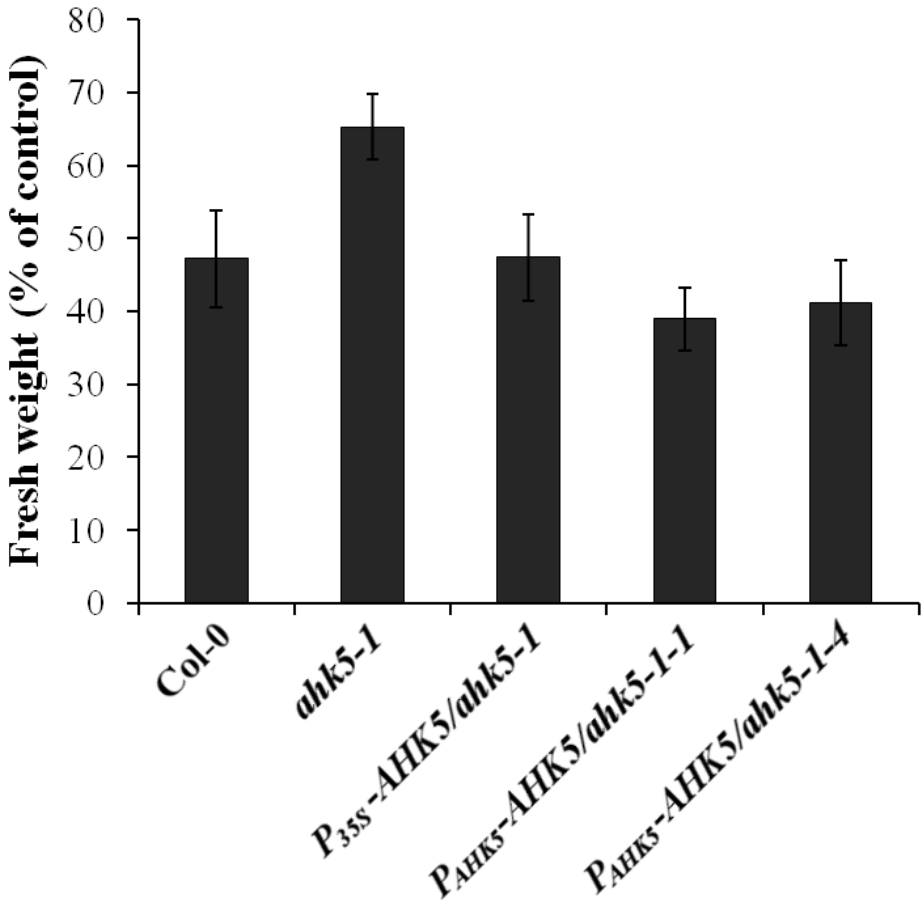


Figure 4.10 Shoot fresh weight of mature soil grown plants watered with 250mM NaCl for two weeks. Data presented are mean values (n = six plants).

4.3.8 *Effect of drought stress on soil grown mature plants*

As salt and drought signalling pathways show overlaps, the response of plants to drought stress was also tested. Withholding water from soil grown plants for 10 days resulted in visually more wilting in wild-type plants compared to *ahk5-1* mutant plants (Figure 4.11). Determination of shoot fresh weight and water content (relative to dry weight) revealed both parameters to be significantly greater in mutant *ahk5-1* plants than wild-type plants compared to their respective control plants which were kept well-watered (Figure 4.12). The higher water content of *ahk5-1* plants under drought stress suggests that these plants are more efficient at retaining and/or uptake of water (Figure 4.12b). These data suggest that the *ahk5-1* mutant is more drought resistant than wild-type plants.

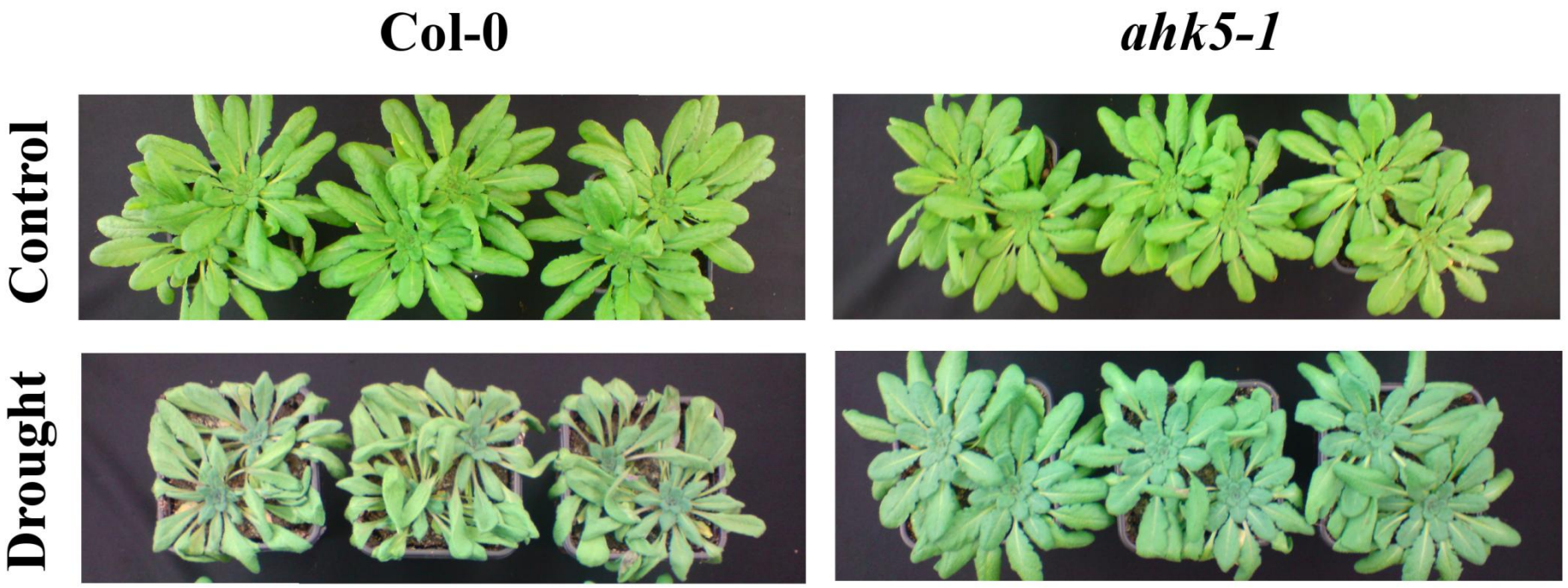


Figure 4.11 Appearance of soil grown plants after 10 days of withholding water to simulate drought stress.

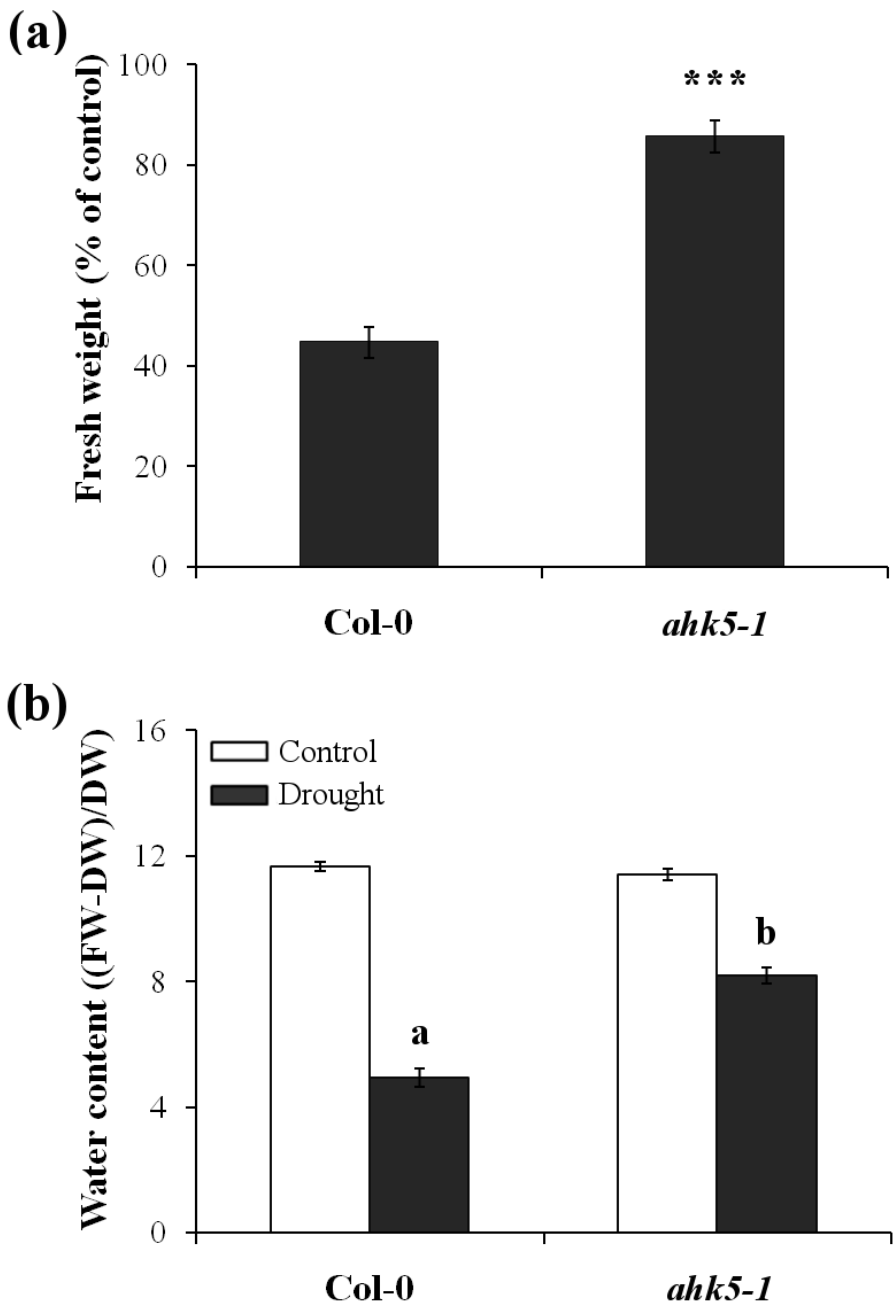


Figure 4.12 Effect of drought stress on (a) fresh shoot weight and (b) water content of shoots. Drought stress created by withholding water from soil grown plants for 10 days. Asterisks and the letters **a** and **b** denote a significant difference between wild-type and mutant responses as determined by the Student's t-test (*** = $p<0.0005$).

4.4 Discussion

The first study of AHK5 function by Iwama et al. (2007) indicated that this histidine kinase acted as a negative regulator of ABA/ethylene-induced inhibition of root growth. To further investigate the extent of the function of AHK5 in root responses, root elongation of the *ahk5-1* mutant in response to heat, cold, salt and drought stress was tested.

4.4.1 *The* ahk5-1 *mutant is not defective in response to low and elevated temperatures*

In this study, the contribution of AHK5 in response to heat and cold stress was tested. Roles for histidine kinases in mediating temperature responses in Cyanobacteria have been described, raising the possibility of similar function of HKs in plants. In Cyanobacteria, the expression of HSPs in response to heat stress is regulated by the activity of the histidine kinase Hik34 which in its normally autophosphorylated form negatively regulates HSP expression (Suzuki et al., 2005). Elevated temperatures are indirectly sensed through changes in the amount of autophosphorlated Hik34, which decreases on increasing temperature, which in turn relieves the repression on HSP expression (Suzuki et al., 2005). This balance between active and inactive Hik34 ensures that HSPs are produced only when required (i.e., on heat stress).

Detection of decreased temperature in Cyanobacteria is also mediated by two other histidine kinases, the membrane bound Hik33 and the soluble Hik19, mutations in which result in the inability to upregulate expression of some cold-responsive genes on exposure to cold stress (Suzuki et al., 2000; Suzuki et al., 2001; Mikami et al., 2002). Hik19 is thought to act downstream of Hik33 in transduction of the cold signal (Suzuki et al., 2000). More recently in *A. thaliana,* AHK2 and AHK3 were found to mediate cold stress responses (Jeon et al., 2010). Since AHK5 is the only histidine kinase predicted and shown to have a cytosolic location, it is possible that AHK5 may act to relay signals from other membrane-bound histidine kinases in response to changes in temperature as with Hik19.

As discussed previously, plants display two types of heat tolerance: basal thermotolerance and acquired thermotolerance. In this study, the *ahk5-1* was not affected in basal thermotolerance when tested by exposure to 38°C for up to 8h and 42°C for up to 2h. Under these conditions, decreased root elongation was seen as expected but occurred to a similar degree in both wild-type and mutant seedlings. The *ahk5-1* mutant also acquired thermotolerance to a normally lethal heat stress of 45°C to the same degree as wild-type

seedlings, suggesting that AHK5 is not required for thermotolerance under the conditions tested using seedlings.

To determine whether AHK5 might be involved in sensing cold stress rather than heat stress, responses to a chilling temperature of 10°C for up to three days were monitored in terms of seedling root growth. Again, as expected, this treatment inhibited root growth, but equally so in both lines tested. A lower temperature of 4°C for up to 24h was also tested (data not shown), but this treatment was not sufficient to inhibit root growth in either wild-type or mutant seedlings.

In conclusion, the evidence suggests that AHK5 does not function in either thermotolerance or responses to cold stress under the conditions tested here. Although no difference in seedling response to heat stress was shown here, it has been noted that seedlings can display different levels of tolerance at different growth stages (Hong et al., 2003; Clarke et al., 2004; Larkindale et al., 2005). It is therefore possible that the *ahk5-1* mutant may be affected in cold or heat stress tolerance at a different growth stage (e.g. vegetative tissues) not investigated here.

4.4.2 *AHK5 contributes to salt sensitivity*

Salinity imposes ion toxicity in plants through excessive uptake of Na^+ and inhibition of cellular processes through inhibition of cellular enzymes and disruption of K^+ uptake (Munns, 2002; Munns and Tester, 2008). In addition to this, salt stress also imposes osmotic stress on the plant (Munns, 2002; Munns and Tester, 2008). In this study, it was found that the *ahk5-1* mutant was more resistant to salinity stress in both seedlings grown in tissue culture and soil grown plants. This increased resistance in the *ahk5-1* mutant was attributed to the loss of AHK5 function as lines complemented with *AHK5* under the control of the endogenous promoter displayed similar responses to salt stress as wild-type at both the seedling and vegetative stages.

In tissue culture, elongation of root length in the *ahk5-1* mutant was less sensitive to the presence of NaCl compared to wild-type, suggesting that AHK5 acts as a negative regulator of root growth under high salinity conditions. Since the root phenotype and germination rate were similar between wild-type and the *ahk5-1* mutant in the presence of sorbitol (to induce osmotic stress) and KCl (to determine the contribution of the ionic component of NaCl), the

altered phenotype in response to NaCl in the *ahk5-1* mutant may be attributed to reduced sensitivity to the presence of Na^+.

Tolerance to salt stress in *Arabidopsis* is mediated in part through efflux of Na^+ by the Na^+/H^+ antiporter SOS1 at the plasma membrane, which is activated upon salt stress by the myristolated calcium binding protein SOS3 and the serine/threonine kinase SOS2 as part of the SOS pathway (Zhu, 2002, 2003). SOS1 was shown to specifically transport Na^+ across the plasma membrane and is unable to transport either Li^+ or K^+ (Qiu et al., 2003). As the phenotype observed in the *ahk5-1* mutant may be due to the ionic component of salt stress, it is possible that AHK5 impacts upon the SOS pathway under conditions of salinity.

In addition to extrusion of Na^+ ions from the cell via SOS1, compartmentalisation of Na^+ ions in the vacuole by Na^+/H^+ antiporters located in the tonoplast membrane also contributes to salt tolerance (Zhu, 2003). Expression of the Na^+/H^+ antiporters AtNHX1 and AtNHX2 is up-regulated by NaCl and this up-regulation requires ABA synthesis and signalling (Shi and Zhu, 2002; Yokoi et al., 2002).

Measurement of sodium and potassium levels in seedlings grown in the presence of 100mM NaCl by ion chromatography suggests that neither Na^+ nor K^+ uptake were significantly different between wild-type and *ahk5-1* seedlings in response to salinity. In the salt-sensitive *sos1*mutant, Na^+ and K^+ levels in salt-treated seedlings accumulated to approximately 180% and 60%, respectively, of that seen in salt stressed wild-type seedlings (Shi et al., 2002). If this is indeed the case, the greater tolerance of the *ahk5-1* mutant to salt stress may be due to more efficient compartmentalisation of Na^+ rather than increased extrusion or a decrease in uptake of this ion. In this scenario, total tissue Na^+ content of salt stressed *ahk5-1* mutants would be similar to that of wild-type (as seen here), but the cellular toxicity caused by Na^+ would be reduced due to compartmentalisation in the vacuole, leading to increased tolerance to salinity.

Interestingly, a study by Jha et al. (2010) investigating difference in salt tolerance between ecotypes of *Arabidopsis* found Na^+ accumulation in shoots did not necessarily correlate with level of salt tolerance, suggesting that the tolerance of plant tissue to Na^+ toxicity rather than the exclusion or inhibition of Na^+ uptake was responsible for the tolerance seen. Additionally, they found no differences in the percentage water content between salt tolerant and salt sensitive ecotypes under salt stress, but found that those with slower growth rates were more tolerant to high salinity. Jha et al. (2010) hypothesised that slower uptake of Na^+ by roots as a

result of slower growth allowed the plants to better manage Na^+ entering the shoots. These findings are in agreement with the results of this study, as salt tolerance of the *ahk5-1* mutant was not attributed to decreased Na^+ accumulation nor associated with a difference in shoot water content (relative to dry weight). Additionally, the *ahk5-1* mutant plants were normally of a smaller stature compared to wild-type plants under normal growth conditions (see Section 3.5). If the rate of Na^+ movement within *ahk5-1* plants is slower due to reduced transpiration, this may suggest greater stomatal closure in *ahk5-1* mutant plants in response to salinity.

Under high salinity, ABA is known to promote primary root elongation through inhibition of ethylene production (Sharp and LeNoble, 2002; Xiong and Zhu, 2002). In this scenario, negative regulation of ABA signalling by AHK5 would result in less root growth under salt stress, with loss of AHK5 function in the *ahk5-1* mutant leading to greater root elongation, as was seen here. In contrary to this, in a seedling root growth assay similar to that used here, Iwama et al. (2007) showed that ABA inhibits root growth and that AHK5 negatively regulates this inhibition, which would suggest that AHK5 functions to promote rather than inhibit root growth. However, it is possible that endogenously, lower levels of ABA are stimulated by salinity stress which promote rather than inhibit root growth. In agreement with this, both wild-type and *ahk5-1* mutant seedlings grown in the presence of a low amount of exogenous ABA (0.1µM) caused a slight promotion of root growth whereas higher concentrations (above 1µM ABA) resulted in inhibition of root growth (see Section 3.6).

Similar to the *ahk5-1* mutant, the *ahk2* and *ahk3* mutants displayed increased tolerance to high salinity, with the *ahk2 ahk3* double mutant more tolerant to salt stress than either single mutant (Tran et al., 2007; Tran et al., 2010), implicating interaction between HKs in stress signalling. A number of stress/ABA-responsive genes were found to be up-regulated in *ahk2 ahk3* double mutants under normal growth conditions, suggesting that AHK2 and AHK3 negatively regulate salt-induced ABA responses (Tran et al., 2007; Tran et al., 2010). In addition to the negative regulation of salt stress responses previously shown for AHK2 and AHK3 (and for AHK5 here), AHK1/AtHK1 (Tran et al., 2007; Wohlbach et al., 2008) and ETR1 (Zhao and Schaller, 2004; Wang et al., 2008b) were shown to act as positive regulators of salt stress tolerance, suggesting *Arabidopsis* HKs play important roles in the salt signalling pathway.

It is therefore hypothesised that AHK5 acts to negatively regulate ABA promotion of root elongation under salt stress and loss of function of AHK5 in the *ahk5-1* mutant results in increased salt tolerance.

Interestingly, measurement of H_2O_2 levels in seedlings treated with 100mM NaCl suggested that H_2O_2 levels to be higher in *ahk5-1* seedlings compared to wild-type seedlings after four, six and eight hours exposure to salt stress. However, after a longer duration to salinity stress of 14 hours, H_2O_2 level in the *ahk5-1* mutant was reduced and less than that measured in wild-type plants at the same time point, which had increased compared to measurements at earlier time points. Thus whereas H_2O_2 levels were initially higher in the *ahk5-1* mutant in response to salt stress, this began to decrease after time, whereas in wild-type seedlings, H_2O_2 levels continued to increase. The significance of this finding is not clear. In a recent report, Xie et al. (2011) found that in response to mild salt stress (10mM NaCl), a biphasic oxidative burst occurred, with a sharp transient peak seen one hour after the onset of stress followed by a second more sustained production of ROS peaking after six hours of salt stress. These two peaks of ROS production (peak I and peak II) were found to be dependent on the NADPH oxidase AtrbohD, loss of function of which abolished the oxidative response to salinity. In the *hy1-100* mutant which is mutated in a gene encoding for a haem oxygenase, peak II was not seen in response to salinity stress and was linked to the salt sensitive phenotype of this mutant (Xie et al., 2011). Induction of the ascorbate peroxidase gene *cAPX1*in response to salt stress was also attenuated in the *hy1-100* mutant (Xie et al., 2011).

These findings suggests that distinct to the oxidative stress caused by salt stress due to disturbances in cellular homeostasis, plants may also induce ROS production for signalling purposes to trigger salt stress tolerance mechanisms, including the production of ROS detoxifying enzymes. It is possible that the greater amount of H_2O_2 seen earlier in the *ahk5-1* mutant may be a reflection of increased ROS production by the plant for the purpose of stress signalling and that the decreased level of H_2O_2 at the later time point was due to the detoxification of ROS by the induced responses. In comparison in wild-type plants, this response is perhaps delayed, thus the lower levels of H_2O_2 seen initially followed by an increase in ROS seen at the end point of the experiment. Whether or not this is the case would require further investigation, such as comparison of the timing of induction of known salt responsive genes in wild-type and mutant plants and a more extensive time course experiment for ROS production as well as antioxidant levels, in response to salinity.

In addition to the salt-insensitive root elongation phenotype, the *ahk5-1* mutant was also insensitive in terms of germination rate in the presence of salt at high concentrations (i.e., 150mM NaCl). Since ABA is also required for seed dormancy/inhibition of germination (Nambara and Marion-Poll, 2005; Nambara et al., 2010), it is tempting to hypothesise that AHK5 also acts upstream of ABA in inhibition of germination in response to salt stress. However, Iwama et al. (2007) observed no difference in germination between wild-type and *ahk5-1* mutant seeds in response to exogenous ABA and found that the ABA pathway involved in inhibition of root elongation is distinct from that involved in germination. In addition, ability to germinate under high salinity does not necessarily translate to increased salt tolerance at later developmental stages (Saleki et al., 1993), suggesting salt tolerance at different developmental stages may be under the control of distinct mechanisms.

The salt resistant phenotype of the *ahk5-1* mutant was also apparent in soil grown plants irrigated with 250mM NaCl. This tolerance manifested as greater shoot fresh weight in the *ahk5-1* mutant compared to wild-type plants. That the increased resistance of the *ahk5-1* mutant was attributed to the loss of AHK5 function was indicated by the three complemented lines, P_{35S}*-AHK5/ahk5-1*, P_{AHK5}*-AHK5/ahk5-1-1* and P_{AHK5}*-AHK5/ahk5-1-2*, expressing wild-type AHK5 which displayed wild-type responses after to irrigation with 250mM NaCl.

4.4.3 *AHK5 contributes to drought stress sensitivity*

A key mechanism in reducing water loss in plants during drought stress is the up-regulation of ABA synthesis, which is known to regulate stomatal closure (Schroeder et al., 2001). Stomatal closure in response to drought stress reduces water loss through the transpiration stream and evaporation of water from the leaf surface (Schroeder et al., 2001). In this study, the *ahk5-1* mutant was found to be more resistant to drought stress, imposed by withdrawal of watering for 10 days in soil grown plants, showing visibly less wilting and greater gain in shoot fresh weight and water content (relative to shoot dry weight) compared to wild-type plants. This suggests that the *ahk5-1* mutant may close stomata more efficiently via ABA in response to drought stress and thus more efficiently control water loss through stomata compared to wild-type plants.

However, stomatal responses in the *ahk5-1* mutant were previously shown to be unaffected in responses to exogenous ABA (Desikan et al., 2008) so how loss of function of AHK5 would enhance drought stress in terms of stomatal closure is not clear. It should be noted that the

responsiveness of the *ahk5-1* mutant to exogenous ABA does not rule out an effect of loss of AHK5 function upstream of ABA perception: it is possible that stimulus-induced production of ABA is altered in the *ahk5-1* mutant rather than ABA perception.

Under the growth conditions used in this study, the *ahk5-1* mutant was noticeably smaller in stature than wild-type plants in the absence of stress, suggesting a slower growth rate and perhaps a slower rate of water uptake. A slower uptake of water by the *ahk5-1* mutant would result in less depletion of water from the soil and therefore increased tolerance to conditions of low water availability. This scenario could also explain the increased tolerance of the mutant to salt stress as discussed above. In addition, the leaves of the *ahk5-1* mutant tended to lie more flat just above the surface of the compost, which would decrease water loss from the leaf by maintaining high humidity at the leaf surface, whereas leaves of wild-type plants tended to grow more upright. To determine whether or not there are differences in the rate of water uptake by the *ahk5-1* mutant and wild-type plants, the water potential (ψ_w) of the compost in which the plants are grown in would need to be measured over time in response to drought stress.

As salt and drought stress show overlaps in signalling pathways, it is perhaps not surprising to find that the *ahk5-1* mutant is affected in response to both stresses. As discussed in Section 1.2, both salt and drought stress result in osmotic stress as both essentially restrict the water available to the plant. That the seedling assay used here to investigate the responses of wild-type and *ahk5-1* mutant plants did not reveal a role for AHK5 in osmotic stress is surprising. It is possible that differences in response to osmotic stress in the wild-type and mutant plants may have been masked by the high humidity conditions which the seedlings were exposed to. In the seedling root growth assay, the seedlings were grown on media in sealed plates; it is possible that in this environment, the humidity was high enough to mask any subtle differences in osmotic stress tolerance between wild-type and mutant plants. That differences in root growth were seen between wild-type and *ahk5-1* mutant plants in response to salinity in the same assay may be a result of the combined effect of osmotic and ionic stress exerted by NaCl, where the ionic component of salt stress is known to have a greater impact on plant growth (Munns, 2002; Verslues et al., 2006; Munns and Tester, 2008).

Alternatively, the lack of difference in osmotic stress phenotypes may be due to the osmoticum used. In this assay, sorbitol was used to simulate osmotic stress in seedlings. It has previously been noted that small molecular weight compounds, such as mannitol and

sorbitol which have commonly been used as osmotica, may be absorbed by the roots and cause stresses other than osmotic stress (Munns, 2002; Verslues et al., 2006). An improvement of this assay would have been to use a high molecular weight compound which is not easily absorbed by the plant to cause osmotic stress, such as polyethylene glycol (PEG) (Verslues et al., 2006).

4.5 Conclusions

The role of AHK5 in responses to abiotic stress was investigated and it was found that whereas AHK5 did not contribute to heat or cold stress responses under the conditions used in this study, AHK5 was found to negatively regulate seedling root elongation in response to salinity. Measurement of H_2O_2 in seedlings under salt stress revealed higher levels in the *ahk5-1* mutant seedlings compared to wild-type at 4, 6 and 8hpt but lower levels at 14hpt. The increased tolerance of the *ahk5-1* mutant in response to salt stress was also true of vegetative tissue and evidence to support the hypothesis that this altered phenotype was due to loss of AHK5 function was obtained using genetically complemented *ahk5-1* lines expressing wild-type AHK5. The *ahk5-1* mutant was also shown to be more resistant to drought stress, which was also linked to the loss of AHK5 function. It is possible that AHK5 acts as a negative regulator of plant responses to salt and drought stress by impacting on the ABA pathway upstream of ABA biosynthesis to modulate growth and transpiration rate. The interaction of AHK5 with the ABA signalling pathway remains to be investigated.

Chapter 5:

The role of AHK5 in response to bacterial infection

5 The role of AHK5 in response to bacterial infection

5.1 Introduction

The bacterium *Pseudomonas syringae* pv. *tomato* DC3000 is a pathogen of both the important crop plant tomato and the model plant *Arabidopsis thaliana.* The availability of the genome sequences of both *A. thaliana* and *P. syringae* pv *tomato* DC3000 and the genetic tractability of both host and pathogen have provided attractive model systems for the study of infection and immunity in plants (Arabidopsis Genome Initiative, 2000; Preston, 2000; 2002; Buell et al., 2003; Quirino and Bent, 2003). Additionally, other pathovars of *Pseudomonas* have also been sequenced, such as *P. syringae* pv. *phaseolicola* 1448A (Joardar et al., 2005), and effector proteins produced by the different *P. syringae* pathovars have been identified (Pseudomonas-Plant Interactions, 2011). The wealth of information available has enabled the study of different types of plant-bacteria interactions, such as compatible, incompatible and non-host interactions.

5.1.1 *Different types of plant-bacteria interactions*

In order to defend against infection by pathogens, plants are able to recognise components specifically associated with the pathogen, such as components of the bacterial flagella. These components which are recognised by the plant are termed pathogen-associated molecular patterns (PAMPs) or, more recently, microbe-associated molecular patterns (MAMPs) as components of non-pathogenic microbes can also elicit a reaction in the plant.

In a compatible interaction, the bacterium is able to ‘disguise’ its presence through the production of effector proteins which act to overcome or subvert plant defence. This allows the pathogen to spread and multiply within the plant tissue, leading to the development of disease symptoms. In the case of the *A. thaliana-Pst*DC3000 interaction, disease is typified by the appearance of water-soaked lesions, chlorosis and *in planta* bacterial multiplication (Preston, 2000; Katagiri et al., 2002). Where the plant is able to recognise the bacterial effector protein, either directly or indirectly, *R*-gene mediated resistance occurs, resulting in an incompatible interaction. In this context, the effector protein is acting as an avirulence determinant, as its presence is detected by the plant. This type of interaction is typically associated with the hypersensitive response (HR) and a biphasic oxidative burst (Levine et

al., 1994). The spread of the pathogen is restricted and it is unable to multiply and establish disease.

In the case where the pathogen cannot overcome plant defences and where multiple effector proteins are recognised by the host, a non-host interaction occurs (Thordal-Christensen, 2003). The inability of the pathogen to overcome multiple recognition events leads to more robust immunity in the plant and is the main basis of non-host interactions (Thordal-Christensen, 2003; Lindeberg et al., 2009). Thus there are different types of plant-bacteria interactions that may occur with different aspects of plant immunity activated depending on the nature of the pathogen.

5.1.2 *The type-III secretion system and effector proteins*

The ability of the bacterium to secrete effector proteins into the host cell is important for overcoming/suppressing innate immunity. The type III secretion system (TTSS) found in many gram-negative bacteria forms a pilus through which the effector proteins are injected into the host cells (Jin and He, 2001). The pilus of the TTSS consists mainly of subunits encoded for by the *hrpA* gene and mutations in this gene lead to an inability to secrete effector proteins and to cause disease symptoms or HR in the context of a compatible or incompatible interaction, respectively (Roine et al., 1997; Wei et al., 1999; Collmer et al., 2000). As mutants of the HrpA subunit are unable to modify plant defences through the action of effector proteins, comparison of plant responses to a *hrpA*- mutant (*Pst*DC3000*(hrpA*$^{-}$*)* with compatible and incompatible interaction can contribute to the understanding of the action of effector proteins in promoting disease and the mechanisms utilised by plants to restrict infection (Jones et al., 2004; de Torres Zabala et al., 2007; Kaffarnik et al., 2009; Allwood et al., 2010).

5.1.3 *Plant hormones in immune signalling*

To mount an immune response against pathogens, signalling via plant hormones salicylic acid (SA), jasmonic acid (JA), and abscisic acid (ABA) is known to be important. This is evident from studies utilising biosynthetic and signalling mutants of these hormones and the observation that *Pst*DC3000 manipulates hormone levels as a virulence strategy (Mohr and Cahill, 2003; Brooks et al., 2005; de Torres Zabala et al., 2007; Katsir et al., 2008; de Torres Zabala et al., 2009).

5.1.3.1 Role of SA in pathogen defence

SA has a major role in resistance to biotrophic pathogens, whereas JA is considered more important in mediating resistance against nectrophic pathogens and herbivores (Glazebrook, 2005). The importance of SA in defence against biotrophic pathogens is evident from the increased susceptibility of mutants unable to accumulate SA, such as the *sid2* (SA induction-deficient 2) mutant (Nawrath and Metraux, 1999) and transgenic plants expressing the SA degrading enzyme salicylate hydroxylase encoded for by the bacterial *nahG* gene. Targeting and manipulation of SA-mediated basal defence by bacteria also highlights the importance of this hormone in defence (DebRoy et al., 2004; Brooks et al., 2005; Uppalapati et al., 2007; de Torres Zabala et al., 2009).

SA-mediated basal defence includes induction of callose deposition in the plant cell wall and activation of pathogenesis-related (*PR*) genes, some of which encode for proteins with anti-microbial properties (Van Loon and Van Strien, 1999; Maleck et al., 2000). SA also mediates HR in response to *R*-gene mediated recognition of bacterial effector proteins together with ROS and nitric oxide (NO) (Zaninotto et al., 2006; Mur et al., 2008). SA is synthesised via two separate pathways, one mediated by phenylalanine ammonia lyase (PAL) and the other by isochorismate synthase (ICS) encoded by two genes, *ICS1/SID2/EDS16* and *ICS2* (Chen et al., 2009). Inhibition of SA accumulation through expression of the *nahG* gene or through suppression or mutation of *PAL* or *ICS* genes results in increased susceptibility to infection with a range of pathogens and an inability to develop systemic acquired resistance (SAR), a phenomenon in which distal uninfected leaves are resistant to subsequent infection (Gaffney et al., 1993; Pallas et al., 1996; Nawrath and Metraux, 1999; Wildermuth et al., 2001).

5.1.3.2 SA signalling triggered by different classes of NB-LRR R-proteins

SA signalling is triggered by the largest class of R-proteins, the nucleotide-binding site leucine rich repeat (NB-LRR) proteins which are subdivided into two subclasses, those with coiled-coil domains at the N-terminus (CC-NB-LRR) and those with a Toll interleukin receptor domain (TIR-NBS-LRR) (Dangl and Jones, 2001). Whereas NDR1 (Non Race-specific Disease Resistance 1) acts downstream of the CC-NB-LRRs, EDS1 (Enhanced Disease Susceptibility 1), PAD4 (Phytolexin Deficient 4) and SAG101 (Senescence Associated Gene 101) act downstream of the TIR-NBS-LRRs, suggesting specificity is

determined by R-protein structure, although some cross-talk between the two pathways does occur (Aarts et al., 1998).

5.1.3.3 Activation of SA signalling by NDR1

NDR1 encodes for a glycosylphosphatidyl-inositol (GPI) anchored plasma-membrane localised protein which plays an important role in SA signalling downstream of SA in response to pathogen recognition by the CC-NB-LRR type R-proteins (Shapiro and Zhang, 2001; Coppinger et al., 2004). Loss of NDR1 function resulted in greater bacterial growth of *Pst*DC3000 strains carrying either *avrB, avrRpm1* or *avrRpt2*, the products of which normally trigger resistance in wild-type plants (Century et al., 1995). On the other hand, over-expression of *NDR1* resulted in increased resistance to both *Pst*DC3000(*avrRpt2*) and virulent *Pst*DC3000 (Coppinger et al., 2004). This suggests that activation of NDR1 functions in response to recognition of bacterial effector proteins. Activation of NDR1 is thought to be mediated through interaction of the R-protein with RIN4 (RPM1-interacting Protein 4), which acts as a negative regulator of R-protein activation and is known to be targeted by the effector proteins AvrB, AvrRpm1 and AvrRpt2 (Kim et al., 2005a; Day et al., 2006; Chung et al., 2011). The sequestering of RIN4 through interaction with NDR1 may relieve the negative regulation on R-proteins (such as RPM1 which recognises AvrRpm1), with interference of RIN4-NDR1 interaction leading to an inability to activate the HR in response to bacterial effector protein where the cognate R-protein is also present (Day et al., 2006).

5.1.3.4 Activation of SA signalling by EDS1, PAD4 and SAG101

EDS1 encodes for a lipase-like protein, mutation of which results in the ability of *Pst*DC3000 carrying the *avrRps4* gene to multiply *in planta* and an inability to induce *PR1* expression, which was restored on exogenous application of SA, placing EDS1 upstream of SA (Aarts et al., 1998; Falk et al., 1999). Loss of function of EDS1 leads to reduced accumulation of *PAD4* and *PR1* transcript levels and of SA in response to both virulent and avirulent (*avrRps4* carrying) *Pst*DC3000 strains (Feys et al., 2001).

In addition to homodimer formation, EDS1 is also able to interact with another lipase –like protein, PAD4, to mediate SA responses (Feys et al., 2001; Feys et al., 2005; Rietz et al., 2011). Evidence suggests that whereas EDS1 and PAD4 monomers are sufficient for

localised reaction, such as the HR, basal resistance involving SA responses and transcription of defence related genes required EDS1-PAD4 complex formation (Rietz et al., 2011). Interaction of EDS1 in the nucleus with another lipase-like protein, SAG101, is thought to link local HR responses with the development of SAR (Rietz et al., 2011). Figure 5.1 summaries the activation of SA signalling downstream of the CC-NB-LRR and TIR-NB-LRR R-proteins mediated by NDR1 and EDS1 and PAD4, respectively.

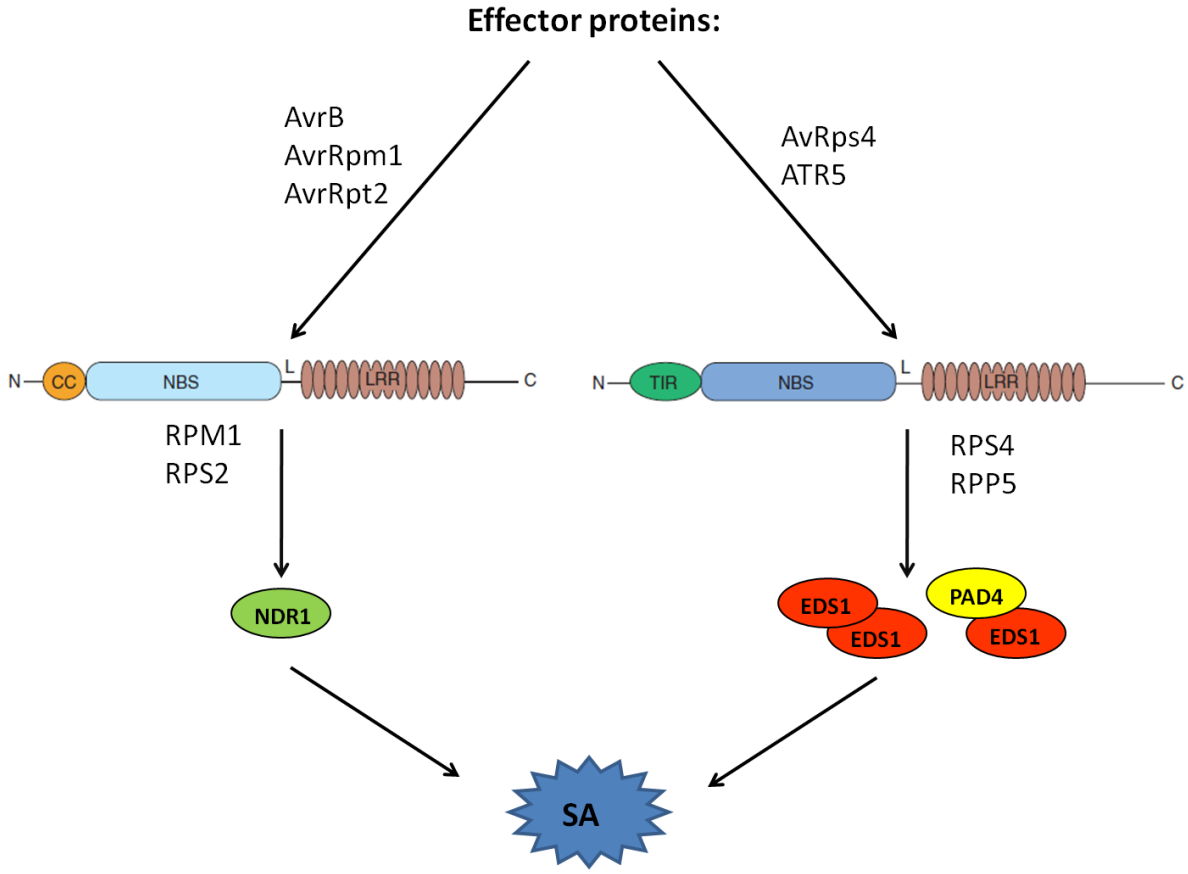


Figure 5.1 Figure showing activation of SA signalling triggered by recognition of pathogen effector proteins by the CC-NB-LRR and TIR-NB-LRR classes of R proteins. Effector proteins such as AvrB, AvrRpm1 and AvrRpt2 are recognised by CC-NBS-LRR R proteins such as RPM1 and RPS2. Activation of the CC-NBS-LRR R protein triggers SA responses through NDR1. TIR-NB-LRR R-proteins such as RPS4 recognise effector proteins such as AvrRps4. Signalling through the TIR-NB-LRR R-proteins is mediated by EDS1 and PAD4. Modified from McHale et al. (2006).

5.1.3.5 Downstream regulators of SA signalling

Downstream of SA, NPR1 (Non-expressor of PR genes 1) is responsible for induction of *PR* gene expression on translocation to the nucleus (Kinkema et al., 2000; Mou et al., 2003). NPR1 exists within the cytosol in an oligomeric state and relocates to the nucleus on dissociation of the NPR1 monomers. This dissociation has been shown to be redox-

controlled; increased concentrations and ratio of reduced glutathione (GSH) and oxidised glutathione (GSSH) on induction of reducing conditions within the cell triggered by the SA functional analog 2,6-dichloroisonicotinic acid (INA) correlated with dissociation of NPR1 to its monomers (Mou et al., 2003). As a result of higher reducing conditions in the cell triggered by SA and catalysed by thioredoxins (TRXs), the intermolecular disulphide bonds mediated by cysteine residues in NPR1 are disrupted by reduction, resulting in release of NPR1 monomers (Mou et al., 2003). Substitution of the cysteine residues at positions 82 or 216 with an alanine residue to mimic reduction of the cysteine residues resulted in an increase in monomeric NPR1, nuclear localisation and constitutive expression of *PR1* (Mou et al., 2003). *S*-nitrosylation via NO of the Cys-156 residue was also found to mediate oligomerisation of NPR1 (Tada et al., 2008). Thus the location of NPR1 is mediated through cellular redox status, with SA-induced redox changes triggering NPR1 monomerisation which is then able to transduce the SA signal to the nucleus.

On translocation to the nucleus, NPR1 activates transcription of SA responsive genes through interaction with TGA transcription factors belonging to the basic leucine-zipper (bZIP) class of transcription factors, mediated by the ankyrin repeat domain of NPR1 (Zhou et al., 2000). TGAs have been shown to act as positive regulators of basal resistance and *PR* gene expression (TGA1, TGA3, TGA4, TGA6) and also in negative regulation of SA responses (TGA2) (Zhang et al., 2003; Kesarwani et al., 2007). Interaction of NPR1 with the transcription factor TGA1 enhances its DNA binding activity to the *as-1*(activating sequence 1) *cis*-element found upstream of SA-responsive genes (Despres et al., 2003; Fobert and Després, 2005). Consistent with the requirement for NPR1 monomerisation and nuclear localisation, this interaction was found to occur only under reducing conditions; under oxidising conditions, the intramolecular disulphide bond between Cys-260 and Cys-266 within TGA1 inhibits interaction with NPR1(Despres et al., 2003; Fobert and Després, 2005) (Figure 5.2). Additionally, *S*-nitrosylation of TGA1 increases the DNA-binding activity of this transcription factor (Lindermayr et al., 2010). As both TGA1 and NPR1 exist in the cell before infection, modification of activity based on cellular redox changes initiated by infection provides a means to switch on protein activity only when required (Ndamukong et al., 2007).

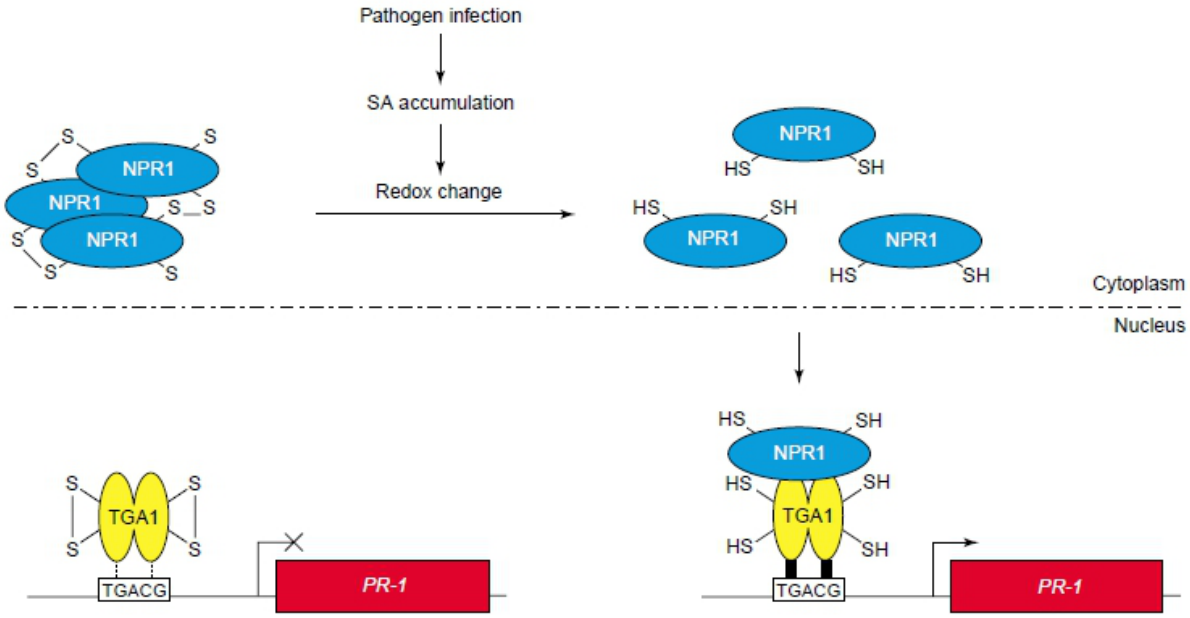


Figure 5.2 Schematic depicting the role of NPR1 in activation of SA-responsive genes. On pathogen infection, SA accumulation leads to changes in cellular redox status which causes dissociation of NPR1 oligomers by reduction of disulphide bridges between NPR1 monomers. Monomeric NPR1 translocates to the nucleus and interacts with a TGA transcription factor, such as TGA1 bound to the *as-1 cis*-element upstream of SA responsive genes such as *PR-1*. Activated TGA1 can then initiate transcription of *PR-1*. *S*-nitrosylation of NPR1 and TGA1 is not shown (see text for details). Figure modified from Pieterse and Van Loon (2004).

5.1.3.6 Antagonism of SA by JA as a virulence strategy

The role of SA in biotrophic interactions and that of JA in response to necrotrophic pathogens is well documented with evidence suggesting a general antagonistic relationship between the two hormone signalling pathways. SA-deficient *nahG* plants display increased JA levels and up-regulation of JA-responsive genes (*LOX2*, *VSP*, *PDF1.2*) coupled with suppression of the SA-responsive *PR-1*gene on infection with *Pst*DC3000 (Spoel et al., 2003; Block et al., 2005). Additionally, the *sid2-2* and *sid2-1* mutants which are more susceptible to *Pst*DC3000 also accumulated more JA on infection, suggesting that SA and JA can act antagonistically (Block et al., 2005; de Torres Zabala et al., 2009). Another example is the *cpr1-1* (*constitutive expressor of PR gene 1*) mutant, which shows elevated levels of SA and are defective in MeJA induction of the JA responsive gene *PDF1.2* (Spoel et al., 2007; Koornneef et al., 2008). Exogenous addition of SA also results in suppression of JA responsive genes, increased expression of SA responsive genes and higher susceptibility to

infection with necrotrophic pathogens and herbivores (Spoel et al., 2007; Koornneef et al., 2008; Leon-Reyes et al., 2009). The evidence therefore suggests that whereas SA is important for defence against biotrophic pathogens, JA is involved in resistance towards nectrotrophic pathogens and activation of one of these pathways can suppress the other.

This general antagonistic relationship may be exploited by pathogens such as *Pst*DC3000 in order to suppress SA-mediated defences. The bacterial phytotoxin coronatine is thought to achieve this through targeting the F-box protein COI1(Coronatine Insensitive 1) which acts to de-repress JA signalling as part of a Skp/Cullin/F-box complex (SCF^{COI1}) which acts as an E3 ubiquitin ligase (Xu et al., 2002). In the absence of JA, the jasmonate ZIM domain (JAZ) proteins suppresses JA signalling thorough interaction with key transcription factors of the JA pathway, such as MYC2, MYC3 and MYC4 (Fernandez-Calvo et al., 2011; Niu et al., 2011). In the presence of JA, COI1interacts with the JAZ proteins in a JA-dependent manner to relieve repression of JA signalling through promotion of ubiquitin-dependent degradation of the JAZ proteins (Katsir et al., 2008). This COI1-dependent degradation of JAZ proteins is dependent on the type of jasmonate present, with the active form of JA, JA-Ile, promoting interaction but not 12-oxo-phytodienoic acid or MeJA (Thines et al., 2007).

Therefore, by targeting COI1, the pathogen can activate JA signalling through manipulation of COI1 function in the absence of JA by acting as a JA-Ile mimic (Melotto et al., 2008b). The resistance of the *coi1* mutant to bacterial infection and insensitivity to both JA and coronatine supports a role for coronatine in JA signalling manipulation (Feys et al., 1994). Additionally, coronatine biosynthetic mutants are able to multiply to similar levels as wild-type *Pst*DC3000 in *nahG* and *sid2-2* plants but not in wild-type plants, suggesting coronatine is required for suppression of SA-defences and is dispensable in the absence of SA (Kloek et al., 2001; Brooks et al., 2005). Furthermore, expression of the *nahG* gene in a *coi1* background negates the negative effect of SA deficiency as these plants are more resistant to bacterial infection (Kloek et al., 2001). It is therefore clear that the interaction between SA and JA is important to the outcome of plant-bacteria interactions.

5.1.3.7 Mediation of SA-JA interactions

The interaction between the SA and JA is mediated by NPR1, with loss of NPR1 abolishing SA inhibition of JA signalling (Spoel et al., 2003; Leon-Reyes et al., 2009; Leon-Reyes et al., 2010). Whereas nuclear localisation of NPR1 is required for activation of SA defences, the

role of NPR1 in mediating negative cross-talk between the SA and JA pathways does not require translocation to the nucleus (Spoel et al., 2003). In support of this hypothesis, a truncated version of NPR1 (*npr1-3*), which is unable to translocate to the nucleus and thus remains in the cytosol, is only affected in SA-mediated gene expression (Leon-Reyes et al., 2009).

The increase in glutathione levels of the cell associated with SA signalling and control of NPR1 function was also correlated with the ability of SA to suppress JA-responsive gene expression (Koornneef et al., 2008). More recent reports suggest that ethylene may over-ride the requirement for NPR1 in SA-JA antagonism, adding an extra layer of control (Leon-Reyes et al., 2009; Leon-Reyes et al., 2010). Additionally, temporal regulation of hormone production may also be an important factor, where timing of the activation of JA/ethylene and SA signalling determines whether the outcome of the interaction is antagonistic. In a study by Koorneef et al. (2008) a time frame within which SA was able to antagonise JA/ethylene signalling was found, whereby exogenous addition of SA applied up to 30 hours prior to MeJA application suppressed expression of *PDF1.2*, but had no effect when applied more than 30 hours before MeJA. This 30 hour window of opportunity correlated with the increase in total glutathione levels which increased within a few hours of SA application and returned to basal levels within this time frame (Koornneef et al., 2008).

The relationship between SA and JA signalling appears to be complex, as synergy between the two hormones has also been shown to occur (Mur et al., 2006). Spatial control of SA and JA has also been implicated in controlling antagonism; whereas infection with virulent *Pst*DC3000 increased local susceptibility to subsequent infection with the necrotrophic pathogen *Alternaria brassicicola* through SA and NPR1-mediated suppression of JA signalling, this antagonism was not systemic (i.e., distal leaves were not affected) (Spoel et al., 2007). Interestingly, this local antagonism of SA and JA signalling was not triggered by avirulent HR-causing bacteria, suggesting antagonism is also dependent on the nature of the interaction (Spoel et al., 2007).

It is therefore clear that the outcome of plant defence signalling is complex, with timing of induction, interaction and spatial distribution of hormones playing a role in the fine-tuning plant responses.

5.1.3.8 Role of ABA in disease progression

More recently, the importance of ABA in plant-pathogen interactions has been unveiled. In the first study to investigate the effects of ABA in the outcome of infection with biotrophic pathogens, ABA was found to increase susceptibility to a normally avirulent strain of *Pst* carrying the avirulence gene *avrRpt2* (*Pst*1065) in a dose dependent manner (Mohr and Cahill, 2003). Additionally, the *aba1-1* mutant which is defective in ABA biosynthesis was less susceptible to infection with virulent strains of the biotrophic oomycete *Hyalonospora arabidopsidis* (formerly *Hyalonospora parasitica*), suggesting ABA negatively regulates resistance against biotrophic pathogens (Mohr and Cahill, 2003). In support of this, pre-treatment of plants with ABA led to a reduction in the levels of endogenous SA in response to infection with *Pst*1065 (Mohr and Cahill, 2007). Analysis of the dynamics of hormone accumulation in response to infection with virulent *Pst*DC3000 suggests this pathogen has evolved to manipulate ABA levels in order to suppress SA defences (de Torres Zabala et al., 2007; de Torres Zabala et al., 2009). Although SA is antagonised by the JA/ethylene pathway, the inhibition of SA by ABA appears to be independent of JA/ethylene and acts both upstream and downstream of SA (Yasuda et al., 2008).

Thus *Pst*DC3000 produces an array of effector proteins and the phytotoxin coronatine (discussed in Sections 1.4.2 and 1.4.3) to ensure establishment of disease and persistence within the host by manipulation of host defences. Clearly the interaction of the plant signalling pathways results in a complex network which is necessary for the fine-tuning of plant defences but which can also be used against the plant through manipulation by pathogens.

5.2 Aims

In this section, the role of AHK5 in compatible, incompatible and non-host interactions was investigated. This was achieved by assessing the ability of different pathovars and strains of *P. syringae* to cause infection in the *ahk5-1* mutant compared to wild-type plants. The bacterial strains used in this study were:

- *Pst*DC3000 – compatible interaction
- *Pst*DC3000(*avrRpm1*) – incompatible interaction
- *Pst*DC3000(*hrpA*-) – non-pathogenic
- *Pph*1448A – non-host interaction

The effect of loss of *ahk5-1* function in resistance against bacterial infection was determined initially by observation of symptom development and *in planta* bacterial growth after infection. As hormones are known to play an important role in plant defences, levels of SA, JA and ABA were measured in response to infection with *Pst*DC3000 in a compatible interaction. Levels of the bacterial phytotoxin coronatine were also measured simultaneously with plant hormones.

In the context of an incompatible interaction, two factors which play an important role in resistance are the hypersensitive response/cell death and the oxidative burst. These responses were monitored by Trypan blue staining and 3, 3'-diaminobezidine (DAB) staining, respectively.

5.3 Results

5.3.1 *Compatible interaction* – Pst*DC3000*

Stomata have been shown to actively defend against bacterial pathogens, with the presence of bacteria on the plant surface triggering their closure (Melotto et al., 2006). This stomatal closure was shown to require an intact ABA signalling pathway and, more recently, AHK5 (Melotto et al., 2006; Desikan et al., 2008). The involvement of AHK5 in defence against bacteria *in planta* was tested first by infiltrating *Pst*DC3000 directly into the apoplast of leaves to by-pass stomatal defences.

5.3.1.1 Syringe infiltration of Pst*DC3000*

Initially, wild-type plants were infiltrated with a range of inoculum densities to determine the optimal inoculum at which subtle changes in symptom development could be seen. An inoculum level of 1 x 10^6 cfu ml^{-1} to 2 x 10^6 cfu ml^{-1} are most commonly used to study *in planta* bacterial growth in plants inoculated by syringe or vacuum infiltration (J. Mansfield, personal communication). To investigate responses of wild-type plants to a range of inocula including bacterial densities above and below that normally used, four inoculm levels of 1.25 x 10^7, 2.5 x 10^6, 5 x 10^5 and 1 x 10^5 cfu ml^{-1} were tested. Figure 5.3 shows the growth of bacteria infiltrated at the different densities. For all inocula, bacterial populations increased approximately two-fold over the course of two days. After this point, bacterial numbers in leaves inoculated with the two higher bacterial densities (1.25 x 10^7 and 2.5 x 10^6 cfu ml^{-1}) dropped. The population counts in leaves infiltrated with the two lower densities (5 x 10^5 and 1 x 10^5 cfu ml^{-1}) continued to increase, albeit at a slower rate. At the end point of the experiment (seven days post inoculation (dpi)), an inverse correlation between initial inoculum density and bacterial populations *in planta* was found: the higher the initial inoculum density, the lower the final bacterial population counts were. Leaves inoculated with the higher inocula showed collapse and drying of the leaves, which was reflected in the decrease in population counts, given that living tissue is required for the multiplication of the bacterium. At the two lower inocula densities, yellowing of the leaves was seen with no collapse of leaf tissue occurring during the course of the experiment. Symptom development with leaves infiltrated with 1 x 10^5 cfu ml^{-1} was variable, with some leaves showing no symptoms, suggesting this inoculum level was too low for reliable monitoring of symptom development.

From this preliminary test, the bacterial density of 5 x 10^5 cfu ml^{-1} was chosen for further experiments as symptoms were consistent, developed gradually and did not result in collapse of leaf tissue, allowing the monitoring of subtle changes in disease phenotypes.

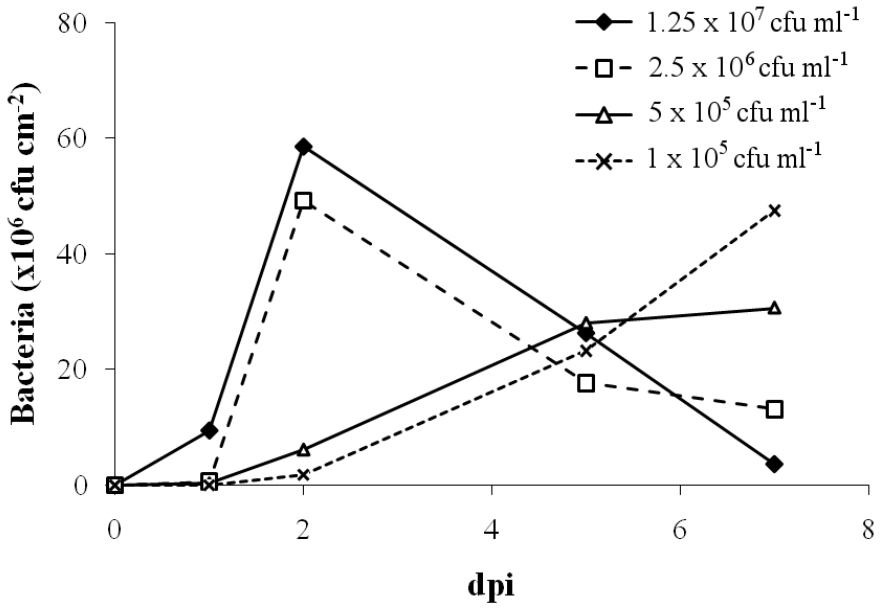


Figure 5.3 *In planta* bacterial populations in wild-type Col-0 leaves after syringe infiltration with *Pst*DC3000 at various densities. Inoculum densities used were 1.25 x 10^7, 2.5 x 10^6, 5 x 10^5 and 1 x 10^5 cfu ml^{-1}.

For reliable monitoring of symptom development in plants inoculated with bacteria, a symptom scoring scale (based on that used by Forsyth et al. (2010)) was used to score disease phenotype progression. Figure 5.4 shows the scoring scale used and the numerical scores assigned to each symptom, with higher numerical scores representing more severe disease phenotypes.

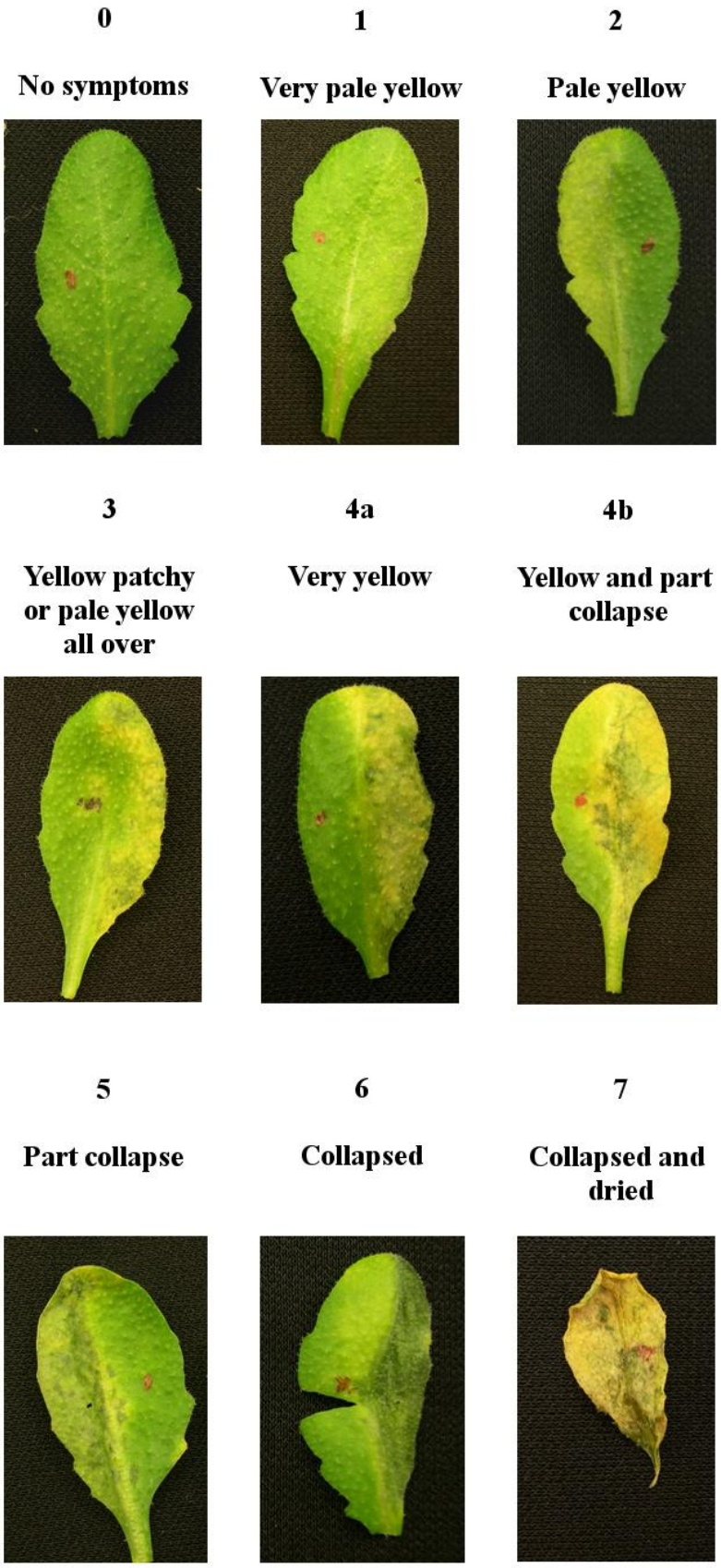


Figure 5.4 Photographs depicting disease symptoms caused by syringe infiltration of Col-0 leaves infiltrated with *Pst*DC3000. Visual descriptions and the numerical scores assigned to each symptom are shown above each photo.

Syringe infiltration of *ahk5-1* plants with 5 x 10^5 cfu ml^{-1} *Pst*DC3000 showed no difference in *in planta* population growth (Figure 5.5a) and symptom development (Figure 5.5b and c) when compared to wild-type Col-0 plants. As a comparison, the *pad4-1* (phytoalexin deficient 4) mutant, which is defective in SA defences, was used to show bacterial growth and symptom development in a susceptible background (Zhou et al., 1998). For all three lines, bacterial population growth was most rapid the first two days after infiltration, with greater bacterial growth in the *pad4-1* mutant evident as early as 1dpi (Figure 5.5a). At 3dpi, bacterial multiplication was at a reduced rate in wild-type and *ahk5-1* plants and close to becoming static. In contrast, bacterial growth rate in the *pad4-1* mutant was still high, after which *in planta* populations decreased, correlating with collapse and drying out of the leaf tissue at 5dpi (Figure 5.5c). The average symptom score at 5dpi for the *pad4-1* mutant was 5.5 (part collapse/collapse), whereas the average symptom score at the same time for wild-type and *ahk5-1* was three (yellow patchy or pale yellow all over) (Figure 5.5b and c).

In conclusion, bacterial growth and symptom development in plants infiltrated with *Pst*DC3000 at a density of 5 x 10^5 cfu ml^{-1} were indistinguishable in wild-type and *ahk5-1* plants.

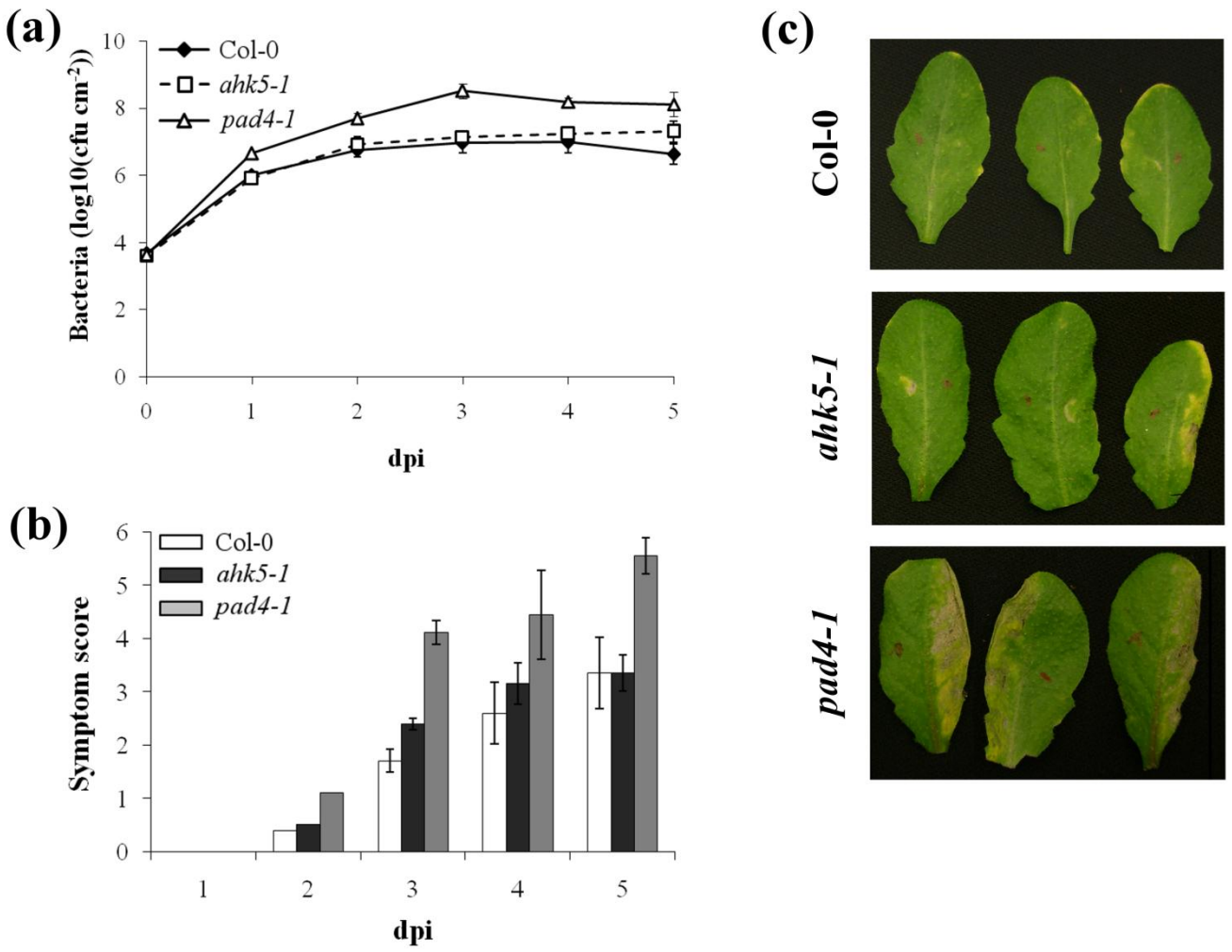


Figure 5.5 Response of plants to syringe infiltration with 5 x 10^5 cfu ml^{-1} of *Pst*DC3000. (a) *In planta* growth, (b) symptom development and (c) photographs of disease symptoms at five days post-inoculation (dpi) are shown. The *pad4-1* mutant was used as an example of a susceptible interaction. Data are mean ± SEM of an average of three experiments.

Since AHK5 is known to act in stomatal defences against bacteria, it is possible that this role is restricted to defence at the plant surface only, as was shown for the flagellin receptor FLS2 (Zipfel et al., 2004). In this scenario, infiltration of bacteria directly into the plant apoplast would mask any defects in surface defences as these are by-passed by the direct introduction of the bacteria into the internal leaf space.

5.3.1.2 Surface inoculation of Pst *DC3000*

Bacteria were inoculated onto the surface of leaves at the higher inoculum density of 4 x 10^8 cfu ml^{-1} since a higher inoculum is required for infection to occur using this method. Visual inspection of symptom progression in plants surface inoculated with *Pst*DC3000 revealed a more severe disease phenotype in *ahk5-1* when compared to wild-type plants (Figure 5.6a). Chlorosis of leaves was patchy and not as uniform as seen with syringe infiltration. Therefore, chlorophyll content of leaves was used to measure progression of symptom development. A greater loss of chlorophyll was seen in *ahk5-1* leaves compared to wild-type at 6dpi (Figure 5.6b), which correlated with a higher bacterial load in which the bacterial population was more than two-fold that found in wild-type leaves (Figure 5.6c). Loss of chlorophyll content in the complemented line P_{AHK5}*-AHK5/ahk5-1-1* on infection with *Pst*DC3000 was found to be simlar to that of wild-type (Figure 5.7), suggesting that the *ahk5-1* mutant is defective in defences against *Pst*DC3000 at the leaf surface and that this defect results in increased susceptibility to infection.

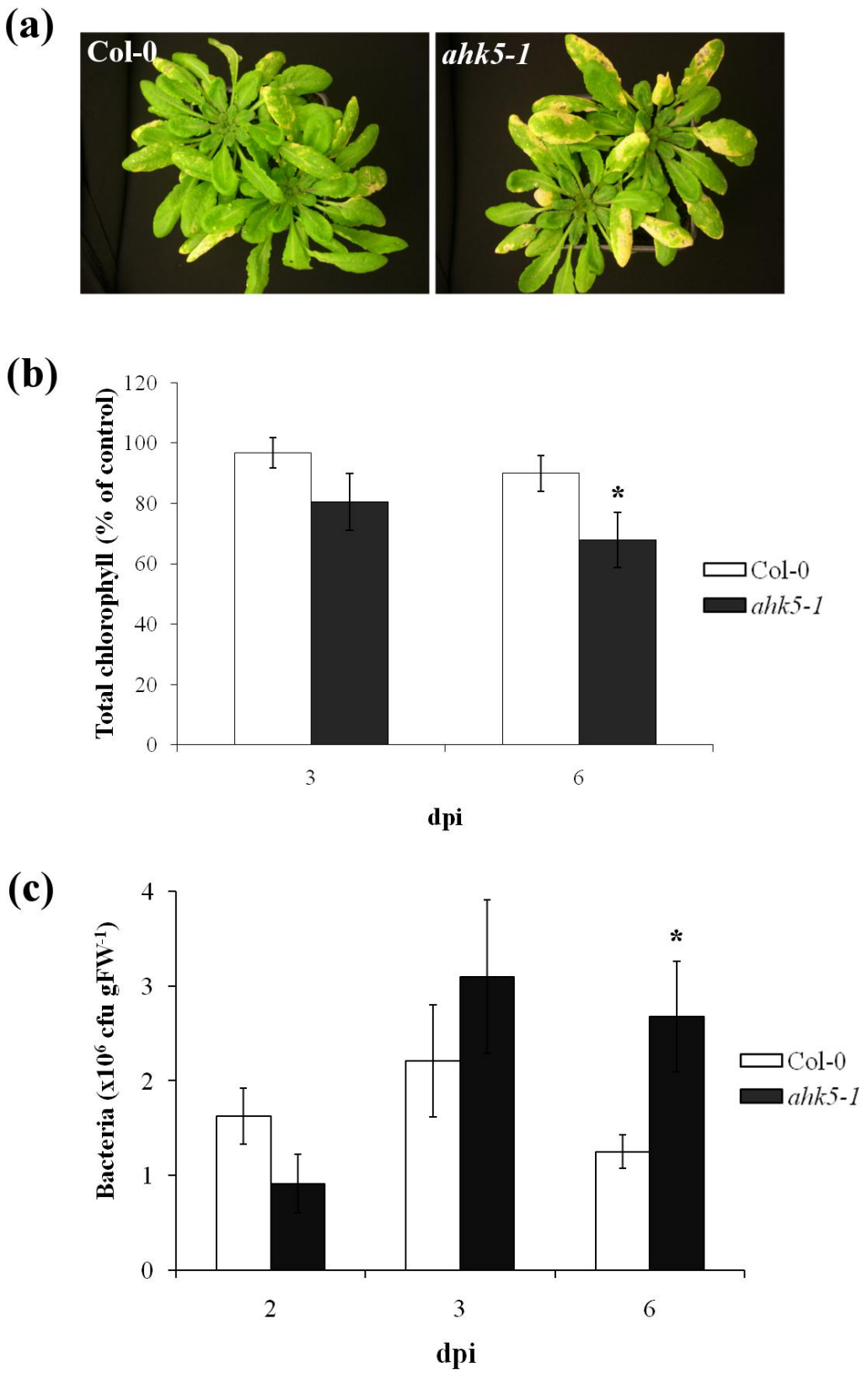


Figure 5.6. Response of wild-type and *ahk5-1* mutant plants to surface inoculation with 4 x 10^8 cfu ml^{-1} *Pst*DC3000. (a) Symptom development at seven days post inoculation (dpi), (b) chlorophyll content and (c) *in planta* bacterial growth. Data are mean ± SEM of an average of six (b) and three (c) independent experiments. The asterisk denotes a significant difference as determined by the Student's t-test (* = $p<0.05$).

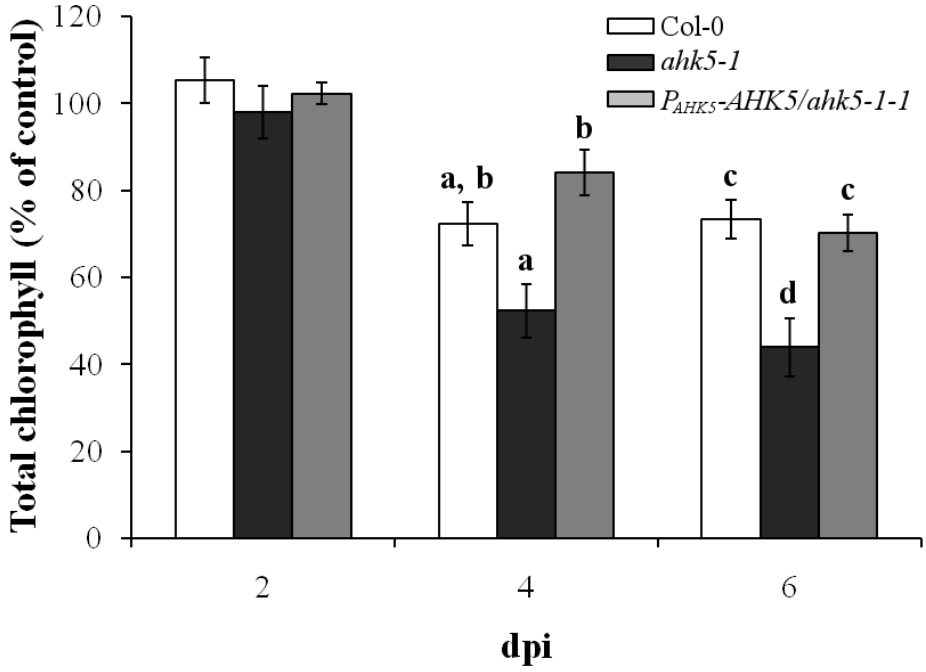


Figure 5.7 Total chlorophyll extracted from leaves of wild-type, *ahk5-1* mutant and P_{AHK5}-*AHK5/ahk5-1-1*surface inoculated with 4 x 10^8 cfu ml^{-1} *Pst*DC3000. Data presented are mean ± SEM of three independent experiments. At each timepoint, bars labelled with different letters were found to be significantly differet as determined by One-way ANOVA with Tukey's post hoc test (at four days post-inoculation (dpi), $p<0.0001$ and at 6dpi, $p<0.001$).

*5.3.1.3 Measurement of hormones and coronatine in Pst*DC3000 *infected leaf tissue*

To determine whether the increased susceptibility of the *ahk5-1* mutant to surface infection with *Pst*DC3000 resulted in alteration in hormone responses, the levels of the plant hormones SA, ABA and JA and the bacterium-derived phytotoxin coronatine was measured over time in infected leaf tissues and are shown in Figure 5.8. In wild-type infected tissue, the levels of both SA and ABA began to rise early at 2dpi, with levels of SA decreasing and ABA increasing over time (Figure 5.8a and b). SA levels in the *ahk5-1* mutant showed the same pattern of induction in wild-type tissue but at much lower levels; at 2dpi, SA levels in wild-type tissue were two-fold higher than that in *ahk5-1* (Figure 5.8a). In contrast, ABA did not rise over initial levels in the *ahk5-1* mutant and was significantly lower than that found in wild-type tissue at 6dpi in which ABA levels were more than 2.5 times higher than that in the *ahk5-1* mutant (Figure 5.8b). JA was seen to increase later than ABA and SA during infection, with highest levels seen at 6dpi in wild-type (Figure 5.8c). JA levels measured at 2dpi and 6dpi were significantly higher in wild-type tissue compared to that of the *ahk5-1* mutant at five-fold and more than three-fold higher, respectively (Figure 5.8c).

On the other side of the interaction, coronatine levels was seen to increase at 2dpi and remained at similar levels throughout the course of the experiment in wild-type (Figure 5.8d). Although coronatine was also seen to increase in the *ahk5-1* mutant, coronatine only accumulated to a quarter of the levels found in wild-type tissue at 2dpi and half the amount of wild-type levels at 4dpi and 6dpi (Figure 5.8d).

Overall, levels of all three hormones and phytotoxin measured were lower in the *ahk5-1* mutant. Levels of the plant hormones were similar between wild-type and mutant leaves mock inoculated with 10mM MgCl, suggesting the differences seen in infected tissue were not due to a difference in endogenous levels, but to induction of hormone production.

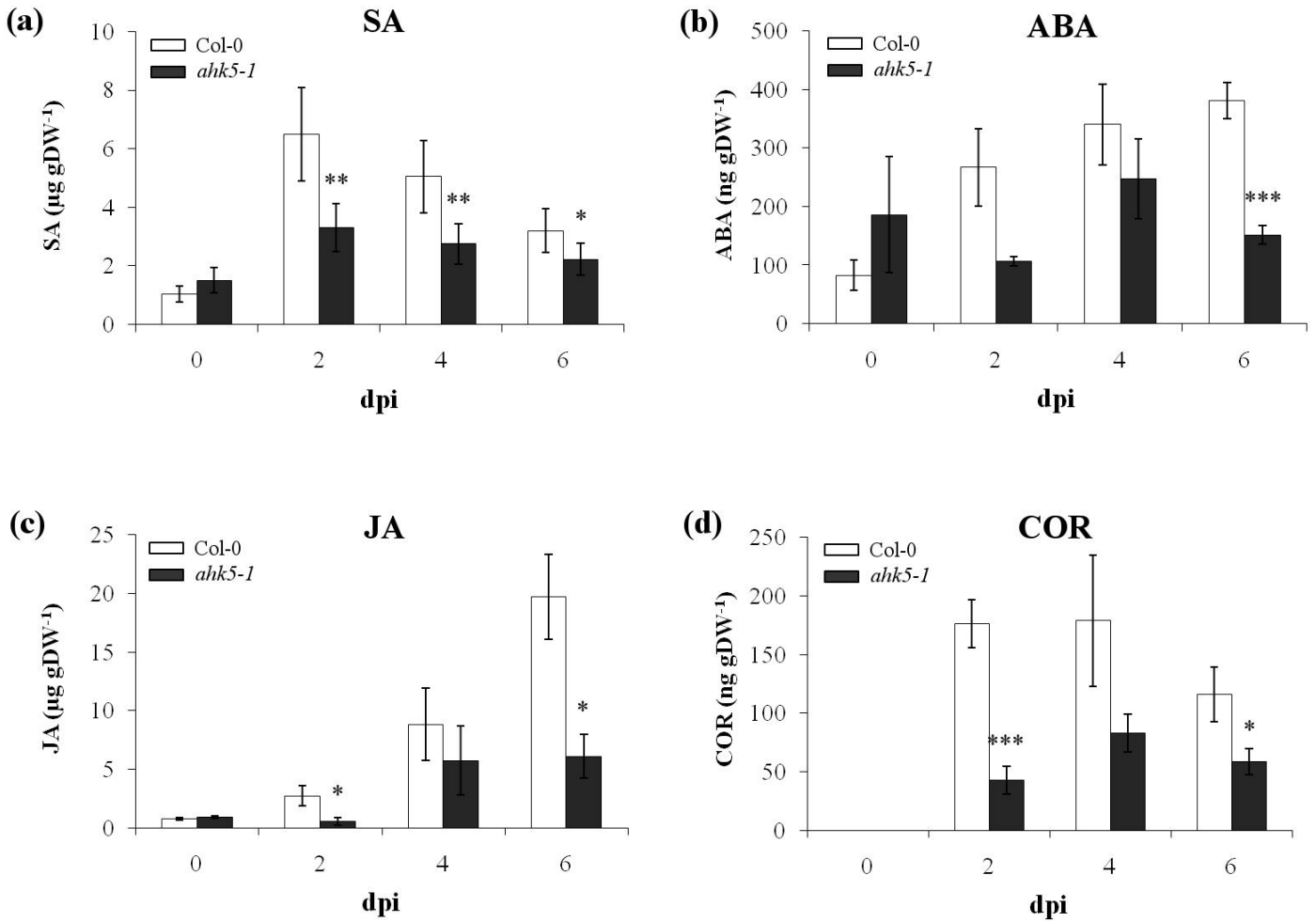


Figure 5.8 Measurement of *in planta* levels of plant hormones and bacterial phytotoxin in response to surface inoculation of leaves with 4 x 10^8 cfu ml^{-1} *Pst*DC3000. Levels of (a) Salicylic acid (SA), (b) abscisic acid (ABA), (c) jasmonic acid (JA) and (d) coronatine (COR) measured by LC-MS/MS over the course of six days post infection. Data presented are mean ± SEM of two independent experiments. Asterisks denote significant differences as determined by the Student's t-test (* = $p<0.05$, ** = $p<0.005$, *** = $p<0.0001$).

In addition to hormone levels, an unknown metabolite with a parent/daughter ion pair of 160/132 Da and a retention time of 11.2 minutes was found in *ahk5-1* mutant leaves in both mock-inoculated and infected leaves (Figure 5.9) which was not present in wild-type plants (data not shown). The levels of this ion increased over the time frame of the experiment to the same degree in both mock-inoculated and infected leaves. This suggests that either the conditions under which the plants were kept or the procedure used for surface inoculation caused the increase in this metabolite and is independent of bacterial infection.

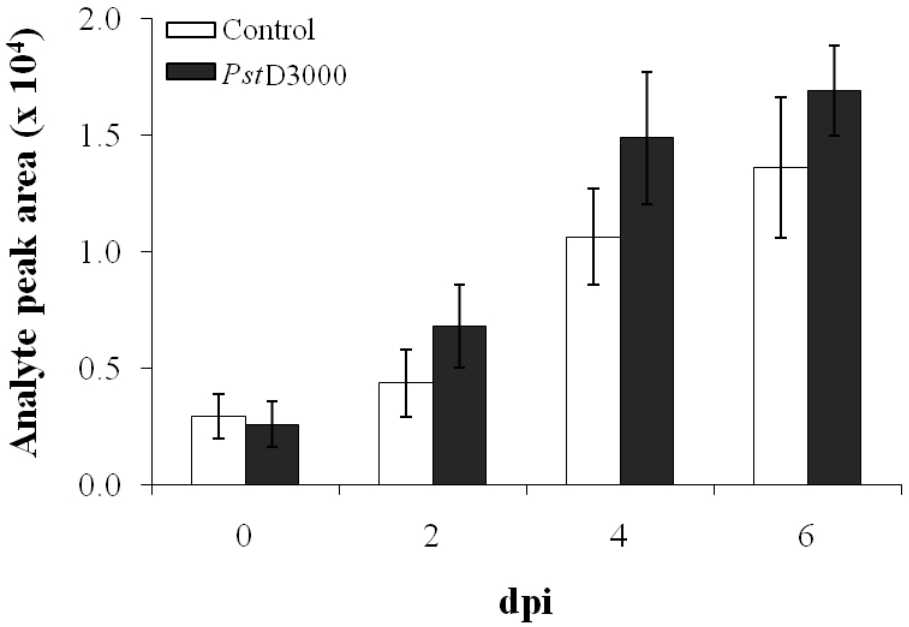


Figure 5.9 Pattern of accumulation of unknown compound with a parent ion of 160Da (retention time of 11.2 minutes) with a daughter ion of 132Da in *ahk5-1* leaf tissue in response surface inoculation. Leaves were either mock-inoculated or inoculated with 4 x 10^8 cfu ml^{-1} *Pst*DC3000.

To determine whether other metabolites with similar retention times and fragmentation patterns were present in wild-type tissues, multiple reaction monitoring (MRM) was used to select for all parent/daughter ion pairs of 160/132 Da. From this analysis, two additional parent ions of 160 Da with daughter ions of 132 Da were identified with retention times of 8.51 and 12.70 minutes (Figure 5.10a). Enhanced product ion (EPI) spectra of these three parent ions to investigate the fragmentation patterns of these three parent ions showed that they have similar fragmentation patterns with main daughter ions of 132 and 158 Da present for all three (Figure 5.10b,c and d), raising the possibility that the novel metabolite found in *ahk5-1* may be a variant of the two compounds with the retention times of 8.51 and 12.70 minutes.

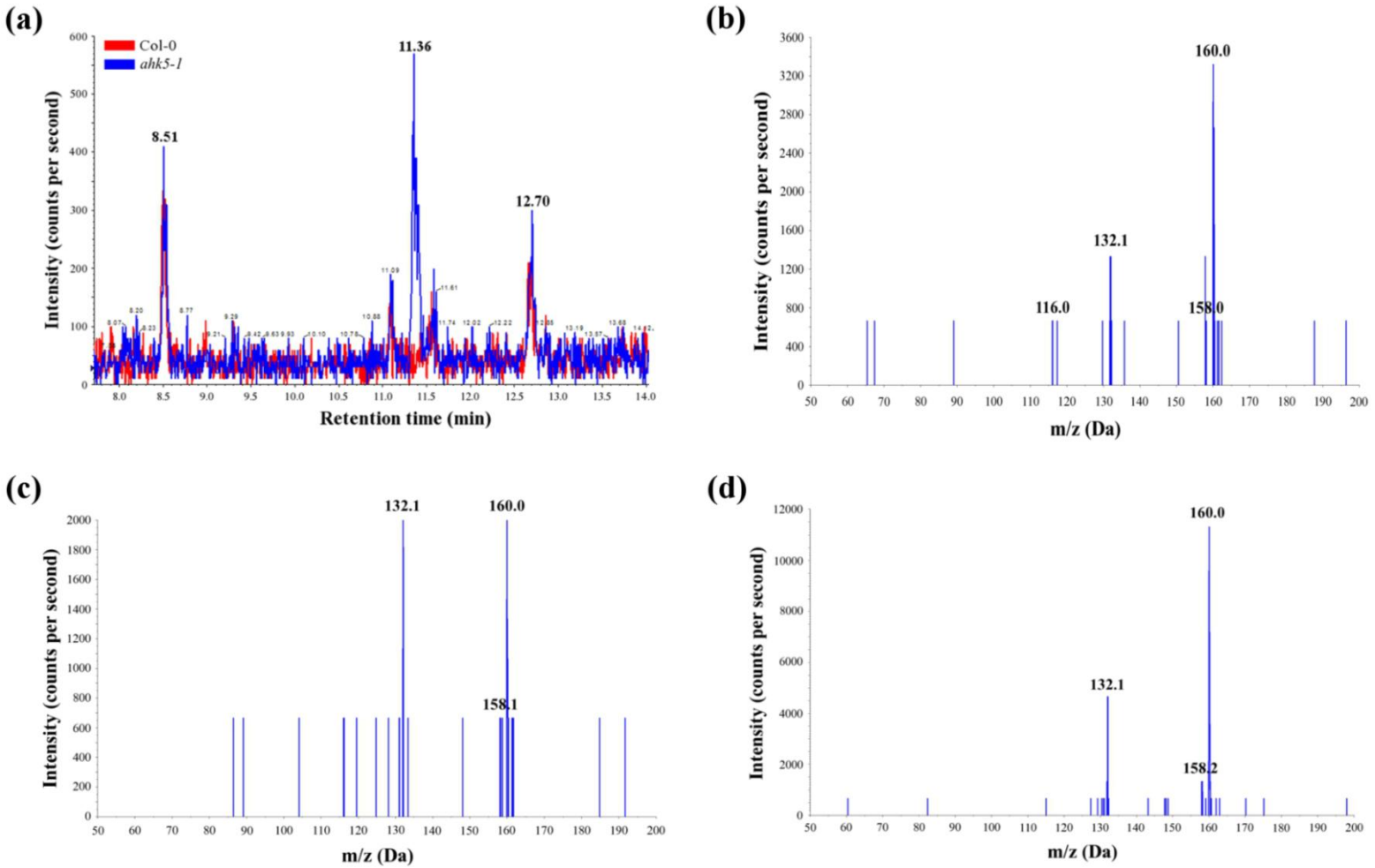


Figure 5.10 Analysis of parent ions of 160Da with a main daughter ion of 132Da (160/132Da) from LC-MS/MS of wild-type and *ahk5-1* mutant leaves surface inoculated with 4 x 10^8 cfu ml^{-1} *Pst*DC3000 at 6dpi. (a) Extracted ion current (XIC) spectra of multiple reaction monitoring (MRM) for parent ions of 160Da with a daughter ion of 132Da (160/132 Da). Enhanced product ion (EPI) spectra of parent/daughter ions pairs of 160/132 Da with retention times of (b) 8.51 minutes (c), 11.36 minutes (d) and 12.70 minutes. See Appendix Appendices XI, XII, XIII and XIV for larger versions of graphs (a), (b), (c) and (d) respectively.

5.3.2 *Incompatible interaction* – Pst*DC3000(avrRpm1)*

In compatible interactions between bacterium and host, the effector proteins secreted by the bacterium act as virulence factors by, for example, suppressing/manipulating plant resistance. To counteract this, plants have evolved to recognise some of these effector proteins and in the case where a bacterium expresses an effector protein which the plant recognises, an incompatible interaction occurs, typified by the prevention of bacterial spread by the HR and an oxidative burst at 3-6hpi (Zeier, 2005).

The interaction between *Arabidopsis thaliana* Col-0 and *Pst*DC3000 strains carrying the gene for the effector protein AvrRpm1 (hereafter referred to as *Pst*DC3000*(avrRpm1)*) represents an incompatible interaction and the response of the *ahk5-1* mutant to this strain was tested here.

In planta population counts in plants infiltrated with 1 x 10^6 cfu ml^{-1} of *Pst*DC3000*(avrRpm1)* showed that bacterial growth increased in both wild-type and *ahk5-1* plants, with maximal population growth at 3dpi, after which bacterial numbers decreased at 5dpi (Figure 5.11a). Although the pattern of bacterial growth in both wild-type and *ahk5-1* were similar, bacterial populations from 2dpi onwards was greater in wild-type plants, with a significant difference seen at 3dpi. At this time point, the bacterial populations counts in wild-type were twice the level in *ahk5-1* plants.

As a measure of the level of cell death, electrolyte leakage was monitored over 72 hours in response to infection with *Pst*DC3000(*avrRpm1*). As no difference in electrolyte leakage was found on comparison of the wild-type and with the *ahk5-1* mutant, this suggests that there was no difference in cell death/HR between wild-type and *ahk5-1* mutant plants (Figure 5.11b), with trypan blue staining at 3dpi confirming this conclusion (Figure 5.11c).

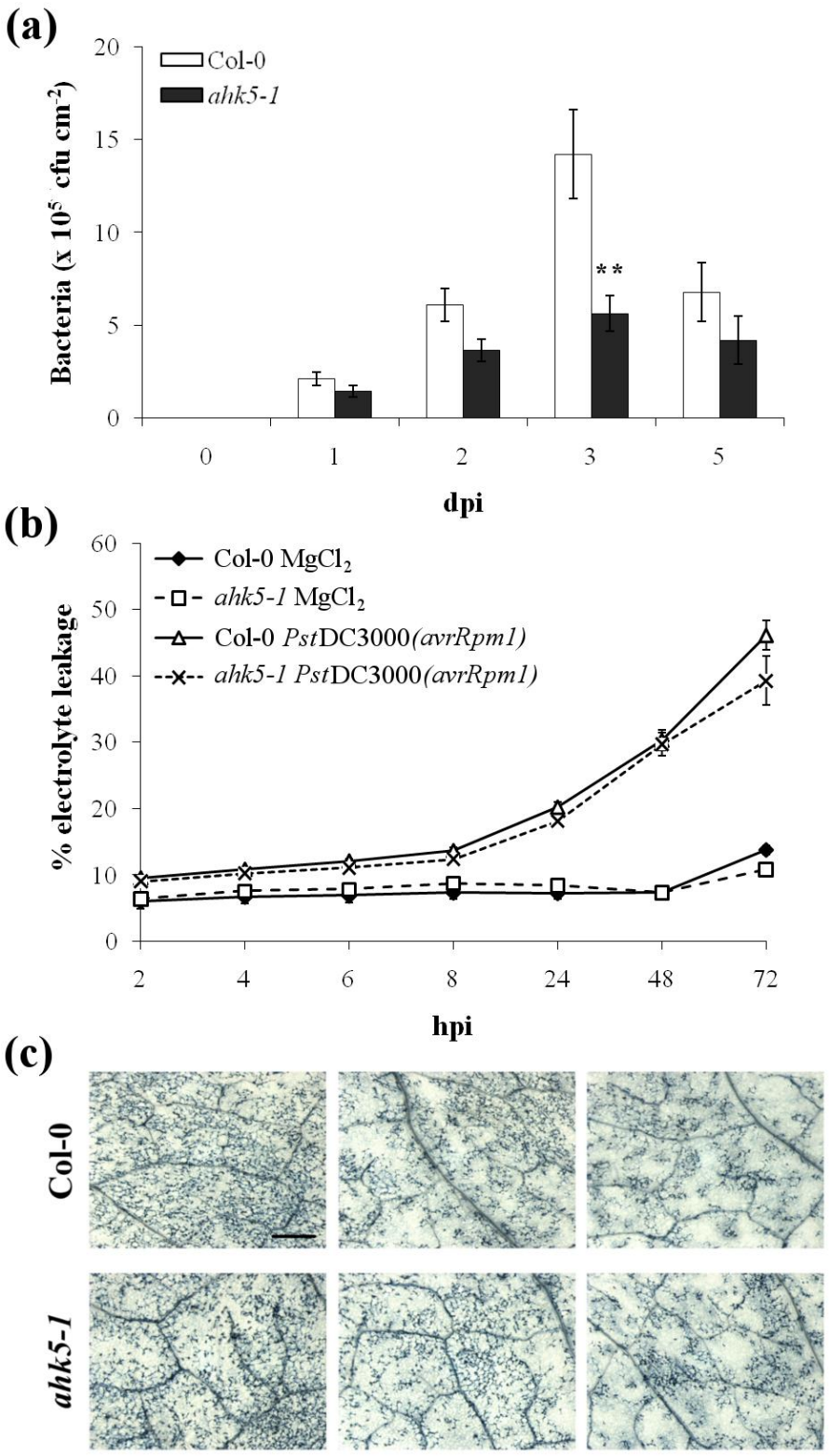


Figure 5.11 Response of wild-type Col-0 and the *ahk5-1* mutant to syringe infiltration with 1 x 10^6 cfu ml^{-1} *Pst*DC3000*(avrRpm1)*. (a) *In planta* population growth of *Pst*DC3000(*avrRpm1*), (b) electrolyte leakage and (c) Trypan blue staining of leaf tissue at 3dpi (scale bar = 500µm). Data in the graphs represent mean ± SEM of three independent experiments. For Trypan blue staining, experiments were repeated three times with similar results and representative pictures are shown. Asterisks denote a significant difference between wild-type and the *ahk5-1* mutant as determined by the Student's t-test (** = $p<0.005$).

As the difference in *in planta* bacterial population growth between wild-type and *ahk5-1* mutant plants was not associated with alterations in the HR, the production of ROS during the oxidative burst in response to *Pst*DC3000(*avrRpm1*) infection was investigated. ROS production was visualised by histochemical staining with 3, 3'-diaminobenzidine (DAB) which forms an insoluble brown precipitate on reaction with H_2O_2 (Šnyrychová et al., 2009). For this, plants were infiltrated with a higher inoculum of 5 x 10^6 cfu ml^{-1} of bacteria as DAB staining was more visible at this density than at that used for determination of *in planta* bacterial population growth. Leaves were DAB stained for ROS at 1, 3, 5 and 7hpi as the oxidative burst was previously shown to occur within this time frame (Levine et al., 1994). DAB staining was seen at all time points in both wild-type and *ahk5-1* mutant leaves and was similar between the two lines at 1, 3 and 7hpi. At 5hpi however, visibly more DAB staining was seen in wild-type leaves compared to *ahk5-1* mutant leaves (Figure 5.12a). Quantification of the staining seen at this time point revealed two-fold more staining in wild-type leaves compared to *ahk5-1* mutant leaves with this difference being statistically significant (Figure 5.12b). This suggests that the *ahk5-1* mutant is altered in its response to infection with *Pst*DC3000(*avrRpm1*) in terms of ROS production.

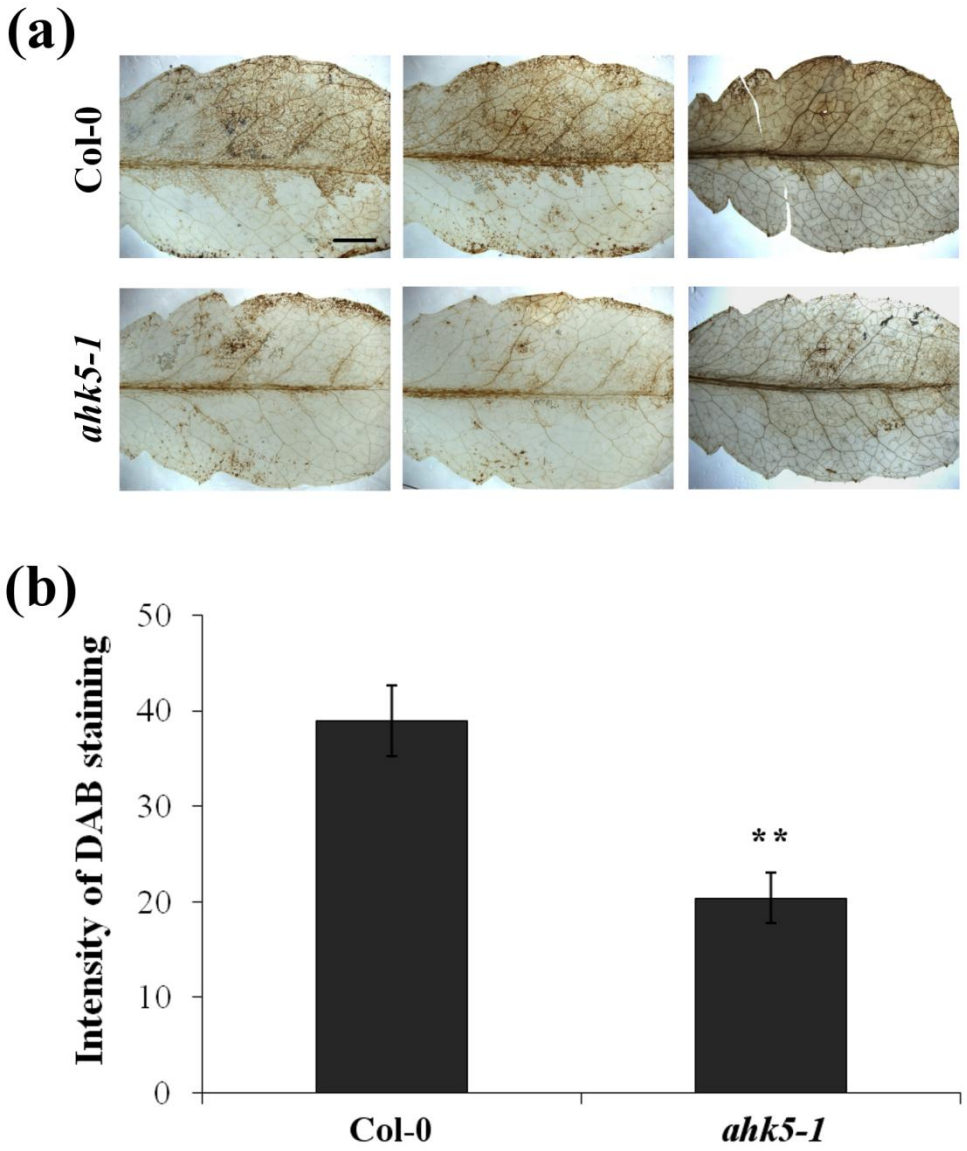


Figure 5.12 ROS production in leaves infiltrated with 5 x 10^6 cfu ml^{-1} *Pst*DC3000 *(avrRpm1)*. (a) DAB staining of leaves at 5hpi (scale bar = 2mm). The experiment was repeated twice and representative pictures are shown. (b) Average intensity of DAB staining in leaves at 5hpi. Values are mean ± SEM of measurements from eight leaves from two independent experiments. Asterisks denote a significant difference between wild-type and *ahk5-1* values as determined by the Student's t-test (**= $p<0.005$).

5.3.3 *Response to the non-pathogenic* Pst*DC3000*(hrpA$^-$) *mutant*

The *Pst*DC3000(*hrpA*$^-$) mutant is a type III secretion system (TTSS) mutant which is unable to deliver effector proteins to the plant cell which usually acts to suppress and manipulate the plant immune response. These bacteria are therefore non-pathogenic as basal plant defences are activated by the presence of bacterial PAMPs such as flagellin.

AHK5 was shown to be involved in detection of flagellin peptide 22 (flg22) by stomata but is not required for sensing EF-Tu peptide 26 (elf26) (Desikan et al., 2008). To test the involvement of *AHK5* in basal resistance to bacterial infection, plants were syringe infiltrated with the *Pst*DC3000(*hrpA*$^-$) mutant and bacterial populations and symptom development *in planta* were monitored. As the *Pst*DC3000(*hrpA*$^-$) mutant is defective in its ability to cause disease, the mutant was infiltrated at the higher concentrations of 1.25 x 10^8 cfu ml^{-1} and 5 x 10^7 cfu ml^{-1} for determination of symptom development and bacterial population growth, respectively. Analysis of both symptom development (Figure 5.13a) and population growth (Figure 5.13b) showed no difference between wild-type and the *ahk5-1* mutant.

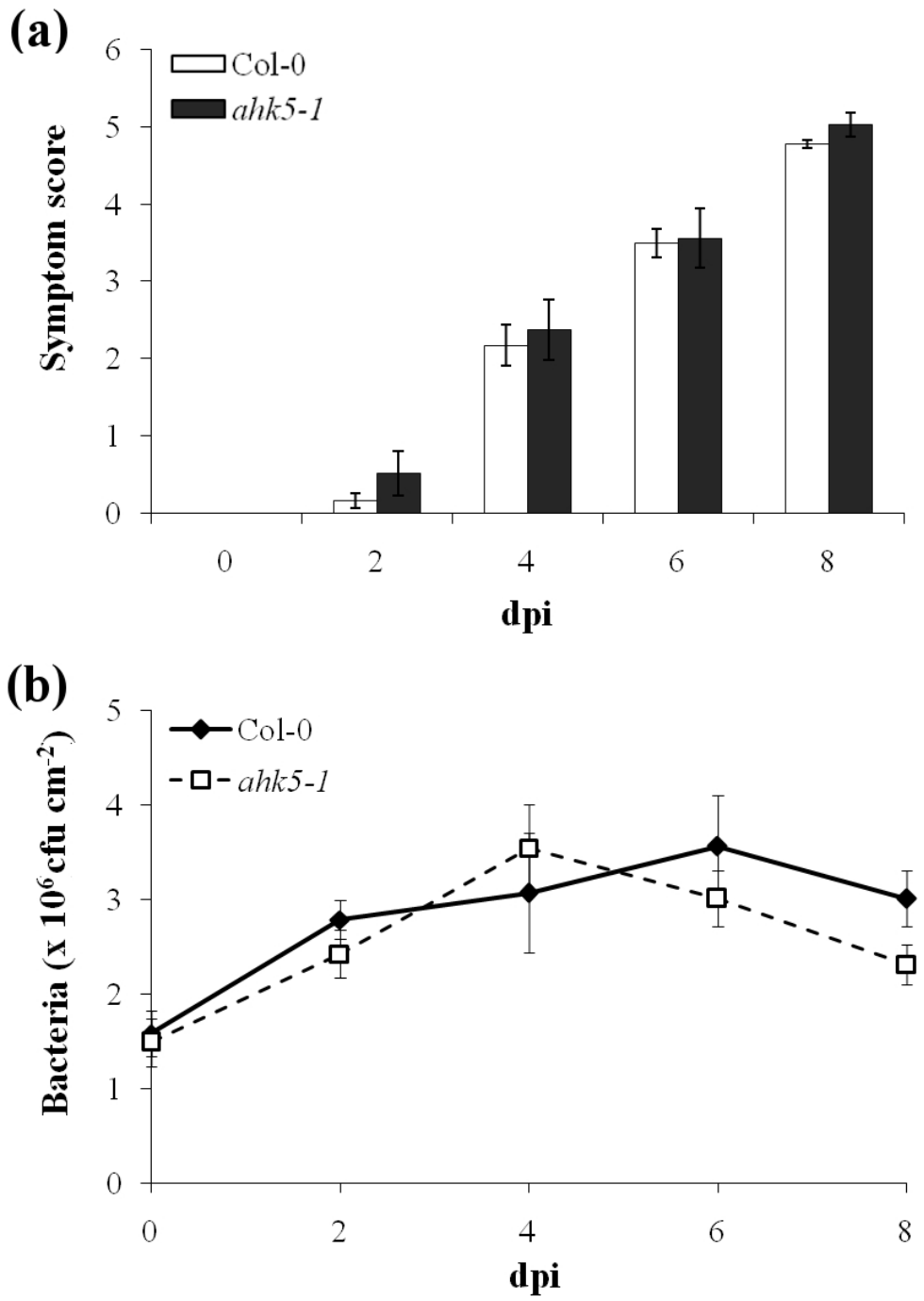


Figure 5.13 Response of wild-type and *ahk5-1* mutant plants to infiltration with the non-pathogenic *Pst*DC3000(*hrpA*$^-$) mutant. (a) *In planta* population growth and (b) symptom development in plants syringe infiltrated with 5 x 10^7 cfu ml^{-1} and 1.25 x 10^8 cfu ml^{-1}, respectively. Data are mean ± SEM of four (a) and three (b) independent experiments.

5.3.4 *Non-host interaction – the bean pathogen* Pph*1448A*

Similar to the incompatible interaction where establishment of disease is prevented by the recognition by the plant of an avirulence gene product produced by the bacterium, in a non-host interaction the plant is able to recognise multiple bacterial avirulence gene products, resulting in robust resistance which contributes to the restriction in host range of the pathogen (Thordal-Christensen, 2003). Analysis of the interaction between the bean pathogen *Pseudomonas phaseolicola* 1448A (*Pph*1448A) and wild-type and *ahk5-1* mutant plants revealed no difference in the symptom development (Figure 5.14a) or *in planta* growth of the bacterium (Figure 5.14b). The maximum increase in *Pph*1448A population was four-fold over the initial inoculum, reflecting the inhibition of bacterial growth by the plant immune response.

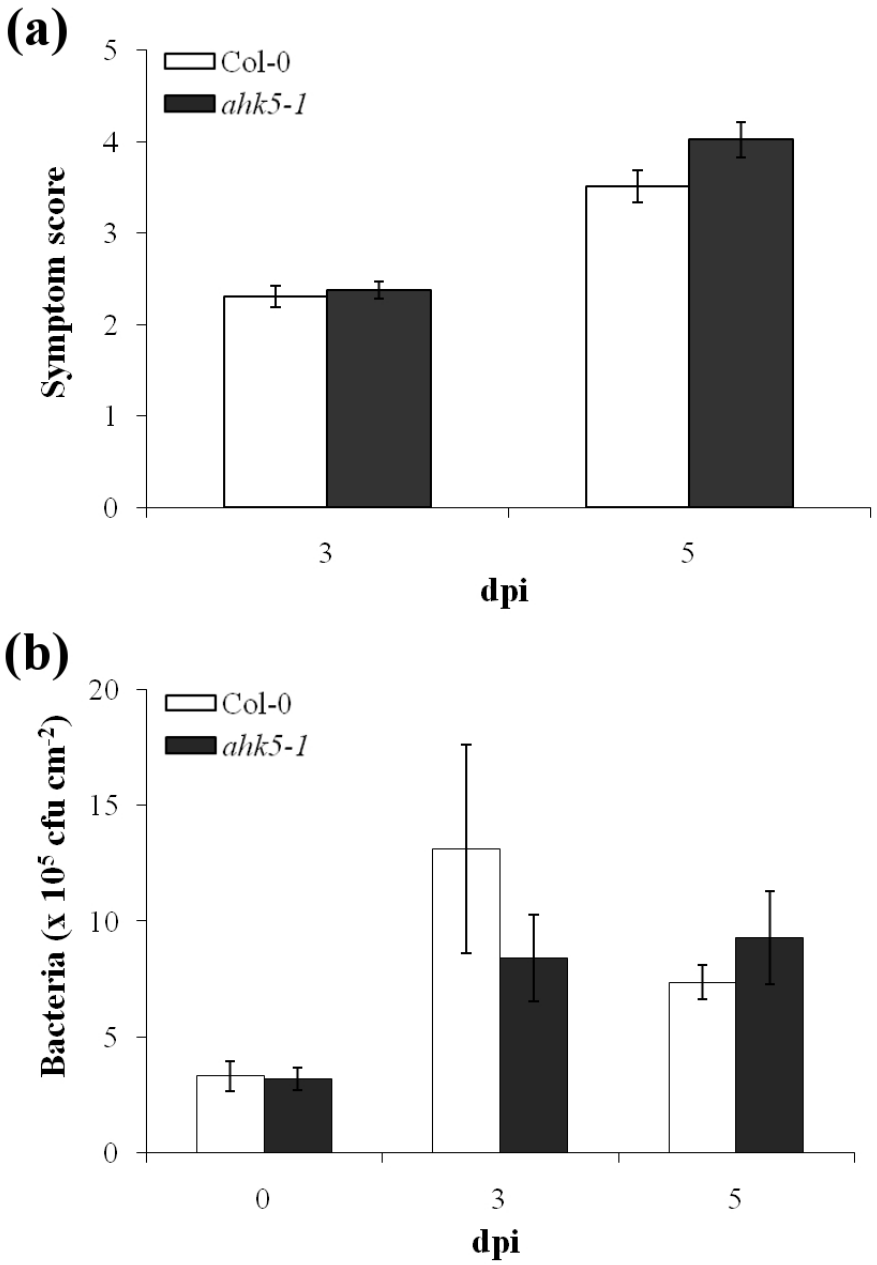


Figure 5.14 Response of wild-type and *ahk5-1* mutant plants to infiltration with the bean pathogen *Pph*1448A. (a) Symptom development in plants syringe infiltrated with 2.25 x 10^8 cfu ml^{-1} bacteria and (b) *in planta* bacterial population growth in plants infiltrated with 4.5 x 10^7 cfu ml^{-1} bacteria. Data are mean ± SEM of three independent experiments.

5.4 Discussion

As the *ahk5-1* mutant was previously shown to be defective in stomatal responses to *Pst*DC3000 and flagellin (Desikan et al., 2008), the role of AHK5 in response to bacterial infection beyond that of stomata was investigated. To accomplish this and to investigate different aspects of plant immunity, the *ahk5-1* mutant was phenotypically screened for differences in response to infection with virulent (*Pst*DC3000), avirulent (*Pst*DC3000(*avrRpm1*)) and non-pathogenic (*Pst*DC3000(*hrpA*-)) strains of *Pst*DC3000 and also with a non-*Arabidopsis* pathogen (*Pph*1448A).

5.4.1 *The* ahk5-1 *mutant is more susceptible to Pst*DC3000 *after surface inoculation but not after syringe infiltration*

Stomata were recently shown to form an important role in defence against bacterial infection by sensing the presence of bacteria on the leaf surface. Closure of stomata in response to bacteria was shown to prevent bacterial ingress into the leaf interior and is triggered through recognition of the bacterial PAMP flagellin as part of PTI (Melotto et al., 2006; Underwood et al., 2007; Melotto et al., 2008a; Zeng et al., 2010). Additionally, the *fls2* mutant which is defective in flagellin perception is more susceptible to *Pst*DC3000 when inoculated onto the leaf surface but not when syringe infiltrated (Zipfel et al., 2004). Similarly, coronatine biosynthetic mutants which are unable to overcome stomatal defences are defective in the ability to cause disease if surface inoculated but can multiply *in planta* to similar levels as wild-type bacteria (at least in the first few days) if infiltrated into the leaf, highlighting the importance of surface defences in disease resistance (Brooks et al., 2004; Melotto et al., 2006). That virulent bacteria have evolved mechanisms to stimulate reopening of stomata suggests stomata are barriers to bacterial infection.

In this study, symptom development and *in planta* bacterial growth was more severe in the *ahk5-1* mutant compared to wild-type Col-0 plants on surface inoculation of bacteria but not when syringe infiltration was used. The increased susceptibility of the *ahk5-1* mutant to surface inoculated bacteria is in agreement with the stomatal phenotype of the mutant previously shown by Desikan et al. (2008), whereby the inability of stomata to close in response to bacteria may allow for higher numbers of bacteria to enter the leaf interior. Using GFP-labelled bacteria and confocal microscopy, Melotto et al. (2006) demonstrated that the ability of bacteria to reopen stomata correlated with a greater number of bacteria able to cross

the leaf epidermis, which occurred as early as 3hpi. This would suggest that greater ingress of bacteria soon after application to the leaf surface results in a greater effective inoculum, which on multiplication within the leaf apoplast results in greater population counts. It may therefore be expected that differences in bacterial population may be seen early after infection in plants defective in stomatal responses to bacteria, such as the *fls2* mutant. On spraying of plants with 5 x 10^8 cfu ml^{-1} *Pst*DC3000, Zipfel et al. (2004) found a difference in symptom and bacterial population counts in the *fls2-17* mutant compared to wild-type plants at 4dpi. This is similar to the time frame in which a difference was seen in this study for the *ahk5-1* mutant, suggesting the higher rate of bacterial entry early after inoculation on the leaf surface (i.e., within hours) may not necessarily be detected by the method used to determine *in planta* population counts in this study.

A direct correlation between the stomatal phenotype of the *ahk5-1* mutant previously observed by Desikan et al. (2008) and the ability of *Pst*DC3000 to cross the leaf epidermis early after inoculation of the leaf surface is yet to be shown. However, given the evidence from previous studies discussed above, it can be hypothesised that altered perception of *Pst*DC3000 at the leaf surface by the *ahk5-1* mutant leads to increased susceptibility to bacterial infection. That no difference was observed between wild-type and *ahk5-1* mutant plants on syringe infiltration of *Pst*DC3000 also supports this hypothesis.

5.4.2 *The* ahk5-1 *mutant is altered in hormone responses to* Pst*DC3000*

The importance of hormones in disease resistance is well documented (Glazebrook, 2005; Ton et al., 2009; Vlot et al., 2009; Verhage et al., 2010). To determine whether the increased susceptibility of the *ahk5-1* mutant resulted in altered hormone responses, the tissue levels of the plant hormones SA, ABA and JA in response to bacterial infection from surface inoculation with virulent *Pst*DC3000 were determined. Hormone levels were measured from 0dpi to 6dpi, the timeframe in which the differences in symptom development/chlorophyll loss and *in planta* bacterial population counts were observed. In addition, the level of the bacterial phytotoxin coronatine was also monitored.

In wild-type Col-0 infected leaves, SA levels increased early after infection and gradually decreased over time whereas ABA levels continued to increase over the time course of the experiment. This is in agreement with the roles of SA in plant immunity and ABA in suppression of SA defences (de Torres Zabala et al., 2007; de Torres Zabala et al., 2009; Fan

et al., 2009; Vlot et al., 2009). In the case of JA, increases in this hormone are seen later than for SA and ABA; JA levels remains low early on and steadily increases after time. This later increase in JA levels relative to SA and ABA was also previously observed by de Torres Zabala et al. (2007). Levels of the bacterial phytotoxin coronatine were also high in wild-type plants throughout the course of the experiment.

Interestingly, although the pattern of hormone accumulation was similar between wild-type and the *ahk5-1* mutant, total levels of each hormone was consistently lower in the mutant in response to bacterial infection. Surprisingly, the levels of coronatine in *ahk5-1* infected tissue was also lower than that found in wild-type leaves, which was unexpected given the role of coronatine in suppression of basal defences and maintenance of *in planta* bacterial growth (Brooks et al., 2004; Brooks et al., 2005; Uppalapati et al., 2007). As discussed earlier in Section 5.1.3.6, coronatine may target the F-box protein COI1 as a virulence strategy (Feys et al., 1994; Kloek et al., 2001; Katsir et al., 2008; Melotto et al., 2008b). The role of coronatine in the ability of *Pst*DC3000 to reopen stomata in order to gain entry into the leaf interior was previously demonstrated to require the *COI1* gene, as the *coi1-20* mutant was insensitive to coronatine-mediated reopening of stomata (Melotto et al., 2006). Additionally, a coronatine deficient mutant multiplied to the same level as virulent *Pst*DC3000 on surface inoculation of SA biosynthetic mutant (*eds16*-2) or SA deficient (*nahG*) plants, which are also defective in stomatal responses to bacteria (Melotto et al., 2006). This suggests that (1) coronatine is required to reopen stomata to enable bacteria to enter the leaf interior, (2) in the absence of stomatal closure, coronatine is dispensable for the ability of the bacterium to colonise the leaf apoplast and (3) SA signalling contributes to stomatal defences.

Bearing this in mind, an explanation for the low levels of hormones and coronatine found in the *ahk5-1* mutant can be postulated. The defect in stomatal closure in the *ahk5-1* mutant may allow more bacteria to enter the leaf interior initially, relieving the requirement for coronatine production. Since evidence suggests that coronatine stimulates JA production (Block et al., 2005; Brooks et al., 2005; Uppalapati et al., 2005; Uppalapati et al., 2007), the reduced production of coronatine by the bacteria in the *ahk5-1*mutant also reduces the stimulation of JA production in the plant. As SA is required for stomatal defences (Melotto et al., 2006), defective detection of bacteria at the leaf surface in the *ahk5-1* mutant may result in a delay in/attenuation of activation of SA responses, resulting in the reduced SA levels measured. A virulence strategy utilised by *Pst*DC3000 is the inhibition of SA-mediated defences through stimulation of increased ABA production, which also involves the action of coronatine (de

Torres Zabala et al., 2007; de Torres Zabala et al., 2009). The reduced coronatine levels may therefore lead to less induction of ABA accumulation. Since SA levels are also reduced in the *ahk5-1* mutant, this reduction in ABA accumulation may not negatively affect the ability of the bacteria to establish disease. The overall reduction in hormone responses may lead to a dampened immune response in the *ahk5-1* mutant, allowing greater *in planta* growth of the bacteria.

That syringe infiltration did not result in any difference in disease progression or *in planta* bacterial population growth would be in agreement with the above theory. By directly introducing the bacteria into the leaf apoplast, the 'advantage' which the bacteria gain from the unresponsive stomata of the *ahk5-1* mutant is by-passed, resulting in similar levels of establishment of infection and disease progression in both wild-type and mutant plants.

5.4.3 *A novel metabolite is present in* ahk5-1 *leaves but not wild-type Col-0 leaves*

Interestingly, a novel metabolite was identified in *ahk5-1* leaf tissue that was not found in wild-type tissue by LC-MS/MS. This metabolite was found in both mock-inoculated and *Pst*DC3000-infected *ahk5-1* tissue and increased to the same extent over the course of the experiment in response to both treatments. This suggests that the induction of the metabolite was not in response to bacterial infection and was either a result of the method of inoculation used or the high humidity conditions under which the plants were kept during the experiment. As the metabolite was present at the highest concentration at the endpoint of the experiment (6dpi) and is slightly higher in *Pst*DC3000 infected tissue (but not significantly so), extracts from *Pst*DC3000 infected tissue 6dpi was used for further investigation by LC-MS/MS.

Multiple reaction monitoring (MRM) of parent ions with a mass of 160Da identified three parent ions eluting at 8.51, 11.36 and 12.70 minutes, each with a main daughter ion of 132Da. The parent ions eluting at 8.51 and 12.70 minutes were found in both wild-type Col-0 and *ahk5-1* tissue, whereas the parent ion eluting at 11.36 minutes was only seen in *ahk5-1* leaves. Operating in the ion trap mode for parent ions of a fixed mass of 132Da, enhanced product ion (EPI) spectra were obtained for all three parent ions to visualise the full fragmentation patterns of these parent ions and to identify daughter ions other than the most abundant ion of 160Da. The fragmentation patterns of the three parent ions were similar, raising the possibility that the parent ion eluting at 11.36 minutes seen only in the *ahk5-1*

mutant may be a variant of one of the other two metabolites, such as a conjugate or a *cis/trans* isomer (M. Bennett, personal communication).

Whether or not this unknown metabolite is involved in the increased susceptibility to infection of *Pst*DC3000 is not clear. The fragmentation pattern of this unknown metabolite suggests that it may be an indolic compound (M. Bennett, personal communication). As indolic compounds, including the well studied phytoalexin camalexin and indole glucosinolates, are known to play important roles in defence against pathogens and to accumulate in response to infection, it would be interesting to determine whether this compound is indeed an indole (Hagemeier et al., 2001; Kliebenstein, 2004; D'Auria and Gershenzon, 2005; Forcat et al., 2010; Simon et al., 2010).

If the presence of this metabolite leads to a predisposition to bacterial infection, it may be expected that an increase in susceptibility of the *ahk-5-1* mutant would be seen with syringe infiltration of bacteria, which was not seen here. However, as mentioned previously, this metabolite increased over time irrespective of infection and may have been due to the high humidity conditions (~80% humidity) under which the plants were kept after surface inoculation to prevent the inoculum from drying too quickly. Plants which were syringe infiltrated were not kept under high humidity (55-65% humidity) and it is possible that high humidity contributes to increased susceptibility through increased production of this metabolite. The high humidity may also exacerbate the defect in stomatal closure by providing conditions that encourage stomatal opening and thus bacterial entry into the leaf. Why this metabolite is present only in the *ahk5-1* mutant is unclear. It is possible that AHK5 may modulate metabolite production; as many secondary metabolites in *A. thaliana* are derived from common starting components, such as shikimic acid and aromatic amino acids which are differentially modified to produce an array of secondary metabolites (Bennett and Wallsgrove, 1994; Kliebenstein, 2004), AHK5 may contribute towards regulating certain modifications. Thus the novel metabolite identified in *ahk5-1* eluting at 11.36 minutes may be an intermediate of the compound(s) eluting at 8.51 and/or 12.70 minutes which accumulates due to a defect in the final modifications required to produce the latter two compounds.

5.4.4 *The* ahk5-1 *mutant is more resistant to infection with* Pst*DC3000*(avrRpm1) *but unaltered in response to the avirulent* hrpA$^-$ *mutant and the bean pathogen* Pph*1448A*

In addition to PAMP-triggered immunity (PTI) which targets common and conserved components of the bacterium, the plant is also able to recognise specific bacterial effector proteins mediated through plant R-proteins to trigger effector-mediated immunity (ETI). The effector protein AvrRpm1 targets the host protein RIN4 for phosphorylation and this modification is detected by the RIN4-associated R-protein RPM1 which 'guards' RIN4 and triggers ETI (Mackey et al., 2003; Kim et al., 2005b; Chung et al., 2011).

To determine whether *ahk5-1* is defective in ETI, responses to infection with *Pst*DC3000 expressing *avrRpm1* (*Pst*DC3000*(avrRpm1)*) was tested. As the expression of *avrRpm1* results in an incompatible interaction and restriction of bacterial growth in wild-type Col-0, the response of plants to *Pst*DC3000*(avrRpm1)* was tested by syringe infiltration. Monitoring *in planta* bacterial populations revealed a pattern of restricted bacterial growth in the *ahk5-1* mutant compared to wild-type plants, with the largest difference seen at 3dpi. At 3dpi, bacterial populations were two-fold higher in wild-type plants compared to *ahk5-1* mutant plants. This suggests that the *ahk5-1* mutant may be enhanced in ETI.

As ETI is associated with the HR, the amount of cell death in response to infection with *Pst*DC3000*(avrRpm1)* was measured by electrolyte leakage. Measurement of cellular electrolyte leakage up to 3dpi when the difference in *in planta* bacterial populations was noted did not reveal any difference in cell death between mutant *ahk5-1* and wild-type plants. This observation was supported by Trypan blue staining at 3dpi which also indicated no difference in cell death. This suggests that the restriction of *Pst*DC3000*(avrRpm1)* growth in the *ahk5-1* mutant was not due to an increased HR response. Although gene-for-gene resistance is typically associated with the HR, evidence suggests that resistance against bacteria carrying avirulence genes can be uncoupled from this response. For example, the *dnd1* (*defence, no death 1)* mutant shows enhanced gene-for-gene resistance against *P. syringae* expressing *avrRpm1*, *avrRps4* or *avrB* without any cell death (Yu et al., 1998). Gene-for-gene resistance in Col-0 against bacteria carrying the avirulence genes *avrRps4* or *hopPsyA* also occurs without the HR (Gassmann, 2005).

In addition to the HR, the 'oxidative burst' is also associated with *R*-gene mediated resistance and occurs within hours of infection (Levine et al., 1994). To monitor production of ROS in leaves in response to infection, leaves were stained with 3, 3'-diaminobenzidine (DAB) which on oxidation in the presence of ROS results in the formation of an insoluble brown precipitate. At 5hpi, considerably less DAB staining was seen in *ahk5-1*mutant leaves compared to wild-type leaves suggesting an attenuated oxidative response in the mutant. As the oxidative burst is associated with resistance, it is not clear how this observation is linked to the suppression of bacterial growth in the *ahk5-1* mutant. Reciprocal regulation of ROS and NO (Zaninotto et al., 2006) raises the possibility that the attenuation of ROS in the *ahk5-1* mutant in response to *Pst*DC3000(*avrRpm1*) may have resulted in increased NO production leading to greater restriction in bacterial multiplication. Observation of NO production in the *ahk5-1* mutant would be required to determine whether this is the case.

Response to an avirulent *hrpA*$^-$ mutant defective in the TTSS and therefore unable to deliver effector proteins, and the bean pathogen *Pph*1448A which results in an incompatible or non-host interaction in *A. thaliana,* were also tested. As with *Pst*DC3000*(avrRpm1),* due to the inability of *Pst*DC3000(*hrpA*$^-$) and *Pph*1448A to establish disease and to multiply to high levels *in planta* in wild-type plants, response to these bacteria were tested by syringe infiltration. In both cases symptom development and bacterial growth was similar between wild-type Col-0 and *ahk5-1* mutant plants. The loss of ability of the *hrpA*$^-$ mutant to secrete effector proteins (He and Jin, 2003) allows for the investigation of defects in PTI in plants in the absence of the suppressive effects of effector proteins. The unaltered response of the *ahk5-1* mutant to infection with *Pst*DC3000(*hrpA*$^-$) suggests no defects in basal resistance on infiltration of the bacterium, in agreement with the observations from syringe infiltration of *Pst*DC3000. Additionally, the loss of function of *AHK5* did not result in more favourable conditions for the growth of *Pph*1448A which is not a pathogen of *A. thaliana.*

5.5 Conclusions

In summary, the histidine kinase AHK5 positively contributes to surface defences against the virulent pathogen *Pst*DC3000 but not towards *Pst*DC3000 directly infiltrated into the leaf apoplast nor towards the avirulent *hrpA*$^-$ mutant or the bean pathogen *Pph*1448A. Hormone responses in the *ahk5-1* mutant are compromised in response to surface inoculation with *Pst*DC3000, which may be linked to the defect in stomatal defences previously observed by Desikan et al. (2005a). In addition to altered responses to virulent bacteria, loss of AHK5

function resulted in increased resistance towards a strain expressing the effector protein *avrRpm1* which is recognised by the R-protein RPM1, resulting in an incompatible interaction. This increased resistance to *Pst*DC3000*(avrRpm1)* was not due to alteration of the HR response but was associated with decreased early ROS production.

Thus AHK5 positively contributes to resistance against virulent *Pst*DC3000 but appears to negatively regulate *RPM1 R*-gene mediated resistance.

Chapter 6:

AHK5 function in response to the necrotrophic pathogen *Botrytis cinerea*

6 AHK5 function in response to the necrotrophic pathogen *Botrytis cinerea*

6.1 Introduction

The fungal pathogen *Botrytis cinerea* is the cause of grey mould and soft rot disease of economically important crop plants and is unique in its ability to infect a wide range of plants, with a host range of over 200 plant species. As a necrotrophic pathogen, the mode of infection employed by this pathogen differs from that of the biotroph which relies on a living host; *B. cinerea* produces an array of toxins and degradative enzymes which breakdown host tissue before and during colonisation to release nutrients for assimilation by the fungus (discussed in Section 1.5.1) (van Kan, 2006; Choquer et al., 2007; Laluk and Mengiste, 2010).

6.1.1 *Infection by* B. cinerea

The versatility in the host on which *B.cinerea* can infect, that it can survive for prolonged periods as either mycelia, sclerotia or conidia and the many different virulent factors produced by this pathogen, many of which act redundantly, makes the task of controlling this pathogen difficult (Williamson et al., 2007).

A well known characteristic of infection with *B. cinerea* is the production of a 'grey mould' that appears on the surface of infected tissue which are the conidophores carrying the conidia/spores of the fungus (Agrios, 2005). The symptoms of infection with *B. cinerea* can vary, depending on the host species and the organ infected (Williamson et al., 2007). In *Arabidopsis*, symptoms consist of the appearance of water-soaked lesions/'wet-rot' of tissue in which the fungus grows, with the periphery of the lesion expanding with the growth of the fungus (van Baarlen et al., 2007).

Initiation of germination of spores on contact with the host surface is through detection of substrate properties, such as hardness, hydrophobicity and the presence of nutrients (Blakeman, 1975; Doehlemann et al., 2006). On germination and development of the fungal infection structure called the appressorium, enzymes such as cutinases and lipases are secreted in order to breach the host surface to gain access to host tissue where the fungus grows (van Kan, 2006). As the plant cuticle acts as a physical barrier to fungal infection

(Kerstiens, 1996) and that *B. cinerea* actively degrades the plant cuticle would suggest that defects in the plant cuticle would enhance the susceptibility of the plant. However, the opposite relationship seems to be true; that is, defects in the plant cuticle increases resistance towards infection. The *bre1* (*botrytis-resistant 1*)*/lacs2* mutant of a long-chain acyl-CoA synthetase 2 involved in cuticle biosynthesis which has a more permeable cuticle was also found to be more resistant to infection with *B. cinerea* and the related fungal pathogen *Sclerotinia sclerotiorum* (Bessire et al., 2007). This seemingly contradictory finding was shown to be due to leaching of anti-microbial compounds on to the leaf surface which inhibits infection by *B. cinerea,* with the more permeable membrane proposed to aid earlier recognition of the fungus by the plant and thus trigger earlier induction of defence responses (Bessire et al., 2007).

6.1.2 *The role of cell death and ROS*

Progression of lesion development and fungal growth is associated with and enhanced by host cell death; whereas cell death in the form of the HR protects against infection with biotrophs, pre-infection of leaves with HR-inducing bacteria increases susceptibility to infection with *B. cinerea* at the site of infection (Levine et al., 1994; Govrin and Levine, 2000). In addition, the accelerated cell death (*acd*) mutants which display cell death in the absence of pathogen infection are also more susceptible towards *B. cinerea* (van Baarlen et al., 2007).

B. cinerea is thought to take advantage of the decrease in plant resistance linked to cell death by stimulating production of ROS by the plant, altering cellular redox status to induce cell death (Govrin and Levine, 2000; Muckenschnabel et al., 2002; Asai et al., 2010). In agreement with this, prevention of host derived ROS production by the use of the NADPH oxidase inhibitor DPI resulted in a reduction in host cell death and fungal spread (Govrin and Levine, 2000). On the other hand, pre-treatment of leaves with the catalase inhibitor 3-aminotriazole or the addition of xanthine oxidase or glucose oxidase with their substrates xanthine and glucose to produce $O_2^{\cdot-}$ and H_2O_2, respectively, enhanced cell death and fungal infection (Govrin and Levine, 2000). Thus it appears that *B. cinerea* requires the production of host derived ROS for successful infection.

However, host ROS production can also contribute to plant defences against *B. cinerea* as early ROS production is linked to resistance rather than susceptibility (Asselbergh et al.,

2007). Thus the timing of ROS production by the host may be important in determining whether the outcome of infection is resistance or susceptibility. In addition to host derived ROS, *B. cinerea* also produces ROS. The role of ROS in fungal development and pathogenicity was discussed in Section 1.5.1.1. Analysis of ROS levels during infection may therefore provide clues as to whether the defence responses in the plant are being activated or if the fungus is manipulating ROS levels to cause cell death.

6.1.3 *Camalexin in defence against* B. cinerea

Recognition by the plant of infection with *B. cinerea* can be triggered through perception of the degradation products of fungal action on the plant cell wall, such as the production of oligogalacturonides, and one defence mechanism induced upon detection is the production of the secondary metabolite camalexin (Denby et al., 2004; Kliebenstein et al., 2005; Ferrari et al., 2007).

Camalexin has been shown to increase in leaf tissue directly surrounding lesions and is known to inhibit *B. cinerea* growth *in vitro* and *in planta*, with lower camalexin levels correlating with greater lesion development (Denby et al., 2004). Camalexin has been shown to exert its toxic effects in bacteria through disruption of membrane integrity and may also do so in fungi (Rogers et al., 1996; Rauhut and Glawischnig, 2009).

As mentioned earlier, characteristic of *B.cinerea* infection of *A. thaliana* is the formation of spreading lesions. As lesion size reflects the extent of fungal growth, and camalexin positively correlates with resistance to this fungus, the extent of lesion spread and measurement of camalexin surrounding infected tissue can be used as indicators of disease severity and resistance, respectively.

The sensitivity of the fungus to camalexin appears to be strain specific and is linked to the ability of the fungus to detoxify phytoalexins through active efflux of fungitoxic compounds via the BcatrB ABC transporter (Denby et al., 2004; Stefanato et al., 2009). The ability of *B. cinerea* to convert camalexin to less toxic metabolites *in vitro* may similarly contribute to camalexin tolerance *in planta* (Pedras et al., 2011). The production and spatial distribution of other plant metabolites, such as glucosinolates, is also influenced by infection with *B. cinerea*, although the role of these other metabolites in defences against this fungal pathogen is not clear (Kliebenstein et al., 2005).

It is apparent that the interaction between *B. cinerea* and its host is complex and that timing of plant response to infection is an important determinant in whether the interaction results in disease or resistance.

6.2 Aims

In this study, the role of AHK5 in mediating resistance against the necrotrophic pathogen *B. cinerea* was investigated. The main questions to be answered were:

- How does loss of AHK5 function affect resistance/susceptibility towards this fungal pathogen?
- Does alteration of plant-derived ROS contribute towards the *ahk5-1* phenotype in response to *B. cinerea?*

To answer the first question, susceptibility of plants towards infection with *B. cinerea* was determined by visual inspection of lesion development and measurement of lesion size. As camalexin is known to play a role in resistance against *B. cinerea,* levels of this phytoalexin were measured in wild-type and *ahk5-1* infected tissue to determine whether increased susceptibility was associated with defects in camalexin production.

Plant-derived ROS has previously been indicated in both resistance against and susceptibility towards infection with *B. cinerea* and was investigated here by histochemical staining for H_2O_2 using 3, 3'-diaminobenzidine (DAB).

Monitoring of fungal growth *in planta* was by staining of fungal structures with Trypan blue to aid correlation of lesion development/plant susceptibility with fungal growth.

6.3 Results

6.3.1 *The* ahk5-1 *mutant is more susceptible to infection with* B. cinerea

To test the response of the *ahk5-1* mutant to a necrotrophic pathogen, detached leaves were inoculated on the abaxial side with 10µl inocula droplets containing *B. cinerea* spores at a density of 2 x 10^5 spores ml^{-1} in 1/8th strength PDB. Lesion development was assessed over eight days using a scoring system (devised by J Mansfield) with scores of 0, 0.5, 1 2, 3 and 4 assigned to distinct stages of disease progression, with a score of 0 for no lesions present and a score of 4 representing tissue collapse and sporulation, the final stage of disease (Figure 6.1).

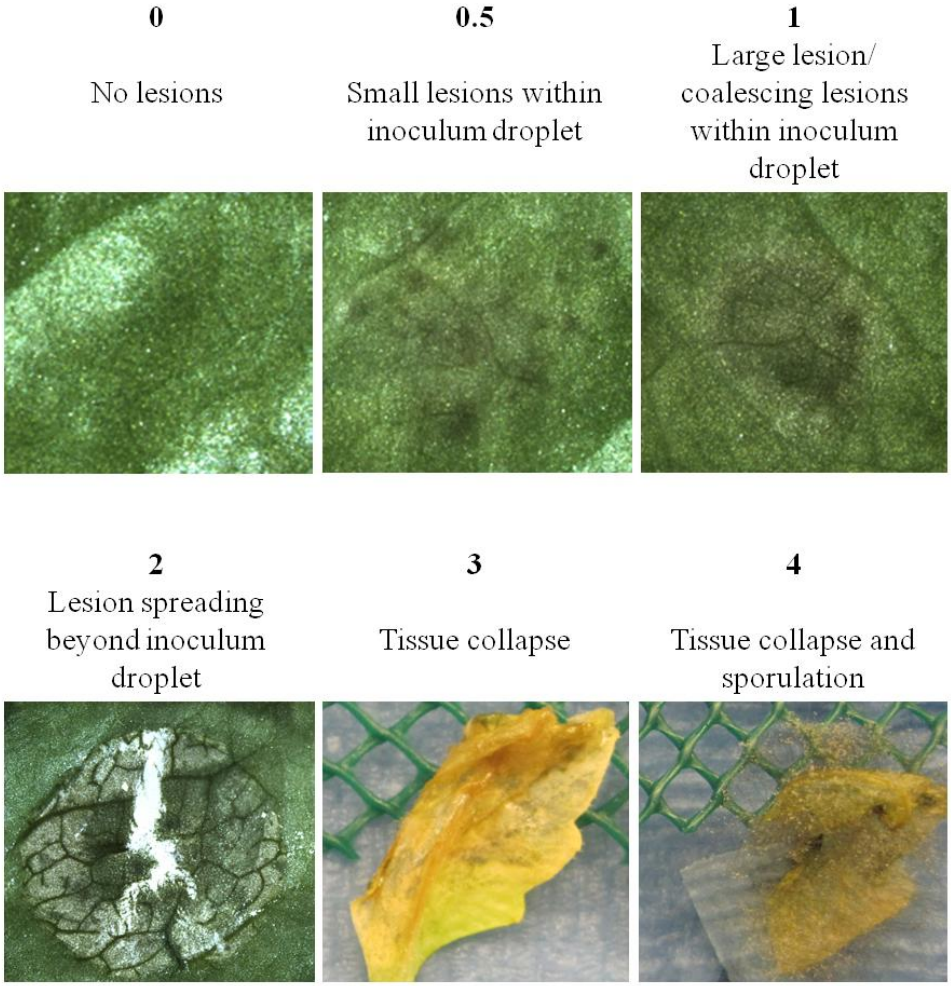


Figure 6.1 Scoring system used to determine disease progression in leaves inoculated with *B. cinerea*. Numbers above the description of disease stage shown in the photos are the scores used to denote each stage of lesion development.

From visual inspection of disease progression, the *ahk5-1* mutant appeared to be more susceptible towards infection with *B. cinerea* as lesion spread to uninoculated leaf tissue was more advanced, compared to wild-type plants (Figure 6.2a). Using the scoring system shown in Figure 6.1, the average symptom score was higher in the *ahk5-1* mutant when compared to lesions in wild-type plants or a complemented line carrying the carrying a *GFP-AHK5* fusion construct under the control of the CaMV 35S promoter in the mutant background (P_{35S} *-AHK5/ahk5-1*) (Figure 6.2b). The difference in lesion score became fully apparent at 4dpi, with significant differences between the *ahk5-1*mutant and wild-type seen at 6 and 8dpi, with larger lesions/more severe disease progression observed in the *ahk5-1* mutant. Lesion formation in the P_{35S} *-AHK5/ahk5-1* line was similar to that seen in wild-type, suggesting loss of AHK5 function in the *ahk5-1* mutant was responsible for the increased susceptibility of the mutant towards infection with *B. cinerea* (Figure 6.2b).

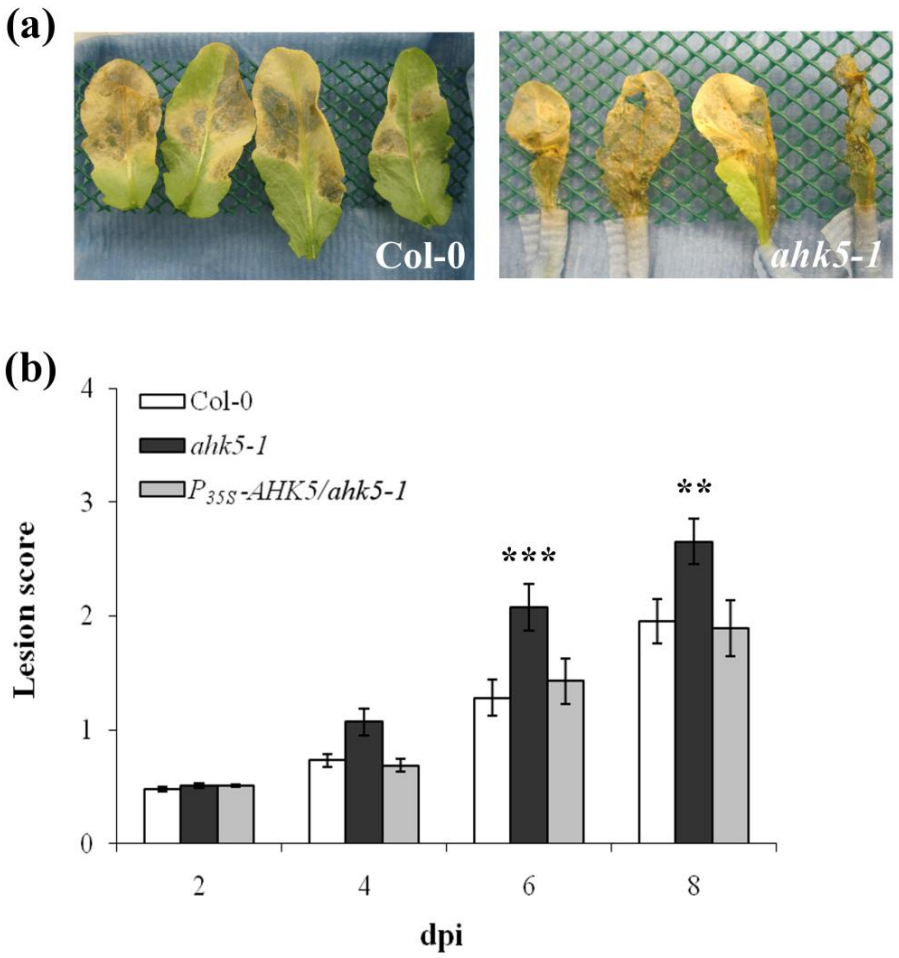


Figure 6.2 Lesion scores observed in wild-type and *ahk5-1* mutant leaves infected with 2 x 10^5 spores ml^{-1} of *B. cinerea*. (a) Representative photographs showing disease symptoms in Col-0 and *ahk5-1* leaves at 7dpi. (b) Bar chart showing average lesion score up to 8dpi. Asterisks denote a significant difference between wild-type and mutant lesion scores using the Kruskal-Wallis Test and Dunn's Multiple Comparison Test (** = $p< 0.005$, *** = $p<0.0001$). Values are mean ± SEM of 63-95 lesions.

Although the average symptom scores shown in Figure 6.2b provides an indication of the increased susceptibility of the *ahk5-1* mutant to *B. cinerea*, the variability in the appearance of the different lesion types is masked by the pooling of symptom scores at each time point. To understand the dynamics of disease progression, the percentage frequency of the different lesion scores for each time point was analysed (Figure 6.3). At 2dpi, the majority of lesions visible scored 0.5 for all plant lines tested, resulting in an even distribution of the data around the 0.5 score (Figure 6.3a). At 4dpi, the percentage appearance of higher symptom scores increased for all plant lines tested, resulting in a skewing of the distribution of scores towards the higher end of the scale (Figure 6.3b). At this time point, the highest lesion score in wild-type and the P_{35S} *-AHK5/ahk5-1* complemented line was a score of 2, whereas in *ahk5-1*, the highest score seen was a score of 3. Six days after inoculation, the difference in symptom severity between wild-type and the P_{35S}*-AHK5/ahk5-1* complemented line with *ahk5-1* was more apparent, with a greater percentage of severe symptom scores (i.e., a score or 3 or 4) seen for the mutant line (Figure 6.3c); in the wild-type and the P_{35S}*-AHK5/ahk5-1* complemented line, lesions scoring 3 made up 14.6% and 21.8%, respectively, of the total lesions present, with no lesions scoring 4, whereas in the *ahk5-1* mutant, 37.5% of lesions scored 3 and 4.2% scored 4. This difference was reflected in the distribution of the data, where two peaks were seen corresponding to the distribution of lesion types in the different plant lines. The maximum lesion scores seen at this time were a score of 3 in the wild-type and P_{35S}*-AHK5/ahk5-1* complemented line and a score of 4 for the *ahk5-1* mutant. At the end of the experiment at 8dpi, lesion scores were more skewed towards the higher lesion scores with all plant lines showing lesions falling into the most severe disease category (Figure 6.3c). However, the *ahk5-1* line still displayed a higher percentage of more severe symptoms with 77.1% of lesions scoring 3 or 4 compared to 41.6% and 37.5% in wild-type and the P_{35S}*-AHK5/ahk5-1* line, respectively. In conclusion, the full range of lesion types appear in all the plant lines tested but differed in the timing and number of appearances of each lesion type, with the appearance of more severe lesion types occurring earlier and at a higher frequency in the *ahk5-1* mutant.

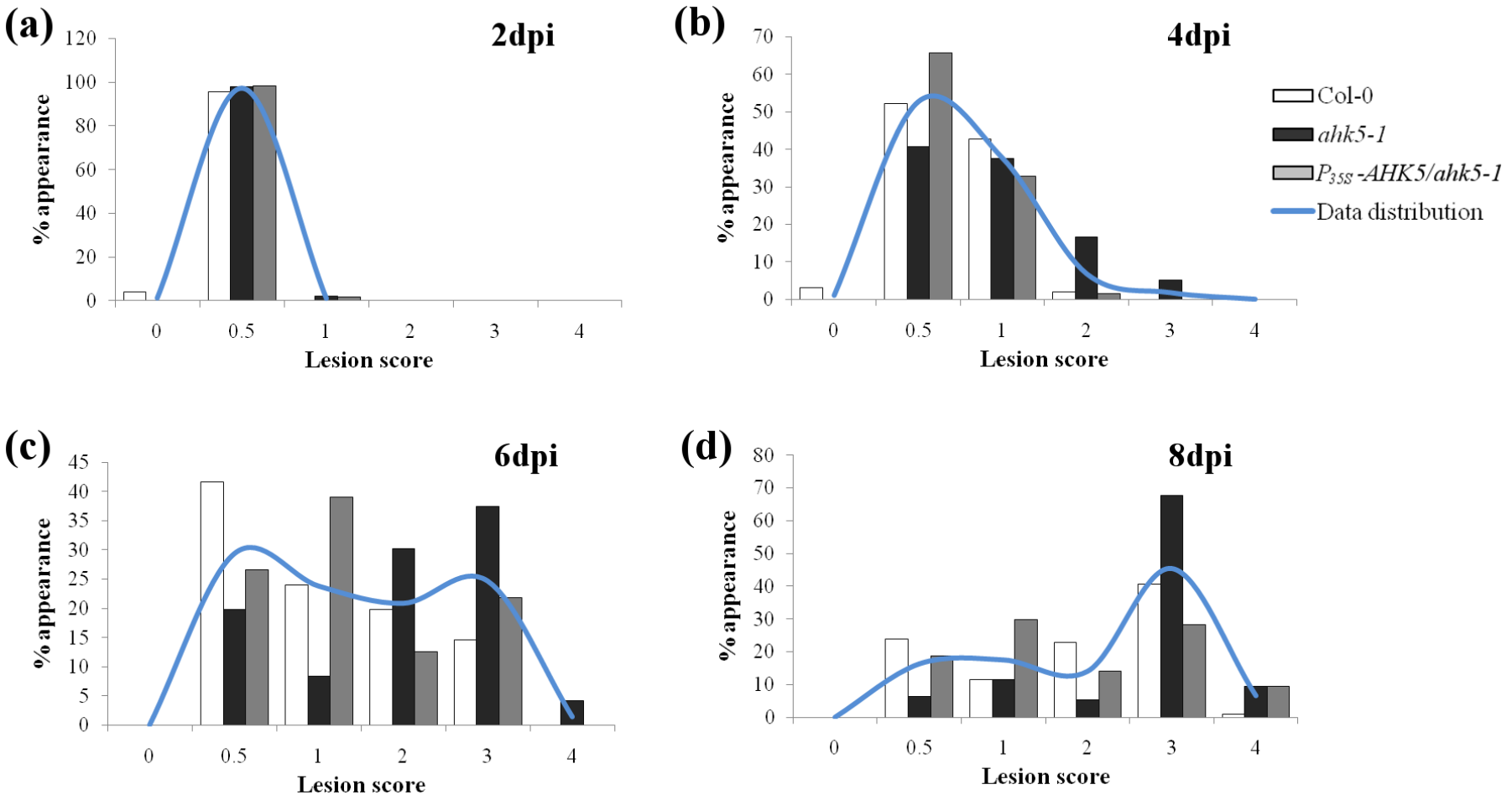


Figure 6.3 The appearance and proportion of different lesion types in leaves of wild-type, *ahk5-1*mutant and the complemented *P_{35S}-AHK5/ahk5-1* line inoculated with 2 x 10^5 spores ml^{-1} *B. cinerea*. The graphs show the frequency expressed as percentage appearance of each lesion score seen for each line at (a) 2dpi, (b) 4dpi, (c) 6dpi and (d) 8dpi. To determine the distribution of lesion scores at each time point, the percentage appearance of each lesion type from all three plant lines used were pooled and plotted on each graph as the data series labelled 'Data distribution'. Percentage appearance of lesions was calculated from 63-95 lesions for each plant line at each time point.

Analysis of disease progression (Figure 6.2) and monitoring of the appearance of different lesion types (Figure 6.3) suggests that disease progression in the *ahk5-1*mutant in response to inoculation with *B. cinerea* is accelerated. As the spread of the lesion is correlated with progression of disease, the size of lesions were measured at 3dpi to determine earlier differences which may not be reflected in lesion scores. At this time point, a significant difference between lesion size in leaves of wild-type Col-0 and *ahk5-1* mutants was seen (Figure 6.4) in agreement with the visual observation of symptom development (Figure 6.2).

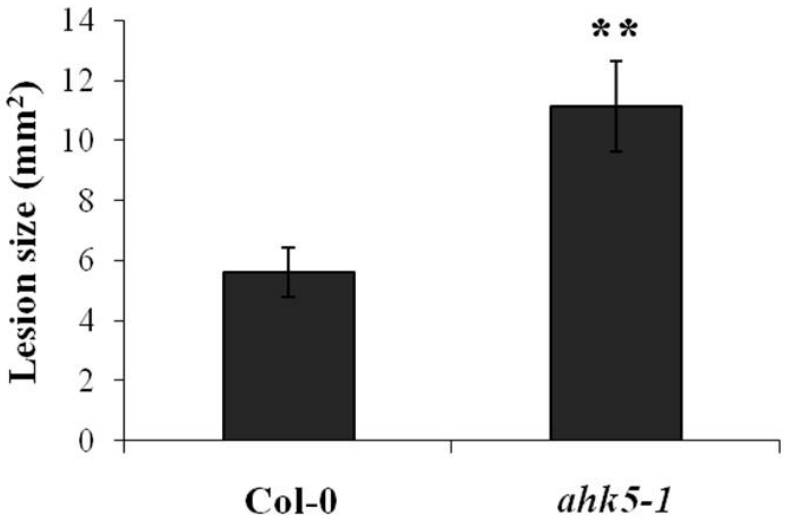


Figure 6.4 Average lesion size in wild-type and *ahk5-1* mutant leaves caused by inoculation with 2 x 10^5 spores ml^{-1} of *B. cinerea* at 3dpi. Lesions were measured by the Image J software. Asterisks denote a significant difference as determined by the Student's t-test (** = $p<0.005$). Data are mean ± SEM of 30 lesions per genotype. The experiment was performed twice with similar results. A representative experiment is shown.

6.3.2 *The* ahk5-1 *mutant is not defective in camalexin production*

The phytoalexin camalexin has been shown to be involved in resistance against *B. cinerea* (Ferrari et al., 2003; Kliebenstein et al., 2005). To determine whether increased susceptibility of the mutant was due to a deficiency in camalexin production, phytoalexin levels in *B. cinerea* infected leaf tissue was measured by HPLC coupled to a fluorescence detector.

Since living tissue is required for production of camalexin and accumulates at the site of infection (Kliebenstein et al., 2005), camalexin was extracted from lesions up to 4dpi before complete collapse of tissue. The extraction process was optimised for extraction of camalexin from individual lesions. To determine whether camalexin from single lesions could be detected, each excised lesion was subjected to successive extractions with camalexin

extracted at each step measured separately by HPLC. Since the intended experiment was to run from 1dpi through to 4dpi, camalexin was extracted from lesions at these two time points as they represent time points at which camalexin measured would be at the lowest and highest levels expected to be measured, respectively. From lesions at 1dpi, camalexin was measureable in the first and second extractions and became undetectable on the third extraction. Assuming the total amount of camalexin from the first two successive extractions represented extraction of 100% of camalexin from the lesion, processing the sample once resulted in extraction of 80.2% of total camalexin and processing the sample twice resulted in extraction of 100% of total camalexin (Figure 6.5a). Lesions at 4dpi required three successive extractions to extract 100% of camalexin, with a total of 88.9% and 98.4% of camalexin recovered from one and two extractions, respectively (Figure 6.5b).

From these preliminary experiments, it was determined that camalexin extracted from single lesions was measurable and a total of three successive extractions were needed to extract over 95% of camalexin from each lesion.

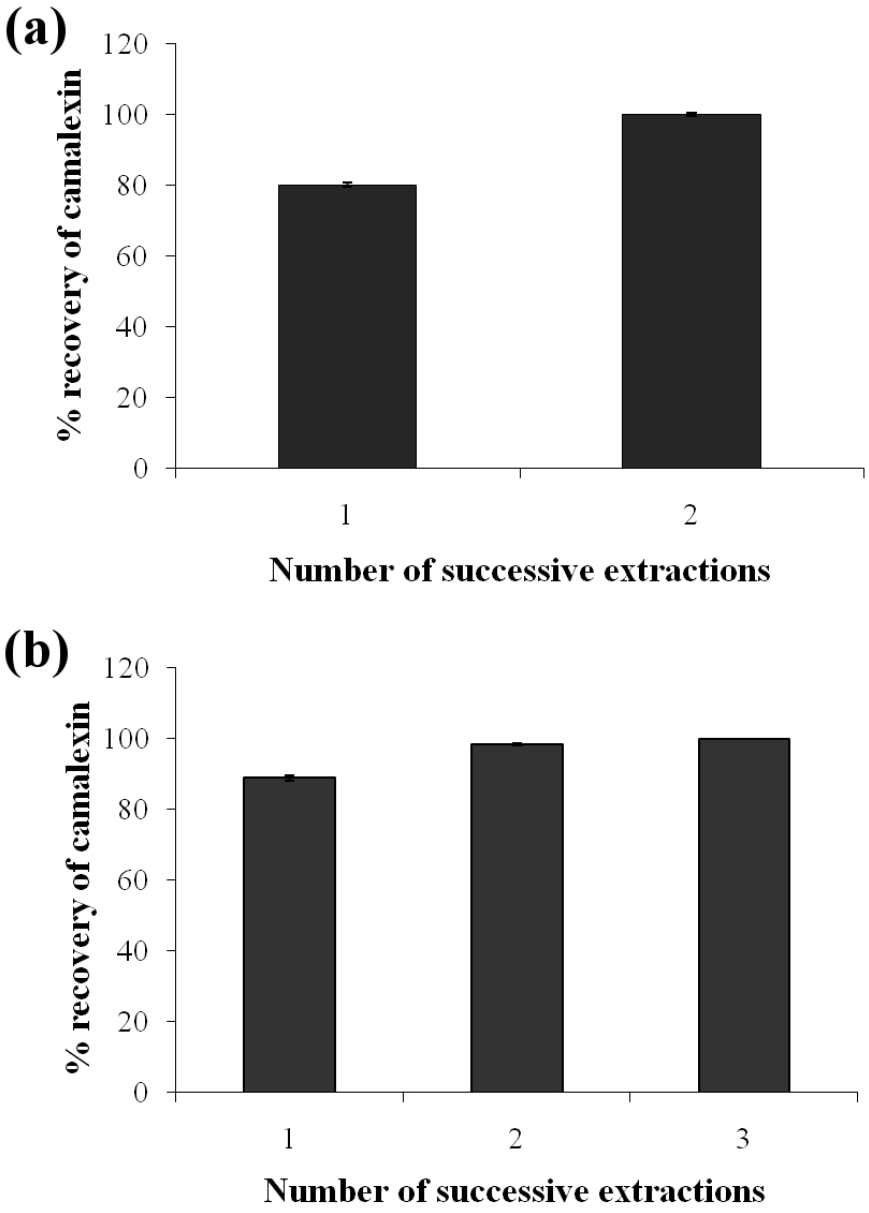


Figure 6.5 Optimisation of camalexin extraction. Total percentage recovery of camalexin from successive extractions from lesions taken at (a) 1dpi and (b) 4dpi from wild-type Col-0 leaves inoculated with 2 x 10^5 spores ml^{-1} of *B. cinerea*. Data are mean ± SEM of three lesions.

As a significant difference in lesion size was measurable at 3dpi (Figure 6.4), it was expected that any difference in camalexin levels between wild-type and the *ahk5-1* mutant would be seen within the time frame of the experiment. Camalexin was found to increase over time in response to infection with *B. cinerea* as expected and this increase was similar in both wild-type and *ahk5-1* mutant plants (Figure 6.6a), suggesting that the increased rate of *B. cinerea* lesion progression on the *ahk5-1* mutant was not due to a defect in camalexin production. In addition, camalexin levels in leaves treated with the abiotic elicitor silver nitrate at a

concentration of 10mM was also tested at three days post treatment (dpt). Although the level of camalexin was consistently lower in *ahk5-1* mutant tissue, this difference was not statistically significant (Figure 6.6b).

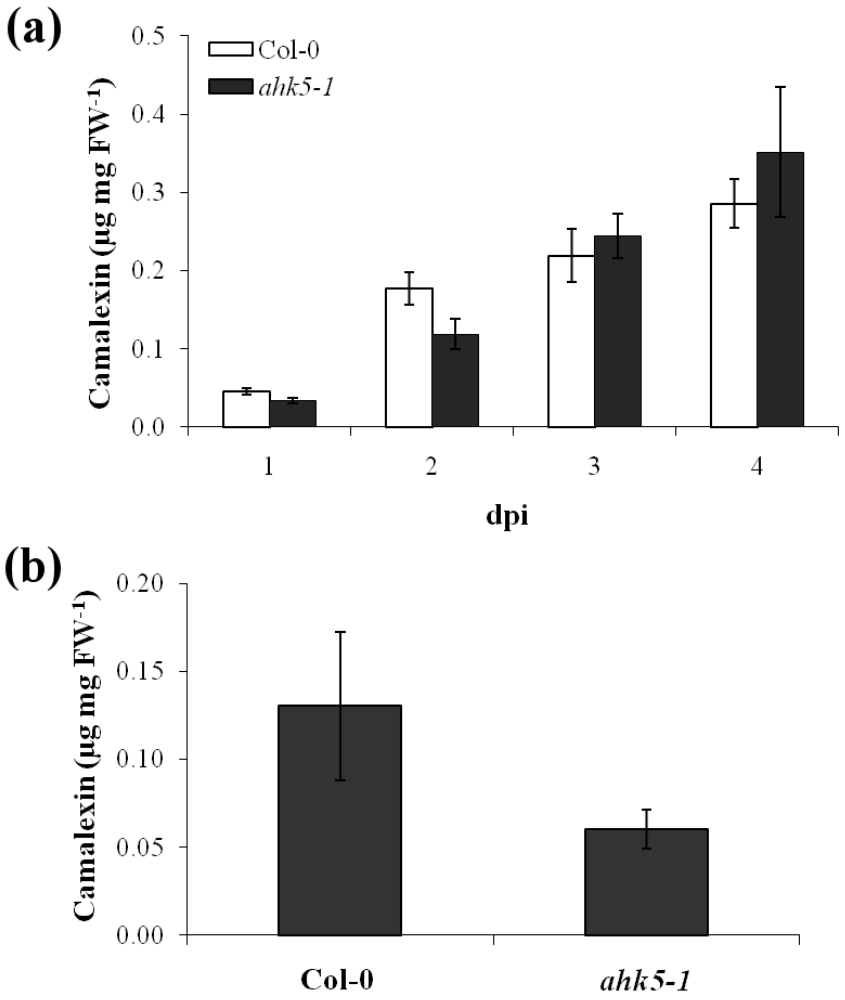


Figure 6.6. Camalexin production of leaves of wild-type and *ahk5-1* mutant plants in response to (a) inoculation with 2 x 10^5 spore ml^{-1} of *B. cinerea* infection up to 4dpi and (b) spraying with 10mM silver nitrate at 3dpt. Values for camalexin content from *B.cinerea* infected leaves are mean ± SEM of 20 lesions from two independent experiments. Camalexin levels for silver nitrate treated tissue are mean ± SEM from nine samples from three independent experiments.

Chassot et al. (2008b) previously found that wounding of *Arabidopsis* leaves prior to infection led to accelerated accumulation of camalexin after inoculation with *B. cinerea*, which prevented the establishment of disease. Wounding of leaves before inoculation afforded the *ahk5-1* mutant with the same protection against infection with *B. cinerea* as it did for leaves of wild-type plants (Figure 6.7). This suggests that the signalling pathways

activated by damage were retained in the *ahk5-1* mutant and also suggesting that camalexin production in the mutant is not compromised.

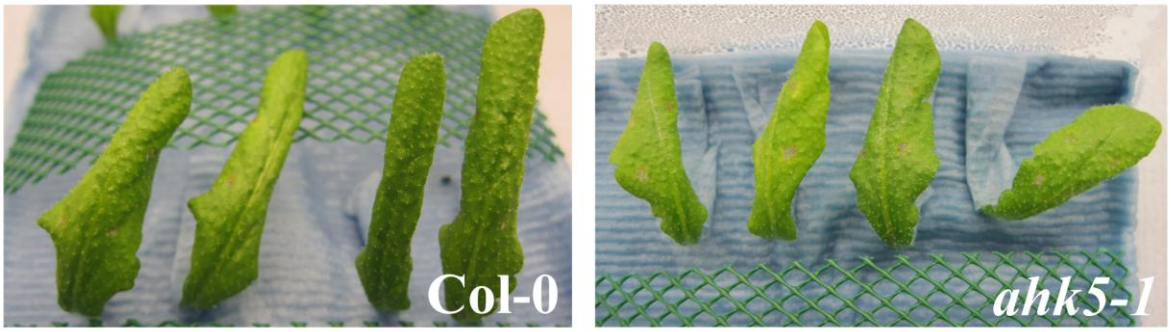


Figure 6.7 Wounding before inoculation with *B. cinerea* prevents symptom development. Leaves of wild-type Col-0 and the *ahk5-1* mutant were wounded by scraping the leaf surface with a razor blade immediately before inoculation with a spore suspension of 2 x 10^5 spores ml^{-1} of *B. cinerea*. Photos were taken 8dpi when unwounded inoculated leaves had collapsed.

6.3.3 *The growth of* B. cinerea *on the* ahk5-1 *mutant is accelerated*

The production of ROS is known to play a role in defence against *B.cinerea* and it has been shown that AHK5 plays a central role in the ROS signalling pathway (Asselbergh et al., 2007; Desikan et al., 2008). To determine whether the difference in establishment of disease between wild-type and mutant plants was due to a difference in the pattern of ROS production, inoculated leaves were treated with 3,3'-diaminobenzidine (DAB) to stain for ROS. ROS production was detected as early as 8hpi, with slightly more staining visible within the vicinity of the inoculation site, with this difference most noticeable at 12hpi and less so at 24hpi (Figure 6.8). Closer inspection of the area of staining at 12hpi when the difference was most noticeable showed that the increased DAB staining seen was associated with fungal hyphae, with no DAB staining seen in plant cells (Figure 6.9). However, it was unclear whether the increased amount of DAB staining seen in the *ahk5-1* mutant was due to an increase in the amount of fungal generated ROS or the presence of more fungal structures. Staining with Trypan blue confirmed that fungal hyphae grew longer on leaves of the *ahk5-1* mutant than on wild-type Col-0 and this difference was measurable and significantly different as early as 8hpi (Figure 6.10).

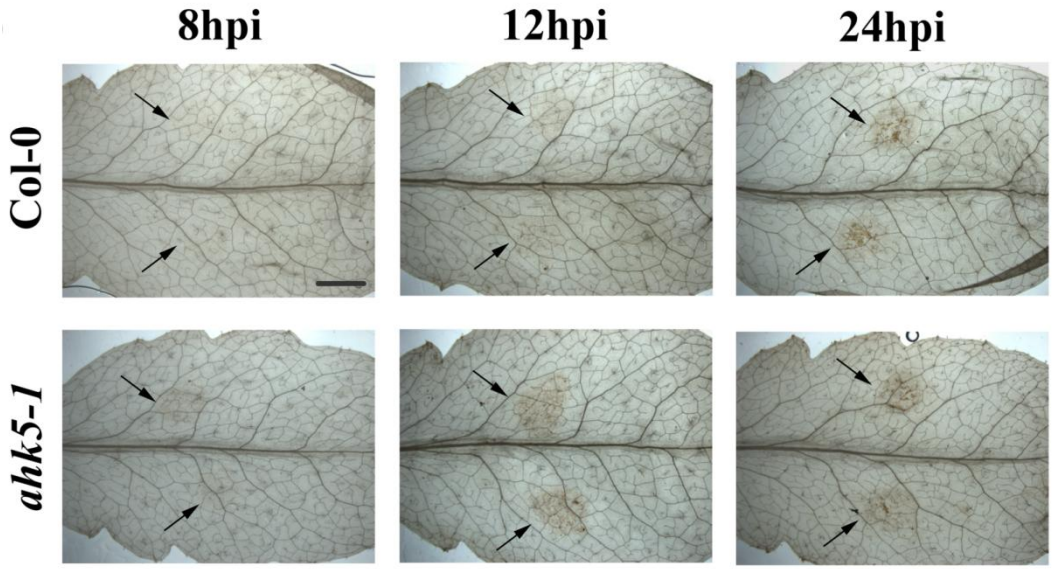


Figure 6.8 ROS production in wild-type and *ahk5-1* mutant leaves associated with the area of inoculation with 2 x 10^5 spore ml^{-1} of *B. cinerea* visualised by DAB staining at 8, 12 and 24hpi. Arrows indicate site of inoculation (Scale bar = 3mm).

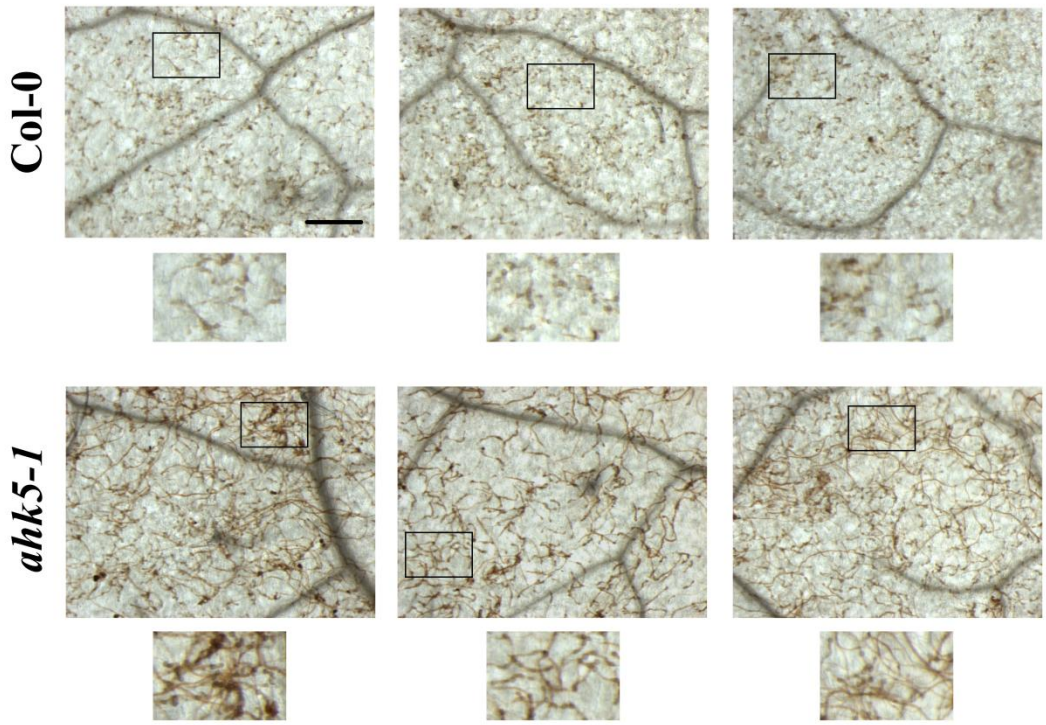


Figure 6.9 ROS associated with fungal hyphae of *B. cinerea* growing on wild-type and *ahk5-1* mutant leaves at 12hpi. Leaves were inoculated with 2 x 10^5 ml^{-1} spores of *B. cinerea* and pictures taken at the site of inoculation. ROS production was visualised by DAB staining. Three representative pictures are shown for each plant line. The smaller pictures shown below each main photo represents the areas within the black frames which have been enlarged x2 (scale bar = 200µm).

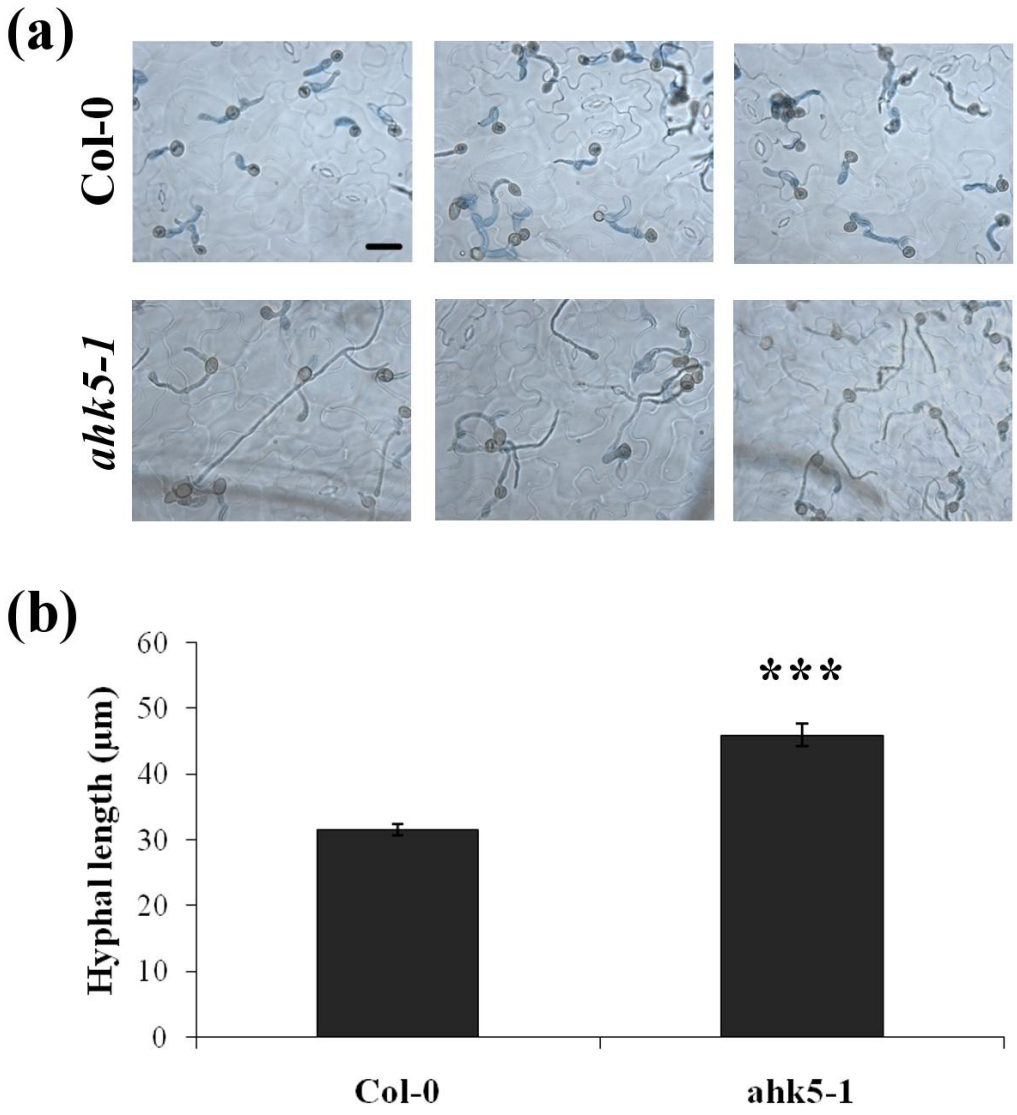


Figure 6.10 Growth of *B. cinerea* on wild-type and *ahk5-1* mutant leaves at 8hpi. (a) Trypan blue staining of fungal hyphae growing on leaves 8hpi (scale bar = length of 5µm). (b) Length of fungal hyphae at 8hpi measured using the Image J software. Asterisks denote a significant difference as determined by the Student's t-test (*** = $p<0.0001$). Data are mean ± SEM of 237-271 measurements.

At 24hpi, close examination of the site of infection by microscopy revealed cellular DAB staining in the plant epidermal cells (Figure 6.11a), with significantly less staining seen in the *ahk5-1*mutant (Figure 6.11b). This suggests that ROS production by the *ahk5-1* mutant is attenuated in response to *B. cinerea* and this attenuated response is seen after the difference in *B. cinerea* growth was seen.

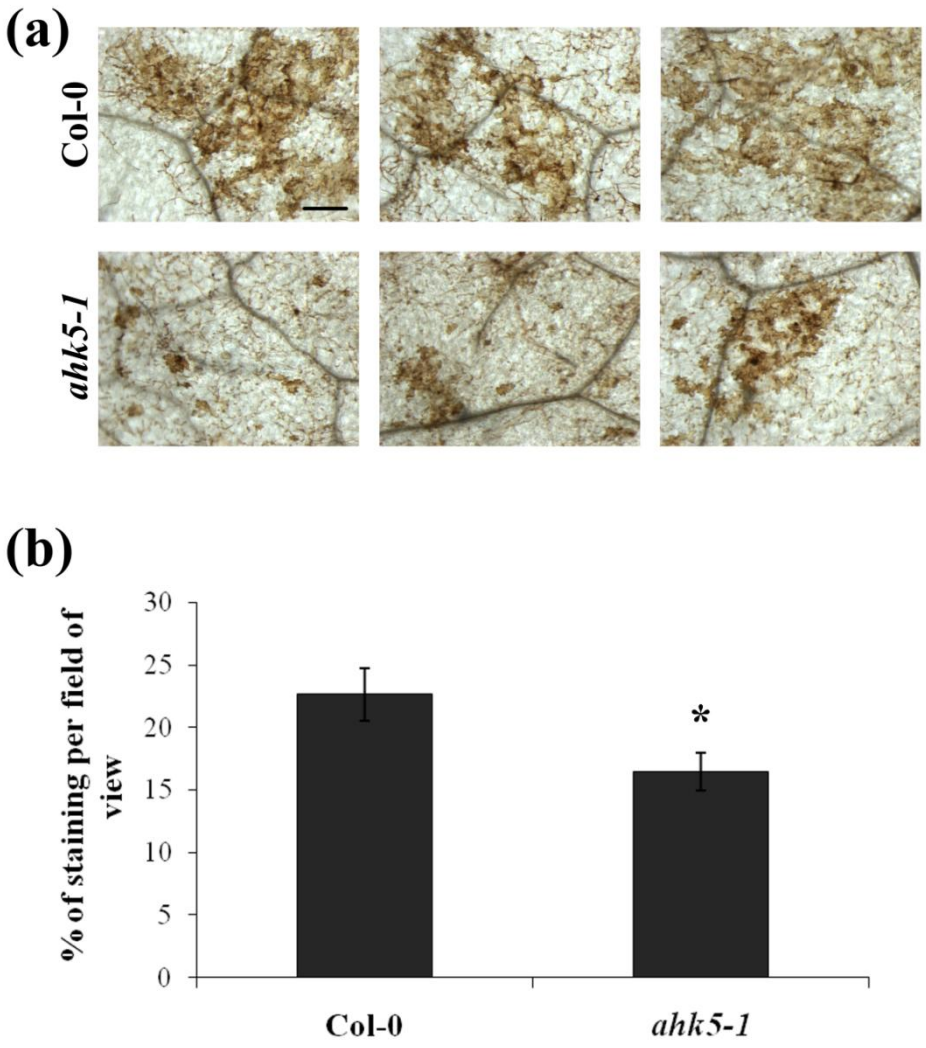


Figure 6.11 ROS production in wild-type and *ahk5-1*mutant leaves in response to inoculation with 2 x 10^5 spores ml^{-1} of *B. cinerea* 24hpi. (a) Representative images of DAB stained cells in leaves at the site of inoculation (scale bar = 200µm). (b) Measurement of the percentage of DAB staining observed per field of view using the Image J software. Data are mean ± SEM of 20 fields of view. The asterisk denotes a significant difference as determined by the Students's t-test (* = $p<0.05$).

6.4 Discussion

6.4.1 *The* ahk5-1 *mutant is more susceptible to infection with* B. cinerea *which is not due to a defect in camalexin production*

To determine whether the *ahk5-1* mutant is altered in responses to necrotrophic pathogens, the phenotype of this mutant in response to infection with *B. cinerea* was investigated. Infection with *B. cinerea* caused larger spreading lesions in the *ahk5-1* mutant, which was measureable by 3dpi. Analysis of lesions scores revealed that more severe disease symptoms

appeared earlier in the *ahk5-1* mutant, suggesting that growth of the fungus may be less restricted in the mutant.

As camalexin is known to play a role in resistance against this phytopathogenic fungus, the level of camalexin in infected tissue was measured. As the production of camalexin requires living tissue, measurements were carried out up to 4dpi, at which time complete maceration of leaf tissue within the inoculated area was not yet seen. Camalexin levels were seen to increase over time as expected, but the levels of camalexin extracted were not significantly different between wild-type and *ahk5-1* mutant tissue, suggesting that the defect in resistance in the mutant was not due to alteration in camalexin production. In addition to infection, camalexin is also induced by abiotic stimuli such as UV-B light and silver nitrate (Mert-Turk et al., 2003b; Mert-Turk et al., 2003a). To test for abiotic elicitation of camalexin production, leaves of wild-type and *ahk5-1* mutant plants were sprayed with 10mM silver nitrate and camalexin levels measured 3dpt. Although the amount of camalexin produced in response to silver nitrate in the *ahk5-1* mutant was approximately half that produced in wild-type, this difference was not statistically significant. Additionally, camalexin produced in wild-type plants in response to silver nitrate was half that found in tissue inoculated with *B. cinerea* at 3dpi, suggesting that *B. cinerea* is a stronger inducer of camalexin than silver nitrate.

Elicitation of camalexin is known to vary in response to different stimuli, as was shown here in response to *B. cinerea* and silver nitrate. Previously, it was demonstrated that wounding of leaves prior to inoculation with *B. cinerea* prevented establishment of infection, with this protective effect thought to be mediated by camalexin (Chassot et al., 2008b). To further investigate the role of camalexin in defence, leaves of both wild-type and *ahk5-1* mutant plants were wounded before inoculation with *B. cinerea*. Wounding of leaves prior to inoculation prevented infection in both wild-type and *ahk5-1* mutant plants, with no lesions visible even at 8dpi, at which point the majority of non-wounded inoculated leaves showed tissue collapse. This suggests that the wounding pathway leading to camalexin production is intact in the *ahk5-1* mutant.

The ability of the *ahk5-1* mutant to produce camalexin in response to *B. cinerea* and silver nitrate and the protective effect of wounding on *B. cinerea* infection indicate that the *ahk5-1* mutant is not defective in induction or production of camalexin. This suggests that the increased susceptibility of the *ahk5-1* mutant is not due to alteration of defence responses involving camalexin but in other resistance pathways. The *Botrytis*-susceptible mutant *bos3*

accumulates higher levels of camalexin in response to infection with *B. cinerea* than wild-type plants whilst being more susceptible (Veronese et al., 2004) and the *pad2* mutant which produces more camalexin than the *pad3* mutant is less resistant to *B. cinerea* (Ferrari et al., 2003), confirming that factors other than camalexin contribute towards resistance against this necrotrophic pathogen.

6.4.2 *The growth of* B. cinerea *on the* ahk5-1 *mutant is accelerated and ROS production in the* ahk5-1 *mutant in response to infection is attenuated*

ROS has been shown to play an important role in the infection process and contributes to both susceptibility and resistance towards *B. cinerea* in plants. On the one hand, inhibition of plant derived ROS by pre-infiltration of leaves with the NADPH oxidase inhibitor diphenyleneiodonium (DPI) before inoculation restricted lesion spread, whereas inhibition of plant catalase enhanced disease progression, suggesting plant-derived ROS is required for full virulence by *B. cinerea* (Govrin and Levine, 2000). On the other hand, timing of ROS production by plants also contributes to the outcome of the interaction, as earlier ROS production in the ABA-deficient *sitiens* tomato mutant confers resistance (Asselbergh et al., 2007). The earlier production of ROS in the *sitiens* mutant coincided with earlier induction of cellular modifications associated with resistance such as cell wall modifications, whereas pre-treatment of *sitiens* leaf discs with catalase or ascorbate prior to inoculation with *B. cinerea* increased and restored susceptibility, respectively, adding another layer of complexity to plant-fungal interactions (Asselbergh et al., 2007). ROS production by the fungus is also known to occur during infection, but the source and role of this fungal-derived ROS in the infection process is unknown (Tenberge et al., 2002; Segmuller et al., 2008). Identification of a fungal superoxide dismutase BCSOD1 and NADPH oxidases BCNOXA and BCNOXB which were required for full virulence of *B. cinerea* suggested that this fungus may dismutate superoxide generated by BCNOXA and BCNOXB through the action of BCSOD1 (Rolke et al., 2004; Segmuller et al., 2008). However, the *bcnoxA* and *bcnoxB* mutants were not defective in ROS production and addition of DPI to wild-type spores had no effect on fungal ROS production, indicating that these NADPH oxidases are not the source of fungal ROS (Govrin and Levine, 2000; Segmuller et al., 2008). It is possible that BCSOD1 dismutates host derived as opposed to fungal derived superoxide, which would be in agreement with the restriction of lesion formation on inhibition of host NADPH oxidases, although conclusive

evidence for the requirement of plant-derived ROS for infection by *B. cinerea* is still lacking (Govrin and Levine, 2000; Heller and Tudzynsk, 2011).

To investigate the involvement of ROS in the susceptibility of the *ahk5-1* mutant towards *B. cinerea*, ROS production was monitored in response to infection by staining with the histochemical stain 3, 3'-diaminobenzidine (DAB). ROS production was measured early after infection 8hpi up to 72hpi. ROS staining was seen at 8hpi within the area of the inoculum droplet and the intensity increased over time. More intense DAB staining was observed in the *ahk5-1* mutant at 8, 12 and 24hpi. On closer inspection, the ROS staining seen at the two earliest time points were associated with fungal hyphae, with more fungal hyphae seen on the *ahk5-1* mutant, suggesting accelerated fungal growth. As DAB staining was not uniform along the whole fungal hyphae, Trypan blue which stains all fungal structures was used to visualise fungal growth by microscopy. Trypan blue staining confirmed that fungal growth was indeed accelerated on the *ahk5-1* mutant, with fungal hyphae measurably longer on the *ahk5-1* mutant as early as 8hpi. The trigger for this early increase in fungal growth is not clear, although it is possible that properties of the leaf surface, such as the structure and composition of the leaf surface. In *Arabidopsis*, changes in the cuticle composition leading to increased permeability is linked to increased exudation of anti-microbial compounds onto the leaf surface and increased resistance (Bessire et al., 2007; Chassot et al., 2008a; Curvers et al., 2010). Whether the reverse is true (i.e. decreased permeability leading to attenuation of resistance due to inhibition of exudation of anti-microbial compounds) is not known.

On the other hand, the *ahk5-1* mutant may exude compounds which stimulate fungal growth. As part of the inoculation process, the *B. cinerea* spores are suspended in one-eighth strength potato dextrose broth (PDB) as a nutrient source, with higher concentration of PDB resulting in more rapid formation of lesions. The addition of nutrients to the inoculation droplet is required to overcome the inhibitory effects of epiphytic bacteria on the leaf surface on *B. cinerea* germination and hyphal growth through competition for nutrients (Blakeman, 1975; Clark and Lorbeer, 1977; Rossall and Mansfield, 1980). As sugars and amino acids found on the leaf surface have been shown to promote *B. cinerea* germination (Blakeman, 1975), it is conceivable that in the *ahk5-1* mutants, nutrients may leach out onto the leaf surface more readily than in wild-type plants and is therefore able to support greater fungal growth.

Although attenuation of cellular ROS production was also seen in the *ahk5-1* mutant, this was seen at 24hpi, after the increased fungal growth was measurable. This suggests that defective

resistance due to attenuation of ROS production was not the cause of this early increase in fungal growth but may have contributed to further acceleration of fungal growth and tissue colonisation, leading to more severe disease symptoms seen later and measurable at 3dpi.

The dual role of ROS was previously demonstrated in *A. thaliana* in response to the necrotrophic fungal pathogen *Alternaria brassicicola.* Mutation of the NADPH oxidase AtrbohD resulted in a greater amount of cell death and marked increase in SA and ethylene levels, inhibition of which led to decreased cell death (Pogany et al., 2009). Interestingly, the distribution of H_2O_2 production in response to infection differed between wild-type and the *atrbohD* mutant; whereas H_2O_2 was produced in single cells in wild-type plants in response to infection with *A. brassicicola*, H_2O_2 production in the *atrbohD* mutant was diffuse and not restricted to single infected cells, but was found in groups of cells (Pogany et al., 2009). This suggests that AtrbohD is required for activation of cell death in response to infection and also in restricting cell death to areas of infection through modulation of SA and ethylene levels (Pogany et al., 2009). In agreement with the role of AtrbohD in restriction of cell death, over-expression of *AtrbohD* in the *lsd1(lesion stimulating disease 1)* mutant resulted in increased ROS production and restriction of the runaway cell death (RCD) phenotype of this mutant in response to either *Pst*DC3000(*avrRpm1*) or *B. cinerea* (Torres et al., 2005).

That the increased cell death seen in the *lsd1 atrbohD* double mutant and the *atrbohD* single mutant were not associated with increased fungal growth of *B. cinerea* or *A. brassicicola,* respectively, suggests that the function of AtrbohD is in the restriction of cell death as opposed to restriction of pathogen growth (Torres et al., 2005; Pogany et al., 2009). It is possible that the reduced ROS in response to *B. cinerea* seen in the *ahk5-1* mutant contributes to greater symptom development/cell death at the later stages of infection rather than in the facilitation of fungal growth. This is in agreement with the observations of this study where increased fungal growth on the *ahk5-1* mutant was seen before any host-derived ROS was triggered in either wild-type or *ahk5-1* mutant leaves in response to *B. cinerea.*

However, as mentioned previously, inhibition of plant NADPH oxidase activity through the pharmacological inhibitor DPI restricts lesion spread and growth of *B. cinerea in planta,* seemingly in contradiction of the role of AtrbohD in restricting cell death only (Govrin and Levine, 2000). However, *A. thaliana* encodes for 10 *Atrboh* genes *(AtrbohA-AtrbohJ)* (Torres et al., 1998; Torres et al., 2002; Kwak et al., 2003; Torres and Dangl, 2005) and inhibition of

all NADPH oxidase function by DPI may have given rise to the difference observed from targeted mutation of AtrbohD function.

Thus the role of ROS in infection is complex with seemingly contradictory functions, whereby ROS is required for both resistance and susceptibility towards *B. cinerea.* It is clear that more detailed analysis of ROS production in the *ahk5-1* mutant is required to further dissect the role of AHK5 in resistance towards *B. cinerea.* In addition to ROS, nitric oxide (NO) may also be important, but was not investigated in this study. In *Nicotiana benthamiana,* NO was found to negatively regulate ROS production in response to *B. cinerea,* with inhibition of NO production either through pharmacological suppression of nitric oxide synthase (NOS) activity with the NOS inhibitor L-NAME or through virus-induced silencing (VIGS) of the tobacco NOS gene *NbNOA1* resulting in more ROS produced and increased susceptibility (Asai and Yoshioka, 2009; Asai et al., 2010). As the *ahk5-1* mutant was found to be defective in stomatal responses to both H_2O_2 and NO, it is possible that AHK5 may also function to integrate both ROS and NO signalling in defence against *B. cinerea* (Desikan et al., 2008).

6.4.3 *A role for AHK5 in hormone signalling in response to* B. cinerea*?*

Another possible factor contributing to the increased susceptibility of the *ahk5-1* mutant is the alteration of hormone levels in response to *B. cinerea* infection, although these have not been demonstrated here. ABA has previously been linked to responses to *B. cinerea* in tomato, with the ABA-deficient *sitiens* mutant more resistant towards infection (Audenaert et al., 2002; Asselbergh and Hofte, 2007; Curvers et al., 2010). As exogenous addition of ABA was shown to restore susceptibility of the *sitiens* mutant to *B. cinerea* but did not have a direct stimulatory effect on the fungus, it was suggested that ABA may negatively regulate host defences during infection with *B. cinerea* (Audenaert et al., 2002). The deficiency of ABA in the *sitiens* mutant was associated with early production of cellular ROS, fortification of the cell wall and up-regulation of genes involved in pathogen defence (Asselbergh et al., 2007). Similarly, the ABA biosynthetic mutants *aba2-12* and *aao3-2* of *A. thaliana* were also more resistant to infection with *B. cinerea* than wild-type plants (Adie et al., 2007). Interestingly, *B. cinerea* encodes putative ABA biosynthetic genes and may therefore stimulate plant ABA responses through production of fungal ABA (Siewers et al., 2005; Asselbergh et al., 2008). Alteration of ABA production in the *ahk5-1* mutant is thus a

possible explanation for the increased susceptibility of the mutant towards infection with *B. cinerea.*

Aside from ABA, the plant hormones JA and ethylene are known to play important roles in resistance against necrotrophic pathogens. Mutants in JA signalling (*coi1, aos, jar1*) and ethylene signalling (*etr1-1, ein2, ein3*) were all found to be more susceptible to infection with *B. cinerea*, suggesting important roles for these hormones in defence against this pathogen (Zimmerli et al., 2001; van Baarlen et al., 2007; Rowe et al., 2010). Additionally, the *coi1* and *aos* mutants showed decreased induction of camalexin production on infection compared to wild-type plants (Rowe et al., 2010). SA signalling has also been implicated in resistance against this necrotroph, as pre-treatment of wild-type plants with the SA analogue benzo-(1,2, 3)-thiadiazole-7-carbothioic acid *S*-methyl ester (BTH) decreased the size of lesion caused by *B. cinerea* (Zimmerli et al., 2001). On the other hand, the SA signalling mutant *npr1-1* and the *nahG* expressing line allowed greater fungal spread, suggesting SA plays a role in resistance against infection with *B. cinerea* (Zimmerli et al., 2001; van Baarlen et al., 2007). It is possible that AHK5 acts upstream of hormone responses to positively regulate hormone production and defence responses against *B. cinerea*, but at this time there is insufficient data to determine whether or not this is the case.

6.5 Conclusions

It is clear from the discussion so far that the interaction between different hormone signalling pathways contribute to plant responses towards *B. cinerea.* Thus determination of hormone levels in the *ahk5-1* mutant in response to infection with *B. cinerea* may therefore provide interesting insights into the role of AHK5 in defence against necrotrophic pathogens such as *B. cinerea*. The *ahk5-1* mutant is more susceptible to infection with the necrotrophic fungus *B. cinerea*, reflected in early accelerated growth of the fungus at 8hpi. Later on in infection, the greater susceptibility of the *ahk5-1* mutant is reflected in more severe symptom development and lesion spread. The increased susceptibility was not due to a defect in camalexin production, as the *ahk5-1* mutant was shown to produce camalexin in response to both infection with *B. cinerea* and treatment with the abiotic elicitor silver nitrate. An attenuation of ROS production by the *ahk5-1* mutant was seen at 24hpi. This attenuation in ROS production was seen after the time at which fungal growth on wild-type and *ahk5-1* was noticeably different. This suggests that factors other than ROS (such as nutrient availability) may play a role in the early acceleration of fungal growth on the *ahk5-1* mutant, although the

attenuation of ROS may positively contribute to later development of lesions. Investigation of the role of NO towards the phenotype of the *ahk5-1* mutant may also further shed light on the function of AHK5 as NO has also previously been shown to contribute towards resistance against *B. cinerea*.

Chapter 7:

Function of AHK5 through protein-protein interactions

7 Function of AHK5 through protein-protein interactions

7.1 Introduction

Of the hybrid HKs of *A. thaliana*, the least is known for AHK5 and to date, only two studies focused on investigating the function of AHK5 have been published (Iwama et al., 2007; Desikan et al., 2008). As such, not much is known about the signalling pathways in which AHK5 participates in and how AHK5 acts to mediate these pathways. One approach in which to further elucidate the role of AHK5 in plant signalling is to identify protein interaction partners.

As discussed earlier, HKs of the TCS have been shown to interact with proteins such as AHPs and ARRs, with most known for the cytokinin signalling pathway (see Section 1.8.2). Since interaction with HPt-domain proteins and response regulators are a key feature of the TCS conserved across different species, it is likely that AHK5 also interacts with these proteins. However according to a TCS interaction network, non-TCS proteins also appear to be part of the signalling system (Dortay et al., 2008)

7.1.1 *Prediction of AHK5 interacting proteins*

One approach which can be used to investigate protein-protein interactions before conducting 'wet lab' experiments is to use online tools to mine databases for predicted protein interactions. One such tool is the Predicted Arabidopsis Interactome Resource (PAIR, Version 3.3, http://www.cls.zju.edu.cn/pair/) which utilises data from different sources to computationally predict interactions based on direct evidence, such as interactions which have been shown experimentally, and on indirect evidence such as homologous interactions in other species, co-localisation and co-expression (Lin et al., 2011). This database is predicted to cover 24% of all Arabidopsis protein interaction with each computational prediction having a confidence of 44% (Lin et al., 2011). Validation of predicted interactions with data not included in the interaction databases at the time of testing showed PAIR outperformed other predicted interactomes, such as the *Arabidopsis thaliana* protein interactome database (Lin et al., 2011).

Querying the AHK5 protein sequence against the PAIR database identified 11 hypothetical interactions, including AHK5 itself (Figure 7.1). In addition to prediction of homodimer

formation (a common feature of HK function), AHK5 was predicted to interact with known TCS proteins, such as the HKs ETR2, AHK4/CRE1/WOL and the AHPs AHP1 and AHP2 and the pseudo-AHP AHP6. AHK5 was also predicted to interact with the divergent HK EIN4. Interestingly, MAP3K delta 4 (At4g23050), a Raf-related MAPKKK, was also identified as a potential interacting partner of AHK5. This raises the possibility that AHK5 may modulate the activities of downstream kinases through direct interaction, similar to the interaction of ETR1 with CTR1, also a Raf-related MAPKKK and which acts as a negative regulator of ethylene signalling (Hahn and Harter, 2009). Another kinase, the serine/threonine kinase Non Phototropic hypocotyls 1-like (NLP1, At5g58140), was also highlighted and functions in control of stomatal opening in response to blue light (Takemiya et al., 2005). Two additional proteins, Postmeiotic Segregation 1 (PMS1, At4g02460) and Multihomologue 1 (MLH1, At4g09140) with predicted functions in DNA mismatch repair were also identified.

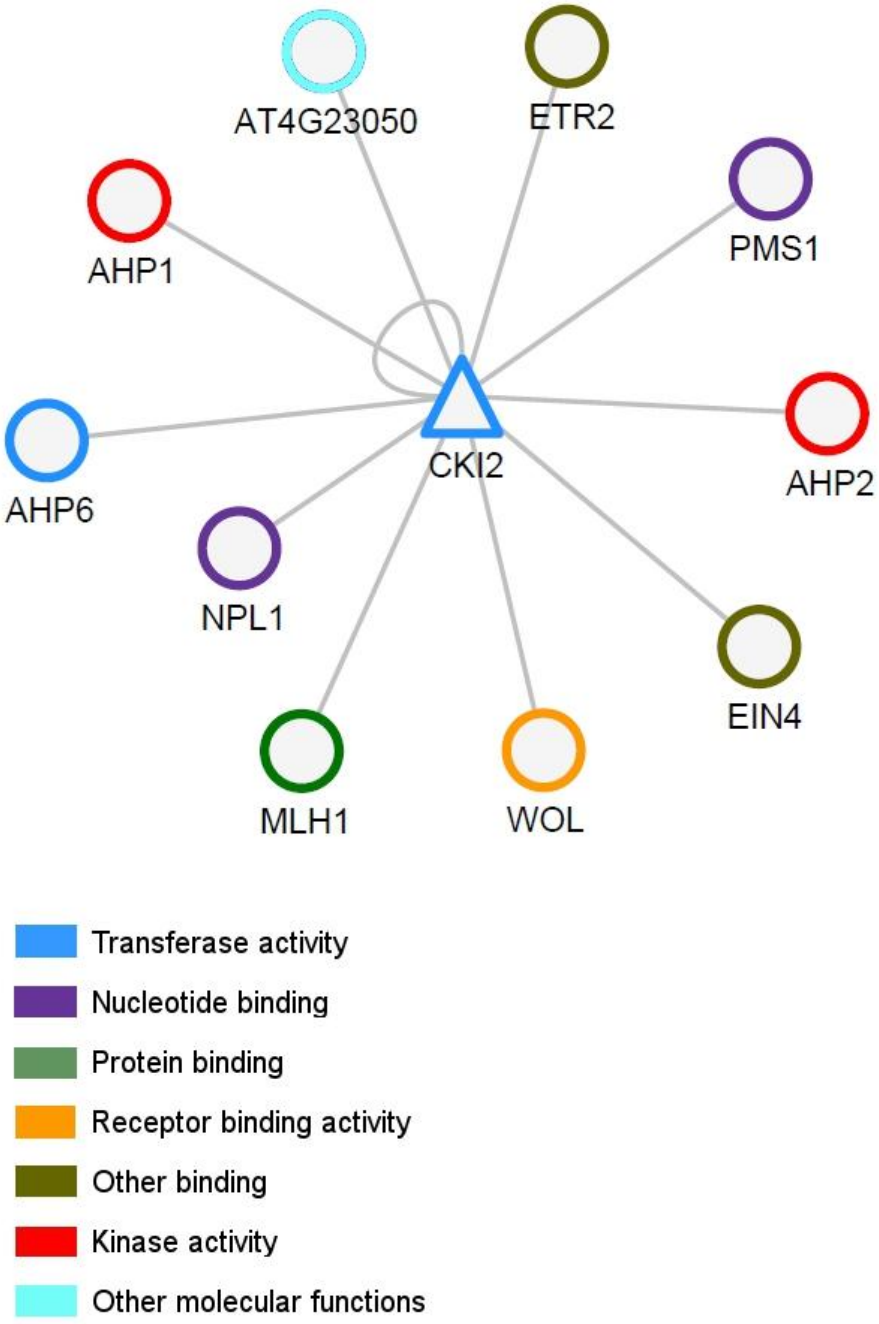


Figure 7.1 Predicted interactors of AHK5 (referred to in the diagram as CKI2) generated by the Predicted Arabidopsis Interactome Resource (PAIR) database. The interactors are colour coded according to known/predicted function.

Although *in silico* methods for prediction of protein interactions are useful tools for guiding the direction of research, ultimately experimental data showing direct interactions are needed as confirmation. From unpublished work it is known that AHK5 is able to interact with AHP1, AHP2 and AHP5 and the Type-A ARR ARR4, but not with AHP4 or AHP6 (R. Desikan, personal communication). Both AHP1 and AHP2 were amongst the proteins

predicted to interact with AHK5 by PAIR, confirming these predictions; AHP6 was also predicted to interact but did not do so under experimental conditions and AHP5 and ARR4 which were found to interact with AHK5 *in planta* were not identified by PAIR. These findings highlight both the usefulness of predictive tools and the importance of experimental verification. Using PAIR to predict interactors of ARR4 however, reveals interactions with AHP1, AHP2 and AHP5, all of which have been experimentally shown (Dortay et al., 2006), providing a link between AHK5 and ARR4 through the three AHPs.

Furthermore, analysis of the 3205 bases upstream of the ATG start codon of *AHK5* using the Signal Scan Search interface of the PLACE database to search for possible cis-acting DNA elements revealed the presence of an ARR1-binding element (Higo et al., 1999). This suggests that AHK5 expression may be regulated by the Type-B ARR1, which is known to act as a transcription factor which positively regulates CK signalling (Mason et al., 2005). However this remains to be proven experimentally.

7.1.2 *Investigating protein-protein interactions experimentally*

A common approach to investigate protein interactions is the use of the yeast two hybrid system which takes advantage of the modular nature of yeast transcription factors. In this system, the protein of interest is fused to the DNA-binding domain (BD) of the yeast transcription factor and a plant cDNA library is transformed into yeast fused to the activation domain (AD) of the transcription factor. On screening of this library and interacton of the BD-fused protein with an AD-fused library protein, the activity of the transcription factor is reconstituted and activates transcription of a reporter gene (Causier and Davies, 2002). Although this method is well established, high levels of false positives occur and that the interactions are taking place in a heterologous system means any interactions must be confirmed *in planta* (Causier and Davies, 2002). In addition, this method is not well suited for the identification of protein complexes involving more than two protein partners.

Another approach is to use *in vitro* biochemical methods such as co-immunoprecipitation. In this method, an antibody raised against the protein of interest is bound to a solid phase, such as protein A/G beads, and incubated with cellular extract (Miernyk and Thelen, 2008). The protein of interest along with any interacting proteins form an immune complex on binding to the antibody and can then be isolated for identification by, for example, liquid-chromatography coupled with tandem mass spectrometry (LC-MS/MS) (Miernyk and Thelen,

2008). One disadvantage of this method is that it is sometimes difficult to generate antibodies which bind with high specificity to the target protein. An alternative is to generate a construct for the expression of the protein of interest fused to an 'affinity tag.' Common affinity tags include the polyhistidine (His) tag, which strongly interacts with transition metals such as Ni^{2+}, and protein A of *Staphylococcus aureus* which binds with high affinity to IgG (Terpe, 2003; Xu et al., 2010).

A further variation of this method is the Tandem Affinity Purification (TAP) tag in which the protein of interest is tagged with more than one affinity tag in tandem, so that two affinity purification steps can be performed to decrease isolation of contaminating proteins and increase the purity of the TAP-tagged protein (Xu et al., 2010). In addition to being used for purification purposes, the tag can also be used for detection of the fused protein. Since the TAP method allows the study of protein interactions which occur under native and physiologically relevant conditions (as the interactions take place *in planta* before extraction) (Rubio et al., 2005; Xu et al., 2010), this method raises the possibility of studying interactions occurring in response to different stresses and stimuli. For these reasons, the TAP method was the method of choice for investigation of AHK5 protein interactions.

7.1.3 *Tandem Affinity Purification*

The use of TAP purification to isolate protein complexes from *Arabidopsis* was first described by Rubio et al. (2005) who used an alternative TAP (TAPa) tag designed for use in *Arabidopsis*. Expression of the TAP-tagged protein in a mutant background lacking the endogenous protein prevents competition for the 'bait' protein between the tagged and endogenous protein. The TAPa tag consists of a region of nine myc repeats, a region of six His repeats, a 3C protease cleavage site and two copies of the protein A IgG binding domain (Figure 7.2).



Figure 7.2 Structure of the C-terminal TAPa tag used in this study. The tag contains two copies of the protein A IgG binding domain for the first purification using IgG beads. Cleavage of the protein for the second purification is mediated by a 3C protease which cuts at the 3C cleavage site. The remaining part of the tag contains a section of nine myc repeats and a section of six His repeats, either of which can be used for the second purification (figure modified from Rubio et al. (2005)).

The TAP method is outlined in Figure 7.3. In the first purification, the tagged protein is bound to IgG immobilised on sepharose beads by the two protein A IgG binding domain (IgG-BD) carried on the end of the TAPa tag. At this stage, any proteins which are not tagged or interacting with the tag should not bind to the beads and are discarded in the flow through. The tagged protein is then eluted from the beads by cleavage at the 3C cleavage site by the human rhinovirus 3C protease. Originally, the TAP tag was developed with a TEV protease cleavage site, but since this protease is not efficient at temperatures below 16°C, this was replaced in the TAPa tag with the 3C protease cleavage site as this protease is active at 4°C, a temperature at which protein interactions are more stable (Puig et al., 2001; Rubio et al., 2005).

After cleavage of the tagged protein from the IgG beads, the protein is then bound to Ni^{2+} beads through interaction of the imidazole side chain of the histidine residues with the transition metal for the second purification (Terpe, 2003). After washing the beads, the tagged proteins are eluted by the addition of free imidazole which competes for binding with Ni^{2+}, displacing the TAPa-tagged protein. The eluted proteins can then be separated and visualised by SDS-PAGE and individual protein bands excised and processed for identification by mass spectrometry.

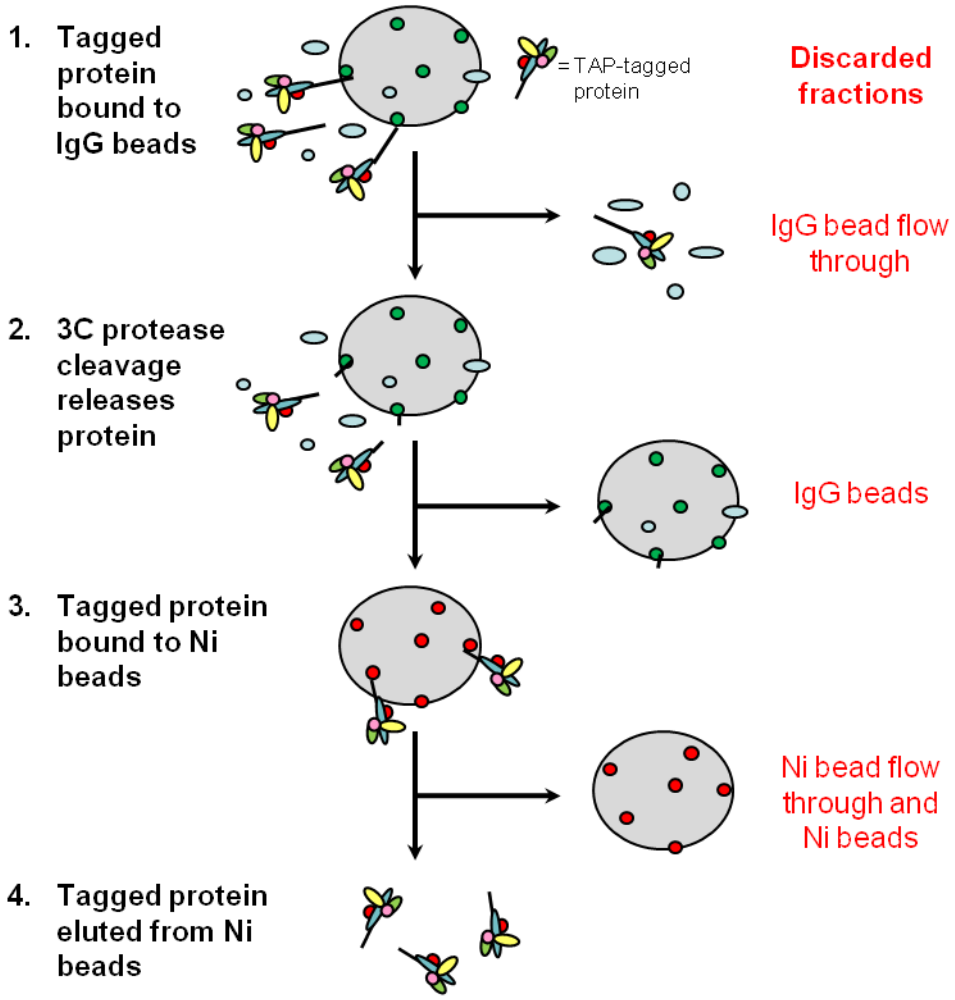


Figure 7.3 Schematic summarising the TAPa purification protocol as described in the text. 1. Cytosolic or microsomal fractions are incubated with IgG beads. TAPa tagged proteins are bound to the IgG beads through the presence of the 2 x IgG binding domains in the tag. The flow-through containing untagged proteins and non-interactors of the tagged proteins are discarded in the flow-through. 2. IgG-bound proteins are cleaved from the beads at the 3C cleavage site upstream of the 2 x IgG binding domains and the IgG beads discarded. 3. Cleaved proteins from step 2 are bound to Ni beads by the 6 x His repeat present in the tag. Flow though containing non-tagged and non-interactors of the tagged protein still remaining are discarded in the flow through. Finally, the tagged protein and any interacting proteins are eluted from the Ni beads and collected for analysis by SDS-PAGE, western-blotting and LC-MS/MS. Modified from Rubio et al. (2005).

7.2 Aims

As AHK5 function may involve protein-protein interactions, a tandem affinity purification (TAP) approach was used in an attempt to isolate TAPa-tagged AHK5 and any interacting proteins occurring *in vivo*. Proteins isolated from this procedure was separation by SDS-PAGE and analysis/identification of proteins was carried out by LC-MS/MS. Soluble and

insoluble proteins were subjected to the TAP procedure separately to determine whether association of AHK5 with the plama membrane or localisation within the cytosol influenced the protein interactors seen.

Seeds for the purpose of TAP were from a transgenic line previously generated by R Desikan, using the *ahk5-3* T-DNA insertion mutant (Desikan et al 2008) complemented with a C-terminal TAPa-tagged *AHK5* construct. Seedlings of this line (P_{35S}-*AHK5/ahk5-3*) were grown on full-strength Murashige and Skoog medium with 1% sucrose for 18 days and approximately 15g of seedling material was harvested for small scale TAP procedure (Rubio et al., 2005).

7.3 Results

7.3.1 *TAP purification of the TAPa-AHK5 protein*

The AHK5 protein is predicted to have a mass of 104KDa, whereas the TAPa-tag is 33KDa in size (Rubio et al., 2005). The TAPa-AHK5 fusion protein was therefore expected to have a size of approximately 137KDa. However, since the TAP procedure involves cleavage of part of the TAPa tag, the purified TAPa-AHK5 protein is expected to be in the region of 122KDa in size.

As AHK5 is predicted and shown to localise to both the cytosol and the plasma membrane (Desikan et al., 2008), it is possible that the proteins with which AHK5 interacts with depends on whether AHK5 is in the cytosol or associated with the plasma membrane. To determine whether this is the case, extracted soluble (cytosolic) and insoluble (microsomal membrane) proteins were separated, concentrated by acetone precipitation and subjected to the TAP protocol separately. At each step of the procedure, the eluted fractions were collected for analysis by SDS-PAGE. The final fraction was eluted with an elution buffer containing 50mM Imidazole.

Figure 7.4 shows SDS-PAGE analysis of fractions collected from TAP purification of soluble and insoluble proteins. From SDS-PAGE analysis of protein fraction collected at each stage of the TAP procedure, a greater amount of soluble proteins were collected than insoluble, a reflection of the total amount of protein in the starting material (2.8mg ml^{-1} of soluble proteins were present in the starting material compared to 0.4mg ml^{-1} insoluble proteins collected). The final fraction collected from the procedure which should contain the TAPa-AHK5 showed a more complex banding pattern for cytosolic proteins (Figure 7.4a) than for membrane proteins (Figure 7.4b). A band in the final fraction obtained from cytosolic proteins migrated to an estimated size of approximately 100KDa, close to the predicted size of the TAPa-AHK5 protein. This band along with six other bands were excised from the final fraction obtained from cytosolic proteins as indicated in Figure 7.4a (lane 'TAP'). In the final fraction obtained from membrane proteins, only one clear band of approximately 50KDa was visible. This band was excised in addition to a band which migrated to a size between 37 and 50KDa in the fraction containing proteins not bound to Ni-NTA beads (Figure 7.4b, lane 'I').

To determine whether the TAPa-AHK5 protein could be detected in the protein extracts used for the TAP procedure, total protein extract and the soluble and insoluble extracts before

purification were subjected to western blot analysis and probed with anti-AHK5 and anti-myc antibodies for visualisation of cross-reacting proteins (Figure 7.5a and b). A band of approximately 50KDa was identified as cross-reacting with both anti-AHK5 and anti-myc in all three extracts. Bands of between 75-100KDa were seen in all three extracts with anti-AHK5 antibody (Figure 7.5a) and was only seen in the soluble extract with anti-myc antibody (Figure 7.5b). This band was fainter than that seen with anti-AHK5 suggesting that perhaps the anti-myc antibody is less sensitive and the signal for this band in the seedling and insoluble fraction was too weak for detection. Specifically seen with anti-AHK5 was a band migrating to a size between that of the 25 and 37KDa markers (Figure 7.5a). On the membrane probed with anti-myc, the antibody was seen to bind to a band of a size close to 100KDa and a band between 37 and 50KDa in the soluble fraction (Figure 7.5b).

As mentioned earlier, the expected size of uncleaved TAPa-tagged AHK5 is 137KDa. Here, the largest proteins detected by anti-AHK5 or anti-myc was between 75-100KDa and it is possible that these bands represent TAPa-tagged AHK5. The bands of smaller size detected may be degradation products of AHK5; degradation of TAPa-tagged protein as a result of the detergent used (in this case 3-([3-cholamidopropyl]dimethylammonio)-1-propanesulfonic acid (CHAPS)) has previously been shown to occur (Rivas et al., 2002).

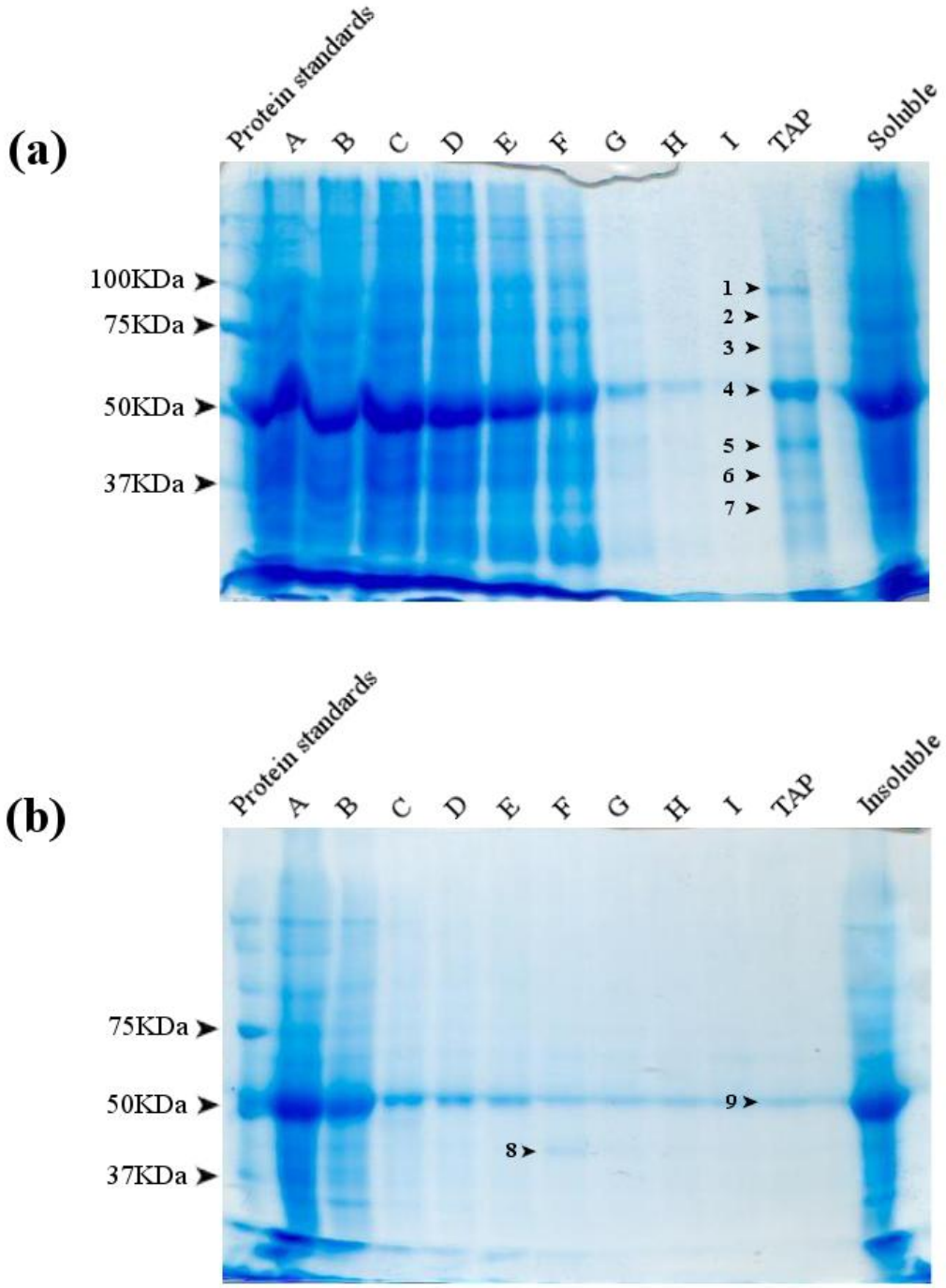


Figure 7.4 Proteins obtained from TAP purification. Proteins from *P_{35S}-AHK5/ahk5-3* seedling extract subjected to TAP purification were separated into soluble/ cytosolic proteins (a) and insoluble/ microsomal proteins (b) and resolved on a 12.5% SDS-PAGE gel and visualised by Colloidal Coomassie Blue staining. Lanes A-I and TAP are protein fractions collected at different stages of the purification process. The first number in parentheses represent the percentage of the fraction loaded from TAP purification of soluble proteins and the second number in parentheses represents the percentage loaded from TAP purification of insoluble proteins; A = supernatant containing proteins not bound to IgG beads (0.3%; 8%), B-E = proteins obtained from consecutive washes of IgG beads (8%; 13%), F = proteins not bound to Ni-NTA beads (13%; 13%), G-I = proteins from consecutive washes of Ni-NTA beads (13%; 13%), TAP = proteins cleaved from Ni-NTA beads (13%; 13%), Soluble/ insoluble = soluble/ insoluble proteins extracted from seedling material for TAP purification (0.3%; 8%). Numbered arrowheads indicate bands excised for identification by LC-MS/MS.

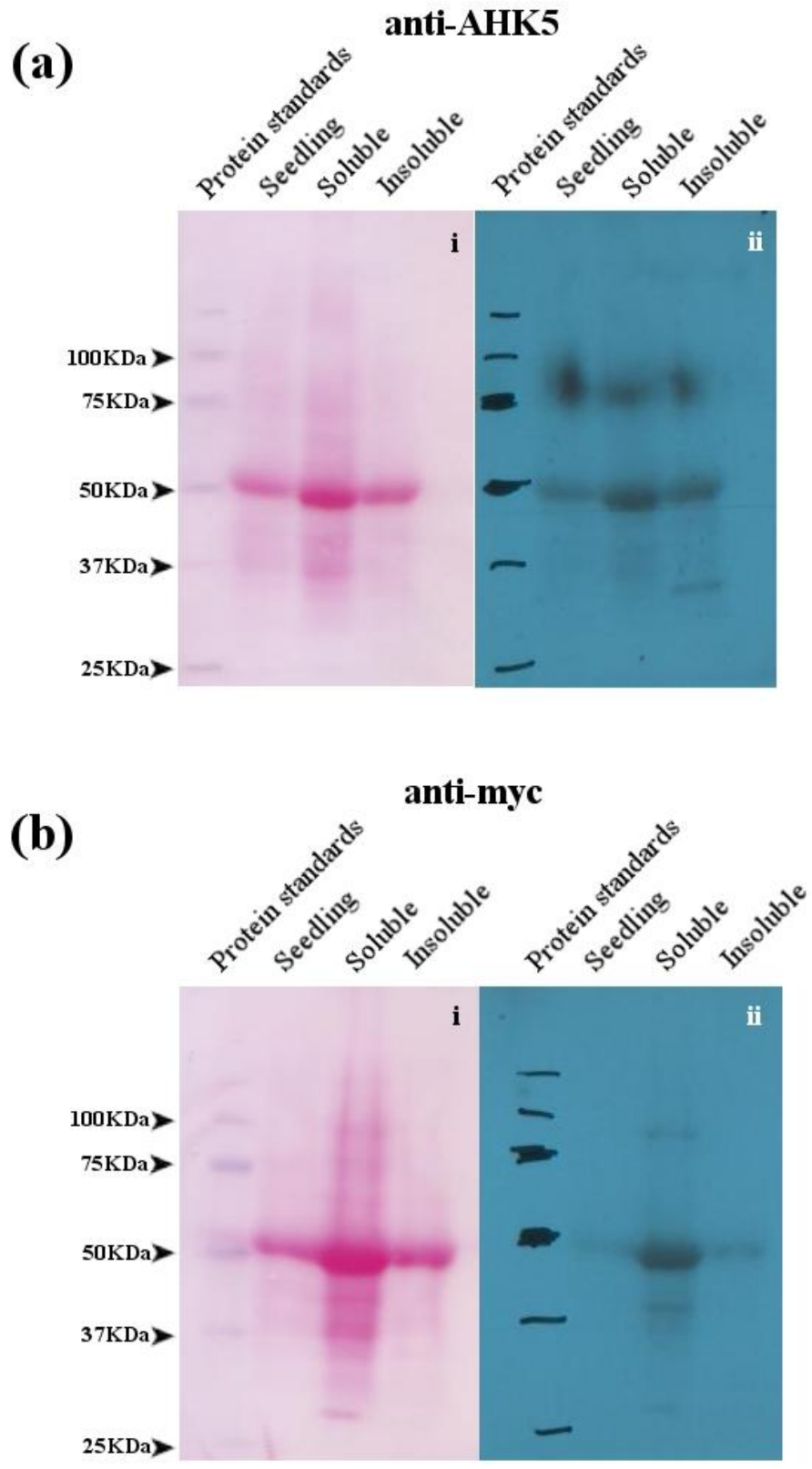


Figure 7.5 Western blot of proteins extracted from 18 day old *P_{35S}-AHK5/ahk5-3* seedlings separated into soluble and insoluble fractions. 'Seedlings' refers to total crude protein extract. The membranes were stained with Ponceau S to confirm transfer of proteins (i) and probed with either anti-AHK5 (a) or anti-myc (b) antibodies to visualise cross-reacting proteins (ii).

In total, nine proteins were excised for analysis by LC-MS/MS, seven from the soluble fraction and two from the insoluble fraction. Of these proteins, identities were obtained for only four of these proteins using the MASCOT algorithm, none of which included proteins from the insoluble fraction. The proteins for which identities were obtained were phospholipase D α1 (At3g15730), catalase 3 (At1g20620), phosphoglycerate kinase (At3g12780) and fructose-bisphosphate aldolase (At2g21330). Ribulose 1, 5-bisphosphate oxygenase (RuBisCO) large subunit (ATCG00490), a common contaminant, was also identified in the band containing catalase 3. Table 7.1 summaries the identities for each excised band identified by MASCOT.

Table 7.1 Identification of proteins obtained from TAP purification of proteins extracted from 18 day old *P_{35S}-AHK5/ahk5-3* seedlings analyses by LC-MS/MS and matched using the MASCOT algorithm. Bands 1-7 were cytosolic proteins and bands 8-9 were membrane proteins. See Appendix IX for peptide sequences matched by MASCOT.

Band Number	Approx. MW on gel (KDa)	Protein identified by MASCOT	MW of identified protein (KDa)	Number of peptides matched	Score
1	100	Phospholipase D α1 (At3g15730)	92	1	69
2	75	-	-	-	-
3	60	Catalase 3 (At1g20620)	57	6	351
		RuBisCO (ATCG00490)	53	4	115
4	50	Phosphoglycerate kinase (At3g12780)	50	2	104
5	40	Fructose-bisphosphate aldolase (At2g21330)	43	2	110
6	37	-	-	-	-
7	30	-	-	-	-
8	40	-	-	-	-
9	50	-	-	-	-

The TAPa-AHK5 protein was not identified in any of the bands recovered for LC-MS/MS analysis. Possible reasons for this include:

- Loss/degradation of proteins during the separation of the proteins into soluble and insoluble fractions and subsequent concentration by acetone precipitation
- Insufficient cleavage of bound proteins from IgG beads
- Failure of proteins to elute from Ni-NTA beads

As such, another TAP procedure was repeated with 15g of 18 day old *P_{35S}-AHK5/ahk5-3* seedling material with the protocol modified by:

- Concentration of total proteins extracted by ultrafiltration without separation into soluble and insoluble fractions
- Increasing incubation with the 3C protease from 1h to overnight
- Increasing imidazole concentration in the final buffer used to elute proteins from Ni-NTA beads from 50mM to 250mM.

SDS-PAGE analysis of the final fraction obtained from TAP purification of total protein extract preformed with the above modifications revealed the presence of two bands, one migrating to a size of slightly larger than the 53KDa marker and another migrating to a size just below the 53KDa marker (Figure 7.6). One of these bands was identified as the RuBisCo large subunit and the other band was found to contain two proteins: RuBisCO activase and phosphoglycerate kinase. Table 7.2 summarises the proteins identified.

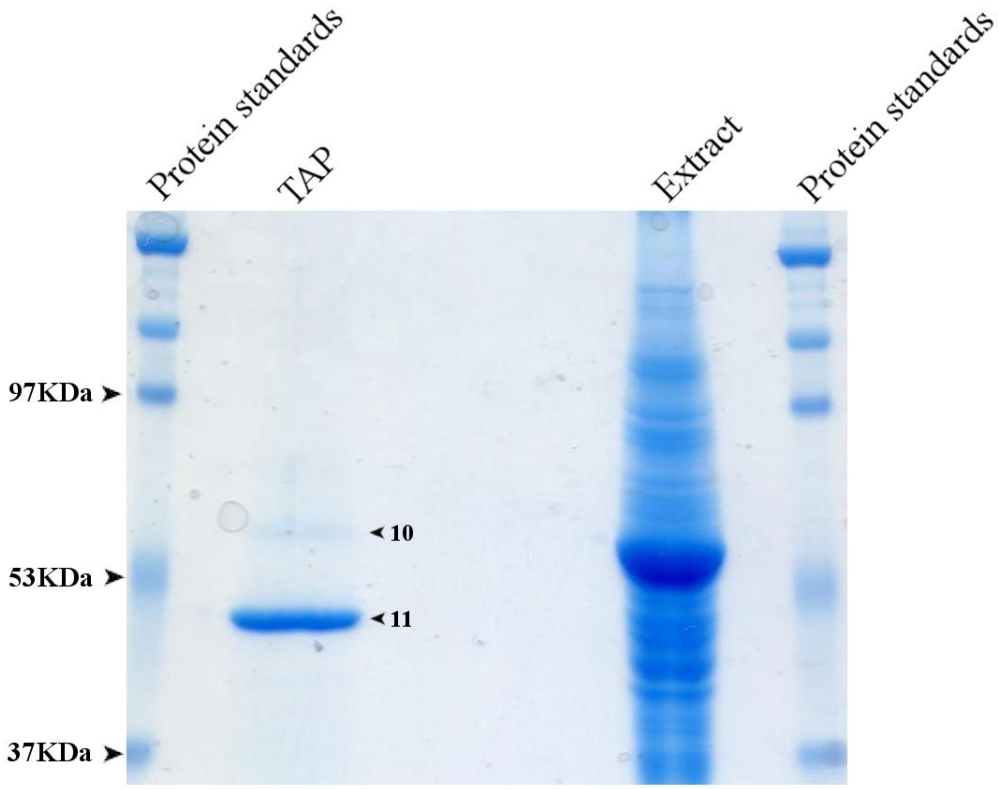


Figure 7.6 SDS-PAGE of proteins obtained from TAP purification of total protein extracts from 15g of 18 day old *P_{35S}-AHK5/ahk5-3* seedling material with modifications. Modifications to the TAP procedure are described in the text. 'TAP' refers to the final fraction obtained (16% of fraction loaded) and 'Extract' refers to the proteins extracted from seedling material and concentrated by ultrafiltration before being subjected to the TAP procedure (0.2% of extract loaded). The numbered arrowheads indicate bands excised for analysis by LC-MS/MS.

Table 7.2 Identification of proteins obtained from TAP purification of proteins extracted from 18 day old *P_{35S}-AHK5/ahk5-3* seedlings analysed by LC-MS/MS and matched using the MASCOT algorithm. See Appendix X for peptide sequences matched by MASCOT.

Band Number	Approx. MW on gel (KDa)	Protein identified by MASCOT	MW of identified protein (KDa)	Number of peptides matched	Score
10	>53KDa	RuBisCO (ATCG00490)	53	6	155
11	<53KDa	Rubisco activase (At2g39730)	52	4	56
		Phosphoglycerate kinase (At3g12780)	50	2	46

7.4 Discussion

In studying the physiological role of a protein for which function is unknown, identification of interacting partners may provide valuable insight into the mechanism by which the protein functions. In this study, the method of Tandem-Affinity Purification (TAP) was used to investigate protein interactors of AHK5. This method was chosen as interacting proteins are isolated under native conditions and the purification of proteins is not dependent on knowledge of their functions. In addition, the two-step purification eliminates most non-specific proteins, reducing complexity of the sample for downstream identification of proteins by mass spectrometry (Xu et al., 2010).

As a member of the TCS in which the functions of the components are highly conserved between species, AHK5 is expected to interact with other members of the TCS, such as HPt-domain containing proteins and ARRs. Previous experimental data suggests that AHK5 may interact with AHP1, AHP2, AHP5 and ARR4, whereas prediction of interactions using an *in silico* method provided a list of 11 possible interactors which included other TCS HKs (AHK4/CRE1/WOL, ETR2 and AHK5 itself) and downstream AHPs (AHP1, AHP2 and the pseudo-AHP AHP6). In addition, non-TCS proteins were also identified which were classed as kinases (NLP1 and MAP3K delta 4) and as functioning in DNA mis-match repair (MLH1 and PMS1). It was expected that TAP purification of AHK5 from a line expressing a TAPa-AHK5 fusion protein (*P_{35S}-AHK5/ahk5-3*) would result in the identification of some of these proteins, or proteins with similar functions.

7.4.1 *Proteins identified from TAP purification of* P_{35S}-AHK5/ahk5-3 *seedling material*

AHK5 does not contain any transmembrane domains and is predicted to reside in the cytosol, but was shown to localise to both the plasma membrane and the cytoplasm (Desikan et al., 2008). Since it is possible that the interactors of AHK5 may depend on the cellular localisation of the HK, proteins extracted from *P_{35S}-AHK5/ahk5-3* were separated into soluble and insoluble fractions and subjected to the TAP protocol separately. To visualise the proteins obtained from the TAP purifications, the final fraction which should contain the TAPa-tagged protein and any interacting proteins were subjected to SDS-PAGE. Nine bands were then selected for in-gel trypsin digestion to generate peptides for protein identification by LC-MS/MS. Of these nine bands (seven soluble and two insoluble), protein identities were obtained for four, all from TAP purification of soluble proteins. These proteins were

phospholipase Dα1 (At3g15730), catalase 3 (At1g20620), phosphoglycerate kinase (At3g12780) and fructose-bisphosphate aldolase (At2g21330). In addition to the identification of catalase 3 in the band of approximately 60KDa, the Ribulose 1, 5-bisphosphate oxygenase (RuBisCO) large subunit (ATCG00490) was also identified. Of these five proteins, phosphoglycerate kinase and RuBisCo have previously been identified as common contaminating proteins obtained from the TAP procedure (Rohila et al., 2006; Van Leene et al., 2008; Rohila et al., 2009).

From the results of this study, AHK5 was implicated in responses to both salt and drought stress (see Chapter 4) and was previously shown to negatively regulate ABA/ethylene inhibition of root growth (Iwama et al., 2007). That phospholipase D α1 and catalase 3 were identified are interesting given the link between phospholipases and catalases with the ABA and salt signalling pathways, respectively. Although no members of the TCS were identified here, which AHK5 as a histidine kinase would be expected to interact with, AHK5 does possess two coiled coil domains at its N-terminus which may act to mediate interactions with non-TCS proteins.

Members of the phospholipase D (PLD) enzyme family are known to play important roles in stress signalling and PLDs have been shown to function in ABA/drought stress-induced stomatal closure in addition to resistance to salinity stress (Jacob et al., 1999; Wang, 2002; Zhang et al., 2004; Bargmann et al., 2009). PLD activity leads to the hydrolysis of structural phospholipids to produce phosphatidic acid (PA) which acts as a signalling molecule (Wang, 2002). Interestingly, PA has been shown to interact with the PPC2 phosphatase ABI1, a negative regulator of ABA signalling (Zhang et al., 2004). In the presence of ABA, PA levels increase through the action of PLDα1 and interaction of PA with ABI1 relieves repression on ABA signalling in response to drought stress (Zhang et al., 2004). Increased responsiveness to ABA in plants over-expressing PLDα1 suggests this enzyme has a role in modulating ABA signalling (Sang et al., 2001). PLDα1 activity was also shown to promote resistance to salinity stress, which was linked to levels of PA production (Bargmann et al., 2009). Modulation of PLDα1 by AHK5 under salinity and drought stress is thus conceivable.

Catalase 3 (CAT3), which catalyses the detoxification of H_2O_2, was shown to interact with the serine/threonine kinase SOS2 of the salt signalling pathway (Verslues et al., 2007). It was hypothesised that the interaction of CAT3 with SOS2 mediates interaction of SOS2 with redox-sensitive proteins through the local detoxification of H_2O_2 (Verslues et al., 2007). It is

possible that CAT3 may also mediate oxidative modification of AHK5 to modulate the function of this histidine kinase in response to salt stress as oxidative modification of AHK5 *in vitro* by H_2O_2 has been observed (R. Desikan, personal communication), although the relevance of this modification to the function of this protein remains to be determined.

The significance of fructose-bisphosphate and aldolase phosphoglycerate kinase, both of which are glycolytic enzymes found in the mitochondria and chloroplasts, is not apparent. Whether or not AHK5 would form biologically relevant interactions with these enzymes is uncertain. It has been noted that proteins involved in metabolic processes are frequently identified in protein purification due to their abundance over regulatory proteins which are mostly expressed at low levels (such as AHK5) suggesting that these proteins may be contaminants (Rose et al., 2004; Van Leene et al., 2008).

Although a band of approximately the same size as that predicted for TAPa-AHK5 (122KDa) was detected in the soluble fraction by immunoblot analysis using anti-myc antibody, TAPa-AHK5 was not identified in this band or any of the other bands by LC-MS/MS. It is possible that recovery of TAPa-AHK5 was too low for detection by LC-MS/MS or that the tryptic digest did not work efficiently for this protein. One problem associated with proteins of low abundance is that they appear as false negatives and the identification of more abundant contaminants within the sample over these proteins (Van Leene et al., 2008). In an attempt to improve recovery, the TAP procedure was repeated with slight modifications. To reduce the loss of proteins through increased processing, the proteins were not separated into soluble and insoluble fractions. Also, in the first attempt of the TAP procedure, the proteins were concentrated using acetone precipitation; it has been noted that ultrafiltration of proteins results in better recovery of proteins and was therefore used to concentrate the protein extract used for the second attempt (Jiang et al., 2004). The duration of the 3C protease cleavage step was also increased from one hour to an overnight incubation to maximise release of tagged protein from IgG beads and imidazole concentration of the final elution buffer was increased from 50mM to 250mM to maximise elution of TAPa-AHK5 from Ni-NTA beads. The final fraction was analysed by SDS-PAGE and two bands of between 50 and 60KDa were seen, neither one of which were close to the size of TAPa-AHK5. The proteins in these two bands were subsequently identified as RuBisCO and RuBisCO activase, both of which are considered contaminants (Rohila et al., 2006; Van Leene et al., 2008; Rohila et al., 2009). Phosphoglycerate kinase (At3g12780) was also identified in the band containing RuBisCO activase.

That the banding patterns of proteins and the proteins identified in the final fraction differed between the two repeated TAP procedures (except for the contaminant RuBisCO and phosphoglycerate kinase) and that TAPa-AHK5 was not identified on either occasions suggests that the proteins identified here are possibly not interactors of AHK5. However, it is possible that the change in the profile of proteins identified from the two purifications was due to the altered conditions used. To determine whether proteins identified are likely to be true interactors or contaminating proteins would require a parallel mock TAP purification using proteins extracted from a plant line of the same genetic background not expressing TAPa-AHK5. Since only TAPa-AHK5 and interacting proteins should be obtained in the final fraction of the procedure, any proteins obtained which are common to the mock purification can be eliminated as non-specific interactors/contaminants.

7.4.2 *Improving recovery of AHK5 interactors*

A problem that is associated with purification of protein complexes is obtaining enough material for downstream analysis and the success of the protocol therefore depends on the abundance of the protein complex isolated (Van Leene et al., 2008). In the first study using stably transformed plant lines over-expressing a TAPa-tagged protein (CSN3-TAPa), Rubio et al. (2005) combined the final fraction of six independent samples to provide enough protein for identification by mass spectrometry.

To increase the expression of the TAPa-AHK5 protein, an over-expressor line of this construct was used in an *ahk5* null background. However, it has previously been noted that even under the control of a constitutive promoter, the expression levels of the tagged protein varies depending on the nature of the protein (Rubio et al., 2005; Van Leene et al., 2007). It is possible that the line used here did not express TAPa-AHK5 at a level sufficient enough for detection of the tagged protein and its interacting partners by SDS-PAGE and mass spectrometry. One possibility to explain low expression of the tagged protein is interference by the TAPa tag itself. As the TAPa tag is very large at a size of 33KDa, the position of the tag may have interfered with the structure and/or function of AHK5. It has been noted that simply changing the position of the tag from one terminus to the other may improve the expression/function of the tagged protein (Puig et al., 2001; Terpe, 2003). In this study, a C-terminal tagged-protein was used; although AHK5 does not possess an N-terminal transmembrane sensing domain typical of sensor HKs, the N-terminal does contain two coiled coil domains which have been suggested to mediate interactions with proteins in the

cytoplasm (Hwang et al., 2002). Therefore, tagging of the N-terminal was not deemed suitable in this case.

In this study, proteins were separated by SDS-PAGE and gel bands extracted for analysis by mass spectrometry. The limitation of this approach is that the amount of sample which can be loaded onto a standard SDS gel and that not all proteins may be resolved or will be visible, problems which are exacerbated in the case of low abundance proteins. In such cases, an in-solution digestion rather than the in-gel digestion used here may increase the probability of identification of proteins which are expressed at low levels.

One of the main features of the TAP protocol is the suitability of the final sample for mass spectrometry analysis. Although the two purification steps involved in the TAP protocol reduces the amount of contaminating proteins, the greater level of sample processing leads to lower recovery of the tagged protein complex as each step is associated with loss of protein and increases probability of complex dissociation (Rose et al., 2004; Morsy et al., 2008). It is possible that the TAPa-AHK5 protein and its interacting partners were lost during the purification procedure.

7.5 Conclusions

In this study, a TAP purification approach was used in an attempt to identify AHK5 interacting proteins. Although potential interactors were identified by LC-MS/MS, these await confirmation. Improvement of the TAP procedure in the future would involve performing a large scale purification in order to obtain enough of the TAPa-AHK5 protein for identification by LC-MS/MS. Demonstration of direct interaction with AHK5 *in vivo* by methods such as bimolecular fluorescence complementation (BiFC) for *in planta* visualisation of interactions would be required for confirmation of potential AHK5 protein partners identified.

Chapter 8:

Final discussion

8 Final discussion

8.1 The histidine kinase AHK5 negatively regulates salt and drought resistance and contributes towards resistance against *Pst*DC3000 and *B. cinerea*

Prior to this study, AHK5 was shown to act as a negative regulator of ABA/ethylene-induced inhibition of root elongation (Iwama et al., 2007) and in pathogen-, darkness- and ethylene-induced stomatal closure via ROS production (Desikan et al., 2008). Here, the role of AHK5 in abiotic and biotic stress signalling has been shown to extend to negative regulation of salt and drought stress tolerance and positive regulation of resistance towards both biotrophic and necrotrophic pathogens. In nature, plants are exposed to numerous stresses and stimuli which occur concurrently and in different combinations. It is therefore apparent that identification of key integrators of multiple signalling pathways and the mechanism by which they fulfil this role is of interest in the race to develop more robust and stress resistant crops.

8.2 Does AHK5 modulate hormone responses to multiple stimuli?

8.2.1 *Abiotic stress*

The signalling pathways leading to salt and drought tolerance show extensive overlap as both stresses result in water deficit. In the case of salt stress, the high ionic content of the soil results in the soil having a higher water potential than the roots, preventing water uptake, whereas lack of water available in the soil leads to water deficit in drought stress. The plant hormone ABA mediates responses to water deficit in both salt and drought stress (Zhu, 2002; Zhang et al., 2006). In seedlings, root elongation of the *ahk5-1* mutant was greater compared to wild-type in the presence of salt. In vegetative tissue, resistance manifested as greater gain in fresh weight. That no phenotypic difference in response to osmotic stress was found between wild-type and *ahk5-1* mutant seedlings would suggest that the increased resistance of the *ahk5-1* mutant was largely towards the ionic component of salt stress. Plant responses to the ionic component of salt stress are largely under the control of the SOS-pathway (Mahajan et al., 2008), suggesting AHK5 may interact with this pathway under conditions of high salinity to modulate salt responses. In addition to the SOS pathway, the vacuolar Na^+/H^+ antiporters AtNHX also play a role in salt tolerance, in which AtNHX1 and AtNHX2 are induced by both ABA and high salinity and AtNHX5 by high salinity (Yokoi et al., 2002).

In response to drought stress, the *ahk5-1* mutant displayed visibly less wilting and greater gain in fresh weight and higher water content compared to wild-type plants. This suggests that AHK5 negatively regulates resistance towards both salt and drought stress. The greater fresh weight gain in the *ahk5-1* mutant in response to both drought and salinity would suggest reduction of water loss, perhaps through reduction of transpiration/increased stomatal closure triggered by increased ABA biosynthesis or ABA hypersensitivity. Given that the *ahk5-1* mutant was previously shown to be altered in stomatal responses to various stimuli (Desikan et al., 2008), it is possible that AHK5 may also be involved in stomatal responses towards drought and salinity stress. Previously, the *ahk5-1* mutant was shown to be unaffected in ABA-mediated stomatal closure, suggesting stomatal phenotypes in this mutant may not be ABA-related (Desikan et al., 2008). However, that the *ahk5-1* mutant is not affected in stomatal closure in response to exogenous ABA does not rule an effect of the *ahk5-1* mutation upstream of ABA production; whether or not guard cells of the *ahk5-1* mutant are affected in perception of stimulus or ABA biosynthesis in response to stimuli as opposed to perception and response to ABA itself is not known. Basal levels of ABA in *ahk5-1* mutant plants under control conditions in this study were similar to that found in wild-type plants (62.2 ng $gDW^{-1}$and 62.0 ng gDW^{-1}, for *ahk5-1* and wild-type Col-0 plants, respectively). Therefore any differences in ABA production in the *ahk5-1* mutant compared to wild-type plants in response to stimuli is more likely to be due to alterations in stimulus-induced ABA biosynthesis rather than a defect in endogenous ABA biosynthesis *per se*.

Interestingly, using the PLACE interface for identification of plant *cis*-acting regulatory DNA elements (Higo et al., 1999), ABA-responsive *cis*-elements were identified in the 5' UTR of *AHK5*, such as the ABRELATERD1 motif which is found upstream of drought responsive genes (Yazaki et al., 2004). If ABA up-regulates *AHK5* expression and AHK5 negatively regulates drought and salinity stress tolerance as suggested here, it is possible that AHK5 acts to inhibit ABA biosynthesis in response to stimuli as part of a negative feedback loop. In this scenario, loss of AHK5 function would relieve repression of ABA biosynthesis leading to increased ABA levels and increased tolerance towards these two stresses.

In roots however, loss of AHK5 function resulted in altered response to ABA/ethylene-induced inhibition of root growth (Iwama et al., 2007), suggesting that AHK5 can also act downstream of ABA. It is possible that the position of AHK5 function in ABA signalling may be dependent upon the tissue type in question. Further investigation into the stomatal responses and ABA production of the *ahk5-1* mutant towards drought and salinity stress may

shed more light onto the function of AHK5 in mediating responses to these two stresses and its role in ABA signalling.

8.2.2 *Biotic stress*

With respect to biotic stress, AHK5 was found to have a role in defence responses towards the hemi-biotrophic bacterial pathogen *Pseudomonas syringae* pv. *tomato* DC3000 and the necrotrophic fungal pathogen *Botrytis cinerea.* Interestingly, disruption of AHK5 function led to increased susceptibility to both *Pst*DC3000 and *B. cinerea.* As discussed earlier, due to the contrasting lifestyles of these pathogens, different defence mechanisms are effective against biotrophs and necrotrophs. Whereas cell death is effective in preventing spread of infection against biotrophs and is used in the form of the hypersensitive response (HR), this defence response enhances rather than suppresses growth of necrotrophs which triggers cell death as a virulence mechanism. However, as resistance mechanisms against virulent *Pst*DC3000 does not involve cell death and no difference in cell death was observed in the *ahk5-1* mutant compared to wild-type plants in response to the avirulent *Pst*DC3000(*avrRpm1*) strain, the increased susceptibility of the *ahk5-1* mutant to infection with *B. cinerea* does not appear to be linked to the HR.

Differences in the defence responses utilised against biotrophs and necrotrophs is reflected in the observation that salicylic acid (SA) mediated defences are associated with resistance against biotrophs whereas jasmonic acid (JA) and ethylene mediated responses are linked to infection with necrotrophs (Glazebrook, 2005). As such, antagonism between SA and JA/ethylene responses can occur and previous studies have shown a general trend in which increased SA signalling is required for resistance to biotrophs but increases susceptibility to necrotrophs and *vice versa.* For example, exogenous application of SA to *A. thaliana* leaves increased lesion size in response to the necrotroph *Alternaria brassicicola* and suppressed JA-responsive *PDF1.2* expression (Spoel et al., 2007). In addition, inoculation of leaves with *Pst*DC3000 prior to infection with *A. brassicicola* increased susceptibility (Spoel et al., 2007). On the other hand, the SA-signalling *npr1-1* mutant and the SA-deficient *nahG* transgenic line show increased susceptibility to the biotrophic oomycetes *H. arabidopsidis* but not in response to *A. brassicicola* or *B. cinerea* compared to wild-type plants (Thomma et al., 1998). In the JA-insensitive *coi1-1* mutant, the opposite was seen, with this mutant more susceptible to necrotrophs (*A. brassicicola* and *B. cinerea*) but unaffected in response to the biotroph *H. arabidopsidis* (Thomma et al., 1998).

Thus if AHK5 participates in a specific hormone signalling pathway, it would be expected that the effect of the *ahk5-1* mutation on resistance towards *Pst*DC3000 would have an opposite or no effect on resistance towards *B. cinerea.* This does not appear to be the case here. From measurement of hormone levels in response to surface inoculation with *Pst*DC3000, it was found that in general whereas the pattern of SA, ABA and JA accumulation was similar between wild-type and *ahk5-1* mutant plants, the absolute levels of hormones was consistently lower in mutant plants in response to infection. In the *A. thaliana*-*Pst*DC3000 interaction, the bacterium is known to stimulate ABA biosynthesis as a virulence mechanism to suppress SA signalling/defences, with the ABA-deficient *aao3* mutant less sensitive to infection with *Pst*DC3000 and exhibiting higher accumulation of SA on infection (de Torres Zabala et al., 2009), whereas over-expression of the ABA biosynthetic genes *NCED3* and *NCED5* resulted in a tenfold increase in the *in planta* growth of virulent *P. syringae* pv. maculicola ES4326 (Fan et al., 2009). Evidence also indicates that *Pst*DC3000 manipulates JA signalling to facilitate infection (Kloek et al., 2001; Ishiga et al., 2010). As levels of SA, JA and ABA measured here in response to *Pst*DC3000 surface inoculation were all reduced in the *ahk5-1*mutant compared to wild-type tissue, this suggests that AHK5 may act to integrate multiple signalling pathways rather than participating in a single signalling pathway. Thus a general defect in hormone accumulation is more likely to be the cause of the increased susceptibility seen in the *ahk5-1* mutant towards both *Pst*DC3000 and *B. cinerea*. In this situation, AHK5 may be acting at the point of stimulus perception/upstream of activation of hormone biosynthesis. In corroboration with this hypothesis, stomata of the *ahk5-1* mutant were found to be unresponsive to the presence of bacteria or the bacterial PAMP flg22 (Desikan et al., 2008), suggesting a defect in pathogen perception/activation of downstream signalling events. Hormone measurements in response to infection with *B. cinerea* may contribute to providing a clearer picture of the role of AHK5 in hormone production in response to pathogens.

8.3 AHK5 as an integrator of multiple stimuli

Thus AHK5 mediates signalling in response to both abiotic and biotic stresses but how does this protein mediate responses to multiple stimuli? Common to the stimuli in which AHK5 was shown to have a function in is the involvement of the ABA pathways in the outcome of the interaction; the role of ABA in mediating salt and drought stress resistance is well documented (Zhu, 2002; Zhang et al., 2006) and has also previously been shown to promote

susceptibility towards both *Pst*DC3000 and *B. cinerea* (Audenaert et al., 2002; Mohr and Cahill, 2003; Asselbergh and Hofte, 2007; de Torres Zabala et al., 2007; de Torres Zabala et al., 2009; Fan et al., 2009; Curvers et al., 2010). Thus it is tempting to hypothesise that AHK5 acts to suppress ABA synthesis, the loss of function of which leads to increased ABA biosynthesis and responses, resulting in greater tolerance to salt and drought stress but increased susceptibility towards *Pst*DC3000 and *B. cinerea.*

However, the phenotypes observed in this study cannot be fully explained by modulation of ABA signalling alone. It does not, for example, explain why the *ahk5-1* mutant is more susceptible to infection with *Pst*DC3000 and yet shows lower levels of ABA (and other hormones) compared to wild-type plants. Thus, although AHK5 may participate in ABA signalling, the evidence here suggests that the function of AHK5 in stress responses extends beyond that of ABA. From the evidence presented, it is hypothesised that AHK5 has opposing functions in abiotic and biotic stress responses; in response to salinity and drought stress, AHK5 may negatively regulate tolerance upstream of ABA biosynthesis, whereas in response to *Pst*DC3000 and *B. cinerea,* AHK5 may positively regulate resistance by acting upstream of hormone responses (Figure 8.1).

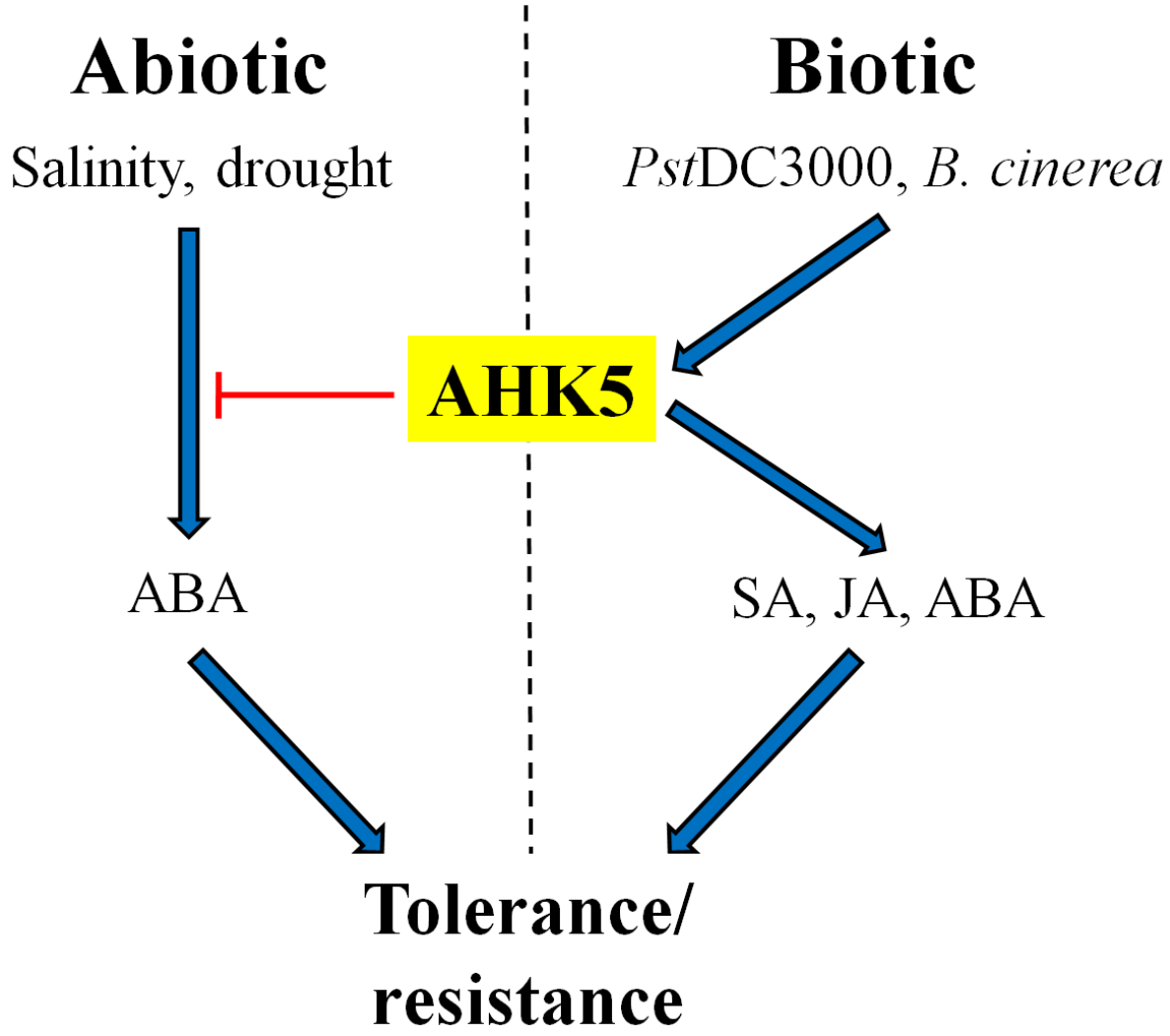


Figure 8.1 Schematic showing the hypothesised opposing functions of AHK5 in tolerance to abiotic stress and resistance towards pathogen infection. In response to salinity and drought stress, ABA positively regulates tolerance to these stresses; AHK5 may act to negatively regulate this tolerance by inhibiting ABA biosynthesis. In response to infection with *Pst*DC3000 and *B. cinerea,* AHK5 may act upstream of hormone responses to initiate hormone biosynthesis to activate resistance responses.

In addition to differences in hormone levels, a novel metabolite was found in *ahk5-1* leaf tissue, the accumulation of which was not dependent on infection with *Pst*DC3000. As this metabolite was seen to increase over the time course of the experiment to similar levels in both mock-inoculated and *Pst*DC3000 infected plants, it is possible that this increase was due to the high humidity conditions under which the plants were kept. If and how this metabolite contributes to the increased susceptibility of the *ahk5-1* mutant towards infection with *Pst*CDC3000 is not clear. As the infection assay with *B. cinerea* was also under conditions of high humidity, it is possible that this novel metabolite may also increase during the course of this experiment. In this study, the *ahk5-1* mutant was shown to support accelerated and

greater growth of *B. cinerea* and was attenuated in ROS production in response to infection compared to wild-type plants. Whether or not this metabolite contributes towards the increased susceptibility of the *ahk5-1* mutant towards this necrotroph, or indeed *Pst*DC3000, remains to be determined.

8.4 ROS – the missing link?

In addition to modulation of hormone responses, the evidence here also suggests AHK5 function in plant responses to multiple stresses may also be through regulation of ROS production and responses. In stomata, AHK5 was found to function both upstream and downstream of ROS in mediating stomatal closure (Desikan et al., 2008). As ROS are produced in response to many stimuli, including those tested in this study, a role for AHK5 in modulating ROS signalling may also explain how one protein can mediate multiple responses. ROS production was attenuated in the *ahk5-1* mutant in response to infection with *B. cinerea* and the incompatible strain of *Pst*DC3000 carrying the avirulence gene *avrRpm1* and also in response to salinity. Coupled with the previously observed defect in ROS responsiveness in *ahk5-1* guard cells and ROS production in response to ethylene, darkness and bacterial flagellin (Desikan et al., 2008), the evidence suggests a general role of AHK5 in ROS perception and signalling.

An example of a single protein modulating responses to multiple stimuli via redox signalling is provided in the case of DELLA proteins which modulate growth, development rate and stress tolerance in response to necrotrophic and biotrophic pathogens and salt stress (Achard et al., 2006; Achard et al., 2008; Navarro et al., 2008; Smirnoff and Grant, 2008). DELLA proteins act as negative regulators of cell elongation and division in plants, repression of which is relieved in the presence of gibberellins (GA). In *A. thaliana*, there are five genes encoding for DELLA proteins of which GA1 and RGA are most important in DELLA-mediated regulation of plant growth (Achard et al., 2006). In response to high salinity, whereas a quadruple-DELLA mutant was less salt tolerant, constitutive DELLA activity in the *gai* mutant or deficiency in GA production in the *ga1-3* mutant significantly increased survival rate, suggesting DELLA-mediated repression of growth contributes to tolerance to high salinity (Achard et al., 2006). DELLAs were also shown to contribute toward resistance against *B. cinerea* infection (Achard et al., 2008). DELLA function in tolerance against salt stress and infection with *B. cinerea* appears to be linked to the control of ROS production/ accumulation via up-regulation in both transcript and protein levels of the two *Arabidopsis*

Cu/Zn SODs CDS1 and CDS2 suggesting a general function for DELLAs in mediating stress responses via control of ROS levels (Achard et al., 2008).

In addition to alteration of ROS levels, DELLAs also mediate hormone responses and is required for ABA-mediated inhibition of root growth, ethylene-induced delay in flowering and JA and SA signalling in response to pathogen infection (Achard et al., 2006; Navarro et al., 2008). More recently, DELLAs were shown to interact with the JA signalling repressor JAZ1, preventing interaction of this inhibitor with the downstream MYC2 transcription factor, relieving repression of JA-responsive gene transcription by JAZ1 (Hou et al., 2010). Thus DELLAs function in responses to both abiotic and biotic stresses through modulation of both ROS and hormone signalling. In this study, AHK5 was also found to function in response to pathogens and abiotic stress and to modulate hormone responses and ROS production.

Another example of a single gene functioning in response to multiple stimuli is the R2R3MYB transcription factor BOS1 (Botrytis susceptible 1) which mediates responses to both biotic and abiotic stimuli (Mengiste et al., 2003). A T-DNA loss-of-function *bos1* mutant was found to be more susceptible to infection with the necrotrophs *B. cinerea* and *A. brassicicola* and presented accelerated symptom development in response to the biotrophs *Pst*DC3000 and *H. arabidopsidis* in addition to increased susceptibility towards salt and drought stress (Mengiste et al., 2003). These observations are very similar to the finding of this study in which the *ahk5-1* mutant was also found to be affected in response to *B. cinerea*, *Pst*DC3000, salinity and drought stress, although AHK5 seems to have opposing contributions to resistance against abiotic and biotic stresses. The *bos1* mutant was also found to be more sensitive to oxidative stress and up-regulation of the *BOS1* transcript in response to *B. cinerea* infection was impaired in the *coi1* mutant suggesting roles for *BOS1* in both ROS and hormone (at least JA) signalling (Mengiste et al., 2003).

Thus the control of plant responses to multiple stimuli mediated by a single gene product is not a novel phenomenon and has been observed previously. Although it is evident that a single protein can act to integrate different signalling pathways and as such contribute to responses to multiple stimuli, the exact mechanism by which this is achieved is not clear.

As previously discussed in Section 1.7, ROS may modify protein structure and function directly through modification of the oxidative state of certain residues, such as cysteine and methionine residues. As ROS is produced in response to many stresses and stimuli, it is

possible that the ability of AHK5 to interact with other proteins is modified in response to different conditions by ROS. *In vitro* modification of AHK5 by H_2O_2 suggests that control of AHK5 activity by ROS is a possibility (R. Desikan, personal communication). Another level of complexity which may introduce some specificity in the activation of AHK5 function is the type, amount and duration of ROS induced by specific stimuli. Different types of ROS may induce different types of modifications to the same target protein and thus have different effects on the function of that protein. For example, whereas H_2O_2 reacts with cysteine residues in proteins, superoxide ($O_2^{\cdot -}$) reacts mostly with Fe-S centres of proteins (Moller et al., 2007; Rinalducci et al., 2008). The type of modification may affect the proteins in which AHK5 is able to interact with. Conversely, modification of AHK5-interacting proteins may be of equal importance in determining the signalling outcomes. Taking these factors into consideration, the control of AHK5 activity in response to specific and multiple stimuli is conceivable.

8.5 AHK5 may participate in responses to multiple stimuli through interaction with different proteins

The ability of AHK5 to impact on multiple signalling pathways may also lie in its activity as a histidine kinase. As a member of the two-component system (TCS), AHK5 would be predicted to interact with other members of this system. Preliminary data suggests that AHK5 can interact with AHPs which mediate phosphotransfer from the stimulus-activated HK to downstream ARRs which in turn activate responses to the stimuli (Stock et al., 2000; Grefen and Harter, 2004; Romir et al., 2009). Therefore, AHK5 may modulate stress responses through activation of downstream ARRs. In support of this theory, ARRs which function in response to pathogen infection and salinity stress have been found. The type-B ARR ARR2 has been shown to interact with the SA-responsive transcription factor TGA3 to activate resistance against *Pst*DC3000 (Choi et al., 2010) and also functions in the mediation of ethylene and H_2O_2-induced stomatal closure (Desikan et al., 2006). Interestingly, the predicted AHK5 interactor AHK4/CRE1/WOL interacts with ARR2 through AHP1 and AHP2 (Dortay et al., 2006; Dortay et al., 2008), providing a putative link between AHK5 function and resistance against *Pst*DC3000. Additionally, ARR1 and ARR12 (also type-B ARRs) suppress expression of AtHKT1, a high-affinity K^+ transporter involved in limiting accumulation of Na^+ in plant shoots (Mason et al., 2010). Interestingly, the presence of an ARR1-binding element was found upstream of AHK5, perhaps providing a mechanism

through which *AHK5* transcription is induced by high salinity as part of a negative regulatory feedback loop on salt tolerance responses.

It is also possible that the histidine kinase activity of AHK5, in addition to functioning as part of the TCS, may also control the interaction of AHK5 with signalling partners. For example, the HK and ethylene receptor ETR1 forms heterodimers with other proteins, including the ethylene receptor EIN2 and this interaction is dependent on the phosphorylation state of the conserved histidine residue in the HK domain of ETR1 (Bisson and Groth, 2010). In the autophosphorylated state, affinity of ETR1 for EIN2 is low whereas in the unphosphorylated state, increased interaction between ETR1 and EIN2 is observed (Bisson and Groth, 2010).

The evidence presented in this study suggests that AHK5 may act to integrate responses to different stresses, but the mechanisms by which it does so remains to be determined. A key step towards this end would be to identify AHK5 interactors and to investigate further the role of these interactors in stress responses. This would provide valuable insight into the signalling pathways into which AHK5 is integrated.

In silico prediction of AHK5 interactors indicated that AHK5 may form homodimers and interact with other HKs (EIN4, ETR2 and AHK4/CRE/WOL), AHPs (AHP1, AHP2, AHP6), a serine/threonine kinase (NLP1, At5g58140), a MAPKKK (At4g23050) and two proteins involved in DNA-mismatch repair (PMS1, At4g02460 and MLH1, At4g09140). As discussed earlier (Section 1.8.2), AHK1/AtHK1, AHK2, AHK3 and AHK4/CRE/WOL have been implicated in the mediation of plant responses towards salinity and drought stress; interestingly, in addition to being predicted as an AHK5 interactor, AHP2 has previously been shown to interact with AHK4/CRE1/WOL in a yeast two hybrid screen (Urao et al., 2000b). Additionally, AHP5 which interacts with AHK5 (R. Desikan, personal communication) is also known to interact with AHK4/CRE1/WOL (Dortay et al., 2006). Similar to AHK4/CRE1/WOL, AHK5 was found to negatively regulate responses towards salinity and drought stress in this study, suggesting AHK5 function may overlap with that of AHK4/CRE1/WOL, perhaps through activation of common downstream components of the TCS (Tran et al., 2007; Tran et al., 2010). These may include ARRs, such as ARR4 which is part of the AHK5 TCS (R. Desikan, personal communication) and is predicted to interact with AHP2 using the PAIR interface (Higo et al., 1999).

As suggested above, interacting partners of AHK5 may not be limited to those belonging to the TCS. For example, in a yeast two hybrid screen carried out by Dortay et al. (2008)

AHK2, AHK3 and AHK4/CRE1/WOL were found to interact with proteins outside of the TCS, which included proteins involved in developmental and metabolic processes. The HK ETR1 is also known to interact with CTR1, a MAPKKK, suggesting HKs function in cellular signalling pathways outside of the TCS. Unique to AHK5 is the presence of two coiled coil domains at the N-terminus which has been proposed to mediate protein-protein interaction (Hwang et al., 2002) and perhaps enables AHK5 to interact with proteins outside of the TCS.

In this study, identification of AHK5 interacting proteins by tandem-affinity purification (TAP) was attempted using an *ahk5-3* mutant line carrying a TAPa-tagged *AHK5* construct under the control of the CaMV 35S promoter. From two purifications, six different proteins were identified by LC-MS/MS of which three, phospholipase Dα1, catalase 3 and fructose-bisphosphate aldolase may be potential AHK5-interacting proteins. These proteins are interesting as they have been implicated in signalling (phospholipase Dα1) (Zhang et al., 2004; Bargmann et al., 2009), ROS regulation (catalase 3) (Verslues et al., 2007; Mhamdi et al., 2010) and cellular metabolism (fructose-bisphosphate aldolase) (Plaxton, 1996). However, purified TAP-tagged AHK5 was not detected by SDS-PAGE or LC-MS/MS in this study and these identifications are therefore preliminary and require confirmation. The other three proteins identified from the purifications, RuBisCO, RuBisCO activase and phosphoglycerate kinase, were proteins commonly found as contaminants associated with the purification procedure.

8.6 Conclusions and future work

In summary, AHK5 negatively regulates abiotic stress responses and positively contributes to biotic stress defences in response to the stimuli tested here. Thus AHK5 may act to integrate responses to multiple stresses and may do so via a combination of three mechanisms:

- Modulation of hormone production/responses
- Perception of ROS and control of ROS production
- Protein-protein interactions as part of the TCS and with proteins outside of the TCS

These mechanisms are not mutually exclusive and the ability of AHK5 to participate in cellular signalling events at the level of hormones, ROS and protein-protein interactions may be the basis on which AHK5 is able to integrate responses to multiple stimuli. Further work is required to determine the mechanisms by which AHK5 functions in response to individual stresses. Questions arising from this study which remain to be answered include:

1. How does AHK5 affect ion accumulation in response to salt stress?

Initial measurements of ions in whole seedlings in response to salt stress suggest that the increased resistance of the *ahk5-1* mutant is not due to alteration in Na^+ accumulation within the plant. It is possible that AHK5 mediates either the compartmentalisation of Na^+ ions and/ or the distribution of Na^+ in the root and shoots rather than mediating uptake or extrusion of Na^+ by the roots, which may not be reflected in total ion content. Measurement of Na^+ (and K^+) levels separately in roots and shoots may shed light on whether long distance transport of ions is affected in the *ahk5-1* mutant. Fluorescent dyes such as sodium-binding benzofuran isophthalate (SBFI) and CoroNa Green have previously been used to visualise Na^+ accumulation in living cells and organs and may also be useful in providing information on the distribution of Na^+ ions in wild-type and *ahk5-1* plants under salinity stress (Halperin and Lynch, 2003; Park et al., 2009).

2. What is the nature of the unique metabolite found in the *ahk5-1* mutant?

The presence of a unique metabolite found in the *ahk5-1* mutant is intriguing, the identity of which could not be determined by the method of LC-MS/MS used here. This metabolite was noted in *ahk5-1* leaf tissue during hormone measurements in response to infection with *Pst*DC3000 and was found to also be present in non-infected *ahk5-1*control tissue. The metabolite was not found in wild-type tissue. As this metabolite was found at similar levels in both mock-inoculated and infected tissue kept under high humidity, this would suggest that the presence of this metabolite is not dependent on infection. In order to identify this metabolite, the extraction of this metabolite would need to be optimised and LC-MS/MS coupled with a method such as nuclear magnetic resonance (NMR) for identification (Moco et al., 2007).

3. What is the factor triggering early increase in growth of *B. cinerea* on the *ahk5-1* mutant?

B. cinerea growth was noticeably greater at 8hpi on *ahk5-1* mutant leaves compared to growth on wild-type leaves. Although attenuated ROS production was seen in the *ahk5-1* mutant in response to infection with *B. cinerea,* this occured much later (24hpi) than the difference in fungal growth, suggesting a factor other than plant derived ROS triggering this difference, at least in the earlier stages of infection. One possibility is the diffusion of stimulatory factors from the leaf surface into the inoculum droplet which enhances the

growth of the fungus. Analysis of the effect of leaf exudates on the growth of *B. cinerea in vitro* may contribute towards understanding the role of plant factors on fungal growth.

4. What are the AHK5-interacting proteins?

In order to answer this question, the TAP purification method used here will need to be optimised in order to purify enough of the TAPa-tagged AHK5 protein for reliable identification of interacting proteins. This may be achieved by large scale purification. Alternatively, other methods of affinity purification, such as the use of the His-tag commonly used in one-step purifications, may increase the yield of the tagged protein due to the reduced number of steps (Xu et al., 2010). However, increased yield comes at a cost as reduction in sample processing also increases the retention of contaminating/non-specific proteins in the final fraction. Confirmation of interaction with candidate proteins *in planta* by bimolecular fluorescence complementation (BiFC) could also be performed (Walter et al., 2004)

5. What is the function of ABA in AHK5-mediated signalling?

Responses to *Pst*DC3000, *B. cinerea,* drought stress and salinity stress are known to involve ABA signalling. As AHK5 was found to participate in responses towards these stimuli, it is possible that AHK5 mediates part of its effects through ABA. The evidence presented here suggest that AHK5 may act in both ABA-dependent and ABA-independent signalling pathways, thus determining the role of ABA in AHK5 function would be of interest. In this study, hormone measurements were only obtained from plant tissue in response to infection with *Pst*DC3000. Measurements of ABA (and other hormones) in response to *B. cinerea,* drought and salinity stress would give a clearer picture as to how AHK5 modulates hormone responses to different stimuli and whether these responses show a general trend or are stimulus-specific.

6. What is the exact function of ROS in the signal integration pathway – does it affect AHK5 activity or does AHK5 regulate antioxidants to modulate redox levels in plants?

In stomatal guard cells, AHK5 acts upstream of H_2O_2 in response to flg22 and ethylene and downstream of H_2O_2 production in response to flg22, ethylene, NO and darkness (Desikan et al., 2008). Determining the position at which ROS interacts with AHK5 may shed more light on the function of AHK5. AHK5 may possibly regulate ROS accumulation through regulation of cellular levels of antioxidants, as was shown for DELLAs (Achard et al., 2008).

Thus the possible functions of AHK5 in ROS signalling may involve a combination of ROS sensing, stimulation of ROS production and control of ROS accumulation/scavenging. Although AHK5 was previously shown to have HK activity, this was performed in a heterologous system using *E. coli* (Iwama et al., 2007); whether or not AHK5 exhibits HK activity *in planta* in response to stimuli is not known and remains to be determined.

In conclusion, the evidence presented in this study suggests that AHK5 acts to integrate both abiotic and biotic stress signalling. In nature, plants are exposed to many different types of stresses which may occur in parallel; whereas great progress has been made in understanding the role of individual pathways in stress signalling, how these pathways interact to fine-tune and tailor responses to the multitude of stresses which can occur in different combinations is largely unknown. Thus it is clear that in order to better understand plant responses to stress, an integrated approach is required. A step towards this direction is to indentify key proteins which act to regulate responses to multiple stimuli, of which AHK5 is a candidate. Further investigation of the mechanism by which this histidine kinase exerts its effects would provide invaluable insight into the interaction between different signalling pathways and contribute towards the generation of more robust crops resistant to multiple stresses.

Appendices

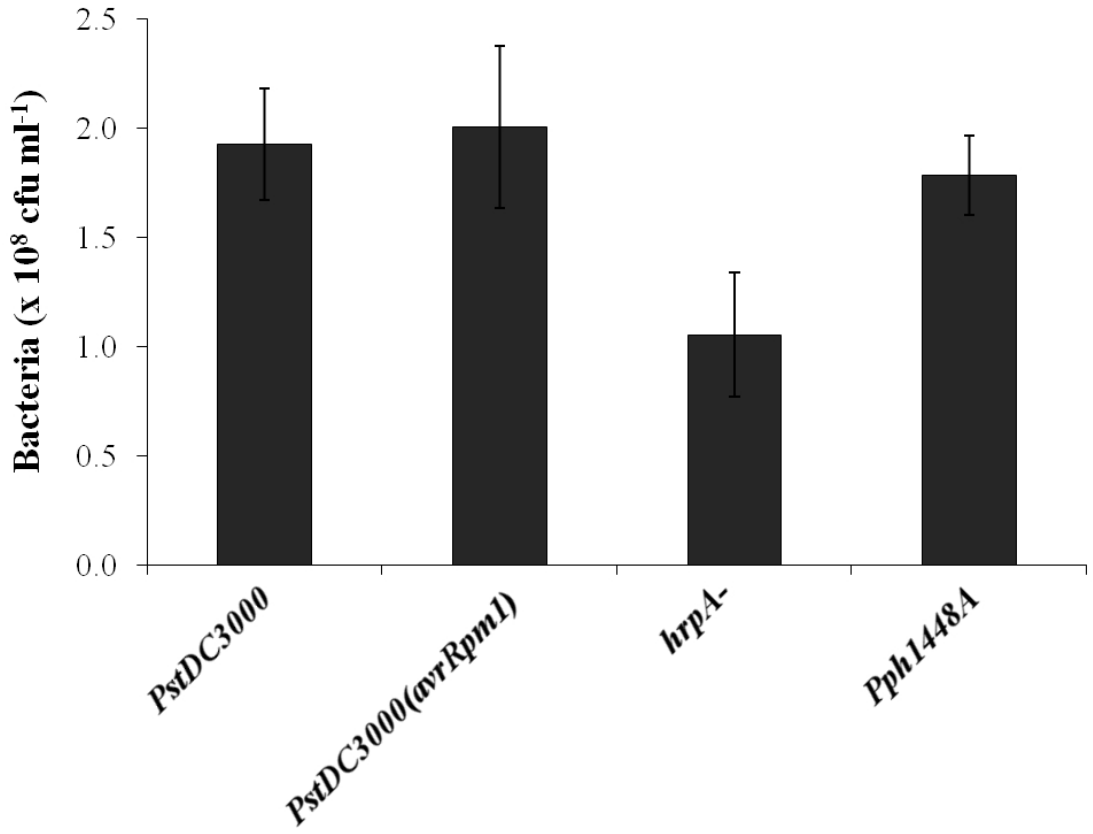
Appendix I: Buffers for TAP purification (Section 2.2.5)

Buffer	Composition
Tris-Saline Tween Buffer	50mM Tris pH 7.5, 150mM NaCl, 0.05% Tween 20
Extration buffer	50mM Tris-HCl (pH7.5), 150mM NaCl, 1mM phenylmethanesulfonyl fluoride (PMSF) (Sigma-Aldrich, Germany), Protease inhibitor cocktail (EDTA-free) (Roche, Germany)
Solubilisation Buffer	Extraction buffer supplemented with 0.5% 3-[(3-cholamidopropyl) dimethylammonio]-1-propanesulfonate (CHAPS) (Fisher Scientific, UK))
Wash Buffer	50mM Tris pH 7.5, 150mM NaCl, 10% glycerol, 0.1% Nonidet P-40
Cleavage Buffer	Wash Buffer supplemented with 1mM DTT
Elution Buffer	Wash Buffer supplemented with 50mM or 250mM Imidazole
1 x Ni-NTA Bind Buffer	300mM NaCl, 50mM Na_2PO_4, 10mM Imidazole, pH 7.5

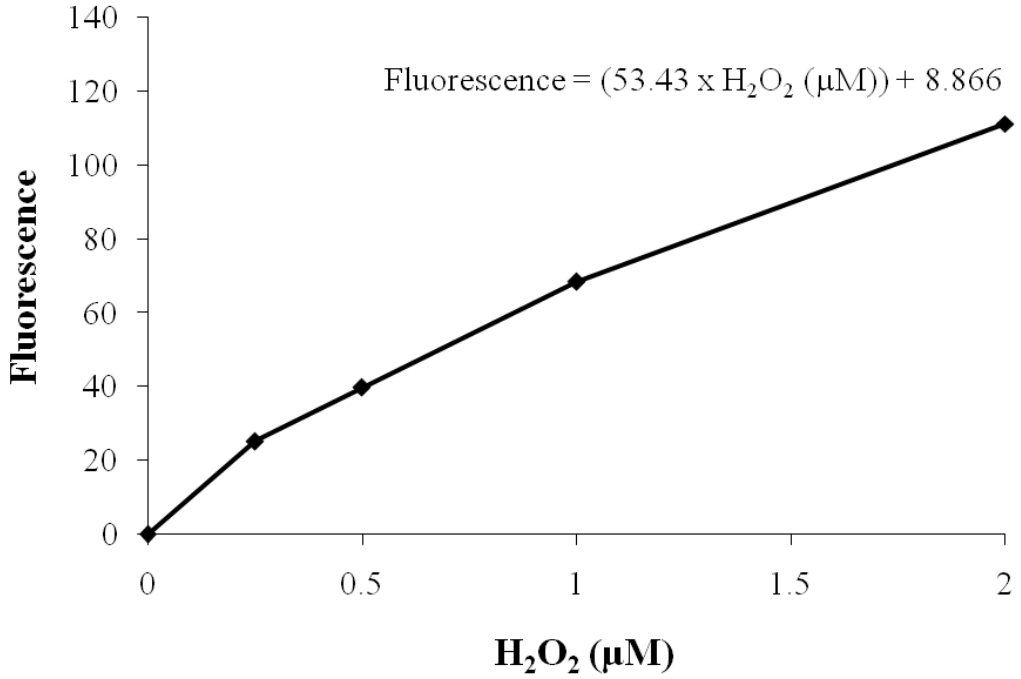
Appendix II: Buffers for western blotting (Section 2.2.7)

Buffer	Composition
Transfer Buffer	10mM 3-(cyclohexylamino)-1-propanesulfonic acid (CAPS) (Fisher, UK), 10% methanol, pH 11.1
Blocking Buffer	5% (w/v) powdered milk, 20mM Tris-HCl (pH 7.6), 137mM NaCl, 0.1% Tween 20 (Fisher, UK)

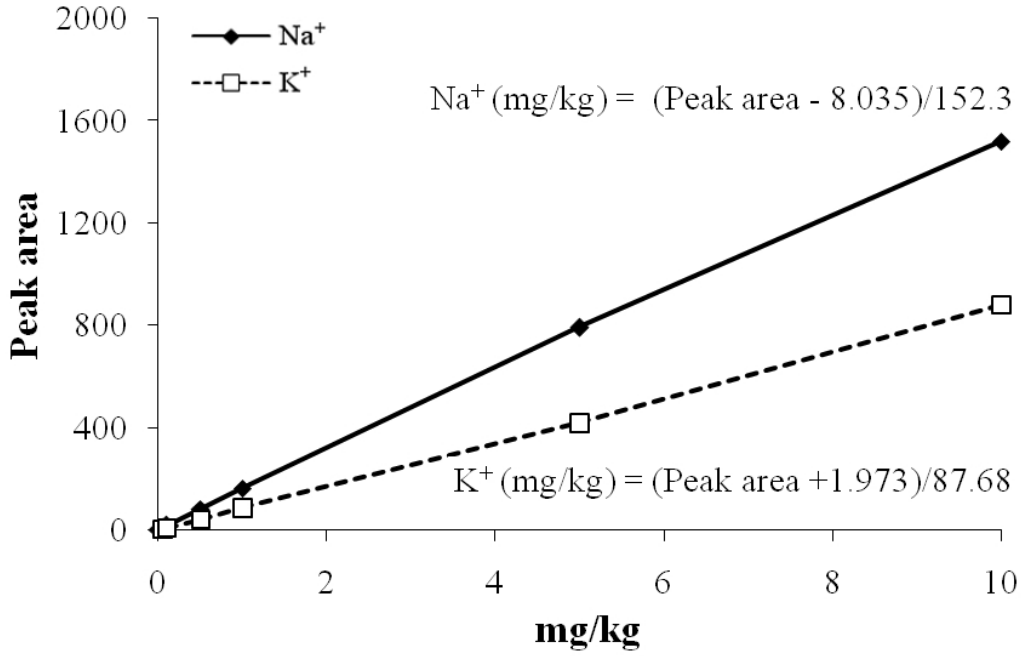
Appendix III: relationship between bacterial suspensions (in 10mM $MgCl_2$) with an optical density (OD600) reading of 0.2 and the number of bacterial colony forming units (cfu) per ml of suspension for each bacterial strain used (Section 2.4.2).



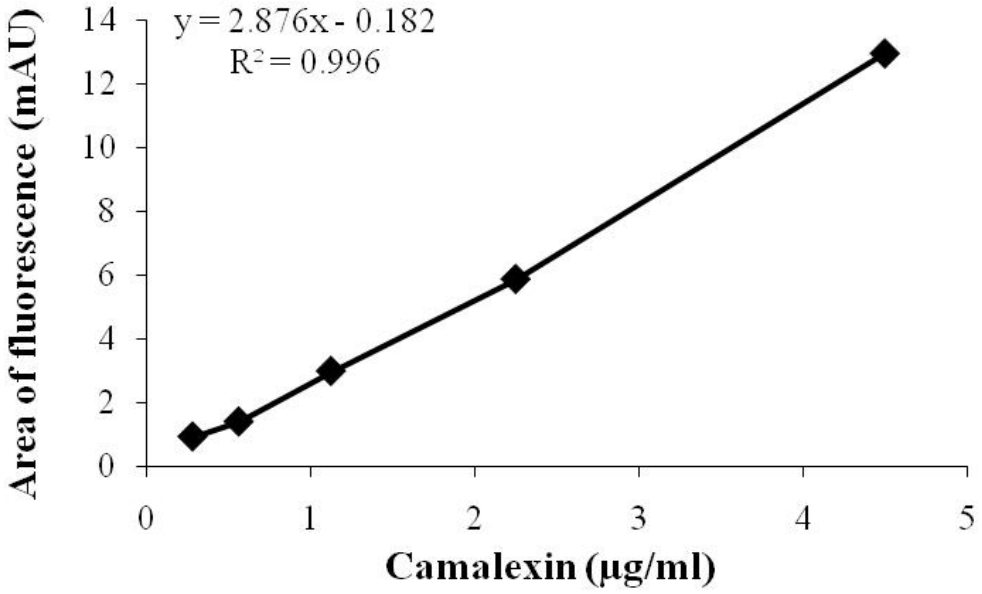
Appendix IV: Amplex red calibration curve for calculation of H_2O_2 concentrations in samples (Section 2.6.1)



Appendix V: Ion chromatography calibration curve for calculation of Na^+ and K^+ concentrations in samples (Section 2.6.2)



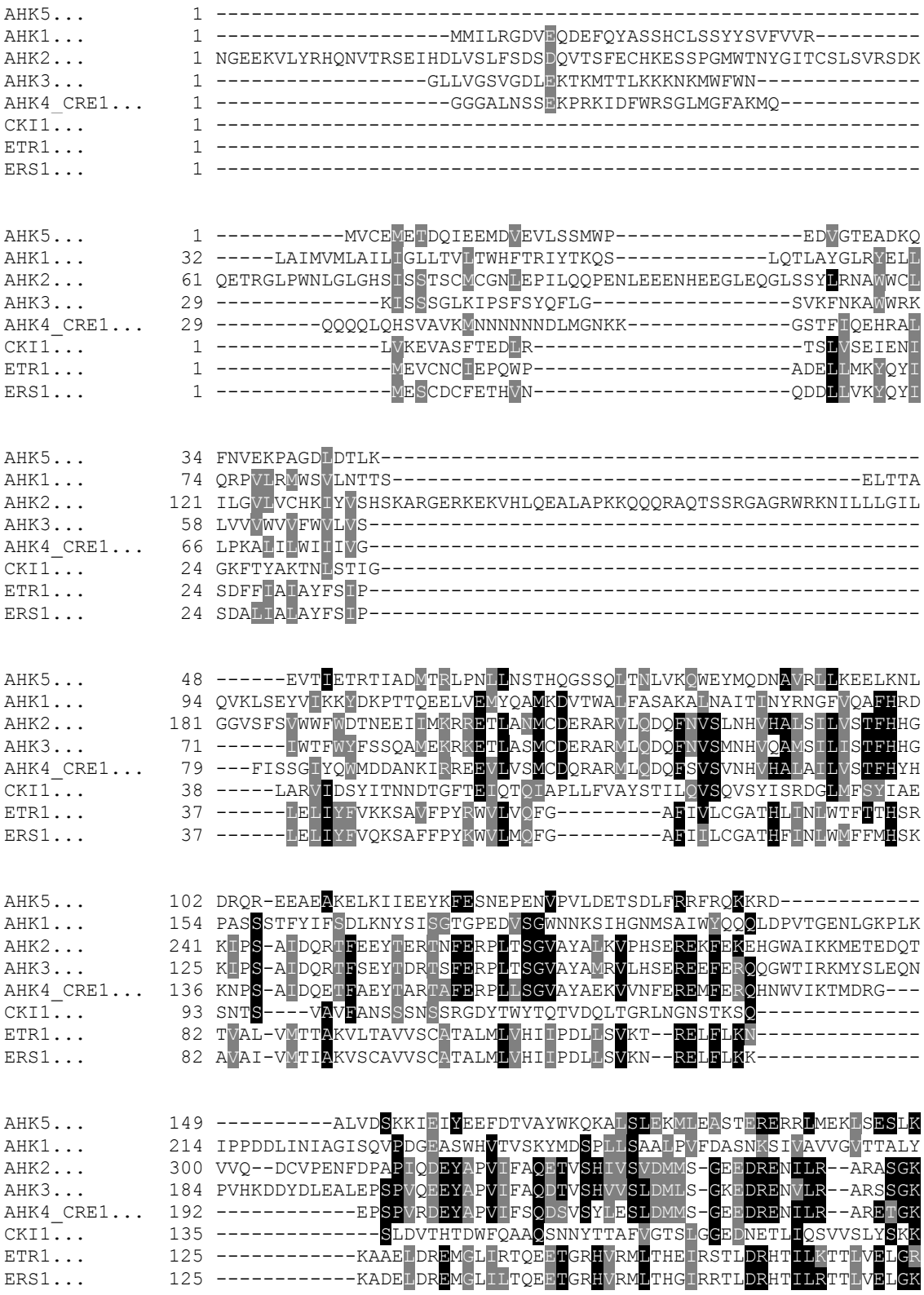
Appendix VI: Camalexin calibration curve relating area of fluorescence measurements given by fluorescence detection to concentration of camalexin used to calculate camalexin concentration in samples (Section 2.6.5).

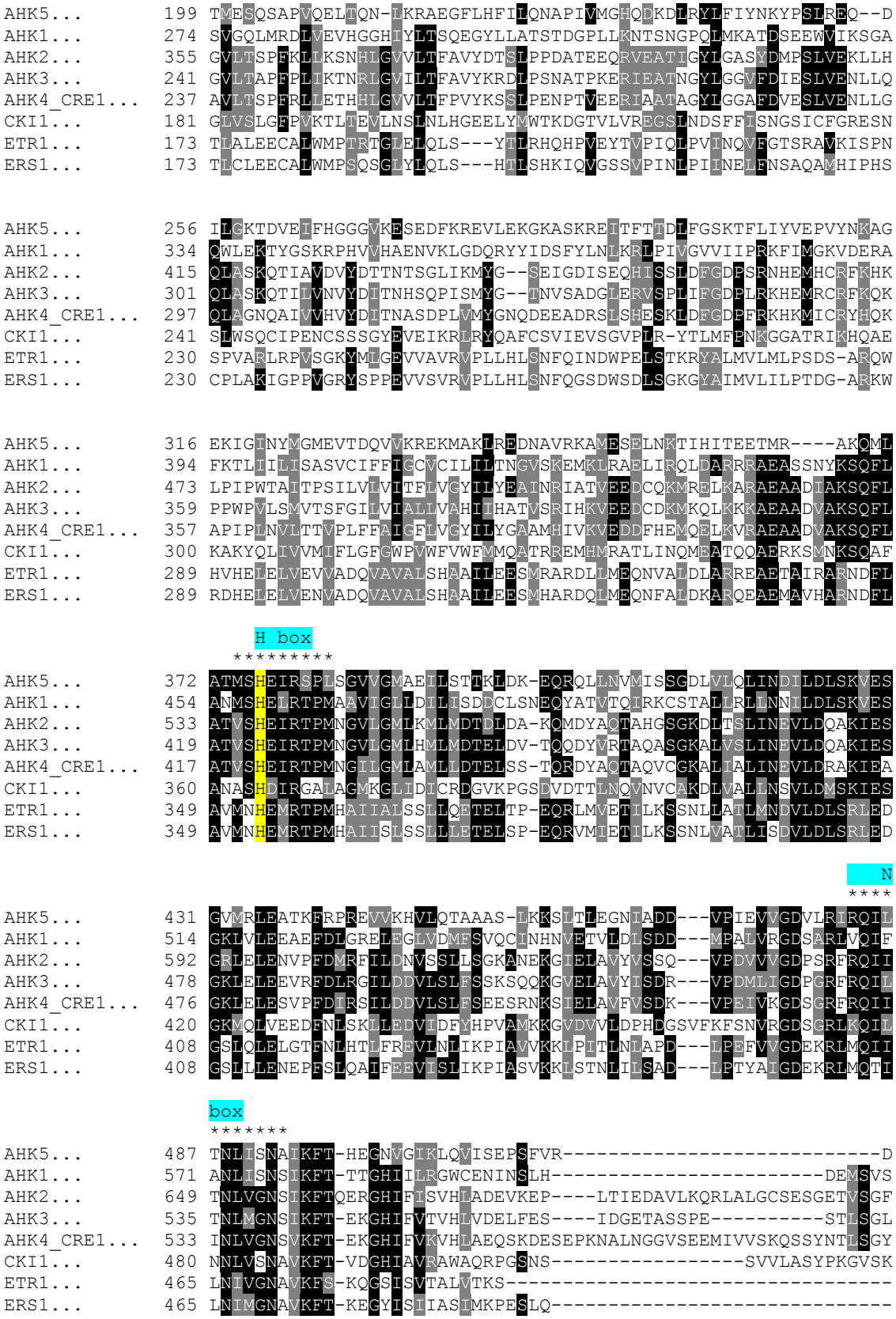


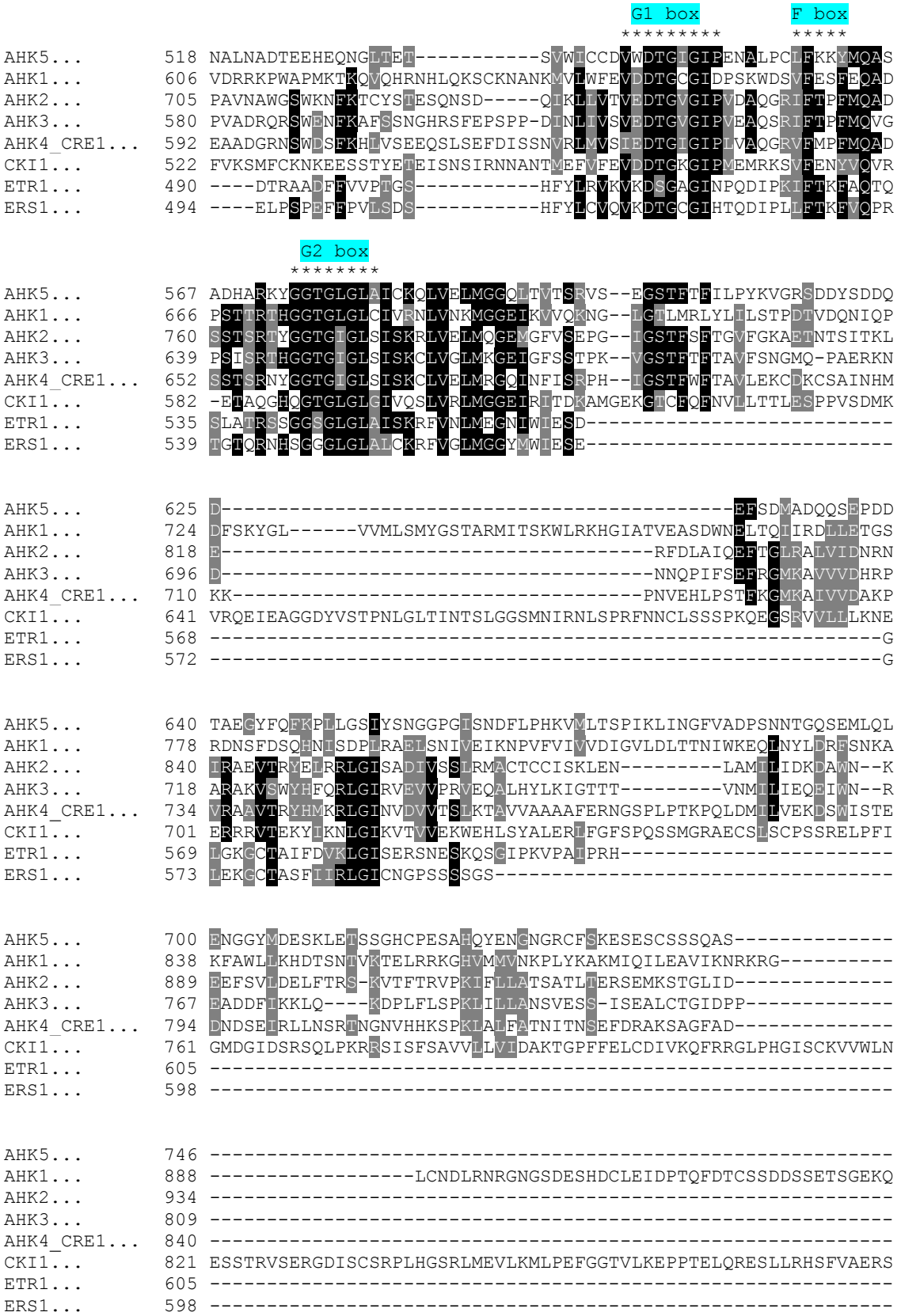
Appendix VII: Buffers for in-gel digestion of proteins (Section 2.6.6)

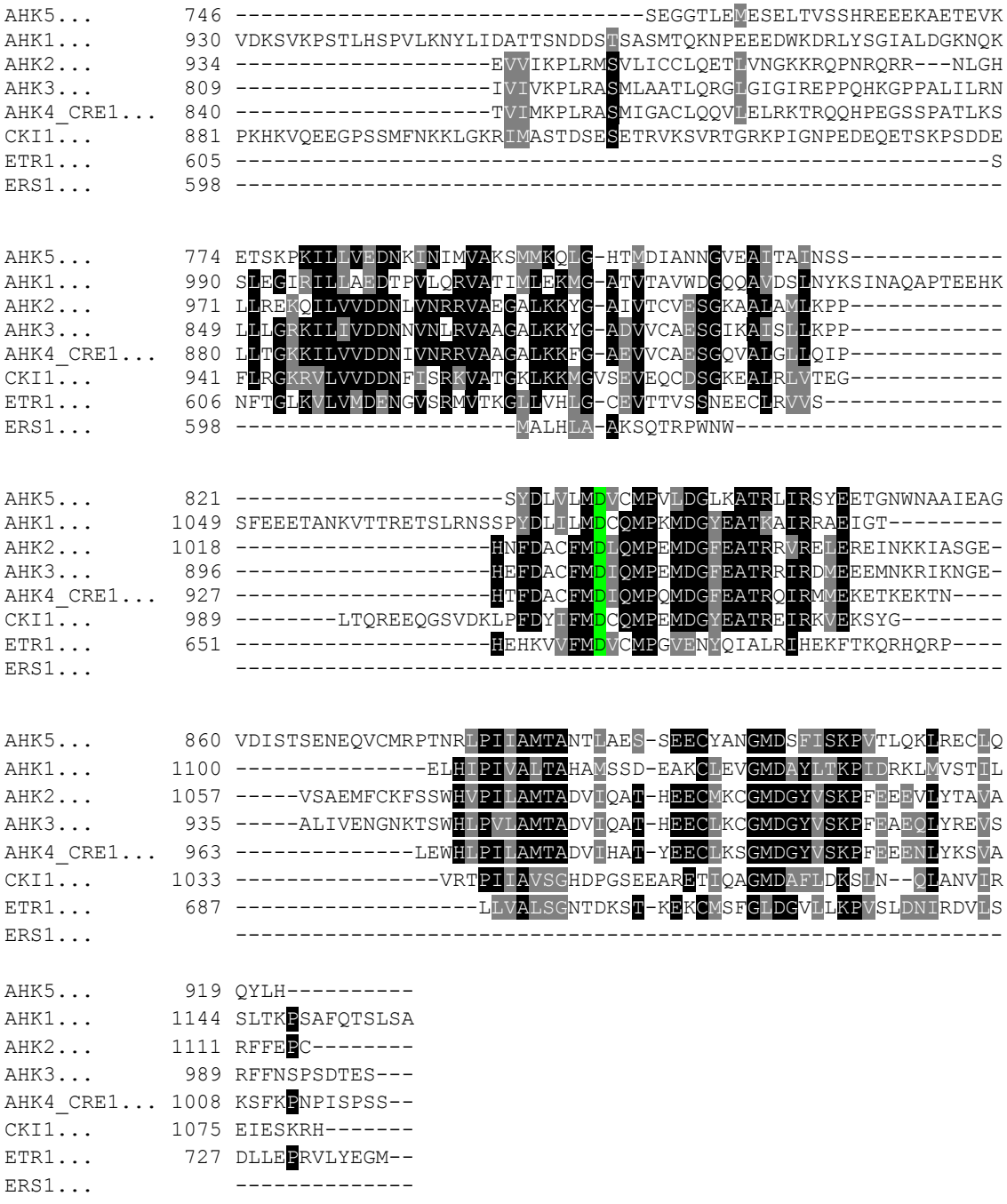
Buffer	Composition
Trypsin Digestion Buffer	25mM Ammonium Bicarbonate, 5mM Calcium Chloride, 10% Acetonitrile
Working Trypsin Solution	Promega Sequencing Grade Trypsin, 20µl Promega Dissolution Buffer, 980µl Trypsin Digestion Buffer

Appendix VIII: Multiple sequence alignment of *A. thaliana* histidine kinases (Section 3.2).




AHK5... 199 TMESQSAPVQELTQN-LKRAEGFLHFILQNAPIVMGHQDKDLRYLFIYNKYPSLREQ--D
AHK1... 274 SVGQLMRDLVEVHGGHIYLTSQEGYLLATSTDGPLLKNTSNGPQLMKATDSEEWVIKSGA
AHK2... 355 GVLTSPEKLLKSNHLGVVLTFAVYDTSLPPDATEEQRVEATIGYLGASYDMPSLVEKLLH
AHK3... 241 GVLTAPEPLIKTNRLGVILTFAVYKRDLPSNATPKERIEATNGYLGGVFDIESLVENLLQ
AHK4_CRE1... 237 AVLTSPERLLETHHLGVVLTFPVYKSSLPENPTVEERIAATAGYLGGAFDVESLVENLLG
CKI1... 181 GLVSLGEPVKTLTEVLNSLNLHGEELYMWTKDGTVLVREGSLNDSFFISNGSICFGRESN
ETR1... 173 TLALEECALWMPTRTGLELQLS---YTLRHQHPVEYTVPIQLPVINQVFGTSRAVKISPN
ERS1... 173 TLCLEECALWMPSQSGLYLQLS---HTLSHKIQVGSSVPINLPIINELFNSAQAMHIPHS
AHK5... 256 ILGKTDVEIFHGGGVKESEDFKREVLEKGKASKREITFTTDLFGSKTFLIYVEPVYNKAG
AHK1... 334 QWLEKTYGSKRPHVVHAENVKLGDQRYYIDSFYLNLKRLPIVGVVIIPRKFIMGKVDERA
AHK2... 415 QLASKQTIAVDVYDTTNTSGLIKMYG--SEIGDISEQHISSLDFGDPSRNHEMHCRFKHK
AHK3... 301 QLASKQTILVNVYDITNHSQPISMYG--TNVSADGIERVSPLIFGDPLRKHEMRCRFKQK
AHK4_CRE1... 297 QLAGNQAIVVHVYDITNASDPLVMYGNQDEEADRSLSHESKLDFGDPFRKHKMICRYHQK
CKI1... 241 SLWSQCIPENCSSSGYEVEIKRLRYQAFCSVIEVSGVPLR-YTLMFPNKGGATRIKHQAE
ETR1... 230 SPVARLRPVSGKYMLGEVVAVRVPLLHLSNFQINDWPELSTKRYALMVLMLPSDS-ARQW
ERS1... 230 CPLAKIGPPVGRYSPPEVVSVRVPLLHLSNFQGSDWSDLSGKGYAIMVLILPTDG-ARKW
AHK5... 316 EKIGINYMGMEVTDQVVKREKMAKLREDNAVRKAMESELNKTIHITEETMR----AKQML
AHK1... 394 FKTLIILISASVCIFFIGCVCILILTNGVSKEMKIRAELIRQLDARRAEASSNYKSQFL
AHK2... 473 LPIPWTAITPSILVLVITFLVGYILYEAINRIATVEEDCQKMRELKARAEAADIAKSQFL
AHK3... 359 PPWPVLSMVTSFGILVIALLVAHIIHATVSRIHKVEEDCDKMKQLKKKAEAADVAKSQFL
AHK4_CRE1... 357 APIPLNVLTTVPLFFAIGFLVGYILYGAAMHIVKVEDDFHEMQELKVRAEAADVAKSQFL
CKI1... 300 KAKYQLIVVMIFLGFGWPVWFVWFMMQATRREMHMRATLINQMEATQQAERKSMNKSQAF
ETR1... 289 HVHEIELVEVVADQVAVALSHAAILEESMRARDLLMEQNVALDLARREAETAIRARNDFL
ERS1... 289 RDHEIELVENVADQVAVALSHAAILEESMHARDQLMEQNFALDKARQEAEMAVHARNDFL
H box
AHK5... 372 ATMSHEIRSPLSGVVGMAEILSTTKLDK-EQRQLLNVMISSGDLVLQLINDILDLSKVES
AHK1... 454 ANMSHELRTPMAAVIGLLDILISDDCLSNEQYATVTQIRKCSTALLRLLNNILDLSKVES
AHK2... 533 ATVSHEIRTPMNGVLGMLKMLMDTDLDA-KQMDYAQTAHGSGKDLTSLINEVLDQAKIES
AHK3... 419 ATVSHEIRTPMNGVLGMLHMLMDTELDV-TQQDYVRTAQASGKALVSLINEVLDQAKIES
AHK4_CRE1... 417 ATVSHEIRTPMNGILGMLAMLLDTELSS-TQRDYAQTAQVCGKALIALINEVLDRAKIEA
CKI1... 360 ANASHDIRGALAGMKGLIDICRDGVKPGSDVDTTLNQVNVCAKDLVALLNSVLDMSKIES
ETR1... 349 AVMNHEMRTPMHAIIALSSLLQETELTP-EQRLMVETILKSSNLLATLMNDVLDLSRLED
ERS1... 349 AVMNHEMRTPMHAIISLSSLLLETELSP-EQRVMIETILKSSNLVATLISDVLDLSRLED
N
AHK5... 431 GVMRLEATKERPREVVKHVLQTAAAS-LKKSLTLEGNIADD---VPIEVVGDVLRIRQIL
AHK1... 514 GKLVLEEAEFDLGRELEGLVDMFSVQCINHNVETVLDLSDD---MPALVRGDSARLVQIF
AHK2... 592 GRLELENVPFDMRFILDNVSSLLSGKANEKGIELAVYVSSQ---VPDVVVGDPSRFRQII
AHK3... 478 GKLELEEVRFDLRGILDDVLSLFSSKSQQKGVELAVYISDR---VPDMLIGDPGRFRQIL
AHK4_CRE1... 476 GKLELESVPFDIRSILDDVLSLFSEESRNKSIELAVFVSDK---VPEIVKGDSGRFRQII
CKI1... 420 GKMQLVEEDFNLSKLLEDVIDFYHPVAMKKGVDVVLDPHDGSVFKFSNVRGDSGRLKQIL
ETR1... 408 GSLQLELGTFNLHTLFREVLNLIKPIAVVKKLPITLNIAPD---LPEFVVGDEKRLMQII
ERS1... 408 GSLLLENEPFSLQAIFEEVISLIKPIASVKKLSTNLILSAD---LPTYAIGDEKRLMQTI
box
AHK5... 487 TNLLSNAIKFT-HEGNVGIKLQVISEPSFVR----------D
AHK1... 571 ANLISNSIKFT-TTGHIILRGWCENINSLH----------DEMSVS
AHK2... 649 TNLVGNSIKFTQERGHIFISVHLADEVKEP----LTIEDAVLKQRLALGCSESGETVSGF
AHK3... 535 TNLMGNSIKFT-EKGHIFVTVHLVDELFES----IDGETASSPE----------STLSGL
AHK4_CRE1... 533 INLVGNSVKFT-EKGHIFVKVHLAEQSKDESEPKNALNGGVSEEMIVVSKQSSYNTLSGY
CKI1... 480 NNLVSNAVKFT-VDGHIAVRAWAQRPGSNS----------SVVLASYPKGVSK
ETR1... 465 LNIVGNAVKFS-KQGSISVTALVTKS----------
ERS1... 465 LNIMGNAVKFT-KEGYISIIASIMKPESLQ----------


G1 box
F box
G2 box
AHK5...
AHK1...
AHK2...
AHK3...
AHK4_CRE1...
CKI1...
ETR1...
ERS1...


AHK5... 746 ----------SEGGTLEMESELTVSSHREEEKAETEVK
AHK1... 930 VDKSVKPSTLHSPVLKNYLIDATTSNDDSTSASMTQKNPEEEDWKDRLYSGIALDGKNQK
AHK2... 934 ----------EVVIKPLRMSVLICCLQETLVNGKKRQPNRQRR---NLGH
AHK3... 809 ----------IVIVKPLRASMLAATLQRGLGIGIREPPQHKGPPALILRN
AHK4_CRE1... 840 ----------TVIMKPLRASMIGACLQQVLELRKTRQQHPEGSSPATLKS
CKI1... 881 PKHKVQEEGPSSMFNKKLGKRIMASTDSESETRVKSVRTGRKPIGNPEDEQETSKPSDDE
ETR1... 605 ----------S
ERS1... 598 ----------
AHK5... 774 ETSKPKILLVEDNKINIMVAKSMMKQLG-HTMDIANNGVEAITAINSS----------
AHK1... 990 SLEGIRILLAEDTPVLQRVATIMLEKMG-ATVTAVWDGQQAVDSLNYKSINAQAPTEEHK
AHK2... 971 LLREKQILVVDDNLVNRRVAEGALKKYG-AIVTCVESGKAALAMLKPP----------
AHK3... 849 LLLGRKILIVDDNNVNLRVAAGALKKYG-ADVVCAESGIKAISLLKPP----------
AHK4_CRE1... 880 LLTGKKILVVDDNIVNRRVAAGALKKFG-AEVVCAESGQVALGLLQIP----------
CKI1... 941 FLRGKRVLVVDDNFISRKVATGKLKKMGVSEVEQCDSGKEALRLVTEG----------
ETR1... 606 NFTGLKVLVMDENGVSRMVTKGLLVHLG-CEVTTVSSNEECLRVVS----------
ERS1... 598 ----------MALHLA-AKSQTRPWNW----------
AHK5... 821 ----------SYDLVLMDVCMPVLDGLKATRLIRSYEETGNWNAAIEAG
AHK1... 1049 SFEEETANKVTTRETSLRNSSPYDLILMDCQMPKMDGYEATKAIRRAEIGT---------
AHK2... 1018 ----------HNFDACFMDLQMPEMDGFEATRRVRELEREINKKIASGE-
AHK3... 896 ----------HEFDACFMDIQMPEMDGFEATRRIRDMEEEMNKRIKNGE-
AHK4_CRE1... 927 ----------HTFDACFMDIQMPQMDGFEATQIRMMEKETKEKTN----
CKI1... 989 --------LTQREEQGSVDKLPFDYIFMDCQMPEMDGYEATREIRKVEKSYG--------
ETR1... 651 ----------HEHKVVFMDVCMPGVENYQIALRIHEKFTKQRHQRP----
ERS1... ----------
AHK5... 860 VDISTSENEQVCMRPTNRLPIIAMTANTLAES-SEECYANGMDSFISKPVTLQKLRECLQ
AHK1... 1100 ---------------ELHIPIVALTAHAMSSD-EAKCIEVGMDAYLTKPIDRKLMVSTIL
AHK2... 1057 -----VSAEMFCKFSSWHVPILAMTADVIQAT-HEECMKCGMDGYVSKPFEEEVLYTAVA
AHK3... 935 -----ALIVENGNKTSWHLPVLAMTADVIQAT-HEECLKCGMDGYVSKPFEAEQLYREVS
AHK4_CRE1... 963 --------------LEWHLPILAMTADVIHAT-YEECIKSGMDGYVSKPFEEENLYKSVA
CKI1... 1033 ----------------VRTPIIAVSGHDPGSEEARETIQAGMDAFLDKSLN--QLANVIR
ETR1... 687 ----------LLVALSGNTDKST-KEKCMSFGLDGVLLKPVSLDNIRDVLS
ERS1... ----------
AHK5... 919 QYLH----------
AHK1... 1144 SLTKPSAFQTSLSA
AHK2... 1111 RFFEPC--------
AHK3... 989 RFFNSPSDTES---
AHK4_CRE1... 1008 KSFKPNPISPSS--
CKI1... 1075 EIESKRH-------
ETR1... 727 DLLEPRVLYEGM--
ERS1... --------------

Appendix IX: Proteins identified by LC-MS/MS. Peptides matched by MASCOT are highlighted. Underlined sequence represents over-lapping sequences of two fragments identified. Band numbers are as shown in Table 7.1 in Section 7.2.1.

Band 1 - phospholipase D alpha 1 At3g15730

MAQHLLHGTLHATIYEVDALHGGGVRQGFLGKILANVEETIGVGKGETQL
YATIDLQKARVGRTRKIKNEPKNPKWYESFHIYCAHLASDIIFTVKDDNP
IGATLIGRAYIPVDQVINGEEVDQWVEILDNDRNPIQGGSKIHVKLQYFH
VEEDRNWNMGIKSAKFPGVPYTFFSQRQGCKVSLYQDAHIPDNFVPRIPL
AGGKNYEPQRCWEDIFDAISNAKHLIYITGWSVYAEIALVRDSRRPKPGG
DVTIGELLKKKASEGVRVLLLVWDDRTSVDVLKKDGLMATHDEETENFFR
GSDVHCILCPRNPDDGGSIVQSLQISTMFTHHQKIVVVDSEMPSRGGSEM
RRIVSFVGGIDLCDGRYDTPFHSLFRTLDTVHHDDFHQPNFTGAAITKGG
PREPWHDIHSRLEGPIAWDVMYNFEQRWSKQGGKDILVKLRDLSDIIITP
SPVMFQEDHDVWNVQLFRSIDGGAAAGFPESPEAAAEAGLVSGKDNIIDR
SIQDAYIHAIRRAKDFIYVENQYFLGSSFAWAADGITPEDINALHLIPKE
LSLKIVSKIEKGEKFRVYVVVPMWPEGLPESGSVQAILDWQRRTMEMMYK
DVIQALRAQGLEEDPRNYLTFFCLGNREVKKDGEYEPAEKPDPDTDYMRA
QEARRFMIYVHTKMMIVDDEYIIIGSANINQRSMDGARDSEIAMGGYQPH
HLSHRQPARGQIHGFRMSLWYEHLGMLDETFLDPSSLECIEKVNRISDKY
WDFYSSESLEHDLPGHLLRYPIGVASEGDITELPGFEFFPDTKARILGTK
SDYLPPILTT

Band 3 - Catalase 3 At1g20620

MDPYKYRPSSAYNAPFYTTNGGAPVSNNISSLTIGERGPVLLEDYHLIEK
VANFTRERIPERVVHARGISAKGFFEVTHDISNLTCADFLRAPGVQTPVI
VRFSTVVHERASPETMRDIRGFAVKFYTREGNFDLVGNNTPVFFIRDGIQ
FPDVVHALKPNPKTNIQEYWRILDYMSHLPESLLTWCWMFDDVGIPQDYR
HMEGFGVHTYTLIAKSGKVLFVKFHWKPTCGIKNLTDEEAKVVGGANHSH
ATKDLHDAIASGNYPEWKLFIQTMDPADEDKFDFDPLDVTKIWPEDILPL
QPVGRLVLNRTIDNFFNETEQLAFNPGLVVPGIYYSDDKLLQCRIFAYGD
TQRHRLGPNYLQLPVNAPKCAHHNNHHEGFMNFMHRDEEINYYPSKFDPV
RCAEKVPTPTNSYTGIRTKCVIKKENNFKQAGDRYRSWAPDRQDRFVKRW
VEILSEPRLTHEIRGIWISYWSQADRSLGQKLASRLNVRPSI

Band 3 - RuBisCO large subunit ATCG00490

MSPQTETKASVGFKAGVKEYKLTYYTPEYETKDTDILAAFRVTPQPGVPP
EEAGAAVAAESSTGTWTTVWTDGLTSLDRYKGRCYHIEPVPGEETQFIAY
VAYPLDLFEEGSVTNMFTSIVGNVFGFKALAALRLEDLRIPPAYTKTFQG
PPHGIQVERDKLNKYGRPLLGCTIKPKLGLSAKNYGRAVYECLRGGLDFT
KDDENVNSQPFMRWRDRFLFCAEAIYKSQAETGEIKGHYLNATAGTCEEM
IKRAVFARELGVPIVMHDYLTGGFTANTSLSHYCRDNGLLLHIHRAMHAV
IDRQKNHGMHFRVLAKALRLSGGDHIHAGTVVGKLEGDRESTLGFVDLLR
DDYVEKDRSRGIFFTQDWVSLPGVLPVASGGIHVWHMPALTEIFGDDSVL
QFGGGTLGHPWGNAPGAVANRVALEACVQARNEGRDLAVEGNEIIREACK
WSPELAAACEVWKEITFNFPTIDKLDGQE

Band 4 - Phosphoglycerate kinase At3g12780

MASAAASSAFSLLKSTGAVASSAGTRARASLLPIPSTSVSARPLGFSATL
DSRRFSLHVASKVESVRGKGSRGVVSMAKKSVGDLTSADLKGKKVFVRAD
LNVPLDDNQTITDDTRIRAAIPTIKYLIENGAKVILSTHLGRPKGVTPKF
SLAPLVPRLSELLGIEVTKADDCIGPEVESLVASLPEGGVLLLENVRFYK
EEEKNDPEFAKKLASLADLYVNDAFGTAHRAHASTEGVTKFLKPSVAGFL
LQKELDYLVGAVSNPKRPFAAIVGGSKVSSKIGVIESLLEKCDILLLGGG
MIFTFYKAQGLSVGSSLVEEDKLELATELLAKAKAKGVSLLLPTDVVVAD
KFAPDANSKIVPASGIEDGWMGLDIGPDSIKTFNEALDTTQTVIWNGPMG
VFEMEKFAAGTEAIANKLAELSEKGVTTIIGGGDSVAAVEKVGVAGVMSH
ISTGGGASLELLEGKVLPGVIALDEAIPVTV

Band 5 - Fructose-bisphosphate aldolase At2g21330

MASSTATMLKASPVKSDWVKGQSLLLRQPSSVSAIRSHVAPSALTVRAAS
AYADELVKTAKTIASPGHGIMAMDESNATCGKRLASIGLENTEANRQAYR
TLLVSAPGLGQYISGAILFEETLYQSTTDGKKMVDVLVEQNIVPGIKVDK
GLVPLVGSYDESWCQGLDGLASRTAAYYQQGARFAKWRTVVSIPNGPSAL
AVKEAAWGLARYAAISQDSGLVPIVEPEIMLDGEHGIDRTYDVAEKVWAE
VFFYLAQNNVMFEGILLKPSMVTPGAEATDRATPEQVASYTLKLLRNRIP
PAVPGIMFLSGGQSELEATLNLNAMNQAPNPWHVSFSYARALQNTCLKTW
GGKEENVKAAQDILLARAKANSLAQLGKYTGEGESEEAKEGMFVKGYTY

Appendix X: Proteins identified by LC-MS/MS. Peptides matched by MASCOT are highlighted. Underlined sequence represents over-lapping sequences of two fragments identified. Band numbers are as shown in Table 7.2 in Section 7.2.1.

Band 10 - RuBisCO large subunit ATCG00490

MSPQTETKASVGFKAGVKEYKLTYYTPEYETKDTDILAAFRVTPQPGVPP
EEAGAAVAAESSTGTWTTVWTDGLTSLDRYKGRCYHIEPVPGEETQFIAY
VAYPLDLFEEGSVTNMFTSIVGNVFGFKALAALRLEDLRIPPAYTKTFQG
PPHGIQVERDKLNKYGRPLLGCTIKPKLGLSAKNYGRAVYECLRGGLDFT
KDDENVNSQPFMRWRDRFLFCAEAIYKSQAETGEIKGHYLNATAGTCEEM
IKRAVFARELGVPIVMHDYLTGGFTANTSLSHYCRDNGLLLHIHRAMHAV
IDRQKNHGMHFRVLAKALRLSGGDHIHAGTVVGKLEGDRESTLGFVDLLR
DDYVEKDRSRGIFFTQDWVSLPGVLPVASGGIHVWHMPALTEIFGDDSVL
QFGGGTLGHPWGNAPGAVANRVALEACVQARNEGRDLAVEGNEIIREACK
WSPELAAACEVWKEITFNFPTIDKLDGQE

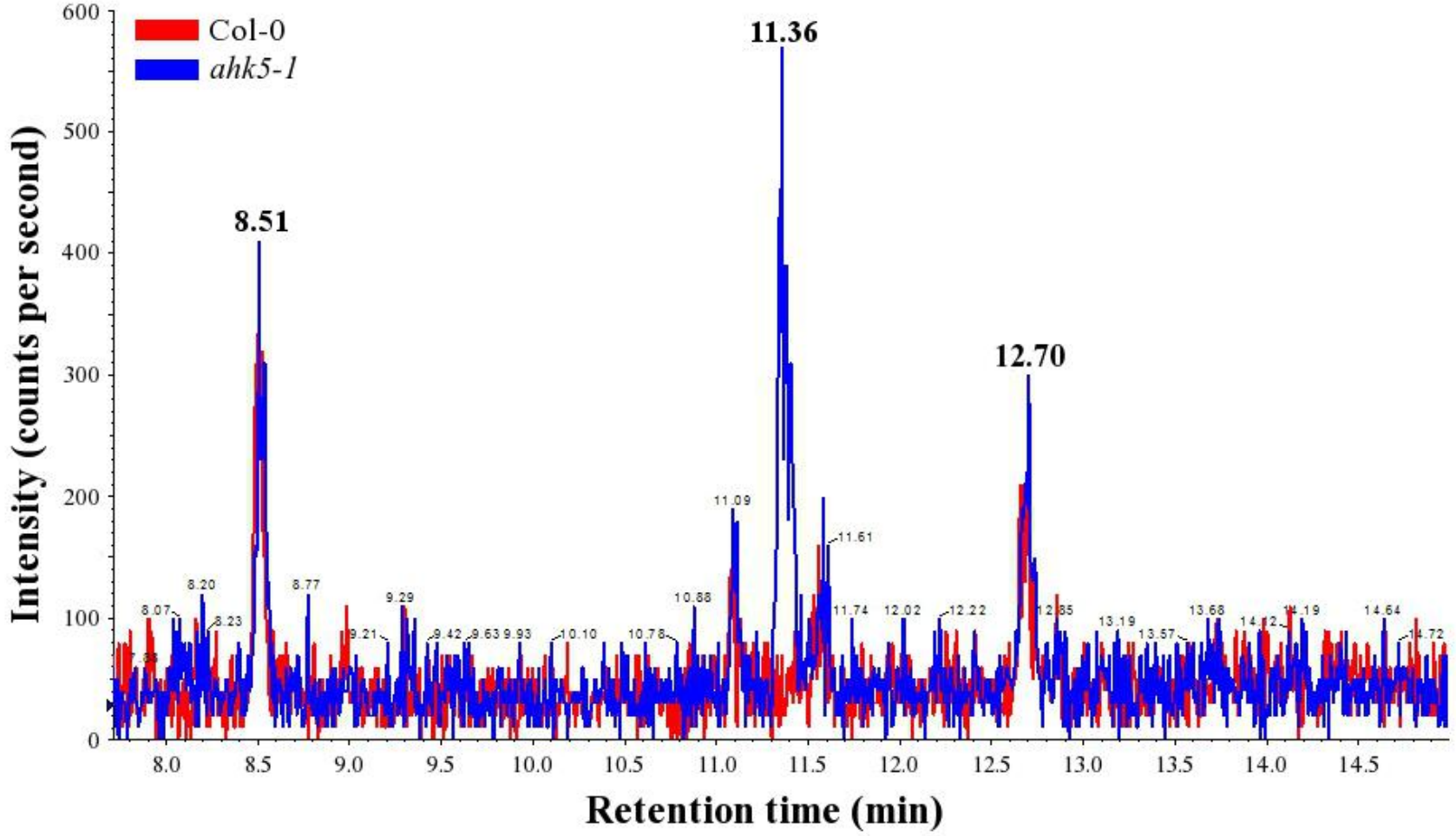
Band 11- RuBisCO activase At2g39730

MAAAVSTVGAINRAPLSLNGSGSGAVSAPASTFLGKKVVTVSRFAQSNKK
SNGSFKVLAVKEDKQTDGDRWRGLAYDTSDDQQDITRGKGMVDSVFQAPM
GTGTHHAVLSSYEYVSQGLRQYNLDNMMDGFYIAPAFMDKLVVHITKNFL
TLPNIKVPLILGIWGGKGQGKSFQCELVMAKMGINPIMMSAGELESGNAG
EPAKLIRQRYREAADLIKKGKMCCLFINDLDAGAGRMGGTTQYTVNNQMV
NATLMNIADNPTNVQLPGMYNKEENARVPIICTGNDFSTLYAPLIRDGRM
EKFYWAPTREDRIGVCKGIFRTDKIKDEDIVTLVDQFPGQSIDFFGALRA
RVYDDEVRKFVESLGVEKIGKRLVNSREGPPVFEQPEMTYEKLMEYGNML
VMEQENVKRVQLAETYLSQAALGDANADAIGRGTFYGKGAQQVNLPVPEG
CTDPVAENFDPTARSDDGTCVYNF

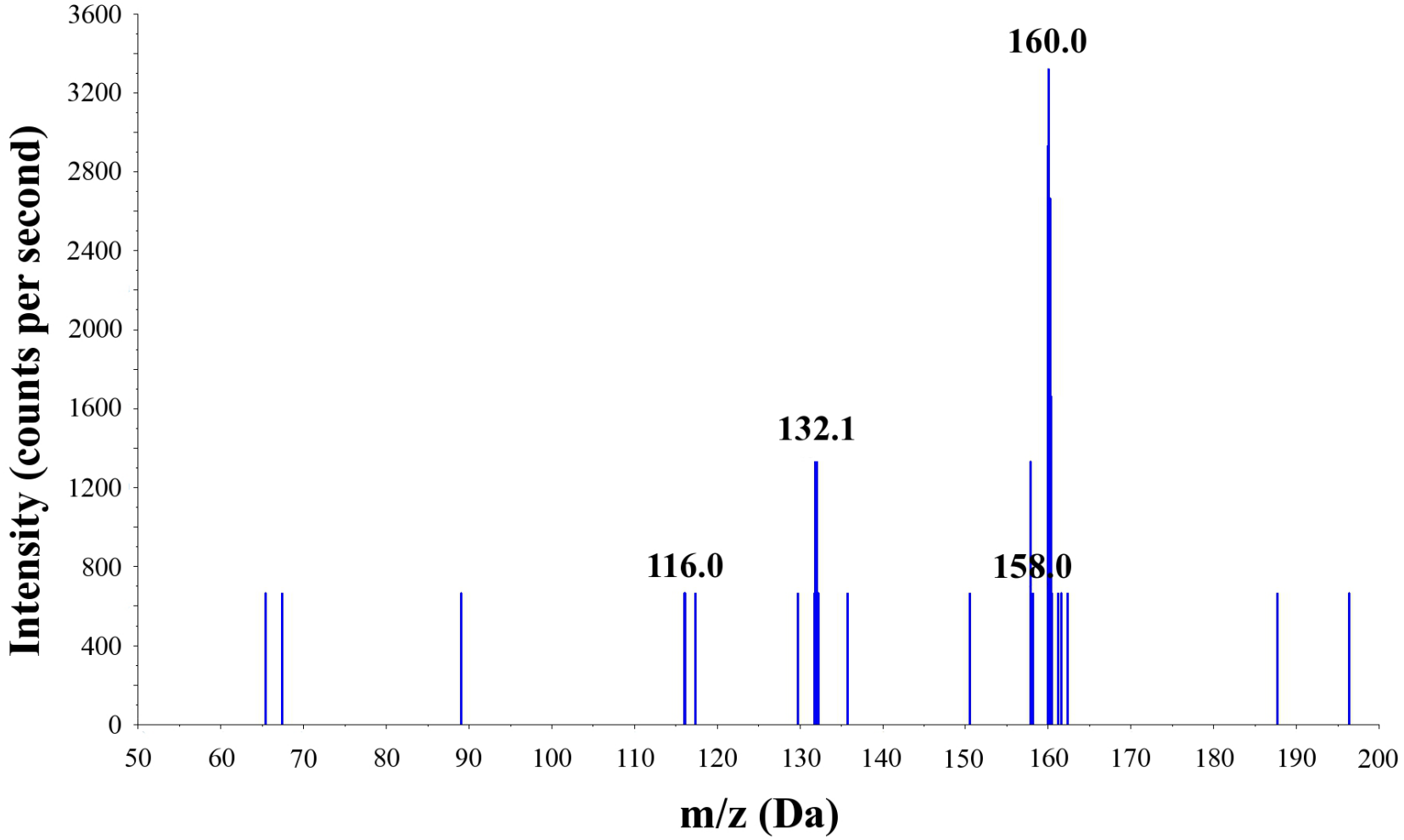
Band 11- Phosphoglycerate kinase At3g12780

MASAAASSAFSLLKSTGAVASSAGTRARASLLPIPSTSVSARPLGFSATL
DSRRFSLHVASKVESVRGKGSRGVVSMAKKSVGDLTSADLKGKKVFVRAD
LNVPLDDNQTITDDTRIRAAIPTIKYLIENGAKVILSTHLGRPKGVTPKF
SLAPLVPRLSELLGIEVTKADDCIGPEVESLVASLPEGGVLLLENVRFYK
EEEKNDPEFAKKLASLADLYVNDAFGTAHRAHASTEGVTKFLKPSVAGFL
LQKELDYLVGAVSNPKRPFAAIVGGSKVSSKIGVIESLLEKCDILLLGGG
MIFTFYKAQGLSVGSSLVEEDKLELATELLAKAKAKGVSLLLPTDVVVAD
KFAPDANSKIVPASGIEDGWMGLDIGPDSIKTFNEALDTTQTVIWNGPMG
VFEMEKFAAGTEAIANKLAELSEKGVTTIIGGGDSVAAVEKVGVAGVMSH
ISTGGGASLELLEGKVLPGVIALDEAIPVTV

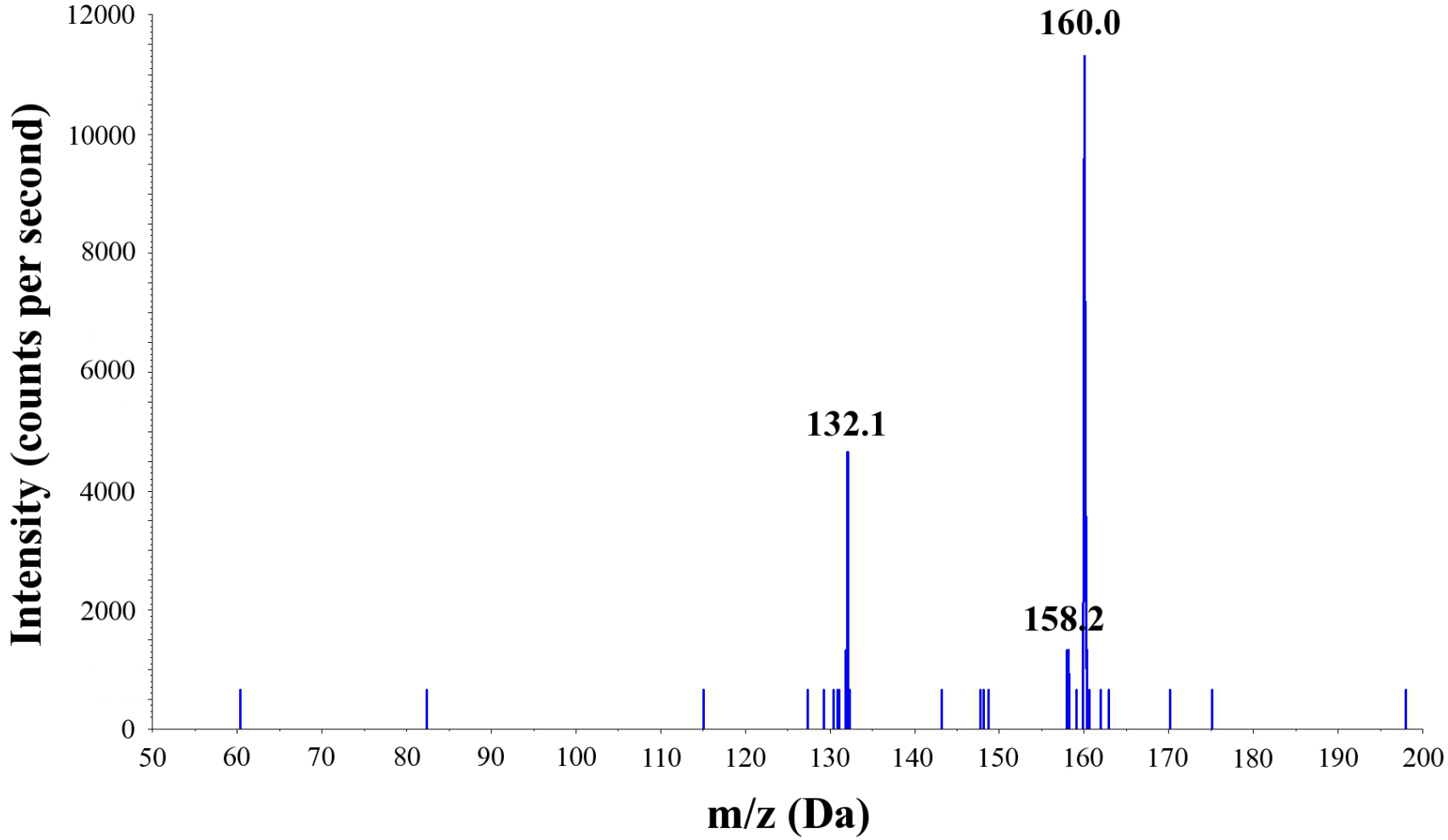
Appendix XI: Enhanced ion current (XIC) spectra of multiple reaction monitoring (MRM) for parent ions of 160Da with daughter ions of 132Da in samples prepared from wild-type Col-0 and *ahk5-1* mutant leaf tissue surface inoculated with 4 x 10^8 cfu ml^{-1} *Pst*DC3000 at 6dpi and analysed by LC-MS/MS (Section 5.3.1).



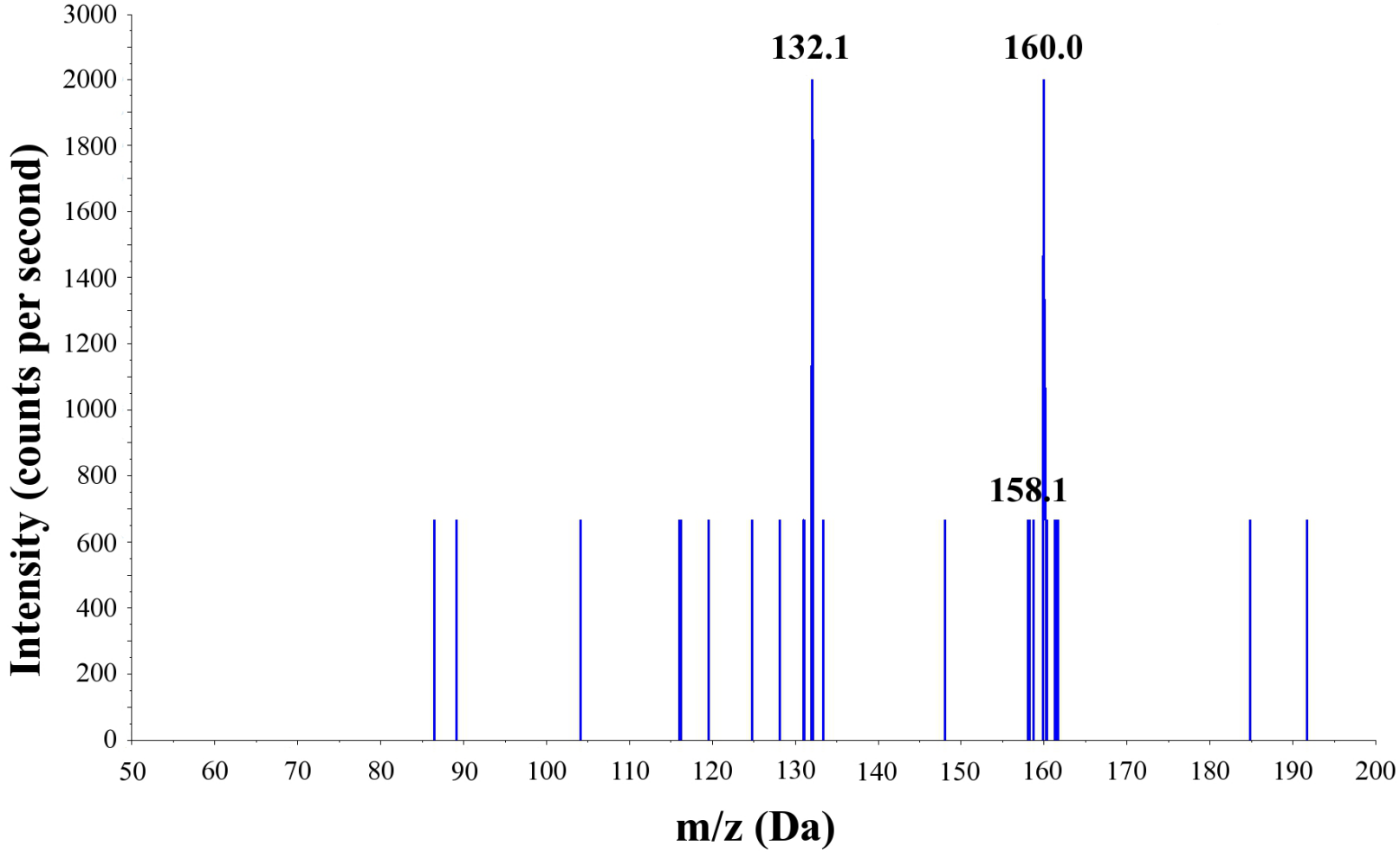
Appendix XII: Enhanced product ion (EPI) spectra of a parent/daughter ion pair of 160/132Da with a retention time of 8.51 minutes from a sample prepared from *ahk5-1* mutant leaf tissue surface inoculated with 4 x 10^8 cfu ml^{-1} *Pst*DC3000 at 6dpi and analysed by LC-MS/MS (Section 5.3.1).



Appendix XIII: Enhanced product ion (EPI) spectra of a parent/daughter ion pair of 160/132Da with a retention time of 11.36 minutes from a sample prepared from *ahk5-1* mutant leaf tissue surface inoculated with 4 x 10^8 cfu ml^{-1} *Pst*DC3000 at 6dpi and analysed by LC-MS/MS (Section 5.3.1).



Appendix XIV: Enhanced product ion (EPI) spectra of a parent/daughter ion pair of 160/132Da with a retention time of 12.70 minutes from a sample prepared from *ahk5-1* mutant leaf tissue surface inoculated with 4 x 10^8 cfu ml^{-1} *Pst*DC3000 at 6dpi and analysed by LC-MS/MS (Section 5.3.1).



References

Aarts, N., Metz, M., Holub, E., Staskawicz, B.J., Daniels, M.J., and Parker, J.E. (1998). Different requirements for EDS1 and NDR1 by disease resistance genes define at least two *R* gene-mediated signaling pathways in *Arabidopsis*. Proceedings of the National Academy of Sciences **95,** 10306-10311.

Abe, H., Yamaguchi-Shinozaki, K., Urao, T., Iwasaki, T., Hosokawa, D., and Shinozaki, K. (1997). Role of *Arabidopsis* MYC and MYB homologs in drought and abscisic acid-regulated gene expression. Plant Cell **9,** 1859 - 1868.

Abramoff, M.D. (2004). Image Processing with ImageJ. Biophotonics International **11,** 36-42.

Abramovitch, R.B., Janjusevic, R., Stebbins, C.E., and Martin, G.B. (2006). Type III effector AvrPtoB requires intrinsic E3 ubiquitin ligase activity to suppress plant cell death and immunity. Proceedings of the National Academy of Sciences of the United States of America **103,** 2851-2856.

Achard, P., Renou, J.P., Berthome, R., Harberd, N.P., and Genschik, P. (2008). Plant DELLAs restrain growth and promote survival of adversity by reducing the levels of reactive oxygen species. Current Biology **18,** 656-660.

Achard, P., Cheng, H., De Grauwe, L., Decat, J., Schoutteten, H., Moritz, T., Van der Straeten, D., Peng, J.R., and Harberd, N.P. (2006). Integration of plant responses to environmentally activated phytohormonal signals. Science **311,** 91-94.

Achou, E.A., Audenaert, K., Meziane, H., and Hofte, M. (2004). The salicylic acid-dependent defence pathway is effective against different pathogens in tomato and tobacco. Plant Pathol. **53,** 65-72.

Adie, B.A.T., Perez-Perez, J., Perez-Perez, M.M., Godoy, M., Sanchez-Serrano, J.J., Schmelz, E.A., and Solano, R. (2007). ABA is an essential signal for plant resistance to pathogens affecting JA biosynthesis and the activation of defenses in *Arabidopsis*. Plant Cell **19,** 1665-1681.

Agrios, G.N. (2005). Plant Pathology. (Oxford: Elsevier Academic Press).

Akutsu, K., Ko, K., and Misato, T. (1981). Role of conidial fusion in infection by *Botrytis cinerea* on cucumber leaves. Annual Meeting og the Phytopathological Society of Japan **47,** 15-23.

Albertyn, J., Hohmann, S., Thevelein, J.M., and Prior, B.A. (1994). *GPD1*, which encodes glycerol-3-phosphate dehydrogenase, is essential for growth under osmotic stress in *Saccharomyces cerevisiae*, and its expression is regulated by the high-osmolarity glycerol response pathway. Mol. Cell. Biol. **14,** 4135-4144.

Alemán, F., Nieves-Cordones, M., Martínez, V., and Rubio, F. (2009). Differential regulation of the *HAK5* genes encoding the high-affinity K^+ transporters of *Thellungiella halophila* and *Arabidopsis thaliana*. Environmental and Experimental Botany **65,** 263-269.

Allan, A.C., and Fluhr, R. (1997). Two distinct sources of elicited reactive oxygen species in tobacco epidermal cells. Plant Cell **9,** 1559-1572.

Allwood, J.W., Clarke, A., Goodacre, R., and Mur, L.A.J. (2010). Dual metabolomics: A novel approach to understanding plant-pathogen interactions. Phytochemistry **71,** 590-597.

Apel, K., and Hirt, H. (2004). Reactive oxygen species: Metabolism, oxidative stress, and signal transduction. Annual Review of Plant Biology **55,** 373-399.

Arabidopsis Genome Initiative. (2000). Analysis of the genome sequence of the flowering plant *Arabidopsis thaliana*. Nature **408,** 796-813.

Arenas, Y.C., Kalkman, E., Schouten, A., Dieho, M., Vredenbregt, P., Uwumukiza, B., Ruiz, M.O., and van Kan, J.A.L. (2010). Functional analysis and mode of action of phytotoxic Nep1-like proteins of *Botrytis cinerea*. Physiological and Molecular Plant Pathology **74,** 376-386.

Argyros, R.D., Mathews, D.E., Chiang, Y.H., Palmer, C.M., Thibault, D.M., Etheridge, N., Argyros, D.A., Mason, M.G., Kieber, J.J., and Schaller, G.E. (2008). Type B response regulators of *Arabidopsis* play key roles in cytokinin signaling and plant development. Plant Cell **20,** 2102-2116.

Asai, S., and Yoshioka, H. (2009). Nitric oxide as a partner of reactive oxygen species participates in disease resistance to necrotrophic pathogen *Botrytis cinerea* in *Nicotiana benthamiana*. Mol. Plant-Microbe Interact. **22,** 619-629.

Asai, S., Mase, K., and Yoshioka, H. (2010). Role of nitric oxide and reactive oxide species in disease resistance to necrotrophic pathogens. Plant signaling & behavior **5,** 872-874.

Aspe, M.P., Sottosanto, J.B., and Blumwald, E. (2003). Vacuolar cation/H^+ exchange, ion homeostasis, and leaf development are altered in a T-DNA insertional mutant of *AtNHX1,* the *Arabidopsis* vacuolar Na^+/H^+ antiporter. Plant J. **36,** 229-239.

Asselbergh, B., and Hofte, M. (2007). Basal tomato defences to *Botrytis cinerea* include abscisic acid-dependent callose formation. Physiological and Molecular Plant Pathology **71,** 33-40.

Asselbergh, B., De Vleesschauwer, D., and Hofte, M. (2008). Global switches and fine-tuning - ABA modulates plant pathogen defense. Mol. Plant-Microbe Interact. **21,** 709-719.

Asselbergh, B., Curvers, K., Franca, S.C., Audenaert, K., Vuylsteke, M., Van Breusegem, F., and Hofte, M. (2007). Resistance to *Botrytis cinerea* in *sitiens*, an abscisic acid-deficient tomato mutant, involves timely production of hydrogen peroxide and cell wall modifications in the epidermis. Plant Physiol. **144,** 1863-1877.

Audenaert, K., De Meyer, G.B., and Hofte, M.M. (2002). Abscisic acid determines basal susceptibility of tomato to *Botrytis cinerea* and suppresses salicylic acid-dependent signaling mechanisms. Plant Physiol. **128,** 491-501.

Bailey-Serres, J., and Mittler, R. (2006). The roles of reactive oxygen species in plant cells. Plant Physiol. **141,** 311-311.

Bargmann, B.O.R., Laxalt, A.M., Riet, B.T., van Schooten, B., Merquiol, E., Testerink, C., Haring, M.A., Bartels, D., and Munnik, T. (2009). Multiple PLDs required for high salinity and water deficit tolerance in plants. Plant and Cell Physiology **50,** 78-89.

Bashan, Y., Sharon, E., Okon, Y., and Henis, Y. (1981). Scanning electron and light microscopy of infection and symptom development in tomato leaves infected with *Pseudomonas tomato*. Physiological Plant Pathology **19,** 139-144.

Batelli, G., Verslues, P.E., Agius, F., Qiu, Q., Fujii, H., Pan, S., Schumaker, K.S., Grillo, S., and Zhu, J.K. (2007). SOS2 promotes salt tolerance in part by interacting with the vacuolar H^+-ATPase and upregulating its transport activity. Molecular and Cellular Biology **27,** 7781-7790.

Battaglia, M., Olvera-Carrillo, Y., Garciarrubio, A., Campos, F., and Covarrubias, A.A. (2008). The enigmatic LEA proteins and other hydrophillins. Plant Physiol. **148,** 6-24.

Bender, C.L., Alarcon-Chaidez, F., and Gross, D.C. (1998). *Pseudomonas syringae* phytotoxins: mode of action, regulation and biosynthesis by peptide and polyketide synthetases. Microbiology and Molecular Biology Reviews **63,** 266-292.

Benedetti, C.E., and Arruda, P. (2002). Altering the expression of the chlorophyllase gene *ATHCOR1* in transgenic *Arabidopsis* caused changes in the chlorophyll-to-chlorophyllide ratio. Plant Physiol. **128,** 1255-1263.

Benedetti, C.E., Costa, C.L., R., T.S., and Arrunda, P. (1998). Differential expression of a novel gene in response to coronatine, methyl jasmonate, and wounding in the *Coi1* mutant of *Arabidopsis*. Plant Physiol. **1998,** 1037-1042.

Bennett, R.N., and Wallsgrove, R.M. (1994). Secondary metabolites in plant defence mechanisms. New Phytol. **127,** 617-633.

Benz, R. (1988). Structure and function of porins from gram-negative bacteria. Annual Review of Microbiology **42,** 359-393.

Bessire, M., Chassot, C., Jacquat, A.C., Humphry, M., Borel, S., Petetot, J.M.C., Metraux, J.P., and Nawrath, C. (2007). A permeable cuticle in *Arabidopsis* leads to a strong resistance to *Botrytis cinerea*. EMBO Journal **26,** 2158-2168.

Bisson, M.M.A., and Groth, G. (2010). New Insight in Ethylene Signaling: Autokinase Activity of ETR1 Modulates the Interaction of Receptors and EIN2. Molecular Plant **3,** 882-889.

Blakeman, J.P. (1975). Germination of *Botrytis cinerea* conidia in vitro in relation to nutrient conditions on leaf surfaces. Transactions of the British Mycological Society **65,** 239-247.

Blatt, M.R. (2000). Cellular Signalling and Volume Control in Stomatal Movements in Plants. Annual Review of Cell and Developmental Biology **16,** 221-241.

Block, A., Schmelz, E., Jones, J.B., and Klee, H.J. (2005). Coronatine and salicylic acid: the battle between *Arabidopsis* and *Pseudomonas* for phytohormone control. Molecular Plant Pathology **6,** 79-83.

Boller, T., and He, S.Y. (2009). Innate Immunity in Plants: An Arms Race Between Pattern Recognition Receptors in Plants and Effectors in Microbial Pathogens. Science **324,** 742-744.

Brimner, T.A., and Boland, G.J. (2003). A review of the non-target effects of fungi used to biologically control plant diseases. Agric. Ecosyst. Environ. **100,** 3-16.

Brooks, D.M., Bender, C.L., and Kunkel, B.N. (2005). The *Pseudomonas syringae* phytotoxin coronatine promotes virulence by overcoming salicylic acid-dependent defences in *Arabidopsis thaliana*. Molecular Plant Pathology **6,** 629-639.

Brooks, D.M., Hernandez-Guzman, G., Kloek, A.P., Alarcon-Chaidez, F., Sreedharan, A., Rangaswamy, V., Penaloza-Vazquez, A., Bender, C.L., and Kunkel, B.N. (2004). Identification and characterization of a well-defined series of coronatine biosynthetic mutants of *Pseudomonas syringae* pv. *tomato* DC3000. Mol. Plant-Microbe Interact. **17,** 162-174.

Buell, C.R., Joardar, V., Lindeberg, M., Selengut, J., Paulsen, I.T., Gwinn, M.L., Dodson, R.J., Deboy, R.T., Durkin, A.S., Kolonay, J.F., Madupu, R., Daugherty, S., Brinkac, L., Beanan, M.J., Haft, D.H., Nelson, W.C., Davidsen, T., Zafar, N., Zhou, L., Liu, J., Yuan, Q., Khouri, H., Fedorova, N., Tran, B., Russell, D., Berry, K., Utterback, T., Van Aken, S.E., Feldblyum, T.V., D'Ascenzo, M., Deng, W.-L., Ramos, A.R., Alfano, J.R., Cartinhour, S., Chatterjee, A.K., Delaney, T.P., Lazarowitz, S.G., Martin, G.B., Schneider, D.J., Tang, X., Bender, C.L., White, O., Fraser, C.M., and Collmer, A. (2003). The complete genome sequence of the *Arabidopsis* and tomato pathogen *Pseudomonas syringae* pv. *tomato* DC3000. Proceedings of the National Academy of Sciences of the United States of America **100,** 10181-10186.

Buist, G., Steen, A., Kok, J., and Kuipers, O.P. (2008). LysM, a widely distributed protein motif for binding to (peptido)glycans. Molecular Microbiology **68,** 838-847.

Bulawa, C.E. (1993). Genetics and Molecular Biology of Chitin Synthesis in Fungi. Annual Review of Microbiology **47,** 505-534.

Causier, B., and Davies, B. (2002). Analysing protein-protein interactions with the yeast two-hybrid system. Plant Molecular Biology **50,** 855-870.

Century, K.S., Holub, E.B., and Staskawicz, B.J. (1995). NDR1, a locus of *Arabidopsis thaliana* that is required for disease resistance to both bacterial and a fungal pathogen. Proceedings of the National Academy of Sciences of the United States of America **92,** 6597-6601.

Chague, V., Danit, L.V., Siewers, V., Gronover, C.S., Tudzynski, P., Tudzynski, B., and Sharon, A. (2006). Ethylene sensing and gene activation in *Botrytis cinerea*: A missing link in ethylene regulation of fungus-plant interactions? Mol. Plant-Microbe Interact. **19,** 33-42.

Chang, C., Kwok, S.F., Bleecker, A.B., and Meyerowitz, E.M. (1993). *Arabidopsis* Ethylene-Response Gene ETR1: Similarity of Product to Two-Component Regulators. Science **262,** 539-544.

Chassot, C., Nawrath, C., and Metraux, J.-P. (2008a). The cuticle: Not only a barrier for plant defence, a novel defence syndrome in plants with cuticular defects. Plant Signal Behav **3,** 142-144.

Chassot, C., Buchala, A., Schoonbeek, H.J., Metraux, J.P., and Lamotte, O. (2008b). Wounding of *Arabidopsis* leaves causes a powerful but transient protection against *Botrytis* infection. Plant J. **55,** 555-567.

Chaves, M.M., Flexas, J., and Pinheiro, C. (2009). Photosynthesis under drought and salt stress: regulation mechanisms from whole plant to cell. Annals of Botany **103,** 551-560.

Chen, Z., Zheng, Z., Huang, J., Lai, Z., and Fan, B. (2009). Biosynthesis of salicylic acid in plants. Plant Signaling and Behaviour **4,** 493-496.

Chenna, R., Sugawara, H., Hideaki, K., Tadashi, L., Rodrigo, G., Gibson, T.J., Higgins, D.G., and Thompson, J.D. (2003). Multiple sequence alignment with the Clustal series of programs. Nucleic Acids Research **31,** 3497-3500.

Chinchilla, D., Bauer, Z., Regenass, M., Boller, T., and Felix, G. (2006). The *Arabidopsis* Receptor Kinase FLS2 Binds flg22 and Determines the Specificity of Flagellin Perception. Plant Cell **18,** 465-476.

Chinchilla, D., Zipfel, C., Robatzek, S., Kemmerling, B., Nurnberger, T., Jones, J.D.G., Felix, G., and Boller, T. (2007). A flagellin-induced complex of the receptor FLS2 and BAK1 initiates plant defence. Nature **448,** 497-500.

Chinnusamy, V., Schumaker, K., and Zhu, J.K. (2004). Molecular genetic perspectives on cross-talk and specificity in abiotic stress signalling in plants. J. Exp. Bot. **55,** 225-236.

Chinnusamy, V., Jagendorf, A., and Zhu, J.K. (2005). Understanding and improving salt tolerance in plants. Crop Sci. **45,** 437-448.

Chinnusamy, V., Zhu, J., and Zhu, J.K. (2007). Cold stress regulation of gene expression in plants. Trends Plant Sci. **12,** 444-451.

Cho, Y.H., and Yoo, S.D. (2007). ETHYLENE RESPONSE 1 histidine kinase activity of *Arabidopsis* promotes plant growth. Plant Physiol. **143,** 612-616.

Choi, J., Huh, S.U., Kojima, M., Sakakibara, H., Paek, K.H., and Hwang, I. (2010). The Cytokinin-Activated Transcription Factor ARR2 Promotes Plant Immunity via TGA3/NPR1-Dependent Salicylic Acid Signaling in *Arabidopsis*. Developmental Cell **19,** 284-295.

Choquer, M., Fournier, E., Kunz, C., Levis, C., Pradier, J., Simon, A., and Viaud, M. (2007). *Botrytis cinerea* virulence factors: new insights into a necrotrophic and polyphageous pathogen. FEMS Microbiol Lett **277,** 1 - 10.

Chung, E.-H., da Cunha, L., Wu, A.-J., Gao, Z., Cherkis, K., Afzal, A.J., Mackey, D., and Dangl, J.L. (2011). Specific Threonine Phosphorylation of a Host Target by Two Unrelated Type III Effectors Activates a Host Innate Immune Receptor in Plants. Cell Host & Microbe **9,** 125-136.

Chung, J.S., Zhu, J.K., Bressan, R.A., Hasegawa, P.M., and Shi, H.H. (2008). Reactive oxygen species mediate Na^+-induced *SOS1* mRNA stability in Arabidopsis. Plant J. **53,** 554-565.

Clark, C.A., and Lorbeer, J.W. (1977). The role of phyllosphere bacteria in pathogenesis of *Botrytis squamosa* and *B. cinerea* on onion leaves. Phytopathology **67,** 96-100.

Clarke, S.M., Mur, L.A.J., Wood, J.E., and Scott, I.M. (2004). Salicylic acid dependent signaling promotes basal thermotolerance but is not essential for acquired thermotolerance in *Arabidopsis thaliana*. Plant J. **38,** 432-447.

Collmer, A., Badel, J.L., Charkowski, A.O., Deng, W.-L., Fouts, D.E., Ramos, A.R., Rehm, A.H., Anderson, D.M., Schneewind, O., van Dijk, K., and Alfano, J.R. (2000). *Pseudomonas syringae* Hrp type III secretion system and effector proteins. Proceedings of the National Academy of Sciences of the United States of America **97,** 8770-8777.

Colmenares, A.J., Aleu, J., Duran-Patron, R., Collado, I.G., and Hernandez-Galan, R. (2002). The putative role of botrydial and related metabolites in the infection mechanism of *Botrytis cinerea*. J. Chem. Ecol. **28,** 997-1005.

Coppinger, P., Repetti, P.P., Day, B., Dahlbeck, D., Mehlert, A., and Staskawicz, B.J. (2004). Overexpression of the plasma membrane-localized NDR1 protein results in enhanced bacterial disease resistance in *Arabidopsis thaliana*. The Plant Journal **40,** 225-237.

Curvers, K., Seifi, H., Mouille, G., de Rycke, R., Asselbergh, B., Van Hecke, A., Vanderschaeghe, D., Hofte, H., Callewaert, N., Van Breusegem, F., and Hofte, M. (2010). Abscisic Acid Deficiency Causes Changes in Cuticle Permeability and Pectin Composition That Influence Tomato Resistance to *Botrytis cinerea*. Plant Physiol. **154,** 847-860.

Cutler, S.R., Rodriguez, P.L., Finkelstein, R.R., and Abrams, S.R. (2010). Abscisic acid: emergence of a core signaling network. Annual Review of Plant Biology **61**.

D'Auria, J., and Gershenzon, J. (2005). The secondary metabolism of *Arabiopsis thaliana:* growing like a weed. Current Opinion in Plant Biology **8,** 308-316.

Dalmais, B., Schumacher, J., Moraga, J., Le Pecheur, P., Tudzynski, B., Collado, I.G., and Viaud, M. (2011). The *Botrytis cinerea* phytotoxin botcinic acid requires two polyketide synthases for production and has a redundant role in virulence with botrydial. Molecular Plant Pathology**,** 564-579.

Dangl, J.L., and Jones, J.D.G. (2001). Plant pathogens and integrated defence responses to infection. Nature **411,** 826-833.

Davletova, S., Schlauch, K., Coutu, J., and Mittler, R. (2005). The zinc-finger protein Zat12 plays a central role in reactive oxygen and abiotic stress signaling in *Arabidopsis*. Plant Physiol. **139,** 847-856.

Day, B., Dahlbeck, D., and Staskawicz, B.J. (2006). NDR1 Interaction with RIN4 Mediates the Differential Activation of Multiple Disease Resistance Pathways in *Arabidopsis*. The Plant Cell Online **18,** 2782-2791.

de Castro, E., Sigrist, C.J.A., Gattiker, A., Bulliard, V., Langendijk-Genevaux, P.S., Gasteiger, E., Bairoch, A., and Hulo, N. (2006). ScanProsite: detection of PROSITE signature matches and ProRule-associated functional and structural residues in proteins. Nucleic Acids Research **34,** W362-W365.

de Torres, M., Mansfield, J.W., Grabov, N., Brown, I.R., Ammouneh, H., Tsiamis, G., Forsyth, A., Robatzek, S., Grant, M., and Boch, J. (2006). *Pseudomonas syringae* effector AvrPtoB suppresses basal defence in *Arabidopsis*. Plant J. **47,** 368-382.

de Torres Zabala, M., Bennett, M.H., Truman, W.H., and Grant, M.R. (2009). Antagonism between salicylic and abscisic acid reflects early host-pathogen conflict and moulds plant defence responses. Plant J **59,** 375-386.

de Torres Zabala, M., Truman, W., Bennett, M.H., Lafforgue, G., Mansfield, J.W., Egea, P.R., Bogre, L., and Grant, M. (2007). *Pseudomonas syringae* pv. *tomato* hijacks the *Arabidopsis* abscisic acid signalling pathway to cause disease. EMBO Journal **26,** 1434-1443.

DebRoy, S., Thilmony, R., Kwack, Y.-B., Nomura, K., and He, S.Y. (2004). A family of conserved bacterial effectors inhibits salicylic acid-mediated basal immunity and promotes disease necrosis in plants. Proceedings of the National Academy of Sciences of the United States of America **101,** 9927-9932.

del Rio, L.A., Corpas, F.J., Sandalio, L.M., Palma, J.M., Gomez, M., and Barroso, J.B. (2002). Reactive oxygen species, antioxidant systems and nitric oxide in peroxisomes. J. Exp. Bot. **53,** 1255-1272.

Denby, K.J., Kumar, P., and Kliebenstein, D.J. (2004). Identification of *Botrytis cinerea* susceptibility loci in *Arabidopsis thaliana*. Plant J. **38,** 473-486.

Desikan, R., Hancock, J.T., and Neill, S.J. (2005a). Reactive oxygen species as signalling molecules. In Antioxidants and Reactive Oxygen Species in Plants, N. Smirnoff, ed (Oxford: Blackwell), pp. 167-195.

Desikan, R., Hancock, J.T., Bright, J., Harrison, J., Weir, L., Hooley, R., and Neill, S.J. (2005b). A role for ETR1 in hydrogen peroxide signaling in stomatal guard cells. Plant Physiol. **137,** 831-834.

Desikan, R., Last, K., Harrett-Williams, R., Tagliavia, C., Harter, K., Hooley, R., Hancock, J.T., and Neill, S.J. (2006). Ethylene-induced stomatal closure in *Arabidopsis* occurs via AtrbohF-mediated hydrogen peroxide synthesis. Plant J. **47,** 907-916.

Desikan, R., Horak, J., Chaban, C., Mira-Rodado, V., Witthoft, J., Elgass, K., Grefen, C., Cheung, M.K., Meixner, A.J., Hooley, R., Neill, S.J., Hancock, J.T., and Harter, K. (2008). The Histidine Kinase AHK5 Integrates Endogenous and Environmental Signals in *Arabidopsis* Guard Cells. Plos One **3,** 15.

Despres, C., Chubak, C., Rochon, A., Clark, R., Bethune, T., Desveaux, D., and Fbert, P.R. (2003). The *Arabidpsis* NDR1 disease resistance protein is a novel cofactor that confers redox regulation of DNA binding activity to the basic domain/leucine zipper transcription factor TGA1. Plant Cell **15,** 2181-2191.

Dodds, P.N., and Rathjen, J.P. (2010). Plant immunity: towards an integrated view of plant-pathogen interactions. Nat. Rev. Genet. **11,** 539-548.

Doehlemann, G., Berndt, P., and Hahn, M. (2006). Different signalling pathways involving a Gα protein, cAMP and a MAP kinase control germination of Botrytis cinerea conidia. Molecular Microbiology **59,** 821-835.

Dortay, H., Mehnert, N., Burkle, L., Schumulling, T., and Heyl, A. (2006). Analysis of protein interactions within the cytokinin-signaling pathway of *Arabidopsis thaliana*. The FEBS Journal **273,** 4631-4644.

Dortay, H., Gruhn, N., Pfeifer, A., Schwerdtner, M., Schmulling, T., and Heyl, A. (2008). Toward an interaction map of the two-component signaling pathway of *Arabidopsis thaliana*. J. Proteome Res. **7,** 3649-3660.

Duckham, S.C., Linforth, R.S.T., and Taylor, I.B. (1991). Abscisic-acid-deficient mutants at the ABA gene locus of *Arabidopsis thaliana* are impaired in the epoxidation of zeaxanthin. Plant, Cell & Environment **14,** 601-606.

Durrant, W.E., and Dong, X. (2004). Systemic acquired resistance. Annu. Rev. Phytopathol. **42,** 185-209.

Ellouzi, H., Ben Hamed, K., Cela, J., Munné-Bosch, S., and Abdelly, C. (2011). Early effects of salt stress on the physiological and oxidative status of *Cakile maritima* (halophyte) and *Arabidopsis thaliana* (glycophyte). Physiologia Plantarum **142,** 128-143.

Espino, J.J., Gutierrez-Sanchez, G., Brito, N., Shah, P., Orlando, R., and Gonzalez, C. (2010). The *Botrytis cinerea* early secretome. Proteomics **10,** 3020-3034.

Falk, A., Feys, B.J., Frost, L.N., Jones, J.D.G., Daniels, M.J., and Parker, J.E. (1999). EDS1, an essential component of *R* gene-mediated disease resistance in *Arabidopsis* has homology to eukaryotic lipases. Proceedings of the National Academy of Sciences **96,** 3292-3297.

Fan, J., Hill, L., Crooks, C., Doerner, P., and Lamb, C. (2009). Abscisic acid has a key role in modulating diverse plant-pathogen interactions. Plant Physiol. **150,** 1750-1761.

Fernandez-Calvo, P., Chini, A., Fernandez-Barbero, G., Chico, J.-M., Gimenez-Ibanez, S., Geerinck, J., Eeckhout, D., Schweizer, F., Godoy, M., Franco-Zorrilla, J.M., Pauwels, L., Witters, E., Puga, M.I., Paz-Ares, J., Goossens, A., Reymond, P., De Jaeger, G., and Solano, R. (2011). The *Arabidopsis* bHLH Transcription Factors MYC3 and MYC4 Are Targets of JAZ Repressors and Act Additively with MYC2 in the Activation of Jasmonate Responses. The Plant Cell Online **23,** 701-715.

Ferrari, S., Plotnikova, J.M., De Lorenzo, G., and Ausubel, F.M. (2003). *Arabidopsis* local resistance to *Botrytis cinerea* involves salicylic acid and camalexin and requires EDS4 and PAD2, but not SID2, EDS5 or PAD4. Plant J. **35,** 193-205.

Ferrari, S., Galletti, R., Denoux, C., De Lorenzo, G., Ausubel, F.M., and Dewdney, J. (2007). Resistance to *Botrytis cinerea* induced in *Arabidopsis* by elicitors is independent of salicylic acid, ethylene, or jasmonate signaling but requires PHYTOALEXIN DEFICIENT3. Plant Physiol. **144,** 367-379.

Feys, B., Benedetti, C.E., Penfold, C.N., and Turner, J.G. (1994). *Arabidopsis* Mutants Selected for Resistance to the Phytotoxin Coronatine Are Male Sterile, Insensitive to Methyl Jasmonate, and Resistant to a Bacterial Pathogen. Plant Cell **6,** 751-759.

Feys, B.J., Moisan, L.J., Newman, M.-A., and Parker, J.E. (2001). Direct interaction between the *Arabidopsis* disease resistance signaling proteins, EDS1 and PAD4. EMBO J **20,** 5400-5411.

Feys, B.J., Wiermer, M., Bhat, R.A., Moisan, L.J., Medina-Escobar, N., Neu, C., Cabral, A., and Parker, J.E. (2005). Arabidopsis SENESCENCE-ASSOCIATED GENE101 Stabilizes and Signals within an ENHANCED DISEASE SUSCEPTIBILITY1 Complex in Plant Innate Immunity. The Plant Cell Online **17,** 2601-2613.

Flowers, T.J. (2004). Improving crop salt tolerance. J. Exp. Bot. **55,** 307-319.

Fobert, P.R., and Després, C. (2005). Redox control of systemic acquired resistance. Current Opinion in Plant Biology **8,** 378-382.

Forcat, S., Bennett, M.H., Mansfield, J.W., and Grant, M.R. (2008). A rapid and robust method for simultaneously measuring changes in the phytohormones ABA, JA and SA in plants following biotic and abiotic stress. Plant Methods **4,** 8.

Forcat, S., Bennett, M., Grant, M., and Mansfield, J.W. (2010). Rapid linkage of indole carboxylic acid to the plant cell wall identified as a component of basal defence in *Arabidopsis* against *hrp* mutant bacteria. Phytochemistry **71,** 870-876.

Forst, S.A., and Roberts, D.L. (1994). Signal transduction by the EnvZ-OmpR phosphotransfer system in bacteria. Research in Microbiology **145,** 363-373.

Forsyth, A., Mansfield, J., Gabov, N., de Torres, M., Sinapidou, E., and Grant, M. (2010). Genetic dissection of basal resistance to *Pseudomonas syringae* pv. *phaseolicola* in accessions of *Arabidopsis*. Mol. Plant-Microbe Interact. **23,** 1545-1552.

Foyer, C.H., and Noctor, G. (2005). Redox Homeostasis and Antioxidant Signaling: A Metabolic Interface between Stress Perception and Physiological Responses. The Plant Cell Online **17,** 1866-1875.

Freeman, B.C., and Beattie, G.A. (2008). An overview of plant defences against pathogens and herbivores. In The Plant Health Instructor (APSnet).

Freeman, B.C., and Beattie, G.A. (2009). Bacterial growth restriction during host resistance to *Pseudomonas syringae* is associated with leaf water loss and localized cessation of vascular activity in *Arabidopsis thaliana*. Mol. Plant-Microbe Interact. **22,** 857-867.

Fu, Z.Q., Guo, M., Jeong, B.-R., Tian, F., Elthon, T.E., Cerny, R.L., Staiger, D., and Alfano, J.R. (2007). A type III effector ADP-ribosylates RNA-binding proteins and quells plant immunity. Nature **447,** 284-288.

Gaffney, T., Friedrich, L., Vernooij, B., Negrotto, D., Nye, G., Uknes, S., Ward, E., Kessmann, H., and Ryals, J. (1993). Requirement for the induction of systemic acquired resistance. Science **261,** 754-756.

Galletti, R., De Lorenzo, G., and Ferrari, S. (2009). Host-derived signals activate plant innate immunity. Plant Signal Behav **4,** 33-34.

Gamble, R.L., Qu, X., and Schaller, G.E. (2002). Mutational analysis of the ethylene receptor ETR1. Role of the histidine kinase domain in dominant ethylene insensitivity. Plant Physiol. **128,** 1428-1438.

Gaspar, T., Franck, T., Bisbis, B., Kevers, C., Jouve, L., Hausman, J.F., and Dommes, J. (2002). Concepts in plant stress physiology. Application to plant tissue cultures. Plant Growth Regulation **37,** 263-285.

Gassmann, W. (2005). Natural variation in the *Arabidopsis* response to the avirulence gene *hopPsyA* uncouples the hypersensitive response from disease resistance. Mol. Plant-Microbe Interact. **18,** 1054-1060.

Gimenez-Ibanez, S., and Rathjen, J.P. (2010). The case for the defense: plants versus *Pseudomonas syringae*. Microbes and Infection **12,** 428-437.

Gimenez-Ibanez, S., Ntoukakis, V., and Rathjen, J.P. (2009a). The LysM receptor kinase CERK1 mediates bacterial perception in *Arabidopsis*. Plant Signal Behav **4,** 539-541.

Gimenez-Ibanez, S., Hann, D.R., Ntoukakis, V., Petutschnig, E., Lipka, V., and Rathjen, J.P. (2009b). AvrPtoB Targets the LysM Receptor Kinase CERK1 to Promote Bacterial Virulence on Plants. Current Biology **19,** 423-429.

Glawischnig, E. (2006). The role of cytochrome P450 enzymes in the biosynthesis of camalexin. Biochemical Society Transactions **34,** 1206-1208.

Glawischnig, E. (2007). Camalexin. Phytochemistry **68,** 401-406.

Glazebrook, J. (2005). Contrasting mechanisms of defense against biotrophic and necrotrophic pathogens. Annu. Rev. Phytopathol. **43,** 205-227.

Goel, A.K., Lundberg, D., Torres, M.A., Matthews, R., Akimoto-Tomiyama, C., Farmer, L., Dangl, J.L., and Grant, S.R. (2008). The *Pseudomonas syringae* Type III Effector HopAM1 Enhances Virulence on Water-Stressed Plants. Mol. Plant-Microbe Interact. **21,** 361-370.

Göhre, V., Spallek, T., Häweker, H., Mersmann, S., Mentzel, T., Boller, T., de Torres, M., Mansfield, J.W., and Robatzek, S. (2008). Plant Pattern-Recognition Receptor FLS2 Is Directed for Degradation by the Bacterial Ubiquitin Ligase AvrPtoB. Current Biology **18,** 1824-1832.

Gómez-Gómez, L., and Boller, T. (2000). FLS2: An LRR Receptor-like Kinase Involved in the Perception of the Bacterial Elicitor Flagellin in *Arabidopsis*. Molecular Cell **5,** 1003-1011.

Gong, Z.Z., Koiwa, H., Cushman, M.A., Ray, A., Bufford, D., Kore-eda, S., Matsumoto, T.K., Zhu, J.H., Cushman, J.C., Bressan, R.A., and Hasegawa, P.M. (2001). Genes that are uniquely stress regulated in *salt overly sensitive (sos)* mutants. Plant Physiol. **126,** 363-375.

Govrin, E.M., and Levine, A. (2000). The hypersensitive response facilitates plant infection by the necrotrophic pathogen *Botrytis cinerea*. Current Biology **10,** 751-757.

Govrin, E.M., and Levine, A. (2002). Infection of *Arabidopsis* with a necrotrophoc pathogen, *Botrytis cinerea*, elicits various defence responses but does not induce systemic acquired resistance (SAR). Plant Molecular Biology **48,** 267-276.

Govrin, E.M., Rachmilevitch, S., Tiwari, B.S., Soloman, M., and Levine, A. (2006). An elicitor from *Botrytis cinerea* induces the hypersensitive response in *Arabidopsis thaliana* and other plants and promotes the gray mold disease. Phytopathology **96,** 299-307.

Grant, S.R., Fisher, E.J., Chang, J.H., Mole, B.M., and Dangl, J.L. (2006). Subterfuge and Manipulation: Type III Effector Proteins of Phytopathogenic Bacteria. Annual Review of Microbiology **60,** 425-449.

Grefen, C., and Harter, K. (2004). Plant two-component systems: principles, functions, complexity and cross talk. Planta **219,** 733-742.

Hagemeier, J., Schneider, B., Oldham, N.J., and Hahlbrock, K. (2001). Accumulation of soluble and wall-bound indolic metabolites in *Arabidopsis thaliana* leaves infected with viruent or avirulent *Pseudomonas syringae* pathovar tomato strains. Proceedings of the National Academy of Sciences **98,** 753-758.

Hahn, A., and Harter, K. (2009). Mitogen-Activated Protein Kinase Cascades and Ethylene: Signaling, Biosynthesis, or Both? Plant Physiol. **149,** 1207-1210.

Halliwell, B. (2006). Reactive species and antioxidants. Redox biology is a fundamental theme of aerobic life. Plant Physiol. **141,** 312-322.

Halperin, S.J., and Lynch, J.P. (2003). Effects of salinity on cytosolic Na^+ and K^+ in root hairs of *Arabidopsis thaliana: in vivo* measurements using the fluorescent dyes SBFI and PBFI. J. Exp. Bot. **54,** 2035-2043.

Hancock, J., Desikan, R., Harrison, J., Bright, J., Hooley, R., and Neill, S. (2006). Doing the unexpected: proteins involved in hydrogen peroxide perception. J. Exp. Bot. **57,** 1711-1718.

Hann, D.R., and Rathjen, J.P. (2010). The long and winding road: virulence effector proteins of plant pathogenic bacteria. Cellular and Molecular Life Sciences **67,** 3425-3434.

Hann, D.R., Gimenez-Ibanez, S., and Rathjen, J.P. (2010). Bacterial virulence effectors and their activities. Current Opinion in Plant Biology **13,** 388-393.

Hass, C., Lohrmann, J., Albrecht, V., Sweere, U., Hummel, F., Yoo, S.D., Hwang, I., Zhu, T., Schafer, E., Kudla, J., and Harter, K. (2004). The response regulator 2 mediates ethylene signalling and hormone signal integration in *Arabidopsis*. EMBO J **23,** 3290-3302.

Hayashi, M., and Maeda, T. (2006). Activation of the HOG Pathway upon Cold Stress in *Saccharomyces cerevisiae*. Journal of Biochemistry **139,** 797-803.

He, S.Y., and Jin, Q. (2003). The Hrp pilus: learning from flagella. Curr. Opin. Microbiol. **6,** 15-19.

Hejatko, J., Ryu, H., Kim, G.-T., Dobesova, R., Choi, S., Choi, S.M., Soucek, P., Horak, J., Pekarova, B., Palme, K., Brzobohaty, B., and Hwang, I. (2008). The Histidine Kinases CYTOKININ-INDEPENDENT1 and ARABIDOPSIS HISTIDINE KINASE2 and 3 Regulate Vascular Tissue Development in *Arabidopsis* Shoots. Plant Cell **21,** 2008-2021.

Hejátko, J., Pernisová, M., Eneva, T., Palme, K., and Brzobohatý, B. (2003). The putative sensor histidine kinase CKI1 is involved in female gametophyte development in female gametophyte development in *Arabidopsis*. Molecular Genetics and Genomics **269,** 443-453.

Heller, J., and Tudzynsk, B. (2011). Reactive oxygen species in phytopathogenic fungi: signaling, development and disease. Annu. Rev. Phytopathol. **49,** 16.11-16.22.

Heyl, A., Wulfetange, K., Pils, B., Nielsen, N., Romanov, G.A., and Schmulling, T. (2007). Evolutioary proteomics identifies amino acids essential for ligand-binding of the cytokinin receptor CHASE domain. BMC Evolutionary Biology **7**.

Higo, K., Ugawa, Y., Iwamoto, M., and Korenaga, T. (1999). Plant cis-acting regulatory DNA elements (PLACE) database: 1999. Nucleic Acids Research **27,** 297-300.

Higuchi, M., Pischke, M.S., Mähönen, A.P., Miyawaki, K., Hashimoto, Y., Seki, M., Kobayashi, M., Shinozaki, K., Kato, T., Tabata, S., Helariutta, Y., Sussman, M.R., and Kakimoto, T. (2004). In planta functions of the *Arabidopsis* cytokinin receptor family. Proceedings of the National Academy of Sciences of the United States of America **101,** 8821-8826.

Hirosawa, M., Hoshida, M., Ishikawa, M., and Toya, T. (1993). MASCOT: multiple alignment system for protein sequences based on three-way dynamic programming. Computer Applications in the Biosciences **9,** 161-167.

Hogenhout, S.A., Van der Hoorn, R.A.L., Terauchi, R., and Kamoun, S. (2009). Emerging Concepts in Effector Biology of Plant-Associated Organisms. Mol. Plant-Microbe Interact. **22,** 115-122.

Hong, S.W., Lee, U., and Vierling, E. (2003). Arabidopsis hot mutants define multiple functions required for acclimation to high temperatures. Plant Physiol. **132,** 757-767.

Hopkins, W.G. (1999). Introduction to Plant Physiology. (New York: John Wiley and Sons).

Hou, X.L., Lee, L.Y.C., Xia, K.F., Yen, Y.Y., and Yu, H. (2010). DELLAs Modulate Jasmonate Signaling via Competitive Binding to JAZs. Developmental Cell **19,** 884-894.

Hruz, T., Laule, O., Szabo, G., Wessendorp, F., Bleuler, S., Oertle, L., Widmayer, P., Gruissem, W., and Zimmermann, P. (2008). Genevestigator v3: a reference expression database for the meta-analysis of transcriptomes. Adv Bioinformatics **2008,** 420747.

Huang, J.K., Pray, C., and Rozelle, S. (2002). Enhancing the crops to feed the poor. Nature **418,** 678-684.

Hutchison, C.E., Li, J., Argueso, C., Gonzalez, M., Lee, E., Lewis, M.W., Maxwell, B.B., Perdue, T.D., Schaller, G.E., Alonso, J.M., Ecker, J.R., and Kieber, J.J. (2006). The *Arabidopsis* Histidine Phosphotransfer Proteins Are Redundant Positive Regulators of Cytokinin Signaling. Plant Cell **18,** 3073-3087.

Hwang, D., Chen, H.C., and Sheen, J. (2002). Two-component signal transduction pathways in *Arabidopsis*. Plant Physiol. **129,** 500-515.

Iizasa, E.i., Mitsutomi, M., and Nagano, Y. (2010). Direct Binding of a Plant LysM Receptor-like Kinase, LysM RLK1/CERK1, to Chitin in Vitro. Journal of Biological Chemistry **285,** 2996-3004.

Ishida, K., Yamashino, T., Yokoyama, A., and Mizuno, T. (2008). Three Type-B Response Regulators, ARR1, ARR10 and ARR12, Play Essential but Redundant Roles in Cytokinin Signal Transduction Throughout the Life Cycle of *Arabidopsis thaliana*. Plant and Cell Physiology **49,** 47-57.

Ishiga, Y., Uppalapati, S., Ishiga, T., and Bender, C. (2010). Exogenous coronatine, but not coronafacic acid or methyl jasmonate, restores the disease phenotype of a coronatine-defective mutant of *Pseudomonas syringae* pv. *tomato* on tomato seedlings. Journal of General Plant Pathology **76,** 188-195.

Ishiga, Y., Uppalapati, S.R., Ishiga, T., Elavarthi, S., Martin, B., and Bender, C.L. (2009a). The phytotoxin coronatine induces light-dependent reactive oxygen species in tomato seedlings. New Phytol. **181,** 147-160.

Ishiga, Y., Uppalapati, S.R., Ishiga, T., Elavarthi, S., Martin, B., and Bender, C.L. (2009b). Involvement of coronatine-inducible reactive oxygen species in bacterial speck disease of tomato. Plant Signaling and Behaviour **4,** 237-239.

Ishitani, M., Liu, J.P., Halfter, U., Kim, C.S., Shi, W.M., and Zhu, J.K. (2000). SOS3 function in plant salt tolerance requires N-myristoylation and calcium binding. Plant Cell **12,** 1667-1677.

Iwama, A., Yamashino, T., Tanaka, Y., Sakakibara, H., Kakimoto, T., Sato, S., Kato, T., Tabata, S., Nagatani, A., and Mizuno, T. (2007). AHK5 histidine kinase regulates root elongation through an ETR1-dependent abscisic acid and ethylene signaling pathway in *Arabidopsis thaliana*. Plant and Cell Physiology **48,** 375-380.

Jacob, T., Ritchie, S., Assmann, S.M., and Gilroy, S. (1999). Abscisic acid signal transduction in guard cells is mediated by phospholipase D activity. Proceedings of the National Academy of Sciences of the United States of America **96,** 12192-12197.

Jakab, G., Ton, J., Flors, V., Zimmerli, L., Metraux, J.P., and Mauch-Mani, B. (2005). Enhancing *Arabidopsis* salt and drought stress tolerance by chemical priming for its abscisic acid responses. Plant Physiol. **139,** 267-274.

Jansen, M.A.K., and van den Noort, R.E. (2000). Ultraviolet-B radiation induces complex alterations in stomatal behaviour. Physiologia Plantarum **110,** 189-194.

Jelenska, J., Yao, N., Vinatzer, B.A., Wright, C.M., Brodsky, J.L., and Greenberg, J.T. (2007). A J Domain Virulence Effector of *Pseudomonas syringae* Remodels Host Chloroplasts and Suppresses Defenses. Current Biology **17,** 499-508.

Jeon, J., Kim, N.Y., Kim, S., Kang, N.Y., Novak, O., Ku, S.-J., Cho, C., Lee, D.J., Lee, E.-J., Strnad, M., and Kim, J. (2010). A Subset of Cytokinin Two-component Signaling System Plays a Role in Cold Temperature Stress Response in *Arabidopsis*. Journal of Biological Chemistry **285,** 23371-23386.

Jha, D., Shirley, N., Tester, M., and Roy, S.J. (2010). Variation in salinity tolerance and shoot sodium accumulation in *Arabidopsis* ecotypes linked to differences in the natural expression levels of transporters involved in sodium transport. Plant, Cell & Environment **33,** 793-804.

Jiang, L., He, L., and Fountoulakis, M. (2004). Comparison of protein precipitation methods for sample preparation prior to proteomic analysis. Journal of Chromatography A **1023,** 317-320.

Jiang, X., Leidi, E.O., and Pardon, J.M. (2010). How do vacuolar NHX exchanges function in plant salt tolerance? Plant Signalling and Behaviour **5,** 792-795.

Jin, Q., and He, S.-Y. (2001). Role of the Hrp Pilus in Type III Protein Secretion in *Pseudomonas syringae*. Science **294,** 2556-2558.

Joardar, V., Lindeberg, M., Jackson, R.W., Selengut, J., Dodson, R., Brinkac, L.M., Daugherty, S.C., DeBoy, R., Durkin, A.S., Giglio, M.G., Madupu, R., Nelson, W.C., Rosovitz, M.J., Sullivan, S., Crabtree, J., Creasy, T., Davidsen, T., Haft, D.H., Zafar, N., Zhou, L.W., Halpin, R., Holley, T., Khouri, H., Feldblyum, T., White, O., Fraser, C.M., Chatterjee, A.K., Cartinhour, S., Schneider, D.J., Mansfield, J., Collmer, A., and Buell, C.R. (2005). Whole-genome sequence analysis of *Pseudomonas syringae* pv. *phaseolicola* 1448A reveals divergence among pathovars in genes involved in virulence and transposition. Journal of Bacteriology **187,** 6488-6498.

Johansson, J.F., Paul, L.R., and Finlay, R.D. (2004). Microbial interactions in the mycorrhizosphere and their significance for sustainable agriculture. FEMS Microbiology Ecology **48,** 1-13.

Jones, A.M.E., Thomas, V., Truman, B., Lilley, K., Mansfield, J., and Grant, M. (2004). Specific changes in the *Arabidopsis* proteome in response to bacterial challenge: differentiating basal and *R*-gene mediated resistance. Phytochemistry **65,** 1805-1816.

Jones, J.D.G., and Dangl, J.L. (2006). The plant immune system. Nature **444,** 323-329.

Kaeriyama, M., Machida, K., Kitakaze, A., Wang, H., Lao, Q., Fukamachi, T., Saito, H., and Kobayashi, H. (2006). OmpC and OmpF are required for growth under hyperosmotic stress above pH 8 in *Escherichia coli*. Lett. Appl. Microbiol. **42,** 195-201.

Kaffarnik, F.A.R., Jones, A.M.E., Rathjen, J.P., and Peck, S.C. (2009). Effector Proteins of the Bacterial Pathogen Pseudomonas syringae Alter the Extracellular Proteome of the Host Plant, Arabidopsis thaliana. Molecular & Cellular Proteomics **8,** 145-156.

Kakimoto, T. (1996). CKI1, a histidine kinase homolog implicated in cytokinin signal transduction. Science **274,** 982-985.

Kakimoto, T. (1998). Cytokinin signaling. Current Opinion in Plant Biology **1,** 399-403.

Kakimoto, T. (2003). Perception and signal transduction of cytokinins. Annual Review of Plant Biology **54,** 605-627.

Kars, I., Krooshof, G.H., Wagemakers, L., Joosten, R., Benen, J.A.E., and van Kan, J.A.L. (2005). Necrotizing activity of five *Botrytis cinerea* endopolygalacturonases produced in *Pichia pastoris*. Plant J. **43,** 213-225.

Katagiri, F., Thilmony, R., and He, S.Y. (2002). The *Arabidopsis thaliana-Pseudomonas syringae* Interaction. The Arabidopsis Book **1,** 1-35.

Katiyar-Agarwal, S., Zhu, J., Kim, K., Agarwal, M., Fu, X., Huang, A., and Zhu, J.K. (2006). The plasma membrane Na^+/H^+ antiporter SOS1 interacts with RCD1 and functions in oxidative stress tolerance in *Arabidopsis*. Proceedings of the National Academy of Sciences of the United States of America **103,** 18816-18821.

Katsir, L., Schilmiller, A.L., Staswick, P.E., He, S.Y., and Howe, G.A. (2008). COI1 is a critical component of a receptor for jasmonate and the bacterial virulence factor coronatine. Proceedings of the National Academy of Sciences of the United States of America **105,** 7100-7105.

Kerstiens, G. (1996). Signalling across the divide: a wider perspective of cuticular structure-function relationships. Trends Plant Sci. **1,** 125-129.

Kesarwani, M., Yoo, J., and Dong, X. (2007). Genetic Interactions of TGA Transcription Factors in the Regulation of Pathogenesis-Related Genes and Disease Resistance in *Arabidopsis*. Plant Physiol. **144,** 336-346.

Kim, H.-S., Desveaux, D., Singer, A.U., Patel, P., Sondek, J., and Dangl, J.L. (2005a). The Pseudomonas syringae effector AvrRpt2 cleaves its C-terminally acylated target, RIN4, from Arabidopsis membranes to block RPM1 activation. Proceedings of the National Academy of Sciences of the United States of America **102,** 6496-6501.

Kim, M.G., da Cunha, L., McFall, A.J., Belkhadir, Y., DebRoy, S., Dangl, J.L., and Mackey, D. (2005b). Two *Pseudomonas syringae* Type III Effectors Inhibit RIN4-Regulated Basal Defense in *Arabidopsis*. Cell **121,** 749-759.

Kinkema, M., Fan, W., and Dong, X. (2000). Nuclear localization of NPR1 is required for activatin of *PR* gene expression. Plant Cell **12,** 2339-2350.

Kishor, P.B.K., Hong, Z., Miao, G.H., Hu, C.A.A., and Verma, D.P.S. (1995). Overexpression of *[delta]-Pyrroline-5-Carboxylate Synthetase* Increases Proline Production and Confers Osmotolerance in Transgenic Plants. Plant Physiol. **108,** 1387-1394.

Kliebenstein, D.J. (2004). Secondary metabolites and plant/environment interactions: a view through *Arabidopsis thaliana* tinged glasses. Plant, Cell & Environment **27,** 675-684.

Kliebenstein, D.J., and Rowe, H.C. (2008). Ecological costs of biotrophic versus necrotrophic pathogen resistance, the hypersensitive response and signal transduction. Plant Sci. **174,** 551-556.

Kliebenstein, D.J., Rowe, H.C., and Denby, K.J. (2005). Secondary metabolites influence *Arabidopsis/Botrytis* interactions: variation in host production and pathogen sensitivity. Plant J. **44,** 25-36.

Kloek, A.P., Verbsky, M.L., Sharma, S.B., Schoelz, J.E., Vogel, J., Klessig, D.F., and Kunkel, B.N. (2001). Resistance to *Pseudomonas syringae* conferred by an *Arabidopsis thaliana coronatine-insensitive (coi1)* mutation occurs through two distinct mechanisms. Plant J. **26,** 509-522.

Konig, J., Baier, M., Horling, F., Kahmann, U., Harris, G., Scharmann, P., and Dietz, K.-J. (2002). The plant-specific function of 2-Cys peroxiredoxin-mediated detoxification of peroxides in the redox-hierarchy of photosynthetic electron flux. Proceedings of the National Academy of Sciences of the United States of America **99,** 5738-5743.

Koornneef, A., Leon-Reyes, A., Ritsema, T., Verhage, A., Den Otter, F.C., Van Loon, L.C., and Pieterse, C.M.J. (2008). Kinetics of salicylate-mediated suppression of jasmonate signaling reveal a role for redox modulation. Plant Physiol. **147,** 1358-1368.

Kotak, S., Larkindale, J., Lee, U., von Koskull-Doring, P., Vierling, E., and Scharf, K.D. (2007). Complexity of the heat stress response in plants. Current Opinion in Plant Biology **10,** 310-316.

Kronzucker, H.J., and Britto, D.T. (2011). Sodium transport in plants: a critical review. New Phytol. **189,** 54-81.

Kwak, J.M., Maser, P., and Schroeder, J.I. (2008). The clickable guard cell, version II: interactive model of guard cell signal transduction mechanisms and pathways. The Arabidopsis Book **6,** 1-18.

Kwak, J.M., Mori, I.C., Pei, Z.M., Leonhardt, N., Torres, M.A., Dangl, J.L., Bloom, R.E., Bodde, S., Jones, J.D.G., and Schroeder, J.I. (2003). NADPH oxidase *AtrbohD* and *AtrbohF* genes function in ROS-dependent ABA signaling in Arabidopsis. EMBO Journal **22,** 2623-2633.

Laluk, K., and Mengiste, T. (2010). Necrotroph attacks on plants: wanton destruction or covert extortion? The Arabidopsis Book **8,** 1-34.

Lamb, C., and Dixon, R.A. (1997). The oxidative burst in plant disease resistance. Annual Review of Plant Physiology **48,** 251-275.

Lan, C.Y., and Igo, M.M. (1998). Differential expression of the OmpF and OmpC porin proteins in *Escherichia coli* K-12 depends upon the level of active OmpR. Journal of Bacteriology **180,** 171-174.

Larkindale, J., and Knight, M.R. (2002). Protection against heat stress-induced oxidative damage in *Arabidopsis* involves calcium, abscisic acid, ethylene, and salicylic acid. Plant Physiol. **128,** 682-695.

Larkindale, J., Hall, J.D., Knight, M.R., and Vierling, E. (2005). Heat stress phenotypes of arabidopsis mutants implicate multiple signaling pathways in the acquisition of thermotolerance. Plant Physiol. **138,** 882-897.

Lee, B.H., and Zhu, J.K. (2009). Phenotypic analysis of *Arabidopis* mutants: root elongation under salt/ hormone-induced stress. Cold Spring Harb Protoc; 2009; doi:10.1101/pdb.prot4968.

Leon-Kloosterziel, K.M., Gil, M.A., Ruijs, G.J., Jacobsen, S.E., Olszewski, N.E., Schwartz, S.H., Zeevaart, J.A.D., and Koornneef, A. (1996). Isolation and characterisation of abscisic acid-deficient *Arabidopsis* mutants at two new loci. Plant J. **10,** 655-661.

Leon-Reyes, A., Du, Y.J., Koornneef, A., Proietti, S., Korbes, A.P., Memelink, J., Pieterse, C.M.J., and Ritsema, T. (2010). Ethylene Signaling Renders the Jasmonate Response of *Arabidopsis* Insensitive to Future Suppression by Salicylic Acid. Mol. Plant-Microbe Interact. **23,** 187-197.

Leon-Reyes, A., Spoel, S.H., De Lange, E.S., Abe, H., Kobayashi, M., Tsuda, S., Millenaar, F.F., Welschen, R.A.M., Ritsema, T., and Pieterse, C.M.J. (2009). Ethylene Modulates the Role of NONEXPRESSOR OF PATHOGENESIS-RELATED GENES1 in Cross Talk between Salicylate and Jasmonate Signaling. Plant Physiol. **149,** 1797-1809.

Levine, A., Tenhaken, R., Dixon, R., and Lamb, C. (1994). H_2O_2 from the oxidative burst orchestrates the plant hypersensitive disease resistance response. Cell **79,** 583-593.

Li, J., Wen, J., Lease, K.A., Doke, J.T., Tax, F.E., and Walker, J.C. (2002). BAK1, an Arabidopsis LRR Receptor-like Protein Kinase, Interacts with BRI1 and Modulates Brassinosteroid Signaling. Cell **110,** 213-222.

Lin, M., Shen, X., and Chen, X. (2011). PAIR: the predicted *Arabidopsis* interactome resource. Nucleic Acids Research **39,** D1134-D1140.

Lindeberg, M., Cunnac, S., and Collmer, A. (2009). The evolution of *Pseudomonas syringae* host specificity and type III effector repertoires. Molecular Plant Pathology **10,** 767-775.

Lindermayr, C., Sell, S., Muller, B., Leister, D., and Durner, J. (2010). Redox Regulation of the NPR1-TGA1 System of *Arabidopsis thaliana* by Nitric Oxide. The Plant Cell Online **22,** 2894-2907.

Lindow, S.E., and Leveau, J.H.J. (2002). Phyllosphere microbiology. Current Opinion in Biotechnology **13,** 238-243.

Liu, J.P., Ishitani, M., Halfter, U., Kim, C.S., and Zhu, J.K. (2000). The *Arabidopsis thaliana SOS2* gene encodes a protein kinase that is required for salt tolerance. Proceedings of the National Academy of Sciences of the United States of America **97,** 3730-3734.

Liu, Q., Kasuga, M., Sakuma, Y., Abe, H., Miura, S., Yamaguchi-Shinozaki, K., and Shinozaki, K. (1998). Two Transcription Factors, DREB1 and DREB2, with an EREBP/AP2 DNA Binding Domain Separate Two Cellular Signal Transduction Pathways in Drought- and Low-Temperature-Responsive Gene Expression, Respectively, in Arabidopsis. The Plant Cell Online **10,** 1391-1406.

Lobell, D.B., Burke, M.B., Tebaldi, C., Mastrandrea, M.D., Falcon, W.P., and Naylor, R.L. (2008). Prioritizing climate change adaptation needs for food security in 2030. Science **319,** 607-610.

Lohrmann, J., and Harter, K. (2002). Plant two-component signaling systems and the role of response regulators. Plant Physiol. **128,** 363-369.

Long, S.P., and Humphries, S. (1994). Photoinhibition of photosynthesis in nature. Annual Review of Plant Physiology and Plant Molecular Biology **45,** 633-662.

Lu, D., He, P., and Shan, L. (2010). Bacterial effectors target BAK1-associated receptor complexes - one stone two birds. Communicative and Integrative Biology **3,** 80-83.

Lushchak, V.I. (2011). Adaptive response to oxidative stress: Bacteria, fungi, plants and animals. Comparative Biochemistry and Physiology Part C: Toxicology & Pharmacology **153,** 175-190.

Lynch, J.P., and St.Clair, S.B. (2004). Mineral stress: the missing link in understanding how global climate change will affect plants in real world soils. Field Crops Research **90,** 101-115.

Ma, S.W., Morris, V.L., and Cuppels, D.A. (1991). Characterization of a DNA region required for production of the phytotoxin coronatine by *Pseudomonas syringae* pv. *tomato*. Mol. Plant-Microbe Interact. **4,** 69-74.

Ma, W., Qi, Z., Smigel, A., Walker, R.K., Verma, R., and Berkowitz, G.A. (2009). Ca^{2+}, cAMP, and transduction of non-self perception during plant immune response. Proceedings of the National Academy of Sciences **106,** 20995-21000.

Mackey, D., Belkhadir, Y., Alonso, J.M., Ecker, J.R., and Dangl, J.L. (2003). *Arabidopsis* RIN4 is a target of the type III virulence effector AvrRpt2 and modulates RPS2-mediated resistance. Cell **112,** 379-389.

Maggio, A., Raimondi, G., Martino, A., and De Pascale, S. (2007). Salt stress response in tomato beyond the salinity tolerance threshold. Environmental and Experimental Botany **59,** 276-282.

Mahajan, S., and Tuteja, N. (2005). Cold, salinity and drought stresses: An overview. Archives of Biochemistry and Biophysics **444,** 139-158.

Mahajan, S., Pandey, G.K., and Tuteja, N. (2008). Calcium- and salt-stress signaling in plants: Shedding light on SOS pathway. Archives of Biochemistry and Biophysics **471,** 146-158.

Mahalingam, R., and Fedoroff, N. (2003). Stress response, cell death and sigalling: the many faces of reactive oxygen species. Physiologia Plantarum **119,** 56-68.

Mähönen, A.P., Higuchi, M., Törmäkangas, K., Miyawaki, K., Pischke, M.S., Sussman, M.R., Helariutta, Y., and Kakimoto, T. (2006a). Cytokinins Regulate a Bidirectional Phosphorelay Network in *Arabidopsis*. Current biology **16,** 1116-1122.

Mähönen, A.P., Bishopp, A., Higuchi, M., Nieminen, K.M., Kinoshita, K., Tormakangas, K., Ikeda, Y., Oka, A., Kakimoto, T., and Helariutta, Y. (2006b). Cytokinin Signaling and Its Inhibitor AHP6 Regulate Cell Fate During Vascular Development. Science **311,** 94-98.

Maleck, K., Levine, A., Eulgem, T., Morgan, A., Schmid, J., Lawton, K.A., Dangl, J.L., and A., D.R. (2000). The transcriptome of *Arabidopsis thaliana* during systemic acquired resistance. Nature Genetics **26,** 403-410.

Mason, M.G., Jha, D., Salt, D.E., Tester, M., Hill, K., Kieber, J.J., and Eric Schaller, G. (2010). Type-B response regulators ARR1 and ARR12 regulate expression of AtHKT1;1 and accumulation of sodium in *Arabidopsis* shoots. The Plant Journal **64,** 753-763.

Mason, M.G., Mathews, D.E., Argyros, D.A., Maxwell, B.B., Kieber, J.J., Alonso, J.M., Ecker, J.R., and Schaller, G.E. (2005). Multiple type-B response regulators mediate cytokinin signal transduction in Arabidopsis. Plant Cell **17,** 3007-3018.

McHale, L., Tan, X., Koehl, P., and Michelmore, R.W. (2006). Plant NBS-LRR proteins: adaptable guards. Genome Biology **7,** 212.210-212.211.

McManus, P.S., Stockwell, V.O., Sundin, G.W., and Jones, A.L. (2002). Antibiotic use in plant agriculture. Annu. Rev. Phytopathol. **40,** 443-465.

Melotto, M., Underwood, W., and He, S.Y. (2008a). Role of Stomata in Plant Innate Immunity and Foliar Bacterial Diseases. Annu. Rev. Phytopathol. **46,** 101-122.

Melotto, M., Underwood, W., Koczan, J., Nomura, K., and He, S.Y. (2006). Plant stomata function in innate immunity against bacterial invasion. Cell **126,** 969-980.

Melotto, M., Mecey, C., Niu, Y., Chung, H.S., Katsir, L., Yao, J., Zeng, W.Q., Thines, B., Staswick, P., Browse, J., Howe, G.A., and He, S.Y. (2008b). A critical role of two positively charged amino acids in the Jas motif of *Arabidopsis* JAZ proteins in mediating coronatine- and jasmonoyl isoleucine-dependent interactions with the COI1F-box protein. Plant J. **55,** 979-988.

Mengiste, T., Chen, X., Salmeron, J., and Dietrich, R. (2003). The *BOTRYTIS SUSCEPTIBLE1* gene encodes an R2R3MYB transcription factor protein that is required for biotic and abiotic stress responses in *Arabidopsis*. Plant Cell **15,** 2551-2565.

Mert-Turk, F., Bennett, M.H., Mansfield, J.W., and Holub, E.B. (2003a). Quantification of camalexin in several accessions of *Arabidopsis thaliana* following inductions with Peronospora parasitica and UV-B irradiation. Phytoparasitica **31,** 81-89.

Mert-Turk, F., Bennett, M., Mansfield, J.W., and Holub, E.B. (2003b). Camalexin accumulation in *Arabidopsis thaliana* following abiotic elicitation or inoculation with virulent or avirulent *Hyaloperonospora parasitica*. Physiological and Molecular Plant Pathology **62,** 137-145.

Mhamdi, A., Queval, G., Chaouch, S., Vanderauwera, S., Van Breusegem, F., and Noctor, G. (2010). Catalase function in plants: a focus on *Arabidopsis* mutants as stress-mimic models. J. Exp. Bot. **61,** 4197-4220.

Miernyk, J.A., and Thelen, J.J. (2008). Biochemical approaches for discovering protein-protein interactions. Plant J. **53,** 597-609.

Mikami, K., Kanesaki, Y., Suzuki, I., and Murata, N. (2002). The histidine kinase Hik33 perceives osmotic stress and cold stress in *Synechocystis sp* PCC 6803. Molecular Microbiology **46,** 905-915.

Miller, G., Suzuki, N., Ciftci-Yilmaz, S., and Mittler, R. (2010). Reactive oxygen species homeostasis and signalling during drought and salinity stresses. Plant Cell and Environment **33,** 453-467.

Mittal, S., and Davis, S.K. (1995). Role of the phytotoxin coronatine in the infection of *Arabidopsis thaliana* by the *Pseudomonas syringae* pv. *tomato*. Mol. Plant-Microbe Interact. **8,** 165-171.

Mittler, R. (2002). Oxidative stress, antioxidants and stress tolerance. Trends Plant Sci. **7,** 405-410.

Mittler, R. (2006). Abiotic stress, the field environment and stress combination. Trends Plant Sci. **11,** 15-19.

Miya, A., Albert, P., Shinya, T., Desaki, Y., Ichimura, K., Shirasu, K., Narusaka, Y., Kawakami, N., Kaku, H., and Shibuya, N. (2007). CERK1, a LysM receptor kinase, is essential for chitin elicitor signaling in *Arabidopsis*. Proceedings of the National Academy of Sciences of the United States of America **104,** 19613-19618.

Mizuno, T. (1997). Compilation of All Genes Encoding Two-component Phosphotransfer Signal Transducers in the Genome of *Escherichia coli*. DNA Research **4,** 161-168.

Mizuno, T. (2005). Two-component phosphorelay signal transduction systems in plants: from hormone responses to circadian rhythms. Bioscience Biotechnology and Biochemistry **69,** 2263-2276.

Moco, S., Bino, R.J., De Vos, R.C.H., and Vervoort, J. (2007). Metabolomics technologies and metabolite identification. Trends in Analytical Chemistry **26,** 855-866.

Mohr, P.G., and Cahill, D.M. (2003). Abscisic acid influences the susceptibility of *Arabidopsis thaliana* to *Pseudomonas syringae* pv. *tomato* and *Peronospora parasitica*. Funct. Plant Biol. **30,** 461-469.

Mohr, P.G., and Cahill, D.M. (2007). Suppression by ABA of salicylic acid and lignin accumulation and the expression of multiple genes, in *Arabidopsis* infected with *Pseudomonas syringae* pv. *tomato*. Funct. Integr. Genomics **7,** 181-191.

Moller, I.M., Jensen, P.E., and Hansson, A. (2007). Oxidative modifications to cellular components. Annual Review of Plant Biology **58,** 459-481.

Morsy, M., Gouthu, S., Orchard, S., Thorneycroft, D., Harper, J.F., Mittler, R., and Cushman, J.C. (2008). Charting plant interactomes: possibilities and challenges. Trends Plant Sci. **13,** 183-191.

Mott, C.L. (2010). Environmental constraints to the geographical expansion of plant and animal species. Nature Education Knowledge **1,** 72.

Mou, Z., Fan, W., and Dong, X. (2003). Inducers of plant systemic acquired resistance regulate NPR1 function through redox changes. Cell **113,** 935-944.

Moussatche, P., and Klee, H.J. (2004). Autophosphorylation Activity of the *Arabidopsis* Ethylene Receptor Multigene Family. Journal of Biological Chemistry **279,** 48734-48741.

Muckenschnabel, I., Goodman, B.A., Williamson, B., Lyon, G.D., and Deighton, N. (2002). Infection of leaves of *Arabidopsis thaliana* by *Botrytis cinerea*: changes in ascorbic acid, free radicals and lipid peroxidation products. J. Exp. Bot. **53,** 207-214.

Mullineaux, P.M., Karpinski, S., and Baker, N.R. (2006). Spatial Dependence for Hydrogen Peroxide-Directed Signaling in Light-Stressed Plants. Plant Physiol. **141,** 346-350.

Mundy, J., Yamaguchi-Shinozaki, K., and Chua, N.H. (1990). Nuclear proteins bind conserved elements in the abscisic acid-responsive promoter of a rice *rab* gene. Proceedings of the National Academy of Sciences **87,** 1406-1410.

Munkvold, K.R., Russell, A.B., Kvitko, B.H., and Collmer, A. (2009). *Pseudomonas syringae* pv. *tomato* DC3000 type III effector HopAA1-1 functions redundantly with chlorosis-promoting factor PSPTO4723 to produce bacterial speck lesions in host tomato. Mol. Plant-Microbe Interact. **22,** 1341-1355.

Munns, R. (2002). Comparative physiology of salt and water stress. Plant Cell and Environment **25,** 239-250.

Munns, R., and Tester, M. (2008). Mechanisms of Salinity Tolerance. Annual Review of Plant Biology **59,** 651-681.

Mur, L., Kenton, P., Lloyd, A., Ougham, H., and Prats, E. (2008). The hypersensitive response; the centenary is upon us but how much do we know? J Exp Bot **59,** 501 - 520.

Mur, L.A.J., Kenton, P., Atzorn, R., Miersch, O., and Wasternack, C. (2006). The outcomes of concentration-specific interactions between salicylate and jasmonate signaling include synergy, antagonism, and oxidative stress leading to cell death. Plant Physiol. **140,** 249-262.

Mustilli, A.-C., Merlot, S., Vavasseur, A., Fenzi, F., and Giraudat, J. (2002). *Arabidopsis* OST1 Protein Kinase Mediates the Regulation of Stomatal Aperture by Abscisic Acid and Acts Upstream of Reactive Oxygen Species Production. The Plant Cell Online **14,** 3089-3099.

Naito, K., Taguchi, F., Suzuki, T., Inagaki, Y., Toyoda, K., Shiraishi, T., and Ichinose, Y. (2008). Amino Acid Sequence of Bacterial Microbe-Associated Molecular Pattern flg22 Is Required for Virulence. Mol. Plant-Microbe Interact. **21,** 1165-1174.

Nakashima, K., and Yamaguchi-Shinozaki, K. (2006). Regulons involved in osmotic stress-responsive and cold stress-responsive gene expression in plants. Physiologia Plantarum **126,** 62-71.

Nambara, E., and Marion-Poll, A. (2005). Abscisic acid biosynthesis and catabolism. Annual Review of Plant Biology **56,** 165-185.

Nambara, E., Okamoto, M., Tatematsu, K., Yano, R., Seo, M., and Kamiya, Y. (2010). Abscisic acid and the control of seed dormancy and germination. Seed Sci. Res. **20,** 55-67.

Navarro-Pedreño, J., Jordan, M.M., Meléndez-Pastor, I., Gómez, I., Juan, P., and Mateu, J. (2007). Estimation of soil salinity in semi-arid land using a geostatistical model. Land Degradation & Development **18,** 339-353.

Navarro, L., Bari, R., Achard, P., Lison, P., Nemri, A., Harberd, N.P., and Jones, J.D.G. (2008). DELLAs control plant immune responses by modulating the balance and salicylic acid signaling. Current Biology **18,** 650-655.

Nawrath, C., and Metraux, J.P. (1999). Salicylic acid induction-deficient mutants of Arabidopsis express *PR-1* and *PR-5* and accumulate hight levels of camalexin after pathogen inoculation. Plant Cell **11,** 1393-1404.

Ndamukong, I., Al Abdallat, A., Thurow, C., Fode, B., Zander, M., Weigel, R., and Gatz, C. (2007). SA-inducible Arabidopsis glutaredoxin interacts with TGA factors and suppresses JA-responsive *PDF1.2* transcription. Plant J. **50,** 128-139.

Neill, S., Desikan, R., and Hancock, J. (2002). Hydrogen peroxide signalling. Current Opinion in Plant Biology **5,** 388-395.

Nilsen, E.T., and Orcutt, D.M. (2000). Soil processes and plant stress physiology. In The Physiology of Plants Under Stress: Soil and Biotic Factors (New Jersey: John Wiley and Sons), pp. 1-236.

Nishimura, M.T., and Dangl, J.L. (2010). *Arabidopsis* and the plant immune system. Plant J. **61,** 1053-1066.

Niu, Y., Figueroa, P., and Browse, J. (2011). Characterization of JAZ-interacting bHLH transcription factors that regulate jasmonate responses in *Arabidopsis*. J. Exp. Bot.

Nomura, K., DebRoy, S., Lee, Y.H., Pumplin, N., Jones, J., and He, S.Y. (2006). A Bacterial Virulence Protein Suppresses Host Innate Immunity to Cause Plant Disease. Science **313,** 220-223.

Nürnberger, T., and Kemmerling, B. (2006). Receptor protein kinases - pattern recognition receptors in plant immunity. Trends Plant Sci. **11,** 519-522.

Oh, D.-H., Lee, S.Y., Bressan, R.A., Yun, D.-J., and Bohnert, H.J. (2010). Intracellular consequences of SOS1 deficiency during salt stress. J. Exp. Bot. **61,** 1205-1213.

Ohta, M., Guo, Y., Halfter, U., and Zhu, J.K. (2003). A novel domasin inthe protein kinase SOS2 mediates interaction with the protein phosphatase 2C ABI2. Proceedings of the National Academy of Sciences **100,** 111771-111776.

Olvera-Carrillo, Y., Campos, F., Reyes, J.L., Garciarrubio, A., and Covarrubias, A.A. (2010). Functional Analysis of the Group 4 Late Embryogenesis Abundant Proteins Reveals Their Relevance in the Adaptive Response during Water Deficit in *Arabidopsis*. Plant Physiol. **154,** 373-390.

Paget, M.S.B., and Buttner, M.J. (2003). Thiol-basedregulatory switches. Annu. Rev. Genet. **37,** 91-121.

Pallas, J.A., Paiva, N.L., Lamb, C., and Dixon, R.A. (1996). Tobacco plants epigenetically suppressed in phenylalanine ammonia-lyase expression do not develop systemic acquired resistance in response to infection by tobacco mosaic virus. The Plant Journal **10,** 281-293.

Pardo, J.M., and Quintero, F.J. (2002). Plants and sodium ions: keeping company with the enemy. Genome Biology **3,** 1017.

Park, M., Lee, H., Lee, J.S., Byun, M.O., and Kim, B.G. (2009). *In planta* measurements of Na^+ using fluorescent dye CoroNa Green. J. Plant Biol. **52,** 298-302.

Pedras, M.S.C., Hossain, S., and Snitynsky, R.B. (2011). Detoxification of cruciferous phytoalexins in *Botrytis cinerea*: Spontaneous dimerization of a camalexin metabolite. Phytochemistry **72,** 199-206.

Penaloza-Vazquez, A., Preston, G.M., Collmer, A., and Bender, C.L. (2000). Regulatory interactions between the Hrp type III protein secretion system and coronatine biosynthesis in *Pseudomonas syringae* pv. *tomato* DC3000. Microbiology-UK **146,** 2447-2456.

Petutschnig, E.K., Jones, A.M.E., Serazetdinova, L., Lipka, U., and Lipka, V. (2010). The Lysin Motif Receptor-like Kinase (LysM-RLK) CERK1 Is a Major Chitin-binding Protein in *Arabidopsis thaliana* and Subject to Chitin-induced Phosphorylation. Journal of Biological Chemistry **285,** 28902-28911.

Pieterse, C.M.J., and Van Loon, L.C. (2004). NPR1: the spider in the web of induced resistance signaling pathways. Current Opinion in Plant Biology **7,** 456-464.

Pinedo, C., Wang, C.M., Pradier, J.M., Dalmais, B., Choquer, M., Le Pecheur, P., Morgant, G., Collado, I.G., Cane, D.E., and Viaud, M. (2009). The sesquiterpene synthase from the botrydial biosynthetic gene cluster of the phytopathogen *Botrytis cinerea*. ACS Chemical Biology **3,** 791-801.

Pischke, M.S., Jones, L.G., Otsuga, D., Fernandez, D.E., Drews, G.N., and Sussman, M.R. (2002). An *Arabidopsis* histidine kinase is essential for megagametogenesis. Proceedings of the National Academy of Sciences of the United States of America **99,** 15800-15805.

Plaxton, W.C. (1996). The organization and regulation of plant glycolysis. Annual Review of Plant Physiology and Plant Molecular Biology **47,** 185-214.

Pogany, M., von Rad, U., Grun, S., Dongo, A., Pintye, A., Simoneau, P., Bahnweg, G., Kiss, L., Barna, B., and Durner, J. (2009). Dual Roles of Reactive Oxygen Species and NADPH Oxidase RBOHD in an *Arabidopsis-Alternaria* Pathosystem. Plant Physiol. **151,** 1459-1475.

Porra, R.J., Thompson, W.A., and Kriedemann, P.E. (1989). Determination of accurate extinction coefficients and simultaneous-equations for assaying chlorophyll-a and chlorophyll-b extracted with four different solvents - verification of the concentration of chlorophyll standards by atomic-absorption spectroscopy. Biochimica Et Biophysica Acta **975,** 384-394.

Posas, F., Wurgler-Murphy, S.M., Maeda, T., Witten, E.A., Thai, T.C., and Saito, H. (1996). Yeast HOG1 MAP Kinase Cascade Is Regulated by a Multistep Phosphorelay Mechanism in the SLN1-YPD1-SSK1 "Two-Component" Osmosensor. Cell **86,** 865-875.

Preston, G.M. (2000). *Pseudomonas syringae* pv. *tomato*: the right pathogen, of the right plant, at the right time. Molecular Plant Pathology **1,** 263-275.

Pseudomonas-Plant Interactions. (2011). *Pseudomonas syringae* genome [Online]. Available at: <http://pseudomonas-syringae.org/home.html> [Accessed 23/05/11].

Puig, O., Caspary, F., Rigaut, G., Rutz, B., Bouveret, E., Bragado-Nilsson, E., Wilm, M., and Seraphin, B. (2001). The tandem affinity purification (TAP) method: a general proceedure of protein complex purification. Methods **24,** 218-229.

Qadir, M., Ghafoor, A., and Murtaza, G. (2000). Amelioration strategies for saline soils: a review. Land Degradation & Development **11,** 501-521.

Qi, Z., and Spalding, E.P. (2004). Protection of Plasma Membrane K^+ Transport by the Salt Overly Sensitive1 Na^{+}-H^+ Antiporter during Salinity Stress. Plant Physiol. **136,** 2548-2555.

Qiu, Q.S., Barkla, B.J., Vera-Estrella, R., Zhu, J.K., and Schumaker, K.S. (2003). Na^+/H^+ exchange activity in the plasma membrane of *Arabidopsis*. Plant Physiol. **132,** 1041-1052.

Quirino, B.F., and Bent, A.F. (2003). Deciphering host resistance and pathogen virulence: the *Arabidopsis/Pseudomonas* interaction as a model. Molecular Plant Pathology **4,** 517-530.

Rabbani, M., Maruyama, K., Abe, H., Khan, M., Katsura, K., Ito, Y., Yoshiwara, K., Seki, M., Shinozaki, K., and Yamaguchi-Shinozaki, K. (2003). Monitoring expression profiles of rice genes under cold, drought, and high-salinity stresses and abscisic acid application using cDNA microarray and RNA gel-blot analyses. Plant Physiol **133,** 1755 - 1767.

Rauhut, T., and Glawischnig, E. (2009). Evolution of camalexin and structurally related indolic compounds. Phytochemistry **70,** 1638-1644.

Reiser, V., Raitt, D.C., and Saito, H. (2003). Yeast osmosensor Sln1 and plant cytokinin receptor Cre1 respond to changes in turgor pressure. The Journal of Cell Biology **161,** 1035-1040.

Rico, A., and Preston, G.M. (2008). *Pseudomonas syringae* pv. *tomato* DC3000 uses constitutive and apoplast-induced nutrient assimilation pathways to catabolize nutrients that are abundant in the tomato apoplast. Mol. Plant-Microbe Interact. **21,** 269-282.

Rietz, S., Stamm, A., Malonek, S., Wagner, S., Becker, D., Medina-Escobar, N., Corina Vlot, A., Feys, B.J., Niefind, K., and Parker, J.E. (2011). Different roles of Enhanced Disease Susceptibility1 (EDS1) bound to and dissociated from Phytoalexin Deficient4 (PAD4) in Arabidopsis immunity. New Phytol.**,** 107-119.

Rinalducci, S., Murgiano, L., and Zolla, L. (2008). Redox proteomics: basic principles and future perspectives for the detection of protein oxidation in plants. J. Exp. Bot. **59,** 3781-3801.

Rivas, S., Romeis, T., and Jones, J.D.G. (2002). The Cf-9 Disease Resistance Protein Is Present in an ~420-Kilodalton Heteromultimeric Membrane-Associated Complex at One Molecule per Complex. The Plant Cell Online **14,** 689-702.

Rogers, E.E., Glazebrook, J., and Ausubel, F.M. (1996). Mode of action of the *Arabidopsis thaliana* phytoalexin camalexin and its role in *Arabidopsis*-pathogen interactions. Mol. Plant-Microbe Interact. **9,** 748-757.

Rohila, J.S., Chen, M., Chen, S., Chen, J., Cerny, R., Dardick, C., Canlas, P., Xu, X., Gribskov, M., Kanrar, S., Zhu, J.K., Ronald, P., and Fromm, M.E. (2006). Protein-protein interactions of tandem affinity purification-tagged protein kinases in rice. Plant J. **46,** 1-13.

Rohila, J.S., Chen, M., Chen, S., Chen, J., Cerny, R.L., Dardick, C., Canlas, P., Fujii, H., Gribskov, M., Kanrar, S., Knoflicek, L., Stevenson, B., Xie, M., Xu, X., Zheng, X., Zhu, J.-K., Ronald, P., and Fromm, M.E. (2009). Protein-Protein Interactions of Tandem Affinity Purified Protein Kinases from Rice. PLoS ONE **4,** e6685.

Roine, E., Wei, W., Yuan, J., Nurmiaho-Lassila, E.-L., Kalkkinen, N., Romantschuk, M., and He, S.Y. (1997). Hrp pilus: An hrp-dependent bacterial surface appendage produced by *Pseudomonas syringae* pv. *tomato* DC3000. Proceedings of the National Academy of Sciences **94,** 3459-3464.

Rolke, Y., Liu, S., Quidde, T., Williamson, B., Schouten, A., Weltring, K.-M., Siewers, V., Tenberge, K.B., Tudzynski, B., and Tudzynski, P. (2004). Functional analysis of H_2O_2-generating systems in *Botrytis cinerea*: the major Cu-Zn-superoxide dismutase (BCSOD1) contributes to virulence on French bean, whereas a glucose oxidase (BCGOD1) is dispensable. Molecular Plant Pathology **5,** 17-27.

Romir, J., Harter, K., and Stehle, T. (2009). Two-component systems in *Arabidopsis thaliana* - A structural view. European Journal of Cell Biology **89,** 270-272.

Rose, J.K.C., Bashir, S., Giovannoni, J.J., Jahn, M.M., and Saravanan, R.S. (2004). Tackling the plant proteome: practical approaches, hurdles and experimental tools. Plant J. **39,** 715-733.

Rossall, S., and Mansfield, J.W. (1980). Investigation of the causes of poor germination of *Botrytis spp.* on broad bean leaves (*Vicia faba* L.). Physiological Plant Pathology **16,** 369-382.

Rowe, H.C., Walley, J.W., Corwin, J., Chan, E.K.F., Dehesh, K., and Kliebenstein, D.J. (2010). Deficiencies in Jasmonate-Mediated Plant Defense Reveal Quantitative Variation in *Botrytis cinerea* Pathogenesis. PLoS Pathogens **6,** 18.

Rubio, V., Shen, Y.P., Saijo, Y., Liu, Y.L., Gusmaroli, G., Dinesh-Kumar, S.P., and Deng, X.W. (2005). An alternative tandem affinity purification strategy applied to Arabidopsis protein complex isolation. Plant J. **41,** 767-778.

Saito, H., and Tatebayashi, K. (2004). Regulation of the osmoregulatory HOG MAPK cascade in yeast. Journal of Biochemistry **136,** 267-272.

Sakai, H., Aoyama, T., and Oka, A. (2000). *Arabidopsis* ARR1 and ARR2 response regulators operate as transcriptional activators. The Plant Journal **24,** 703-711.

Saleki, R., Young, P.G., and Lefebvre, D.D. (1993). Mutants of *Arabidopsis thaliana* capable of germination under saline conditions. Plant Physiol. **101,** 839-845.

Sambrook, J., and Russell, D.W. (2006). The Condensed Protocols from Molecular Cloning: a Laboratory Manual. (New York: Cold Spring Harbour Laboratory Press).

Sang, Y., Zheng, S., Li, W., Huang, B., and Wang, X. (2001). Regulation of plant water loss by manipulating the expression of phospholipase Dα. The Plant Journal **28,** 135-144.

Sangwan, V., Orvar, B.L., Beyerly, J., Hirt, H., and Dhindsa, R.S. (2002). Opposite changes in membrane fluidity mimic cold and heat stress activation of distinct plant MAP kinase pathways. Plant J. **31,** 629-638.

Schaller, G.E., Kieber, J.J., and Shiu, S.-H. (2008). Two-component signaling elements and histidyl-aspartyl phosphorelays. The Arabidopsis Book **6,** 1-12.

Scharein, B., Voet-Van-Vormizeele, J., Harter, K., and Groth, G. (2008). Ethylene signaling: Identification of a putative ETR1-AHP1 phosphorelay complex by fluorescence spectroscopy. Anal. Biochem. **377,** 72-76.

Schechter, L.M., Vencato, M., Jordan, K.L., Schneider, S.E., Schneider, D.J., and Collmer, A. (2006). Multiple Approaches to a Complete Inventory of *Pseudomonas syringae* pv. *tomato* DC3000 Type III Secretion System Effector Proteins. Mol. Plant-Microbe Interact. **19,** 1180-1192.

Schneeberger, W., Darnhofer, I., and Eder, M. (2002). Barriers to the adoption of organic farming by cash-crop producers in Austria. American Journal of Alternative Agriculture **17,** 24-31.

Schneider, D.J., and Collmer, A. (2010). Studying Plant-Pathogen Interactions in the Genomics Era: Beyond Molecular Koch's Postulates to Systems Biology. Annu. Rev. Phytopathol. **48,** 457-479.

Schoonbeek, H., van Nistelrooy, J.G.M., and de Waard, M.A. (2003). Functional Analysis of ABC Transporter Genes From *Botrytis cinerea* Identifies BcatrB as a Transporter of Eugenol. Eur. J. Plant Pathol. **109,** 1003-1011.

Schouten, A., Van Baarlen, P., and Van Kan, J.A.L. (2008). Phytotoxic Nep1-like proteins from the necrotrophic fungus *Botrytis cinerea* associate with membranes and the nucleus of plant cells. New Phytol. **177,** 493-505.

Schroeder, J.I., Ward, J.M., and Gassmann, W. (1994). Perspectives on the physiology and structure of inward-rectifying K^+ channels in higher plants - biophysical implications for K^+ uptake. Annual Review of Biophysics and Biomolecular Structure **23,** 441-471.

Schroeder, J.I., Allen, G.J., Hugouvieux, V., Kwak, J.M., and Waner, D. (2001). Guard cell signal transduction. Annual Review of Plant Physiology and Plant Molecular Biology **52,** 627-658.

Schuhegger, R., Nafisi, M., Mansourova, M., Petersen, B.L., Olsen, C.E., Svatos, A., Halkier, A., and Glawischnig, E. (2006). CYP71B15 (PAD3) catalyzes the final step in camalexin biosynthesis. Plant Physiol. **141,** 1248-1254.

Schultz, J., Copley, R.R., Doerks, T., Ponting, C.P., and Bork, P. (2000). SMART: a web-based tool for the study of genetically mobile domains. Nucleic Acids Research **28,** 231-234.

Schwartz, S.H., Leon-Kloosterziel, K.M., Koornneef, A., and Zeevaart, J.A.D. (1997). Biochemical characterisation of the *aba2* and *aba3* mutants in *A. thaliana*. Plant Physiol. **114,** 161-166.

Segmuller, N., Kokkelink, L., Giesbert, S., Odinius, D., van Kan, J., and Tudzynski, P. (2008). NADPH Oxidases are involved in differentiation and pathogenicity in *Botrytis cinerea*. Mol. Plant-Microbe Interact. **21,** 808-819.

Seki, M., Narusaka, M., Abe, H., Kasuga, M., Yamaguchi-Shinozaki, K., Carninci, P., Hayashizaki, Y., and Shinozaki, K. (2001). Monitoring the expression pattern of 1300 *Arabidopsis* genes under drought and cold stresses by using full-length cDNA microarray. Plant Cell **13,** 61-72.

Seki, M., Narusaka, M., Ishida, J., Nanjo, T., Fujita, M., Oono, Y., Kamiya, A., Nakajima, M., Enju, A., Sakurai, T., Satou, M., Akiyama, K., Taji, T., Yamaguchi-Shinozaki, K., Carninci, P., Kawai, J., Hayashizaki, Y., and Shinozaki, K. (2002). Monitoring the expression profiles of 7000 *Arabidopsis* genes under drought, cold and high-salinity stresses using a full-length cDNA microarray. The Plant Journal **31,** 279-292.

Seo, M., Peeters, A.J.M., Koiwai, H., Oritani, T., Marion-Poll, A., Zeevaart, J.A.D., Koornneef, M., Kamiya, Y., and Koshiba, T. (2000). The *Arabidopsis* aldehyde oxidase 3 *(AAO3)* gene product catalyzes the final step in abscisic acid biosynthesis in leaves. Proceedings of the National Academy of Sciences **97,** 12908-12913.

Shaikhali, J., Heiber, I., Seidel, T., Stroher, E., Hiltscher, H., Birkmann, S., Dietz, K.J., and Baier, M. (2008). The redox-sensitive transcription factor Rap2.4a controls nuclear expression of 2-Cys peroxiredoxin A and other chloroplast antioxidant enzymes. BMC Plant Biol. **8,** 14.

Shan, L.B., He, P., Li, J.M., Heese, A., Peck, S.C., Nurnberger, T., Martin, G.B., and Sheen, J. (2008). Bacterial effectors target the common signaling partner BAK1 to disrupt multiple MAMP receptor-signaling complexes and impede plant immunity. Cell Host & Microbe **4,** 17-27.

Shapiro-Ilan, D.I., Fuxa, J.R., Lacey, L.A., Onstad, D.W., and Kaya, H.K. (2005). Definitions of pathogenicity and virulence in invertebrate pathology. Journal of Invertebrate Pathology **88,** 1-7.

Shapiro, A.D., and Zhang, C. (2001). The Role of NDR1 in Avirulence Gene-Directed Signaling and Control of Programmed Cell Death in *Arabidopsis*. Plant Physiol. **127,** 1089-1101.

Sharp, R.E., and LeNoble, M.E. (2002). ABA, ethylene and the control of shoot and root growth under water stress. J. Exp. Bot. **53,** 33-37.

Shi, H.Z., and Zhu, J.K. (2002). Regulation of expression of the vacuolar Na^+/H^+ antiporter gene AtNHX1 by salt stress and abscisic acid. Plant Molecular Biology **50,** 543-550.

Shi, H.Z., Ishitani, M., Kim, C.S., and Zhu, J.K. (2000). The *Arabidopsis thaliana* salt tolerance gene SOS1 encodes a putative Na^+/H^+ antiporter. Proceedings of the National Academy of Sciences of the United States of America **97,** 6896-6901.

Shi, H.Z., Quintero, F.J., Pardo, J.M., and Zhu, J.K. (2002). The putative plasma membrane Na^+/H^+ antiporter SOS1 controls long-distance Na+ transport in plants. Plant Cell **14,** 465-477.

Shi, H.Z., Lee, B.H., Wu, S.J., and Zhu, J.K. (2003). Overexpression of a plasma membrane Na^+/H^+ antiporter gene improves salt tolerance in *Arabidopsis thaliana*. Nat. Biotechnol. **21,** 81-85.

Shimizu, T., Nakano, T., Takamizawa, D., Desaki, Y., Ishii-Minami, N., Nishizawa, Y., Minami, E., Okada, K., Yamane, H., Kaku, H., and Shibuya, N. (2010). Two LysM receptor molecules, CEBiP and OsCERK1, cooperatively regulate chitin elicitor signaling in rice. The Plant Journal **64,** 204-214.

Shinozaki, K., and Yamaguchi-Shinozaki, K. (2007). Gene networks involved in drought stress response and tolerance. J. Exp. Bot. **58,** 221-227.

Siewers, V., Viaud, M., Jimenez-Teja, D., Collado, I.G., Gronover, C.S., Pradier, J.M., Tudzynski, B., and Tudzynski, P. (2005). Functional analysis of the cytochrome P450 monooxygenase gene *bcbot1* of *Botrytis cinerea* indicates that botrydial is a strain-specific virulence factor. Mol. Plant-Microbe Interact. **18,** 602-612.

Simon, C., Langlois-Meurinne, M., Bellvert, F., Garmier, M., Didierlaurent, L., Massoud, K., Chaouch, S., Marie, A., Bodo, B., Kauffmann, S., Noctor, G., and Saindrenan, P. (2010). The differential spatial distribution of secondary metabolites in *Arabidopsis* leaves reacting hypersensitively to *Pseudomonas syringae* pv. *tomato* is dependent on the oxidative burst. J. Exp. Bot. **61,** 3355-3370.

Sirichandra, C., Gu, D., Hu, H.-C., Davanture, M., Lee, S., Djaoui, M., Valot, B., Zivy, M., Leung, J., Merlot, S., and Kwak, J.M. (2009). Phosphorylation of the *Arabidopsis* AtrbohF NADPH oxidase by OST1 protein kinase. FEBS Letters **583,** 2982-2986.

Skirycz, A., and Inzé, D. (2010). More from less: plant growth under limited water. Current Opinion in Biotechnology **21,** 197-203.

Smirnoff, N., and Grant, M. (2008). Plant biology: Do DELLAs do defence? Current Biology **18,** R617-R619.

Smith, C.A., Melino, V.J., Sweetman, C., and Soole, K.L. (2009). Manipulation of alternative oxidase can influence salt tolerance in *Arabidopsis thaliana*. Physiologia Plantarum **137,** 459-472.

Šnyrychová, I., Ayaydin, F., and Hideg, É. (2009). Detecting hydrogen peroxide in leaves *in vivo* – a comparison of methods. Physiologia Plantarum **135,** 1-18.

Soylu, S. (1998). Analysis of the Responses of *Arabidopsis thaliana* to Infection by *Albugo candida* and Pathovars of *Pseudomnas syringae*. In Wye College (University of London).

Spoel, S.H., Johnson, J.S., and Dong, X. (2007). Regulation of tradeoffs between plant defenses against pathogens with different lifestyles. Proceedings of the National Academy of Sciences of the United States of America **104,** 18842-18847.

Spoel, S.H., Koornneef, A., Claessens, S.M.C., Korzelius, J.P., Van Pelt, J.A., Mueller, M.J., Buchala, A.J., Metraux, J.P., Brown, R., Kazan, K., Van Loon, L.C., Dong, X.N., and Pieterse, C.M.J. (2003). NPR1 modulates cross-talk between salicylate- and jasmonate-dependent defense pathways through a novel function in the cytosol. Plant Cell **15,** 760-770.

Stefanato, F.L., Abou-Mansour, E., Buchala, A., Kretschmer, M., Mosbach, A., Hahn, M., Bochet, C.G., Metraux, J.P., and Schoonbeek, H.J. (2009). The ABC transporter BcatrB from *Botrytis cinerea* exports camalexin and is a virulence factor on *Arabidopsis thaliana*. Plant J. **58,** 499-510.

Sticher, L., MauchMani, B., and Metraux, J.P. (1997). Systemic acquired resistance. Annu. Rev. Phytopathol. **35,** 235-270.

Stock, A.M., Robinson, V.L., and Goudreau, P.N. (2000). Two-component signal transduction. Annual Review of Biochemistry **69,** 183-215.

Suzuki, I., Los, D.A., Kanesaki, Y., Mikami, K., and Murata, N. (2000). The pathway for perception and transduction of low-temperature signals in *Synechocystis*. EMBO Journal **19,** 1327-1334.

Suzuki, I., Kanesaki, Y., Mikami, K., Kanehisa, M., and Murata, N. (2001). Cold-regulated genes under control of the cold sensor Hik33 in *Synechocystis*. Molecular Microbiology **40,** 235-244.

Suzuki, I., Kanesaki, Y., Hayashi, H., Hall, J.J., Simon, W.J., Slabas, A.R., and Murata, N. (2005). The histidine kinase Hik34 is involved in thermotolerance by regulating the expression of heat shock genes in *Synechocystis*. Plant Physiol. **138,** 1409-1421.

Suzuki, N., and Mittler, R. (2006). Reactive oxygen species and temperature stresses: A delicate balance between signaling and destruction. Physiologia Plantarum **126,** 45-51.

Swarbreck, D., Wilks, C., Lamesch, P., Berardini, T.Z., Garcia-Hernandez, M., Foerster, H., Li, D., Meyer, T., Muller, R., Ploetz, L., Radenbaugh, A., Singh, S., Swing, V., Tissier, C., Zhang, P., and Huala, E. (2008). The *Arabidopsis* Information Reseource (TAIR): gene structure and function annotation. Nucleic Acids Research **36,** D1009-D1014.

Szczerba, M.W., Britto, D.T., and Kronzucker, H.J. (2009). K^+ transport in plants: Physiology and molecular biology. Journal of Plant Physiology **166,** 447-466.

Tada, Y., Spoel, S.H., Pajerowska-Mukhtar, K., Mou, Z.L., Song, J.Q., Wang, C., Zuo, J.R., and Dong, X.N. (2008). Plant immunity requires conformational charges of NPR1 via S-nitrosylation and thioredoxins. Science **321,** 952-956.

Taira, S., Tuimala, J., Roine, E., Nurmiaho-Lassila, E.-L., Savilahti, H., and Romantschuk, M. (1999). Mutational analysis of the *Pseudomonas syringae* pv. *tomato hrpA* gene encoding Hrp pilus subunit. Molecular Microbiology **34,** 737-744.

Taiz, L., and Zeiger, E. (1998). Plant Physiology. (Massachusetts: Sinauer Associates, Inc).

Takemiya, A., Inoue, S.-i., Doi, M., Kinoshita, T., and Shimazaki, K.-i. (2005). Phototropins Promote Plant Growth in Response to Blue Light in Low Light Environments. The Plant Cell Online **17,** 1120-1127.

Tenberge, K.B., Beckendorf, M., Hoppe, B., Schouten, A., Solf, M., and von den Driesch, M. (2002). *In situ* localization of AOS in host-pathogen interactions. Microscopy and Microanalysis **8 (Suppl. 2),** 250-251.

Terpe, K. (2003). Overview of tag protein fusions: from molecular and biochemical fundamentals to commercial systems. Applied Microbiology and Biotechnology **60,** 523-533.

Thines, B., Katsir, L., Melotto, M., Niu, Y., Mandaokar, A., Liu, G.H., Nomura, K., He, S.Y., Howe, G.A., and Browse, J. (2007). JAZ repressor proteins are targets of the SCFCO11 complex during jasmonate signalling. Nature **448,** 661-U662.

Thomma, B., Eggermont, K., Broekaert, W.F., and Cammue, B.P.A. (2000). Disease development of several fungi on *Arabidopsis* can be reduced by treatment with methyl jasmonate. Plant Physiology and Biochemistry **38,** 421-427.

Thomma, B., Eggermont, K., Penninckx, I., Mauch-Mani, B., Vogelsang, R., Cammue, B.P.A., and Broekaert, W.F. (1998). Separate jasmonate-dependent and salicylate-dependent defense-response pathways in *Arabidopsis* are essential for resistance to distinct microbial pathogens. Proceedings of the National Academy of Sciences of the United States of America **95,** 15107-15111.

Thordal-Christensen, H. (2003). Fresh insights into processes of nonhost resistance. Current Opinion in Plant Biology **6,** 351-357.

Tierens, K., Thomma, B., Bari, R.P., Garmier, M., Eggermont, K., Brouwer, M., Penninckx, I., Broekaert, W.F., and Cammue, B.P.A. (2002). *esa1,* an *Arabidopsis* mutant with enhanced susceptibility to a range of necrotrophic fungal pathogens, shows a distorted induction of defense responses by reactive oxygen generating compounds. Plant J. **29,** 131-140.

To, J.P.C., Haberer, G., Ferreira, F.J., Deruere, J., Mason, M.G., Schaller, G.E., Alonso, J.M., Ecker, J.R., and Kieber, J.J. (2004). Type-A *Arabidopsis* Response Regulators Are Partially Redundant Negative Regulators of Cytokinin Signaling. Plant Cell **16,** 658-671.

Tolleter, D., Jaquinod, M., Mangavel, C., Passirani, C., Saulnier, P., Manon, S., Teyssier, E., Payet, N., Avelange-Macherel, M.-H., and Macherel, D. (2007). Structure and Function of a Mitochondrial Late Embryogenesis Abundant Protein Are Revealed by Desiccation. The Plant Cell Online **19,** 1580-1589.

Ton, J., Flors, V., and Mauch-Mani, B. (2009). The multifaceted role of ABA in disease resistance. Trends Plant Sci. **14,** 310-317.

Torres, M.A., and Dangl, J.L. (2005). Functions of the respiratory burst oxidase in biotic interactions, abiotic stress and development. Current Opinion in Plant Biology **8,** 397-403.

Torres, M.A., Dangl, J.L., and Jones, J.D.G. (2002). Arabidopsis gp91(phox) homologues AtrbohD and AtrbohF are required for accumulation of reactive oxygen intermediates in the plant defense response. Proceedings of the National Academy of Sciences of the United States of America **99,** 517-522.

Torres, M.A., Jones, J.D.G., and Dangl, J.L. (2005). Pathogen-induced, NADPH oxidase-derived reactive oxygen intermediates suppress spread of cell death in *Arabidopsis thaliana*. Nature Genetics **37,** 1130-1134.

Torres, M.A., Onouchi, H., Hamada, S., Machida, C., Hammond-Kosack, K.E., and Jones, J.D.G. (1998). Six *Arabidopsis thaliana* homologues of the human respiratory burst oxidase (gp91(phox)). Plant J. **14,** 365-370.

Towne, V., Will, M., Oswald, B., and Zhao, Q. (2004). Complexities in horseradish peroxidase-catalysed oxidation of dihydroxyphenoxazine derivaties: appropriate ranges for pH values and hydrogen peroxide concentrations in quantitative analysis. Anal. Biochem. **334,** 290-296.

Tran, L.S.P., Shinozaki, K., and Yamaguchi-Shinozaki, K. (2010). Role of cytokinin responsive two-component system in ABA and osmotic stress signalings. Plant Signal Behav **5,** 148-150.

Tran, L.S.P., Urao, T., Qin, F., Maruyama, K., Kakimoto, T., Shinozaki, K., and Yamaguchi-Shinozaki, K. (2007). Functional analysis of AHK1/ATHK1 and cytokinin receptor histidine kinases in response to abscisic acid, drought, and salt stress in *Arabidopsis*. Proceedings of the National Academy of Sciences of the United States of America **104,** 20623-20628.

Tran, L.S.P., Nakashima, K., Sakuma, Y., Simpson, S.D., Fujita, Y., Maruyama, K., Fujita, M., Seki, M., Shinozaki, K., and Yamaguchi-Shinozaki, K. (2004). Isolation and functional analysis of Arabidopsis stress-inducible NAC transcription factors that bind to a drought-responsive *cis*-element in the *early responsive to dehydration stress 1* promoter. Plant Cell **16,** 2481-2498.

Tran, L.S.P., Nakashima, K., Sakuma, Y., Osakabe, Y., Qin, F., Simpson, S.D., Maruyama, K., Fujita, Y., Shinozaki, K., and Yamaguchi-Shinozaki, K. (2006). Co-expression of the stress-inducible zinc finger homeodomain ZFH1 and NAC transcription factors enhances expression of the *EDR1* gene in *Arabidopsis*. Plant J. **49,** 46-63.

Trewavas, A. (2001). Urban myths of organic farming. Nature **410,** 409-410.

Trewavas, A. (2004). A critical assessment of organic farming-and-food assertions with particular respect to the UK and the potential environmental benefits of no-till agriculture. Crop Protection **23,** 757-781.

Tuteja, N. (2007). Abscisic acid and abiotic stress signaling. Plant Signaling and Behaviour **2,** 135-138.

Ueguchi, C., Koizumi, H., Suzuki, T., and Mizuno, T. (2001). Novel Family of Sensor Histidine Kinase Genes in *Arabidopsis thaliana*. Plant and Cell Physiology **42,** 231-235.

Underwood, W., Melotto, M., and He, S.Y. (2007). Role of plant stomata in bacterial invasion. Cellular Microbiology **9,** 1621-1629.

Uppalapati, S.R., Ayoubi, P., Weng, H., Palmer, D.A., Mitchell, R.E., Jones, W., and Bender, C.L. (2005). The phytotoxin coronatine and methyl jasmonate impact multiple phytohormone pathways in tomato. Plant J. **42,** 201-217.

Uppalapati, S.R., Ishiga, Y., Wangdi, T., Kunkel, B.N., Anand, A., Mysore, K.S., and Bender, C.L. (2007). The phytotoxin coronatine contributes to pathogen fitness and is required for suppression of salicylic acid accumulation in tomato inoculated with Pseudomonas syringae pv. tomato DC3000. Mol. Plant-Microbe Interact. **20,** 955-965.

Uppalapati, S.R., Ishiga, Y., Wangdi, T., Urbanczyk-Wochniak, E., Lshiga, T., Mysore, K.S., and Bender, C.L. (2008). Pathogenicity of *Pseudomonas syringae* pv. *tomato* on tomato seedlings: Phenotypic and gene expression analyses of the virulence function of coronatine. Mol. Plant-Microbe Interact. **21,** 383-395.

Urao, T., Yamaguchi-Shinozaki, K., and Shinozaki, K. (2000a). Two-component systems in plant signal transduction. Trends Plant Sci. **5,** 67-74.

Urao, T., Yamaguchi-Shinozaki, K., and Shinozaki, K. (2001). Plant histidine kinases: an emerging picture of two-component signal transduction in hormone and environmental responses. Sci STKE **2001,** re18.

Urao, T., Noji, M., Yamaguchi-Shinozaki, K., and Shinozaki, K. (1996). A transcriptional activation domain of ATMYB2, a drought-inducible *Arabidopsis* Myb-related protein. The Plant Journal **10,** 1145-1148.

Urao, T., Miyata, S., Yamaguchi-Shinozaki, K., and Shinozaki, K. (2000b). Possible His to Asp phosphorelay signaling in an Arabidopsis two-component system. FEBS Letters **478,** 227-232.

Urao, T., Yakubov, B., Satoh, R., Yamaguchi-Shinozaki, K., Seki, M., Hirayama, T., and Shinozaki, K. (1999). A transmembrane hybrid-type histidine kinase in *Arabidopsis* functions as an osmosensor. Plant Cell **11,** 1743-1754.

Valette-Collet, O., Cimerman, A., Reignault, P., Levis, C., and Boccara, M. (2003). Disruption of *Botrytis cinerea* pectin methylesterase gene *Bcpme1* reduces virulence on several host plants. Mol. Plant-Microbe Interact. **16,** 360-367.

Valliyodan, B., and Nguyen, H.T. (2006). Understanding regulatory networks and engineering for enhanced drought tolerance in plants. Current Opinion in Plant Biology **9,** 1-7.

van Baarlen, P., Woltering, E.J., Staats, M., and van Kan, J.A.L. (2007). Histochemical and genetic analysis of host and non-host interactions of *Arabidopsis* with three *Botrytis* species: an important role for cell death control. Molecular Plant Pathology **8,** 41-54.

Van Der Biezen, E.A., and Jones, J.D.G. (1998). Plant disease-resistance proteins and the gene-for-gene concept. Trends in Biochemical Sciences **23,** 454-456.

van Kan, J. (2006). Licensed to kill: the lifestyle of a necrotrophic plant pathogen. Trends Plant Sci **11,** 247 - 253.

Van Leene, J., Witters, E., Inzé, D., and De Jaeger, G. (2008). Boosting tandem affinity purification of plant protein complexes. Trends Plant Sci. **13,** 517-520.

Van Leene, J., Stals, H., Eeckhout, D., Persiau, G., Van de Slijke, E., Van Istrdael, G., De Clercq, A., Bonnet, E., Laukens, K., Remmerie, N., Henderick, K., De Vijlder, T., Abdelkrim, A., Pharazyn, A., Van Onckelen, H., Inze, D., Witters, E., and De Jaeger, G. (2007). A tandem affinity purification-based technology platform to study the cell cycle interactome in *Arabidopsis thaliana*. Molecular and Cellular Proteomics **6,** 1226-1238.

Van Loon, L.C., and Van Strien, E.A. (1999). The families of pathogenesis-related proteins, their activities and comparative analysis of PR-1 type proteins. Physiological and Molecular Plant Pathology **55,** 85-97.

Verhage, A., van Wees, S.C.M., and Pieterse, C.M.J. (2010). Plant Immunity: It's the Hormones Talking, But What Do They Say? Plant Physiol. **154,** 536-540.

Vermeulen, T., Schoonbeek, H., and De Waard, M.A. (2001). The ABC transporter BcatrB from *Botrytis cinerea* is a determinant of the activity of the phenylpyrrole fungicide fludioxonil. Pest Management Science **57,** 393-402.

Veronese, P., Chen, X., Bluhm, B., Salmeron, J., Dietrich, R., and Mengiste, T. (2004). The *BOS* loci of Arabidopsis are required for resistance to *Botrytis cinerea* infection. Plant J. **40,** 558-574.

Verslues, P.E., Agarwal, M., Katiyar-Agarwal, S., Zhu, J., and Zhu, J.-K. (2006). Methods and concepts in quantifying resistance to drought, salt and freezing, abiotic stresses that affect plant water status. Plant J. **45,** 523-539.

Verslues, P.E., Batelli, G., Grillo, S., Agius, F., Mm, Y.S., Zhu, J., Agarwal, M., Katiyar-Agarwal, S., and Zhu, J.K. (2007). Interaction of SOS2 with nucleoside diphosphate kinase 2 and catalases reveals a point of connection between salt stress and H_2O_2 signaling in *Arabidopsis thaliana*. Molecular and Cellular Biology **27,** 7771-7780.

Very, A.-A., and Sentenac, H. (2003). Molecular mechanisms and regulationof K^+ transport in higher plants. Annual Review of Plant Biology **54,** 575-603.

Vlad, F., Rubio, S., Rodrigues, A., Sirichandra, C., Belin, C., Robert, N., Leung, J., Rodriguez, P.L., Lauriere, C., and Merlot, S. (2009). Protein phosphatases 2C regulate the activation of the Snf1-related kinase OST1 by abscisic acid in *Arabidopsis*. Plant Cell **21,** 3170-3184.

Vlot, A.C., Dempsey, D.A., and Klessig, D.F. (2009). Salicylic Acid, a Multifaceted Hormone to Combat Disease. Annu. Rev. Phytopathol. **47,** 177-206.

Voet-van-Vormizeele, J., and Groth, G. (2008). Ethylene Controls Autophosphorylation of the Histidine Kinase Domain in Ethylene Receptor ETR1. Molecular Plant **1,** 380-387.

Waard, M.A., Georgopoulos, S.G., Hollomon, D.W., Ishii, H., Leroux, P., Ragsdale, N.N., and Schwinn, F.J. (1993). Chemical Control of Plant Diseases: Problems and Prospects. Annu. Rev. Phytopathol. **31,** 403-421.

Wahid, A., Gelani, S., Ashraf, M., and Foolad, M.R. (2007). Heat tolerance in plants: an overview. Environmental and Experimental Botany **61,** 199-233.

Walter, M., Chaban, C., Schütze, K., Batistic, O., Weckermann, K., Näke, C., Blazevic, D., Grefen, C., Schumacher, K., Oecking, C., Harter, K., and Kudla, J. (2004). Visualization of protein interactions in living plant cells using bimolecular fluorescence complementation. The Plant Journal **40,** 428-438.

Wan, J., Zhang, X.-C., Neece, D., Ramonell, K.M., Clough, S., Kim, S.-y., Stacey, M.G., and Stacey, G. (2008). A LysM Receptor-Like Kinase Plays a Critical Role in Chitin Signaling and Fungal Resistance in *Arabidopsis*. Plant Cell **20,** 471-481.

Wang, W.X., Vinocur, B., and Altman, A. (2003). Plant responses to drought, salinity and extreme temperatures: towards genetic engineering for stress tolerance. Planta **218,** 1-14.

Wang, W.X., Vinocur, B., Shoseyov, O., and Altman, A. (2004). Role of plant heat-shock proteins and molecular chaperones in the abiotic stress response. Trends Plant Sci. **9,** 244-252.

Wang, X.C. (2002). Phospholipase D in hormonal and stress signaling. Current Opinion in Plant Biology **5,** 408-414.

Wang, Y., Wang, T., Li, K., and Li, X. (2008a). Genetic analysis of involvement of ETR1 in plant response to salt and osmotic stress. Plant Growth Regulation **54,** 261-269.

Wang, Y., Wang, L., Sun, Y., Chen, Y., Zhu, L., Guo, L., Luo, B., and Wang, H. (2007). Disrupted *ompC* causes osmotic sensitivity of *Escherichia coli* in alkaline medium. Journal of Genetics and Genomics **34,** 1131-1138.

Wang, Y.N., Zhang, W.S., Li, K.X., Sun, F.F., Han, C.K., Wang, Y., and Li, X. (2008b). Salt-induced plasticity of root hair development is caused by ion disequilibrium in *Arabidopsis thaliana*. Journal of Plant Research **121,** 87-96.

Wei, W., Plovanich-Jones, A., deng, W.L., Jin, Q.L., Collmer, A., Huang, H.C., and He, S.Y. (1999). The gene coding for the Hrp pilus structural protein is required for type III secretion of Hrp and Avr proteins in *Pseudomonas syringae* pv. *tomato*. Proceedings of the National Academy of Sciences **97,** 2247-2252.

West, A.H., and Stock, A.M. (2001). Histidine kinases and response regulator proteins in two-component signaling systems. Trends in Biochemical Sciences **26,** 369-376.

Wildermuth, M.C., Dewdney, J., Wu, G., and Ausubel, F.M. (2001). Isochorismate synthase is required to synthesize salicylic acid for plant defence. Nature **414,** 562-565.

Williamson, B., Tudzynsk, B., Tudzynski, P., and van Kan, J.A.L. (2007). *Botrytis cinerea*: the cause of grey mould disease. Molecular Plant Pathology **8,** 561-580.

Wohlbach, D.J., Quirino, B.F., and Sussman, M.R. (2008). Analysis of the *Arabidopsis* histidine kinase ATHK1 reveals a connection between vegetative osmotic stress sensing and seed maturation. Plant Cell **20,** 1101-1117.

Wright, C.A., and Beattie, G.A. (2004). *Pseudomonas syringae* pv. *tomato* cells encounter inhibitory levels of water stress during the hypersensitive response of *Arabidopsis thaliana*. Proceedings of the National Academy of Sciences of the United States of America **101,** 3269-3274.

Wu, S.J., Ding, L., and Zhu, J.K. (1996). *SOS1,* a genetic locus essential for salt tolerance potassium acquisition. Plant Cell **8,** 617-627.

Xiang, T., Zong, N., Zou, Y., Wu, Y., Zhang, J., Xing, W., Li, Y., Tang, X., Zhu, L., Chai, J., and Zhou, J.-M. (2008). *Pseudomonas syringae* Effector AvrPto Blocks Innate Immunity by Targeting Receptor Kinases. Current Biology **18,** 74-80.

Xiang, T.T., Zong, N., Zhang, J., Chen, J.F., Chen, M.S., and Zhou, J.M. (2011). BAK1 Is Not a Target of the *Pseudomonas syringae* Effector AvrPto. Mol. Plant-Microbe Interact. **24,** 100-107.

Xiao, S.Y., Brown, S., Patrick, E., Brearley, C., and Turner, J.G. (2003). Enhanced transcription of the arabidopsis disease resistance genes *RPW8.1* and *RPW8.2* via a salicylic acid-dependent amplification circuit is required for hypersensitive cell death. Plant Cell **15,** 33-45.

Xie, Y.-J., Xu, S., Han, B., Wu, M.-Z., Yuan, X.-X., Han, Y., Gu, Q., Xu, D.-K., Yang, Q., and Shen, W.-B. (2011). Evidence of *Arabidopsis* salt acclimation induced by up-regulation of *HY1* and the regulatory role of RbohD-derived reactive oxygen species synthesis. The Plant Journal **66,** 280-292.

Xiong, L., and Zhu, J.-K. (2002). Salt tolerance. The Arabidopsis Book **1,** 1-22.

Xiong, L., Ishitani, M., Lee, H., and Zhu, J.K. (2001). The *Arabidopsis LOS5/ABA3* locus encodes a molybdenum cofactor sulfurase and modulates cold stress- and osmotic stress-responsive gene expression. Plant Cell **13,** 2063-2083.

Xiong, L.M., Schumaker, K.S., and Zhu, J.K. (2002). Cell signaling during cold, drought, and salt stress. Plant Cell **14,** S165-S183.

Xu, L., Liu, F., Lechner, E., Genschik, P., Crosby, W.L., Ma, H., Peng, W., Huang, D., and Xie, D. (2002). The SCF^{COI1} ubiquitin-ligase complexes are required for jasmonate response in *Arabidopsis*. The Plant Cell **14,** 1919-1935.

Xu, X., Song, Y., Li, Y., Chang, J., zhang, H., and An, L. (2010). The tandem affinity purification method: An efficient system for protein complex purification and protein interaction identification. Protein Expression and Purification **72,** 149-156.

Yamada, H., Suzuki, T., Terada, K., Takei, K., Ishikawa, K., Miwa, K., Yamashino, T., and Mizuno, T. (2001). The *Arabidopsis* AHK4 Histidine Kinase is a Cytokinin-Binding Receptor that Transduces Cytokinin Signals Across the Membrane. Plant and Cell Physiology **42,** 1017-1023.

Yamada, M., Morishita, H., Urano, K., Shiozaki, N., Yamaguchi-Shinozaki, K., Shinozaki, K., and Yoshiba, Y. (2005). Effects of free proline accumulation in petunias under drought stress. J. Exp. Bot. **56,** 1975-1981.

Yamaguchi-Shinozaki, K., and Shinozaki, K. (1994). A novel *cis*-acting element in an *Arabidopsis* gene is involved in responsiveness to drought, low temperature, or high-salt stress. Plant Cell **6,** 251-264.

Yamaguchi-Shinozaki, K., and Shinozaki, K. (2005). Organization of *cis*-acting regulatory elements in osmotic- and cold-stress-responsive promoters. Trends Plant Sci. **10,** 88-94.

Yang, Q., Chen, Z.Z., Zhou, X.F., Yin, H.B., Li, X., Xin, X.F., Hong, X.H., Zhu, J.K., and Gong, Z. (2009). Overexpression of *SOS* (*Salt Overly Sensitive)* genes increases salt tolerance in transgenic *Arabidopsis*. Molecular Plant **2,** 22-31.

Yang, S.J., Vanderbeld, B., Wan, J.X., and Huang, Y.F. (2010). Narrowing Down the Targets: Towards Successful Genetic Engineering of Drought-Tolerant Crops. Molecular Plant **3,** 469-490.

Yasuda, M., Ishikawa, A., Jikumaru, Y., Seki, M., Umezawa, T., Asami, T., Maruyama-Nakashita, A., Kudo, T., Shinozaki, K., Yoshida, S., and Nakashita, H. (2008). Antagonistic interaction between systemic acquired resistance and the abscisic acid-mediated abiotic stress response in *Arabidopsis*. Plant Cell **20,** 1678-1692.

Yazaki, J., Shimatani, Z., Hashimoto, A., Nagata, Y., Fujii, F., Kojima, K., Suzuki, K., Taya, T., Tonouchi, M., Nelson, C., Nakagawa, A., Otomo, Y., Murakami, K., Matsubara, K., Kawai, J., Carninci, P., Hayashizaki, Y., and Kikuchi, S. (2004). Transcriptional profiling of genes responsive to abscisic acid and gibberellin in rice: phenotyping and comparative analysis between rice and *Arabidopsis*. Physiol Genomics **17,** 87 - 100.

Yokoi, S., Quintero, F.J., Cubero, B., Ruiz, M.T., Bressan, R.A., Hasegawa, P.M., and Pardo, J.M. (2002). Differential expression and function of Arabidopsis thaliana NHX Na^+/H^+ antiporters in the salt stress response. Plant J. **30,** 529-539.

Yoshiba, Y., Kiyosue, T., Katagiri, T., Ueda, H., Mizoguchi, T., Yamaguchi-Shinozaki, K., Wada, K., Harada, Y., and Shinozaki, K. (1995). Correlation between the induction of a gene for delta^1-pyrroline-5-carboxylate synthetase and the accumulation of proline in *Arabidopsis thaliana* under osmotic stress. Plant J. **7,** 751-760.

Yu, I.C., Parker, J., and Bent, A.F. (1998). Gene-for-gene disease resistance without the hypersensitive response in *Arabidopsis dnd1* mutant. Proceedings of the National Academy of Sciences of the United States of America **95,** 7819-7824.

Yu, L., Nie, J., Cao, C., Jin, Y., Yan, M., Wang, F., Liu, J., Xiao, Y., Liang, Y., and Zhang, W. (2010). Phosphatidic acid mediates salt stress response by regulation of MAPK6 in *Arabidopsis thaliana*. New Phytol. **188,** 762-773.

Yuan, J., and He, Y. (1996). The *Pseudomonas syringae* Hrp regulation and secretion system controls the production and secretion of multiple extracellular proteins. Journal of Bacterioloogy **178,** 6399-6402.

Zaninotto, F., La Camera, S., Polverari, A., and Delledonne, M. (2006). Cross talk between reactive nitrogen and oxygen species during the hypersensitive disease resistance response. Plant Physiol. **141,** 379-383.

Zeier, J. (2005). Age-dependent variations of local and systemic defence responses in *Arabidopsis* leaves towards an avirulent strain of *Pseudomonas syringae*. Physiological and Molecular Plant Pathology **66,** 30-39.

Zeng, W.Q., and He, S.Y. (2010). A Prominent Role of the Flagellin Receptor FLAGELLIN-SENSING2 in Mediating Stomatal Response to *Pseudomonas syringae* pv *tomato* DC3000 in *Arabidopsis*. Plant Physiol. **153,** 1188-1198.

Zeng, W.Q., Melotto, M., and He, S.Y. (2010). Plant stomata: a checkpoint of host immunity and pathogen virulence. Current Opinion in Biotechnology **21,** 599-603.

Zhang, J., Shao, F., Li, Y., Cui, H., Chen, L., Li, H., Zou, Y., Long, C., Lan, L., Chai, J., Chen, S., Tang, X., and Zhou, J.-M. (2007). A *Pseudomonas syringae* Effector Inactivates MAPKs to Suppress PAMP-Induced Immunity in Plants. Cell Host & Microbe **1,** 175-185.

Zhang, J.H., Jia, W.S., Yang, J.C., and Ismail, A.M. (2006). Role of ABA in integrating plant responses to drought and salt stresses. Field Crops Research **97,** 111-119.

Zhang, W., Qin, C., Zhao, J., and Wang, X. (2004). Phospholipase D α1-derived phosphatidic acid interacts with ABI1 phosphatase 2C and regulates abscisic acid signaling. Proceedings of the National Academy of Sciences of the United States of America **101,** 9508-9513.

Zhang, Y., Tessaro, M.J., Lassner, M., and Li, X. (2003). Knockout analyis of *Arabidopsis* transcription factors *TGA2, TGA5* and *TGA6* reveals their redundant and essential roles in systemic acquired resistance. The Plant Cell **15,** 2647-2653.

Zhao, X.C., and Schaller, G.E. (2004). Effect of salt and osmotic stress upon expression of the ethylene receptor ETR1 in *Arabidopsis thaliana*. FEBS Letters **562,** 189-192.

Zhou, J.M., Trifa, Y., Silva, H., Pontier, D., Lam, E., Shah, J., and Klessing, D.F. (2000). NPR1 differentially interacts with members of the TGA/OBF family of transcription factors that bind an element of the *PR-1* gene required for induction by salicylic acid. Mol. Plant-Microbe Interact. **13,** 191-202.

Zhou, N., Tootle, T.L., Tsui, F., Klessig, D.F., and Glazebrook, J. (1998). PAD4 Functions Upstream from Salicylic Acid to Control Defense Responses in *Arabidopsis*. The Plant Cell Online **10,** 1021-1030.

Zhu, J.H., Fu, X.M., Koo, Y.D., Zhu, J.K., Jenney, F.E., Adams, M.W.W., Zhu, Y.M., Shi, H.Z., Yun, D.J., Hasegawa, P.M., and Bressan, R.A. (2007). An enhancer mutant of *Arabidopsis salt overly sensitive 3* mediates both ion homeostasis and the oxidative stress response. Molecular and Cellular Biology **27,** 5214-5224.

Zhu, J.K. (2002). Salt and drought stress signal transduction in plants. Annual Review of Plant Biology **53,** 247-273.

Zhu, J.K. (2003). Regulation of ion homeostasis under salt stress. Current Opinion in Plant Biology **6,** 441-445.

Zimmerli, L., Metraux, J.P., and Mauch-Mani, B. (2001). beta-aminobutyric acid-induced protection of *Arabidopsis* against the necrotrophic fungus *Botrytis cinerea*. Plant Physiol. **126,** 517-523.

Zipfel, C. (2008). Pattern-recognition receptors in plant innate immunity. Current Opinion in Immunology **20,** 10-16.

Zipfel, C., and Rathjen, J.P. (2008). Plant Immunity: AvrPto Targets the Frontline. Current Biology **18,** R218-R220.

Zipfel, C., Robatzek, S., Navarro, L., Oakeley, E.J., Jones, J.D.G., Felix, G., and Boller, T. (2004). Bacterial disease resistance in *Arabidopsis* through flagellin perception. Nature **428,** 764-767.

Zipfel, C., Kunze, G., Chinchilla, D., Caniard, A., Jones, J.D.G., Boller, T., and Felix, G. (2006). Perception of the Bacterial PAMP EF-Tu by the Receptor EFR Restricts *Agrobacterium*-Mediated Transformation. Cell **125,** 749-760.